Co-processing of drugs and co-crystal formers and its effect on pharmaceutical dosage-form performance

Co-crystallization of urea/ 2-methoxybenzamide, caffeine/ malonic acid, caffeine/ oxalic acid and theophylline/ malonic acid systems: Solid-state characterization including imaging, thermal, X-ray and Raman spectroscopic techniques with subsequent evaluation of tableting behaviour

Asim Yousif Ibrahim Mohamed, MPharm

Submitted for the degree of
Doctor of Philosophy

Drug Delivery Group
School of Pharmacy
University of Bradford
UK

2008

Abstract

Asim Yousif Ibrahim Mohamed, MPharm

Co-processing of drugs and co-crystal formers and its effect on pharmaceutical dosage-form performance

This dissertation has focused on the solid-state characterization of different co-crystal system as well as the effect of co-crystallization of these systems on pharmaceutical dosage form performance. Urea/ 2-MB, caffeine/ malonic acid, caffeine/ oxalic acid and theophylline/ malonic acid co-crystals were prepared using co-grinding- and co-precipitation techniques. In addition, the synthesis of co-crystals through two novel methods has been demonstrated. This includes compaction and convection mixing. The solid-state characterization of the co-crystals has been carried out using XRPD, Raman spectroscopy, DSC, TGA, hot-stage microscopy and SEM. After preparation of co-crystals, tablets have been produced from co-ground-, co-precipitated-, and physical mixtures using Compaction Studies Press (Kaleva), and the data were recorded to compare between the different mixtures, regarding compactibilty, compressibility and deformational properties.

The DSC results showed that the physical mixtures of all systems, formed co-crystals during heating process. For systems of urea/ 2-MB, caffeine/ malonic acid and theophylline/ malonic acid, the co-ground mixture produced tablets with higher tensile strength compared with either co-precipitated or physical mixture. However, for caffeine/ oxalic acid system, the tensile strengths of compacts produced from the physical mixture were greater than those obtained from either co-ground or co-precipitated mixtures. The Heckel data suggested that urea/ 2-MB, caffeine/ malonic acid and theophylline/ malonic acid systems are Type 1 materials, as an extensive linearity during compression was indicative of a plastic deformation mechanism, while the caffeine/ oxalic acid system was Type 2 materials. However, the co-precipitated mixture of urea/ 2-MB system was the least compressible, as it possessed the greatest value of yield pressure (85 MPa) and the highest elastic recovery (7.42%). The co-precipitated mixture of both of caffeine/ malonic acid and theophylline/ malonic acid systems was the most compressible with small yield pressure values of (44 & 80 MPa) and elastic recovery of (7.2% & 6.56%), respectively. The co-ground mixture of caffeine/ oxalic acid possessed the highest value of yield pressure (166 MPa) and thus the lowest compressibility among other mixtures. Furthermore, the addition of microcrystalline cellulose and α-lactose monohydrate has affected the crystallinity as well as the tableting properties of the co-crystals. After the addition of excipients, the tensile strength of compacts was about 2 times higher than any other mixture. Finally, urea/ 2-MB and caffeine/ malonic acid co-crystals were successfully synthesized through convection mixing and compaction.

Keywords:

Co-crystals, urea, 2-methoxybenzamide, caffeine, malonic acid, oxalic acid, theophylline, convection mixing, compaction, tensile strength.

PUBLICATIONS

Sections of this thesis have previously been presented or published in the following forms:

1. Co-crystallisation of hydrochlorothiazide with succinic acid and fumaric acid to improve solubility, Ibrahim, A.Y., Grimsey, I., Bonner, M.C., Blagden, N. and Forbes, R.T., Poster presentation at Bradford university, open day, Bradford, UK, 2008.
2. Solid-state characterization of urea/ 2-MB co-crystal prepared by co-grinding and co-precipitation methods, Ibrahim, A.Y., Grimsey, I., Bonner, M.C., Blagden, N. and Forbes, R.T., Poster presentation at the ASSA international conference, Bamberg, Germany, 2008.
3. Current direction in co-crystal growth, New Journal of Chemistry, Nicholas Blgden, Asim Ibrahim, et al. (2008).
4. Co-crystallization of caffeine/ malonic acid affects tableting behaviour, Ibrahim, A.Y., Grimsey, I., Bonner, M.C., and Forbes, R.T., Poster presentation in the Research Showcase Event at Bradford university, Bradford, UK, 2008.

Acknowledgments

First of all, I wish to express my deep thanks and gratitude to my supervisor Professor Rob Forbes for his kindness, invaluable and constant support, guidance, advice and supervision throughout the period of this research. He has given me the freedom to explore my theories but was always able to share with me any new idea. I would also like to thank my co-supervisors Dr. Ian Grimsey and Dr. Michael Bonner for their valuable help, support, advice and reading of the thesis and the papers.

I should also like to thank Dr. Nicholas Blagden for his help, support, and guidance in exploring one new method of co-crystal synthesis, reading, and publishing the findings.

My thanks are due to the technical staff David Benson for his help in moisture isotherm technique.

Special thanks are due to my colleague Dr Wendy Hulse for her constant help in tableting experiments. My deep thanks are also due to my colleague David Berry for his help in hot-stage microscopy.

I would also like to thank my friends and colleagues within the IPI and Richmond building for their help and support.

I would like to acknowledge the Islamic University of Omdurman and the ministry of higher education in Sudan for the sponsorship.

Finally, I would like to express my thanks to all my friends and family for their continual help, encouragement and support over my post graduate studies.

Table of Contents

LIST OF FIGURES

LIST OF TABLES

List of abbreviations and symbols

API	Active pharmaceutical ingredients
CSD	Cambridge structural data base
DSC	Differential scanning calorimetry
SEM	Scanning electron microscopy
n	Order of reflection
θ	Bragg angle
λ	Applied wave length
đ	Distance between atomic plane
2-MB	2-methoxybenzamide
PXRD	Powder X-ray diffraction
SSNMR	Solid state nuclear magnetic resonance
PVP	Polyvinylpyrrolidone
PVP-CL	Cross-linked polyninylpyrrolidone
UDCA	Ursodeoxychloric acid
HCTZ	Hydrochlorothiazide
MCC	Microcrystalline cellulose
GRAS	Generally recognized as safe
DTA	Differential thermal analysis
TGA	Thermal gravimetric analysis
TA	Thermo gravimetric analysis
RH	Relative humidity
Ts	Tensile strength
D_f	Final bulk density
D_0	Initial bulk density
A	Maximum punch force
B	Punch stroke when punch force is zero
C	Punch stroke when punch force is maximum
D	Punch stroke after decompression
ABC	Gross energy
ABD	Plastic energy
ADC	Elastic energy
E	Elastic recovery
t_1	Minimal thickness of powder bed in the die
t_2	Thickness of the recovered tablet
D	Relative density
P	Applied pressure
KN	Kilo Newton
MPa	Mega Pascal
IR-press	Infra red Press

This thesis is dedicated to the soul
of my mother, my father and my lovely daughter Rana.

1. Introduction

1.1. General introduction

Crystal engineering of pharmaceuticals may open new avenues to improve poorly soluble drugs and provide formulation development options. Solid-state reactions of drugs have been investigated for the preparation of crystalline materials (Caira et al. 1995), (Braga et al. 2002). Solvent free processing, especially the mechanical mixing of solid reactants, has attracted the interest of chemists and technologists, as they often provide fast routes to prepare novel organic and inorganic materials (Rastogi et al. 1963). The literature suggests that the same product can be obtained quantitatively by different methods, e.g. manual grinding, electromechanical ball milling (Boldyrev and Takacova 2000), kneading (Watano et al. 2002), and by seeding the growth of crystals from solution (Seiler and Dunitz 1982).

In recent years, a number of studies have focused on the preparation of molecular co-crystals (Etter 1991). Within crystal engineering of molecular solids assembly may principally be through hydrogen–bonding interactions, as documented by numerous papers on hydrogen bonded crystal engineering strategies (Subramanian and Zaworotka 1995). As a result of the progress in supramolecular and crystal engineering approaches, which are defined as spatial arrangements of intermolecular interactions, organic solid-state materials are intensively investigated in the context of crystal packing and in the design of new solids with enhanced physical and chemical properties (Desiraju 1989).

When formulating an active pharmaceutical ingredient (API) into a specific dosage form, the physical form of a drug substance is carefully selected. However, other factors can determine the solid-state properties of the drug in the final product, e.g. co-processing of

drugs and excipients can change the product performance (Alsaidan et al. 1998). Additionally, processing steps during tablet manufacture, including milling, granulation, drying, compression, as well as the processing conditions has also been found to have a major impact on the physical form of the drug. Ultimately, the choice of API physical form was found to have a great impact on the dissolution rate profile (Phadnis and Suryanayanan 1997).

Few studies have focused on the effect of processing-induced phase transformation (Yoshinari et al. 2003). However, it has been observed that the crystal form of a drug substance can influence the properties of granules and behaviour of tablets (Otsuka et al. 1997).

1.2. Pharmaceutical co-crystals

Co-crystals represent a well-established class of compounds, and an example of which is quinhydrone, which was reported by (Wöhler 1844) and (Ling and Baker 1893). The definition of the term co-crystals is still a matter of topical debate. For example, a broad definition is that a co-crystal is a mixed crystal or crystal that contains two different molecules (Kitaigorodskii 1984). Alternatively, from applying the concept of supramolecular chemistry and crystal engineering, a co-crystal is the consequence of a molecular recognition event between different molecular species (Dunitz 2003). However, pharmaceutical co-crystals are defined as crystalline materials that consist of two or more molecular species held together by non-covalent forces (Aakeröy 1997). These crystalline phases are developed for greater efficacy, stability and solubility in drug formulation (Walsh et al. 2003). It has been suggested that co-crystals are made from reactants that are solid at ambient temperature. It has also been stated that all hydrates and other solvates are

excluded which, in principle, eliminates compounds that are classified as clathrates or inclusion compounds (Aakeröy et al. 2003). However, there is still some disagreement as to whether to include solvates in the category of co-crystals. Some scientists suggest that co-crystals are part of the broader family of multicomponent crystal systems which include salts, solvates, clathrates, inclusion crystals and hydrates, and that solvates differ from hydrates primarily in the physical state of the single components (Morissette et al. 2004). Almarsson and Zaworotka, (2004) argued that solvates are commonplace as they occur as a serendipitous result of crystallization from solution. In addition, solvated crystals are often unstable, because it is common to observe dehydration/desolvation of hydrates/solvates and such evaporation of the solvent may result in crystallising of the amorphous phase into less soluble forms. However, co-crystals are the products of choice, if these have been designed. They are more stable, as the co-crystal formers are solid at room temperature. On the other hand, solvates are described as a special type of multi-component solids. They may be classified according to the molecular network of the solvent molecules into two types:

i) A co-crystal, if the solvent is an integral part of the network structure and forms at least a two-component crystal.

ii) A clathrate, if the solvent does not contribute to the network itself (Rodriguez-Spong et al. 2004).

For distinguishing between multi-component crystalline materials that are comprised of two or more solids, versus those composed of one or more solids and a liquid, the latter have been called solvates or pseudopolymorphs (Nangia 2005).

1.2.1. Groups and classes of pharmaceutical co-crystals

The multi-component crystal is a group of pharmaceutical co-crystals that are formed between a molecular or ionic active pharmaceutical ingredient (API) and co-crystal former that is a solid under ambient conditions. This group also includes salts, solvates, clathrates, inclusion crystals and hydrates as shown in (Figure1). An overlap between these classes exists, since there are crystalline materials that consist of two or more components that are solid under ambient conditions and a liquid component. However, a multi-component system resulting from a molecular co-crystal former and an ionic API would be classified as a pharmaceutical co-crystal (Childs et al. 2004). It is important to bear in mind that, from a supramolecular perspective (which is defined as recurring hydrogen bond and/or intermolecular interaction patterns for crystal engineering (Desiraju 1995)), pharmaceutical co-crystals and solvates are closely related to one another since components within the crystal interact by hydrogen bonding or other directional non-covalent interaction. An example of these is the multiple solvates and co-crystals of carbamazepine (Fleischman et al. 2003). The principal difference between solvates and pharmaceutical co-crystals is the physical state of the isolated pure components (Morissette et al. 2004). For example, if one component is a liquid at room temperature a compound is a solvate; if both components are crystalline solids at room temperature, they are pharmaceutical co-crystals. The solvated forms of spironolactone were found to enhance the drug dissolution rate (Salole and Al-Sarraj 1985). However, solvated crystals are often unstable, leading to desolvation during storage, which may lead to the amorphous phase crystallizing into less soluble forms. Like other crystalline systems, a number of polymorphic co-crystals have been reported to date, including caffeine and glutaric acid co-crystals (Trask et al. 2004).

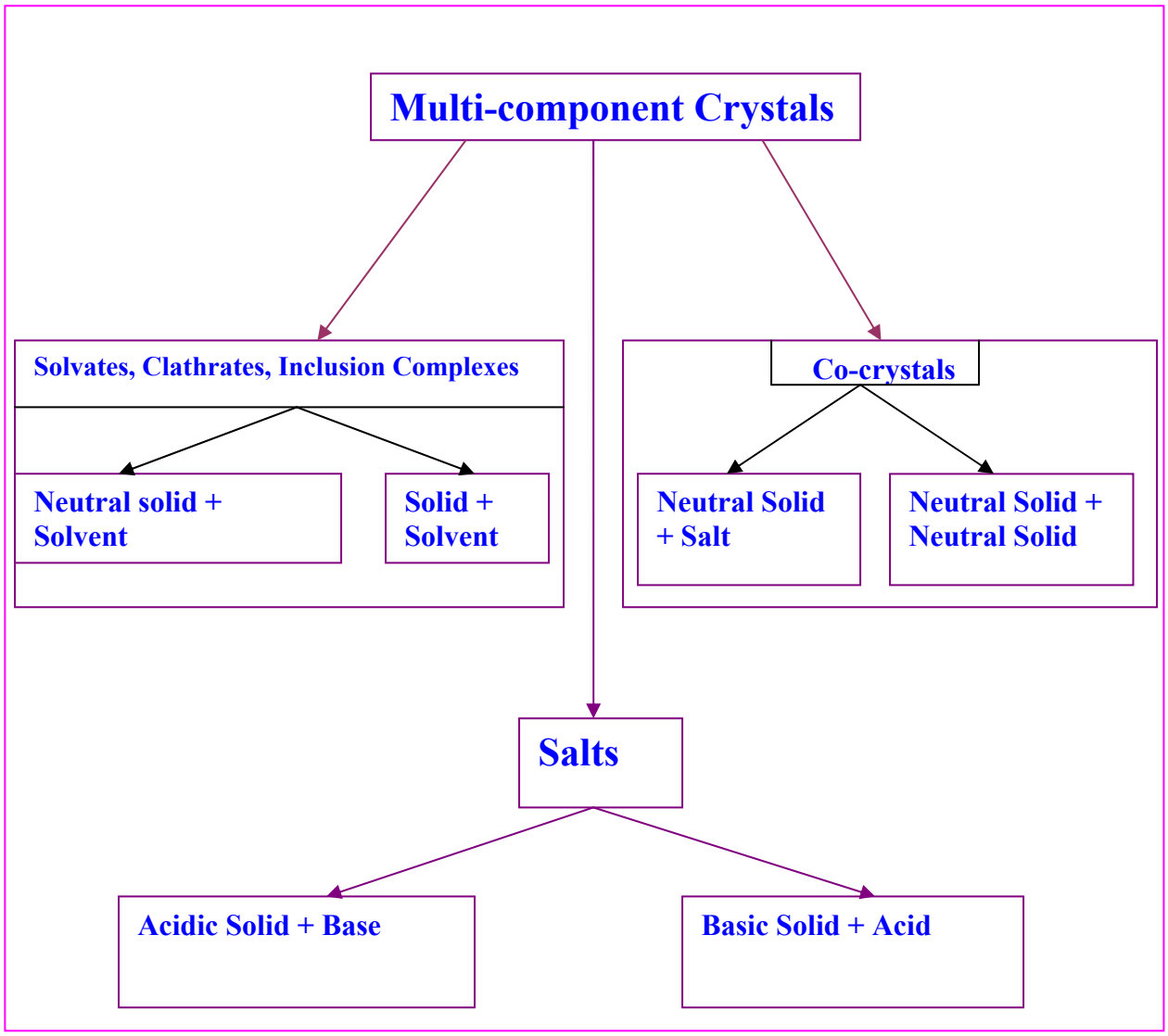

Figure 1: Types of multi-component crystals adopted from Morissette et al., (2004).

1.2.2. Crystal engineering of pharmaceutical co-crystals

Crystal engineering can be defined as the application of the concept of supramolecular chemistry to the solid state. It has been described as the exploitation of non-covalent interactions between molecular or ionic components for the rational design of solid-state structures with other unique properties e.g. electrical, magnetic, and optical phenomena. It is becoming evident that the specificity, directionality, and predictability of intermolecular hydrogen bonds can be used to assemble supramolecular structures of controlled dimensionality (Subramanian and Zaworotka 1995). It is apparent that crystal engineering enjoyed rapid growth during the 1990s, especially in terms of organic solids and metal-organic solids and also in terms of organometallic (Braga et al. 1998), and inorganic structures (Finn et al. 2003). Taking crystal engineering in the context of co-crystals, the structural units of supramolecular synthons (defined as recurring hydrogen bond and/ or intermolecular interaction patterns for crystal engineering) can be formed by synthetic operation involving intermolecular interactions (Desiraju 1995). Pharmaceutical co-crystals are considered to be much more useful in pharmaceutical products than solvates or hydrates for the following reasons:

1. The number of pharmaceutically acceptable solvents is very small.
2. Solvents tend to be more mobile and have higher vapour pressures than small molecular co-crystal formers.
3. Depending on storage conditions, it is rare to observe dehydration/desolvation of hydrates/solvates in solid dosage forms.

4. Additionally, solvates can lose solvent, which may lead to amorphous compounds that are principally less chemically stable and can crystallize resulting in less soluble forms.
5. In contrast to solvates, most co-crystal formers are unlikely to evaporate from solid dosage forms, making phase separation less likely.

As a potential method for the design of co-crystals, the Cambridge Structural Database (CSD) is used to carry out analysis of existing crystal structures. This method enables empirical information about functional groups and confirm their engagement in molecular association, hence the formation of supramolecular synthons. Allen and co-workers (1983) highlighted it when they noted that the systematic analysis of large numbers of related structures is a potential field of research since it has the capability to yield results not achieved by any other method.

Similar to salt screening, co-crystal screening is particularly suited to high-throughput technologies (Morissette et al. 2004). In order to start co-crystallization studies on an API, the co-crystal former(s) with acceptable pharmaceutical properties must first be selected, and should not be toxic (Remenar et al. 2003). This requirement limits the use of co-crystallizing agents to pharmaceutical excipients and compounds that have been approved for consumption by humans. These are classified as generally recognized as safe (GRAS) for use as food additives (U.S. Department of Health and Human Services, 2005).

In order to realize the pharmaceutical applications of these co-crystallizing agents that are classified as GRAS in the formation of co-crystals, the level of active drug and hence the resulting stoichiometric amount of co-crystal agent must be less than the permitted additive level for human administration (Almarsson and Zaworotka 2004).

There has been much co-crystallization research carried out using pharmaceutically acceptable co-crystallizing agents. A recent study of acetaminophen (paracetamol) adducts with ethers and amines provide examples of supramolecular synthons for co-crystal formation (Oswald et al. 2002). However 1,4-dioxane, N-methylmorpholine, morpholine, N,N-dimethylpiperazine, piperazine, and 4,4-bipyridine are not GRAS substances. Piperazine dihydrochloride and morpholine as the salt(s) of one or more fatty acids, are permitted as food additives at the relevant level (Oswald et al. 2002).

It can be concluded that the formation of co-crystals requires a consideration of the hydrogen bond donors and acceptors of the materials to be co-crystallized. Etter (1990) proposed some guidelines to facilitate the rationale design of hydrogen-bonded solids. These rules included the following:

1. All good proton donors and acceptors in hydrogen bonding are used in hydrogen bonding.

2. Six-membered rings intermolecular hydrogen bonds form in preference to intermolecular hydrogen bonds.

3. The best proton donor and acceptor remaining after intermolecular hydrogen-bond formation will form intermolecular hydrogen bonds to one another but not all acceptors will necessarily interact with donors.

1.2.3. Intermolecular Interactions

The attractions between molecules are described by intramolecular bonding which can be divided into covalent, that involves the mutual sharing of a pair of electrons by two atoms, or noncovalent interactions. The covalent bonding of molecules occurs in organic synthesis, while noncovalent bonding interactions occur in supramolecular chemistry.

The directionality of non-covalent interactions and the distance dependence are of importance to crystal engineers. The repeating interactions of a crystalline compound are additive and the relatively weak forces become significant in this context. According to the distance range, non-covalent interactions are divided into Van der Waals interactions, metal coordination, hydrogen bonds and electrostatic ion pairing.

Van der Waals interactions are medium range forces, responsible for molecular shape, close packing of the molecules, and contribute to the overall crystal stability. Hydrogen bonds are longer-range forces, directional and may show some covalent property. The very long-range forces are those between salts, may have specific controls, and constraints on molecular structure.

Supramolecular synthons are defined as recurring hydrogen bond and/ or intermolecular interaction patterns for crystal engineering and the synthetic organic structural features are described by the synthon (Desiraju 1995). However, supramolecular synthons are spatial arrangements of intermolecular interactions. The core objective of crystal engineering is to identify and design synthons that are strong enough to be interchanged between network structures. This ensures an overview eventually leading to the certainty of one, two and three-dimensional patterns fashioned by intermolecular interactions.

In the crystal engineering, the Cambridge Structural Database (Allen 2002) may be utilized to identify stable hydrogen bonding motifs (Bruno et al. 2002) with the objective that the most robust motifs will remain intact a cross a family of related structures. However, the nature of APIs, that is, molecules or ions with exterior functional groups that engage in hydrogen bonding; this makes all APIs inherently predisposed to formation of pharmaceutical co-crystals (Almarsson and Zaworotka 2004; Blagden et al. 2007).

Supramolecular synthons are sub-classified into homothynthons and heterosynthons according to similarities and differences of the interacting complementary functional groups (Scheme 1) (Walsh et al. 2003).

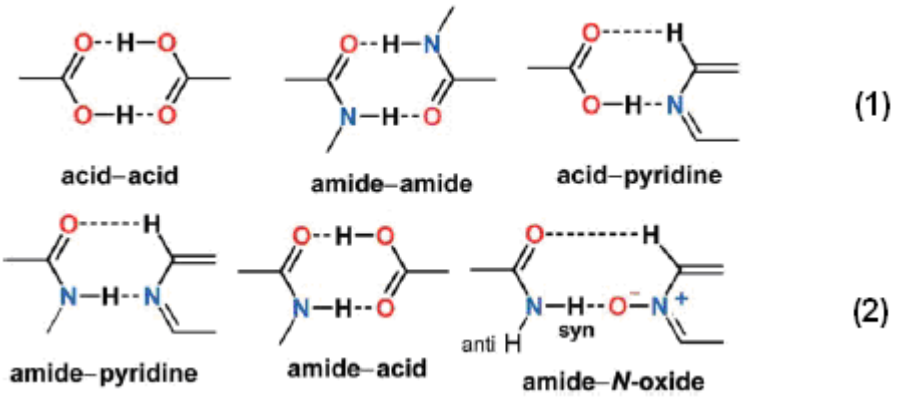

Scheme 1: Examples of homosynthons (1) and heterothynthons (2).

The functional groups in carboxylic acids and amides are self-complementary and have the capability of forming supramolecular heterothynthons; however, they are also complementary with each other and can interact through formation of a supramolecular heterothynthon. This motif has been studied for some time in the context of crystal engineering (Etter 1985; Huang et al. 1973). The interaction of carboxylic acids with heterocyclic bases is perhaps the most widely studied type of synthon (Aakeröy et al. 1998; Caira et al. 1995; Etter 1990). (Aakeröy et al. 2000; Batchelor et al. 2000; Carrow and Wheeler 1998; Edwards et al. 2002; Pedireddi et al. 1998; Pedireddi and PrakashaReddy 2002; Shan et al. 2002b; Shan et al. 2002c; Zhang et al. 2003).

In an attempt to assist the prediction of co-crystal formation, competition and prediction of synthon have been investigated (Etter 1991). This study suggested that the synthon with the

lowest hydrogen bonding energy would often attribute in the co-crystal structure, as this was demonstrated and verified experimentally through comparisons to the generated single-crystal structures.

1.2.4. General methods of preparation of co-crystals

1.2.4.1. Introduction

Co-crystals are usually synthesized by slow evaporation from solutions that contain co-crystal formers, grinding two solid co-crystal formers using a ball mill or mortar and pestle. Sublimation, growth from the melt, and slurry preparation have also been reported (Zaworotka 2005). Recently, a technique of solvent drop grinding is reported to be a promising preparation method. It has been performed by the addition of small amount of suitable solvent to accelerate the process of co-crystallization (Trask et al. 2004). Solvent drop grinding has the advantage over the traditional solvent crystallization techniques in that the former avoids the use of excessive crystallization solvent. Furthermore, the solvent-drop grinding helps in polymorph control and is useful for selective transformation of polymorph (Trask and Jones 2005).

Regardless of the method used to prepare co-crystals, formation of these classes is still challenging for a scientist. There are some difficult situations described in the literature in the context of co-crystal formation. For example, the preparation of a single co-crystal of good quality for single X-ray diffraction analysis can take 6 months (Portalone and Colapietro 2004) and it has been reported that approximately 50 co-crystal agents used for the 10 new co-crystals of carbamazepine, give a success rate of only 20% (Fleischman et al. 2003). Similar to salt formation, co-crystal formation requires a difference of at least two pKa units between a drug and co-crystal former, and in a co-crystal, proton transfer does

not take place between the acidic and the basic component; rather, a hydrogen bond of the type A-H…B is formed between them (Serajuddin and Pudipeddi 2002). Additionally, there are other requirements for co-crystal formation such as functional group complementarity and viable packing interaction (synthon compatibility) (Trask et al. 2005a). If one considers a polymorphic component as a co-crystallizing agent, it has been demonstrated that a chance of bringing such a molecule into a different packing arrangement in coexistence with another molecule is evidently increased (Aakeröy 1997). However, other studies on co-crystal formation from pairs of polymorphic APIs in their pure forms concluded that they appeared to be less prone to polymorphism than the corresponding single component APIs (Banerjee et al. 2005).

It is obvious that polymorphism alone is no guarantee that a compound is able to act as a co-crystallizing agent, however the ability of a molecule to participate in intermolecular interaction is the crucial factor (Aakeröy et al. 2003).

1.2.4.2. Co-grinding

Co-grinding involves the milling of the drug and excipient or between two drugs using high-energy comminution. This additional energy is utilized to cause particle size reduction of the active compound, decrease in drug crystallinity to amorphization (Hancock and Zografi 1997; Yonemochi 1999), or formation of metastable modifications which may lead to an increase in apparent dissolution rate (Miyamae et al. 1994; Takahashi 1985). Drug interaction with carriers can stabilize the system and delay the recrystallization. Many papers review the role of polymorphic modification during the co-grinding process. The dissolution properties of a mixture of glisentide with polyvinylpyrrolidone (PVP) (Mura et al. 2002), hydroxypropylmethylcellulose (HPMC) and nifidipine (Sugimoto et al. 1998),

furosemide and cross-linked (PVP-CL) (Shin et al. 1998), modified gum karaya/gum karaya and other APIs (Murali Mohan Babu et al. 2002) were found to improve after grinding. Grinding was also performed on a mixture of indometacin with PVP and with silica nanoparticles (Watanbe et al. 2003). Furthermore, grinding of the pure active ingredient decreased the intensities of powder X-ray diffraction peaks for ursodeoxycholic acid (UDCA), phenanthrene and anthrone. These peaks were either changed into halo patterns or completely disappeared after grinding, indicating a lowering of crystallinity without any polymorphic change with the drug becoming amorphous (Oguchi et al. 2000).

Reported solubility studies indicate an enhancement of drug dissolution, if components are co-ground. This was solely rationalized by the state of the drug and was irrespective of the carrier species. Amorphous indometacin has been stabilized by co-grinding with silica (Watanbe et al. 2001), talc and $Mg(OH)_2$-SiO_2 mixture (Watanbe et al. 2002). The use of cross-linked (PVP-CL) as an excipient for co-grinding created an amorphous drug form, found to be stable after 1 year (Shin et al. 1998). Also, compatibility studies on excipients reported a decrease in drug melting endotherms upon co-grinding with both linear, and/ or cross-linked forms of polymers as monitored by differential scanning calorimetry (Botha and Lotter 1989). A similar effect to grinding is the preparation of solid dispersions of griseofulvin and saccharides via a roll mixing method (Saito et al. 2002). It has been reported that griseofulvin gradually converted to an amorphous form during mixing with each of the carriers, namely processed starch and cornstarch. This process was also found to improve the dissolution profile of griseofulvin.

The preparation of co-crystals via grinding generally leads to products that are consistent with those produced by solution (Etter et al. 1993). This may signify that hydrogen-bond connectivity patterns are not distinctive or indomitable by non-specific and unmanageable

solvent effects or crystallization conditions. However, there are exceptions. While many co-crystals can be prepared from both solution growth and solid-state grinding, other can only be produced by solid-state grinding (Lynch et al. 1991). For example, the co-crystallization of 2,4,6-trinitrobenzoic acid and indole-3-acetic acid resulted in different crystal forms when prepared by solution compared with grinding (Lynch et al. 1991).

The inability to generate suitable co-crystals arrangements is most likely the reason behind the failure to form co-crystals by grinding rather than the stability of initial phases. If a co-crystal has been formed successfully by solution but not by grinding, solvent inclusion in stabilizing the supramolecular structure may be a reason (Pedireddi et al. 1996). Though co-crystallization by solid-state grinding has been recognized in the 19th century (Ling and Baker 1893), the current technique of solvent drop grinding was found to improve the kinetics and ease the formation of co-crystals and has shown the way to the solid-state grinding as a method of co-crystal preparation (Shan et al. 2002).

When cyclohexene-1, 3cis, 5cis-tricarboxylic acid with bipyridine, that previously was found to crystallize from MeOH solutions, was co-ground for 60 min, only partial conversion occurred, while the addition of some drops of MeOH to the mixture during grinding led to complete conversion into co-crystal after 20 min.

1.2.4.3. Physical mixes and co-crystals

Historically, physical mixtures are prepared by combining of two or more solid compounds using adequate agitation of two or more solid compounds without the addition of any liquid (Harnby et al. 1989). In the pharmaceutical context, this process involves the combination of one or more drugs with one or more excipients. This technique is straightforward and adaptable and is carried out using different mixing mechanisms, e.g. tubular mixer, mortar

and pestle, etc. The use of physical mixes of carriers and drugs is required as standards or a control, against which formulation systems (i.e. solid dispersions) are measured for improvements in physicochemical properties (Tantishiyakul et al. 1996). Additionally, physical mixes of carriers and drug have sometimes been shown to induce molecular conformation changes of the API and lead to an improvement in dissolution profile without any further treatment of the mixes.

Physical mixes of paracetamol and polyethylene glycol 4000 showed a lower heat of solution than the theoretical value calculated from the heats of solution corresponding to the individual components (Lloyed et al. 1999). This may have resulted from the possible formation of a solid dispersion. There is some evidence that hydrogen bonding has been observed in physical mixes of linear PVP and indometacin (Forster et al. 2001). A lowering in crystallinity has also been reported for drug compounds containing cross-linked PVP in physical mixes (Fujii et al. 2005), while other excipients did not show similar results, e.g. microcrystalline cellulose. However, it has been reported that a marked reduction in ibuprofen crystallinity when mixed with cross-linked PVP and an improvement in the dissolution profile was not reproduced on scale up of the batch size or on using different mixing equipment (Lu 2002).

Compared with melting, solvent depositions or co-grinding that induces strong molecular interaction between active pharmaceutical ingredients (APIs) and carriers within delivery systems, mixing is less energetic. As mentioned previously, these systems have the advantages of solid dispersions in that the exposure of the drug molecules to mechanical stress, heat or solvent is avoided.

1.2.4.4. The use of co-crystals in drug formulation

Marketed solid dosage forms of APIs have traditionally been limited to crystal forms of single component solids (i.e. they contain only the API), salts of the API or solvates of the API (Haleblian 1975). The form of the active pharmaceutical ingredient is of great importance in determining key physical properties such as water solubility and bioavailability. The crystal form varies according to crystallization solvent, the rate of cooling, or the presence of other materials in solution (Haleblian 1975).

The pharmaceutical co-crystals, as a new class of multiple component crystalline forms, are able to pack with increased efficiency due to the complementaries of the API and co-crystal former. In polymorphism that occurs in single component crystals or pseudopolymorphism that exists in salts, solvates and single component crystals, the crystal packing can also vary and most active ingredients exhibit this phenomenon.

Since pharmaceutical co-crystals do not involve covalently modifying the API, they offer a great opportunity to enhance the physical properties of the crystal form of APIs without changing their therapeutic attributes.

Studies on the processing of theophylline tablets reported that the crystallinity decreased (Shefter and Higuchi 1963) and phase transformation occurred during dissolution (Urakami et al. 2002). The crystallinity of anhydrous theophylline tablets was found to decrease upon both milling and aqueous wet granulation and this processing-induced decrease in crystallinity accelerated the conversion of anhydrate to monohydrate during dissolution (Debnath and Suryanarayanan 2004). Remenar and co-workers (2003) compared the dissolution of co-crystals of itracanazole (a trizole drug) with succinic acid, maleic acid and tartaric acid, to that of the pure crystalline and amorphous drug. They found that the co-

crystals of itracanazole behaved in a manner similar to the amorphous form rather than the crystalline drug, and the solution concentrations were higher than that of the crystalline drug. This ability to form a supersaturated solution could have a dramatic effect on drug absorption and bioavailability (Kwei et al. 1995). Fleischman et al., (2003) reported that of the melting points of thirteen carbamazepine co-crystals, only two had melting point higher than the pure components.

The stability of solid active materials against atmospheric moisture is important in the pharmaceutical industry, since hydrates can form upon processing, formulation, storage and packaging (Byrn 1999). Examination of the relative humidity stability was carried out for caffeine/dicarboxylic acid co-crystals against the pure crystalline anhydrous caffeine. There have been no co-crystal hydrates observed and the unstable co-crystal with respect to relative humidity tended to dissociate to the crystalline starting materials (Trask et al. 2005a).

Hickey and co-workers (2007) compared the performance of carbamazepine/ saccharine co-crystal with that of the marketed carbamazepine, in an attempt to address the suitability of a model co-crystal as an alternative to the currently marketed versions of carbamazepine (Tegretol® tablets). They reported that the carbamazepine co-crystal was found to have comparable chemical stability to carbamazepine form 3 (the polymorph found in Tegretol tablets), and that the physical stability of the co-crystal appeared to be similar to the anhydrous polymorph form 3. In addition, the co-crystal showed a dependence of dissolution rate on particle size above 150 μm and the resistance of the smaller particle sizes to conversion to dihydrate in aqueous suspension during the time scale of drug absorption. However, the aqueous solubility of carbamazepine has not been affected by co-

crystal formation to such a degree to completely relieve the known dissolution rate limitation of carbamazepine (Hickey et al. 2007).

With regards to marketability of a variety APIs as chloride salts is well documented, and, recently, such chloride salts, specifically fluoxetine hydrochloride has been utilized to generate co-crystals of an amine hydrochloride salt via a chloride-mediated carboxylic acid supramolecular synthon (Childs et al. 2004).

It has also been reported that polymorphism can have significant effects on pharmaceutical processing, e.g., granulation, milling and tableting. It was found that polymorph B of phenylbutazone is more ductile (plastic deformable) and tends to form stronger bonding than polymorph A, and the deformation of polymorph B was more sensitive to compression rate (Tuladhar et al. 1982).

The granulation of chlorpromazine hydrochloride with different solvents can lead to the formation of different polymorphs, and the changes in the crystal form produced different bonding properties of this drug during wet granulation (Wong and Mitchell 1992). Also, form II crystals of chlorpromazine hydrochloride take up water more easily than form I and convert to the hydrate. Consequently, tablets produced from form II were found to crack during storage, while those obtained from form I did not crack under the same storage conditions (Yamako et al. 1982).

Other studies on the tableting behavior of different polymorphic forms of carbamazepine indicated that the tablets have different hardness (Otsuka et al. 1997). It has been reported that the different yield strengths of two polymorphs of acetaminophen are due to their crystal structures (Nichlas and Frampton 1998).

1.2.5. Characterization of pharmaceutical co-crystals

Several methods exist to characterize co-crystals and excellent reviews have been published (for example X-ray powder diffraction (XRPD), Raman spectroscopy, solid-state nuclear magnetic resonance (SSNMR), differential scanning calorimetry (DSC), and scanning electron microscopy (SEM).

1.2.5.1. X-ray Powder Diffraction (XRPD)

X-ray diffraction techniques used for characterizing pharmaceutical solids include the analysis of single crystals and powders. The electrons surrounding the atoms diffract X-rays in a manner described by the Bragg equation:

$$n\lambda = 2d \sin\theta \quad (n = 1, 2, 3 \ldots) \qquad \textbf{equation 1}$$

Where

λ = x-ray wavelength

d = spacing between the diffraction planes

θ = diffraction angle

n = order of reflection

Crystal structures provide important and useful information about solid-state pharmaceutical materials. It is not always possible to grow suitable single crystals of a drug substance. In this case, X-ray diffraction of powder samples can be used for comparison of samples. X-ray diffraction peaks provide definitive proof of crystallinity in a solid. X-ray

powder diffraction (XRPD) is the analysis of powder sample. The typical output is a plot of intensity versus the diffraction angle (2θ). Ruland (1961) using internal comparison (i.e. compare amorphous and crystalline scattering) described the % crystallinity determination. Krimm and Tobosky (1951) provided more approximate methods, using external comparison, which requires the assignation of areas of the diffraction to either amorphous or crystalline scattering.

1.2.5.2. Fourier transfer Raman spectroscopy

The Raman effect was discovered in 1928, but the first commercial FT-Raman instrumentation appeared in 1988 and by the next year, FT-Raman microscopy was possible (Ferraro 1996). Raman spectroscopy has been widely used for the qualitative and quantitative characterization of polymorphic compounds of pharmaceutical interest. This solid-state vibrational spectroscopy can be used to probe the nature of polymorphism on a molecular level, and is therefore considered to be useful in instances where full crystallographic characterization of polymorphism was not found to be possible.

1.2.5.3. Thermal Analysis (TA)

Thermal analysis is defined as "a group of techniques in which a physical property of a substance is measured as a function of temperature whilst the substance is subjected to a controlled temperature programme" (Mackenzie 1979).

Thermal analysis encompasses a wide variety of techniques, including Differential Thermal Analysis (DTA), Differential Scanning Calorimetry (DSC) and Thermogravimetric Analysis (TGA) (Skoog et al. 1998). TA techniques help researchers to study and gain physical and chemical information on substances, such as thermal stability, polymer system

analysis, glass transition, purity, chemical reactions, etc. For more TA application, see Cooper and Johnson.

1.2.5.3.1. Thermo Gravimetric Analysis (TGA)

Thermogravimetric analysis is a thermal analytical technique in which the mass of a sample under a controlled atmosphere is continuously recorded as a function of temperature for a controlled temperature programme (Mackenzie 1979). Many modifications of such devices are used to determine the weight changes with heat, e.g. moisture content of tablet granulations, hydrated substances, and decomposition (Hamed 1995).

1.2.5.3.2. Differential Scanning Calorimetry (DSC)

Differential Scanning Calorimetry (DSC) is a commonly used technique that provides information about thermal changes that do not involve a change in the sample mass (Haines, 2002). Information is obtained by heating or cooling a sample alongside an external reference (an empty sample pan). In power compensated DSC the two pans are maintained at the same temperature by separate heaters and two identical platinum resistive temperature sensors are incorporated in the test chamber, one for the sample and one for the reference. As the pans are heated or cooled during the temperature scan, a differential heating rate will be required to maintain equality in pan temperature if endothermic or exothermic changes occur within the sample. This differential between the sample and the reference is transformed into an electrical signal and transformed into a thermal analysis curve. The comparative nature of this data collection means that thermal changes can be studied free from external thermal effects, i.e. variation will affect both sample and

reference sensors equally. The integral, or area, under the DSC peak is directly proportional to the heat absorbed or evolved by the thermal event (Brittain 1995).

1.2.5.4. Scanning Electron Microscopy (SEM)

In SEM, a high-energy electron beam is thermoionically emitted from a tungsten cathode and is accelerated towards an anode. One or two condenser lenses focus this electron beam. It then passes through a pair of scanning coil in the objective lens, which deflects the beam horizontally and vertically so that it scans over a rectangular area of the sample surface. The energy exchange between the electron beam and the sample results in the emission of electrons and electromagnetic radiation, which can be detected to produce an image.

1.3. Tableting

Tableting is a process in which powder particles are forced into close proximity to each other by compression, which enables the particles to cohere into a porous, solid mass of defined dimension. However, the art of compressing discrete solid particulate matter into a cohesive mass has its roots extended in history and has been practiced since the days of the ancient Egyptians. The involvement of the process in medicinal use was not developed until the mid nineteenth century when (Brockedon 1843) took out a patent for shaping pills, lozenges and black leads by pressure in a die.

Fundamental research began in the 1920s mainly in the field of powder metallurgy, but quickly spread to other disciplines as the implications become more widely realized. There are two broad lines of investigation that may be distinguished: One is the study of the distribution of forces at die and punch walls, and within compacts during compression (Fuhrer 1962; Knoechel et al. 1967; Leigh et al. 1967; Lewis and Shotton 1965; Nelson et

al. 1954; Shotton et al. 1963; Shotton and Obiorah 1960). The second line of investigation is the analysis of the relationships between the applied pressure and the resulting density of compact (Cooper and Eaton 1962; Fell and Newton 1971; Heckel 1961a; Heckel 1961b; Herssy and Rees 1970).

The force transmitted radially to the die wall was first measured by Nelson (1955) and (Windheuser et al. 1963) who cut away a section of the die wall and bonded strain gauges on it. They stated that materials, which permitted good conversion of axial to radial pressure, tend to form better tablets. A residual die wall pressure, after removal of the upper punch was found by (Higuchi et al. 1965). Several workers have reported the instrumentation of this type. They used it to record the compaction profiles of several pharmaceutical materials (Leigh et al. 1967; Long 1960).

1.3.1. Powder compaction and bonding mechanisms

The compression process takes place in a die by the action of two punches, the lower and the upper, by which the compressive force is applied. There are several stages for the formation of the compact, firstly, the rearrangement of particles followed by elastic deformation, plastic deformation and particle fragmentation (Duberg and Nystroem 1986) and cold welding with or without fragmentation (York 1978). Powder compression is defined as the reduction in volume of a powder owing to the application of a force. If these volume reduction mechanisms result in a permanent consolidation into a compact, then bonds must be formed between solid surfaces in the compact. There have been several bonding mechanisms proposed (Fuhrer 1977; Rumpf 1958). However, for tablets, three types are usually observed: (a) solid bridges formed by e.g. a melting process or recrystallization; (b) attractive forces active over a distance, i.e. intermolecular forces

(Karehill et al. 1990); (c) mechanical interlocking, depending on the shape of the particles. The surface area of the individual particles themselves changes during the compaction process. Initially, an increase in surface area is noted due to the fracture as compression forces increase. Eventually, the surface area decreases due to bonding and consolidation of particles at higher compression forces (Hiestand et al. 1977; Nelson et al. 1954).

When a loose powder bed is subjected to a constant pressure, the pressure transmitted through the bed will decrease uniformly with the distance from the source. However, when the powder is filled in a die, there are force losses due to extra forces, which the upper punch has to overcome. The major forces involved in the formation of a tablet compact are illustrated in Figure 2. These forces include die wall friction, which is dependent on powder properties; the state of compaction and the interfacial condition between powders and die wall.

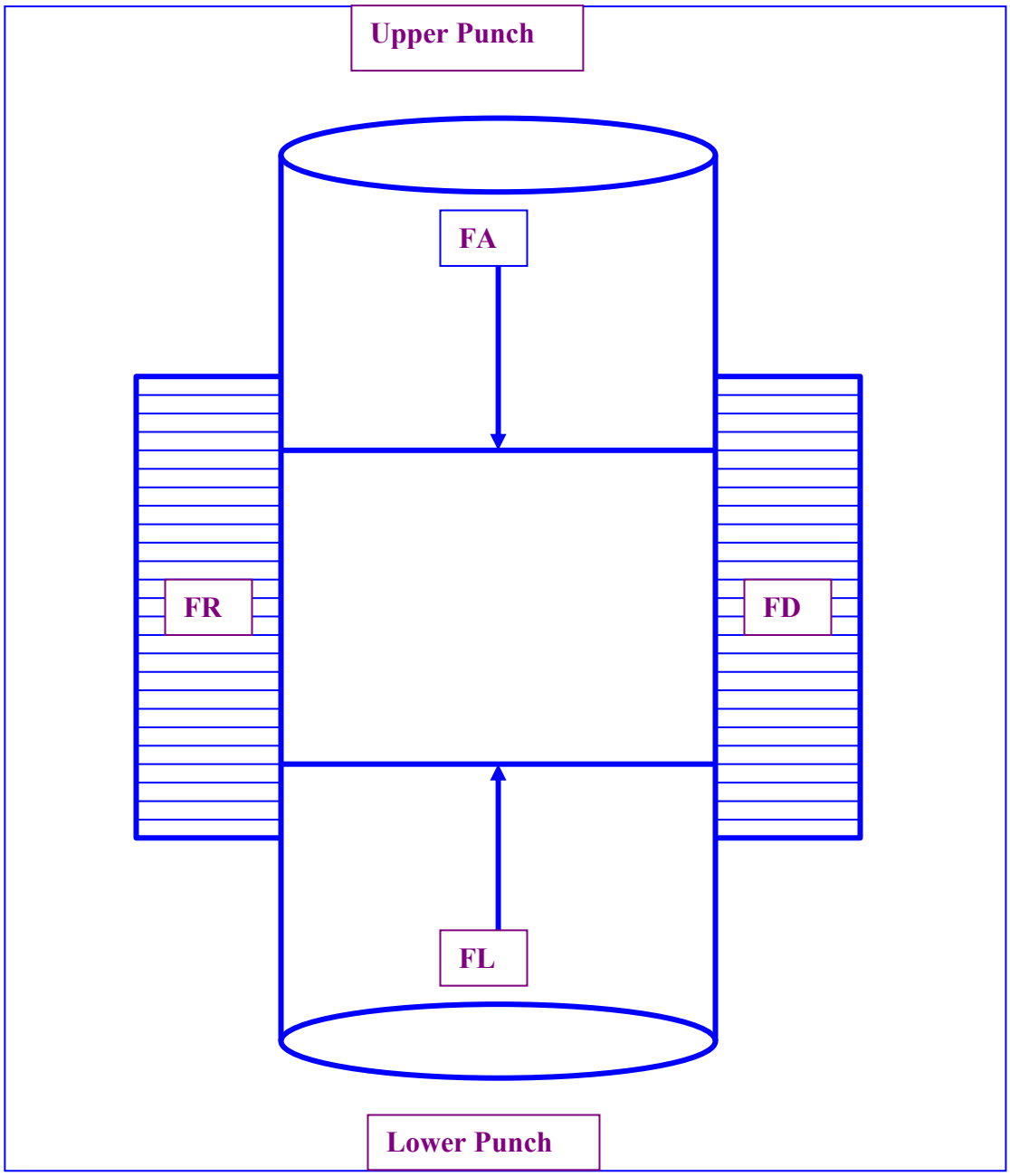

Figure 2: Forces operating on a powder during compression

Where

FA represents the axial pressure, which is the force applied by the upper punch, FL is the force transmitted to the lower punch, FD is the force lost to the die wall and FR is the radial force.

For elastic materials, the elastic strain induced by the application of a load can be recovered by unloading the materials. The change in dimension is generally attributed to the stretching of the atomic bonds and changes in the internal energy of a loaded and unloaded specimen (Stanley-Wood 1983). When a material undergoes a linear stress-strain relationship, the elastic characteristics of the material such as Young modulus and Poisons ratio can be calculated.

Plastic materials are materials, which have non-recoverable strain on unloading when loaded beyond the elastic limit. The process occurs mainly because of the sliding of atoms over each other (Stanley-Wood 1983). The plastic deformation of materials occurs non-homogeneously by means of lattice dislocation within the crystal structure of material.

1.3.2. Pressure/ volume relationship

Many equations have been proposed to account for pressure/ volume relationships during compaction (Kawakita and Ludde 1971). However, the equation developed by Heckel (1961a, 1961b) has been found particularly useful in numerous compaction studies. The Heckel equation essentially describes a first order relationship for the change in pore volume with pressure. This relationship is given by:

$\ln (1/(1-D)) = KP + A$ **equation 2**

Where D is the density of the compact relative to the absolute density of the material being compacted, P is the applied pressure (MPa), K = 1/Y where Y is the yield pressure of the material and A is a function of the original compact volume.

Some researchers have however, expressed caution when analyzing data by the Heckel equation (Rees and Rue 1978; York 1978), since the experimental conditions and methods of measurement influence the numerical values of the parameter (i.e. compressibility) derived from the analysis. Alternatively, by standardizing the experimental procedures it is possible to use the data to compare the compaction behaviour of materials.

When analyzing the compaction properties according to the Heckel relationship, two types of behaviour can be described (Herssy and Rees 1970). Type A was observed for particles with bulk density dependant on the initial particle size. The densification was due to particle rearrangement or slippage, followed by plastic deformation. On the other hand, type B was observed for materials that have higher yield pressures and undergo consolidation by initial fragmentation to form consistent packing followed by plastic deformation. These materials mainly do not maintain the initial bulk density difference due to particle size variation. York and Pilple (1973) distinguished Type C, which shows a very rapid approach to a limiting density for materials with very low yield pressures.

1.3.3. Evaluation of tableting properties

A number of terms and parameters are used to evaluate the tableting behaviour of powders (Joiris et al. 1998). These parameters represent an effective means to describe the compaction properties and enable comparisons of different powder batches.

1.3.3.1. Compressibility

Compressibility is defined as the ability of a material to undergo a reduction in volume as a result of an applied pressure (Joiris et al. 1998). Compressibility describes how a powder bed undergoes volume reduction under compaction pressure. It is calculated from a plot

showing the decrease in tablet porosity with increasing compression force. The lower the compaction pressure at a given compaction force, the better is the compressibility and greater is the interparticulate bonding area in a tablet.

1.3.3.2. Compactibility

Compactibility is defined as the ability of a material to produce tablets with sufficient strength under the densification (Joiris et al. 1998). In many cases, the tensile strength decreases exponentially with increasing porosity (Ryshkewitch 1953). It is interpreted by calculating the tensile strength that is normalized by tablet porosity. By extrapolating the tensile strength to zero porosity, the compactibility plot will indicate the interparticulate bonding strength that may be related to intermolecular/ interionic interaction (Roberts et al. 1991).

1.3.3.3. Tabletability

Under the effect of compression force, the tabletability is the capacity of a powder to transform into a tablet of specified strength. It indicates the effectiveness of the applied pressure in increasing the tensile strength of the tablet (Joiris et al. 1998). Compressibility also describes the relationship between the cause, the compression pressure, and the result, which is the strength of the compact.

1.3.4. Selection of model drugs and co-crystal systems

In this thesis, several model drugs/ co-crystal agents were studied. These were:

1. Urea/ 2-MB

2. Caffeine/ malonic acid
3. Caffeine/ oxalic acid
4. Theophylline/ malonic acid

1.3.4.1. Urea/ 2-methoxybenzamide (2-MB) system

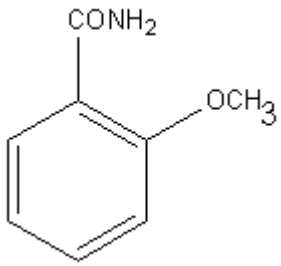

2-MB

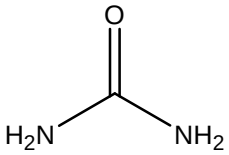

Urea

Figure 3: Chemical structures of 2-MB and urea.

Previous reports have been already established on equimolar complex formation of urea with 2-methoxy-benzamide (2-MB). Complex formation of urea and 2-MB was achieved both by a co-grinding technique and by a co- precipitation method (Moribe et al. 2006). It has been reported that in the urea/2-MB complex, not only show an intermolecular hydrogen bond between urea and 2-MB but also a hydrogen bond network between urea molecules is present and takes part in the overall assembly of the complex. Complexation results in an overall change in conformation. The molecular arrangement of the compound was characterized using the single crystal X-ray diffraction method, and the conformational change of guest molecules has been reported in terms of intramolecular hydrogen bond length and the dihedral angles (Moribe et al. 2006). It has also been reported that the basicity and symmetrical location of amines in guest molecules could be a crucial factor for

the formation of either a corrugated or a laminar structure. It was found that in case of the conventional urea inclusion complexes, a three dimensional hydrogen bonded array of urea formed hexagonal channels with an internal diameter of 5.5-5.8 Å, within which organic molecules such as n-alkenes (Takemoto and Sonoda 1984), fatty acids (Brandstaetter and Burger 1997), and polymer (Rusa et al. 2002) were densely packed through Van der Waals forces. Most of the urea inclusion complex exhibited incommensurate structural properties (Harris and Thomas 1990) (Penner et al. 1992). However, α, ω-dinitriles, di- and tricarboxlic acids have been reported to form specific co-crystals with urea molecules (Videnova-Adrabinska 1996).

1.3.4.2. Caffeine/ malonic and oxalic acid systems

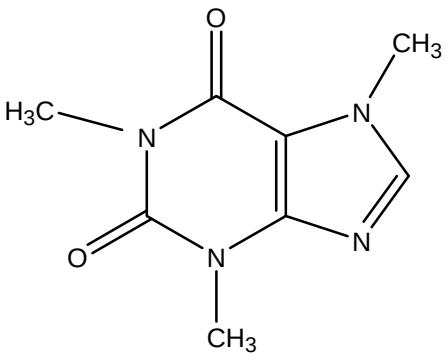

Caffeine

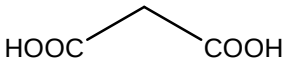

Malonic acid

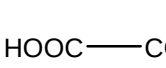

Oxalic acid

Figure 4: Chemical structures of caffeine, malonic acid and oxalic acid.

Caffeine is a central nervous system stimulant and smooth muscle relaxant. It is widely employed as a formulation additive to analgesic remedies. As a model pharmaceutical compound, caffeine is known to exist as two anhydrous crystal forms (α, β) and one

crystalline nonstoichiometric hydrate (Bothe and Cammenga 1980). At high temperature the stable anhydrous β- caffeine crystal form converts to the metastable caffeine (Lehto and Laine 1998). The nonstoichiometric crystalline hydrate of caffeine was found to contain 0.8 moles of water per mole of caffeine which might result from a channel inclusion of water in the hydrate crystal structure (Edwards et al. 1997). The α or β crystalline form of caffeine converts to caffeine hydrate at high relative humidity. Conversely, caffeine hydrate loses its water of hydration at low relative humidity and reverts to β-caffeine (Pirttimaeki and Laine 1994). This hydration behaviour of caffeine has been a challenge to develop this model drug substance into a marketed form and requires a synthesis of a crystalline salt form to enhance its physical properties. However, the only one pharmaceutically acceptable salt form of caffeine revealed by the CSD is a hydrochloride dehydrate (Mercer and Trotter 1978). It seems, however, that the stable anhydrous, pharmaceutically acceptable form of caffeine is not yet known (Stahl and Wermuth 2002). The limited salt forming capability of caffeine is behind the reason for reporting structure of only one pharmaceutically acceptable caffeine. The suitability of co-crystallisation of caffeine in its neutral form has been based on its weak basicity as imidazole nitrogen of caffeine results in a pKa of 3.6. It has already been published that caffeine can form 12 neutral organic co-crystals, including, complexes of caffeine with sulfacetamide (Leger et al. 1977), sulfaproxylline (Ghosh et al. 1991), a co-crystal of caffeine with the sedative barbital (Graven and Gartland 1974) and two other not acceptable co-crystals of caffeine with unionized aromatic carboxylic acids. Recently, a number of co-crystals of caffeine with dicarboxylic acids has been reported, i.e. oxalic acid, malonic acid, maleic acid and glutaric acids (Trask et al. 2005a). For our study, we selected malonic acid and oxalic acid to co-crystallize with caffeine (Figure 4).

1.3.4.3. Theophylline/ malonic system

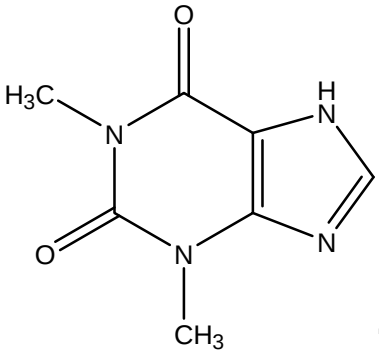

Theophylline

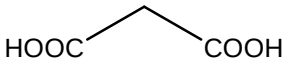

Malonic acid

Figure 5: Chemical structures of theophylline and malonic acid.

Theophylline is a drug used for respiratory treatment. From a physicochemical point of view, the formulation of theophylline represents a challenge because of its interconversion between crystalline anhydrate and monohydrate forms as a function of relative humidity (RH). This interconversion complicates the design of a consistent, reproducible formulation process (Kahnkari and Grant 1995). The reversible hydrate formation causes a stability problem across a range of common processing conditions. It indicates that neither the anhydrate nor the hydrate may be fully stable as reported by several researchers (Hermann et al. 1988; Otsuka and Kaneniwa 1988; Shefter et al. 1973; Suzuki et al. 1989). Theophylline has been found to form a number of co-crystals with guest compounds, including, 5-chlorosalicylic acid, urea, sulfathiazole, phenobarbital, p-nitrophenol, N-2-aminoethyl-carbamate, 5-fluorouracil and water. Recently, co-crystals of theophylline with dicarboxylic acids including: oxalic acid, malonic acid, maleic acid and glutaric acids were

reported (Trask et al. 2005a). For our study, we selected malonic acid and oxalic acid to co-crystallize with theophylline (Figure 5).

1.3.5. Aims and objectives

The aim of this thesis was to investigate the factors that affect the production of co-crystals with enhanced physico-chemical properties including compressibility, compactibility and processability. Moreover, pharmaceutical co-crystals represent a promising area of research and offer a genuine opportunity to enhance the formulation of a compound, optimize the product performance and to improve marketed products.

Objectives of this thesis are:

1. To study the effect of co-processing drug and excipient mix on the crystallographic and solid-state properties and behaviour using model drug substances and different co-crystal formers.

2. To explore the manipulation of the solid-state properties of co-crystals through different methods such as dry and wet grinding and co-precipitation.

3. To investigate any possible crystal transformation during compression and convection mixing.

4. To examine the impact of additives, namely microcrystalline cellulose (MCC) and α-lactose monohydrate on the crystallinity, formation of co-crystals and stability.

5. Finally, the subsequent effect of the modification of the solid-state properties of the model drug on the overall mechanical and deformational characteristics of the compact has also been explored.

1.3.6. Thesis structure

This thesis is structured as follows:

Chapter 1 gives an intensive and detailed introduction about engineering of co-crystals, their groups and classes, methods of preparation, characterizations, and use in the drug formulation. This chapter also introduces the tableting process, bonding mechanisms as well as parameters used to evaluate the tableting behaviour of the co-crystals and the physical mixtures. In addition, reported molecular chemistry, chemical structures and uses of the selected systems have also been introduced.

Chapter 2 describes the materials, material processing, mixing and compaction procedures as well as the analytical techniques used throughout the thesis.

Chapter 3, Chapter 4, Chapter 5 and Chapter 6 presents respectively, the solid-state characterization of urea/ 2-MB, caffeine/ malonic acid, caffeine/ oxalic acid and theophylline/ malonic acid systems and evaluate the effect of co-crystallization by both grinding and precipitation on the compaction and deformational properties.

Chapter 7 examines the impact of additives (α-lactose monohydrate and MCC) on the crystallinity, phase transformation and molecular structure of an in situ co-crystals and subsequent tableting behaviour.

Chapter 8 presents out finding of co-crystal formation of urea/ 2-MB and caffeine/ malonic acid systems during compression using both the Compaction Studies Simulator the IR-Press.

Chapter 9 presents out finding of co-crystal synthesis of urea/ 2-MB systems through convection mixing and investigates the mechanisms of the phase transformation using different analytical techniques.

Chapter 10 discusses and concludes the results given in the previous chapters and gives suggestions for future work.

2. Methodology

2.1. Materials

All materials used in this study are given in Table 1.

Table 1: Materials selected for study.

Material	Purity	Product number	Company
Urea	98%	A 12360 or L05020	Alva Aesar Avocado & Lancaster
2-methoxybebnzamide	98%	A12520 or L05588	Alva Aesar Avocado & Lancaster
Caffeine	100%	A 12360 or L05020	Alva Aesar Avocado & Lancaster
Theophylline	100%	A12520 or L05588	Alva Aesar Avocado & Lancaster
Oxalic acid	98%	58-93-5	Sigma-Aldrich Company Ltd. (United Kingdom)
Malonic acid	98%	62517-86-2	Sigma-Aldrich Company Ltd. (United Kingdom)
α-lactose monohydrate	98%	5989-81-1	Sigma-Altra Company Ltd. (United Kingdom)
Microcrystalline cellulose	98%	9288	Edward Mendell Co., Inc. New York

2.2. Material processing

2.2.1. Preparation of a mixture of urea and 2-MB by co-precipitation

2-MB (1.6 g) was dissolved in 40ml ethanol and heated to 60 ^{0}C. After the addition of 0.8 g of urea, the solution was stirred for 10 min. Then the solution was stored at 25 ^{0}C for 24 h

to obtain the crystals. The precipitated product was collected on a filter paper and dried at room temperature for 24 h.

2.2.2. Preparation of co-ground mixture of urea and 2-MB

Firstly, 0.8 g of 2-MB was added to 0.4 g of urea. The mixture was co-ground with a pestle and mortar for 2 min. Then 0.5 ml of water was added to the mixture. The wet mixture was co-milled gently for 20 min. After that the co-ground mixture was collected on a filter paper and dried at room temperature for 24 h.

2.2.3. Preparation of physical mixture of urea and 2-MB

Urea was physically mixed with 2-MB at molar ratio of 1:1 in a glass vial and shaken by hand for 20 min.

2.2.4. Preparation of a (2:1) caffeine/ oxalic acid co-crystal by co-grinding

Caffeine (0.38g) was added to oxalic acid (0.89g) in a glass mortar and co- ground with 0.5 ml methanol using a pestle for 30 min. The ground mixture then collected on a filter paper and stored at room temperature for 24 h.

2.2.5. Preparation of a (2:1) caffeine/ oxalic acid co-crystal by co-precipitation

Caffeine (4.85g) and oxalic acid (1.12g) were dissolved in 7:2 (v/v) chloroform- methanol (90 ml) and heated to 50 ^{0}C. The solution was removed from heat and allowed to cool at ambient temperature. The precipitated solids were filtered, collected on a filter paper and dried at room temperature for 24 h.

2.2.6. Preparation of the physical mixture of caffeine/ oxalic acid

Caffeine was physically mixed with oxalic acid at molar ratio (2:1) in a glass vial and shaken by hand for 20 min.

2.2.7. Preparation of a (2:1) caffeine/ malonic acid co-crystal by co-grinding

Caffeine (0.30g) was added to malonic acid (0.81g) in a glass mortar and co- ground with 0.5 ml methanol using a pestle for 30 min. The ground mixture was collected on a filter paper and stored at room temperature for 24 h.

2.2.8. Preparation of a (2:1) caffeine/ malonic acid co-crystal by co-precipitation

Caffeine (1.43g) and malonic acid (0.38g) were dissolved in 7:2 (v/v) chloroform-methanol (90 ml) and heated to 50 ^{0}C. The solution was removed from heat and allowed to cool at ambient temperature. The precipitated solids were filtered, collected on a filter paper and dried at room temperature for 24 h.

2.2.9. Preparation of physical mixture of caffeine and malonic acid

Caffeine was physically mixed with malonic acid at molar ratio of 2:1 in a glass vial, and shaken by hand for 10 min.

2.2.10. Preparation of a (1:1) theophylline/ malonic acid co-crystal by co-grinding

Theophylline (149mg) was added to malonic acid (86mg) in a glass mortar and co- ground with 0.5 ml methanol using a pestle for 30 min. The ground mixture was collected on a filter paper and stored at room temperature for 24 h.

2.2.11. Preparation of a (1:1) theophylline/ malonic acid co-crystal by co-precipitation

Theophylline (587mg) and malonic acid (339mg) were dissolved in a mixture of 40 ml chloroform and 2ml methanol (50 ^{0}C). The solution was removed from heat and allowed to cool to ambient temperature. The precipitated solids were filtered, collected on a filter paper and dried at room temperature for 24 h.

2.2.12. Preparation of a physical mixture of theophylline and malonic acid

Theophylline was physically mixed with malonic acid at molar ratio of 1:1 in a glass vial and shaken by hand for 10 min.

2.2.13. Addition of MCC and α-lactose monohydrate to the co-ground mixture of urea and 2-methoxy-benzamide

100 mg of a co-ground mixture of urea/2-MB (Section 2.2.2) (prepared at molar ratio 1:1) was added to 150 mg of MCC and 100 mg of α-lactose monohydrate in a glass vial and shaken by hand for 10 min.

2.2.14. Addition of MCC and α-lactose monohydrate to the co-ground of caffeine and malonic acid

100 mg of a co-ground mixture of caffeine/malonic acid (Section 2.2.18) (prepared at molar ratio 2:1) was added to 150 mg of MCC and 100 mg of α-lactose monohydrate in a glass vial and shaken by hand for 10 min.

2.2.15. Addition of MCC and α-lactose monohydrate to the co-precipitated mixture of urea and 2-methoxy-benzamide

100 mg of a co-precipitated mixture of urea/2-MB (Section 2.2.1) (prepared at molar ratio 1:1) was added to 150 mg of MCC and 100 mg of α-lactose monohydrate in a glass vial and shaken by hand for 10 min.

2.2.16. Addition of MCC and α-lactose monohydrate to the co-precipitated mixture of caffeine and malonic acid

100 mg of a co-precipitated mixture of caffeine/malonic acid (Section 2.2.19) (prepared at molar ratio 2:1) was added to 150 mg of MCC and 100 mg of α-lactose monohydrate in a glass vial and shaken by hand for 10 min.

2.2.17. Addition of MCC and α-lactose monohydrate to the physical mixture of urea and 2-methoxy-benzamide

100 mg of a physical mixture of urea/ 2-MB (Section 2.2.3)(prepared at molar ratio 1:1) was added to 150 mg of MCC and 100 mg of α-lactose monohydrate in a glass vial and shaken by hand for 10 min

2.2.18. Addition of MCC and α-lactose monohydrate to the physical mixture of caffeine and malonic acid

100 mg of physical mixture of caffeine/ malonic acid (Section 2.2.20) (prepared at molar ratio 2:1) was added to 150 mg of MCC and 100 mg of α-lactose monohydrate in a glass vial and shaken by hand for 10 min.

2.3. Compaction procedures

Tablet compactions were performed using a Compaction Studies Press (Caleva Process Solutions Ltd) (Figure 6) and crushing values were obtained using a Schleuniger Hardness Tester Type 4M (Copley Instrument). The thickness and diameter of the tablets were measured using an ID-C Digimatic Indicator (Mitutoyo Corporation).

The die wall of the press was cleaned with acetone and pre-lubricated with magnesium stearate before each compression. An average powder weight of 350 ± 5 mg was used to make each tablet, with the initial compaction load for both speeds studied (10 mm sec^{-1} and

100 mm $sec^{-1)}$ set at 5000N. The compaction load was then increased incrementally by 2500N until a maximum crushing value was obtained. The compaction behavior of the two co-crystals (co-ground –and co-precipitated mixtures) and the physical mixture was evaluated by means of crushing strength measurement of the compact. A graph of crushing strength versus compaction force was then produced for each co-crystal. Experiments were performed in triplicate. The compact tensile strength (Ts) was calculated by the following equation (Fell and Newton, 1970):

$$\mathbf{Ts = 2F/\pi DT} \qquad \textbf{Equation 3}$$

Where F is the compact hardness (N), D and T are the diameter and thickness of the compacts (mm), respectively.

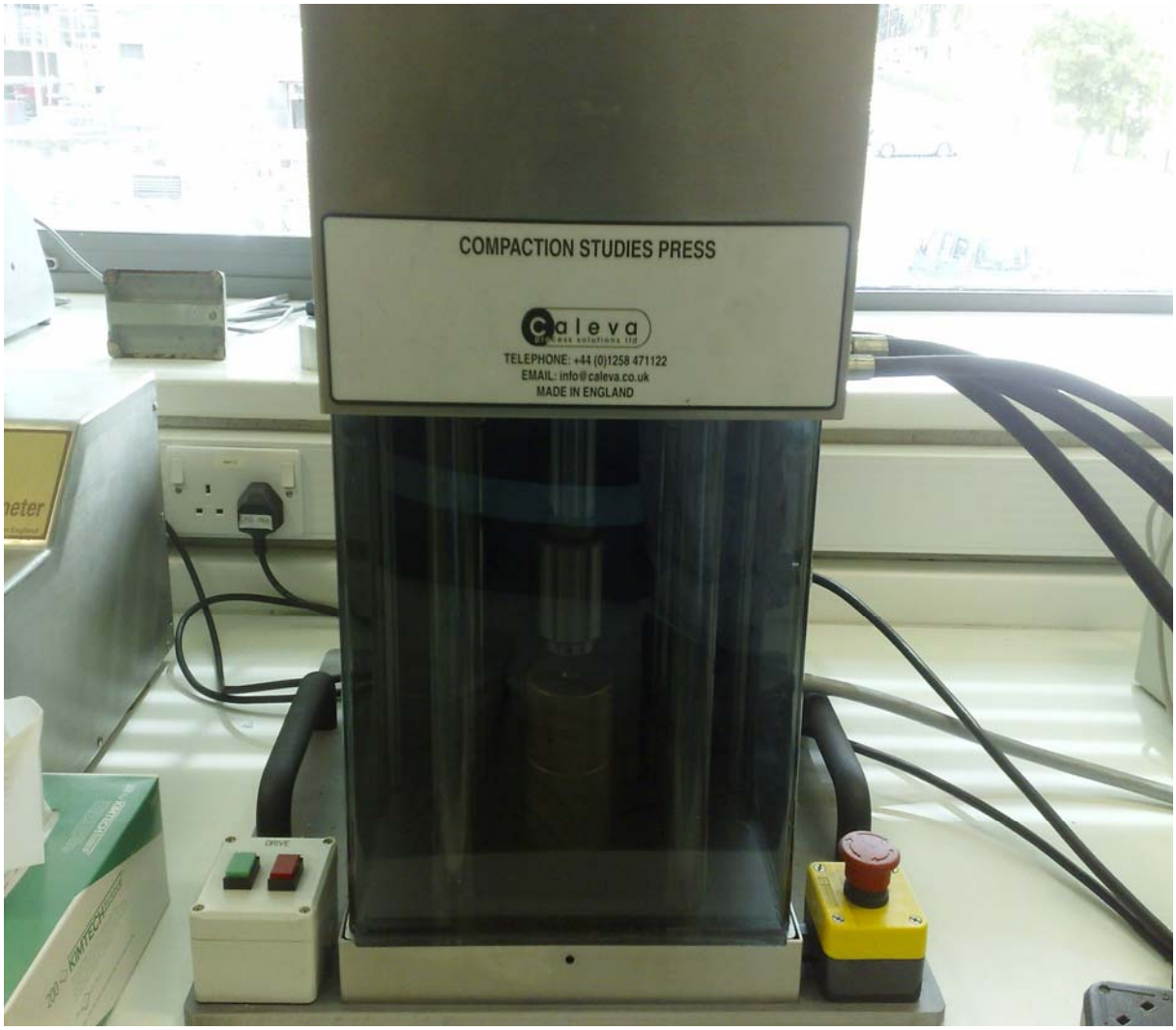

Figure 6: Caleva Compaction Studies Press (Caleva Process Solution Ltd.).

2.3.1. Pycnometric Density Determination

Helium Pycnometry

True density determinations were carried out using a Micromeritics AccuPye 1330 Gas Pycnometer (Micromeritics Limited, UK). The instrument was initially calibrated using a spherical metal standard of known volume. The volume of the empty vessel was calculated by filling with helium gas at a fixed pressure and allowed to equilibrate. This sample vessel was then filled two-thirds full with sample and weighed. The filled sample vessel was pressurized by helium gas and allowed to re-equilibrate. The change in volume between empty and sample vessel at same pressure was measured. The calculated volume of gas displaced by sample at a given pressure was divided by the mass of sample to measure true density of the material.

2.3.2. Bulk density

The bulk density of each co-crystal was determined as follows: A 0.5g quantity of sample was poured into a size graduated measuring cylinder and the initial bulk volume has been taken to calculate the initial bulk density D_0 (also known as fluff or poured bulk density). The powder contained in the measuring cylinder was then mechanically tapped and the final volume read and used to calculate the final bulk density D_f (also known as equilibrium, tapped or consolidated bulk density).

2.3.3. Measurement of elastic and plastic energy

The typical punch stroke against upper punch force is illustrated in Figure 7 where A is maximum punch force, B is punch stroke when punch force is zero, C is punch stroke when punch force is maximum, D is punch stroke after decompression when punch force is zero again. The area of ABC shows the gross energy, and the area of ABD and ADC is plastic

energy and elastic energy, respectively. These areas were calculated for the samples compacted.

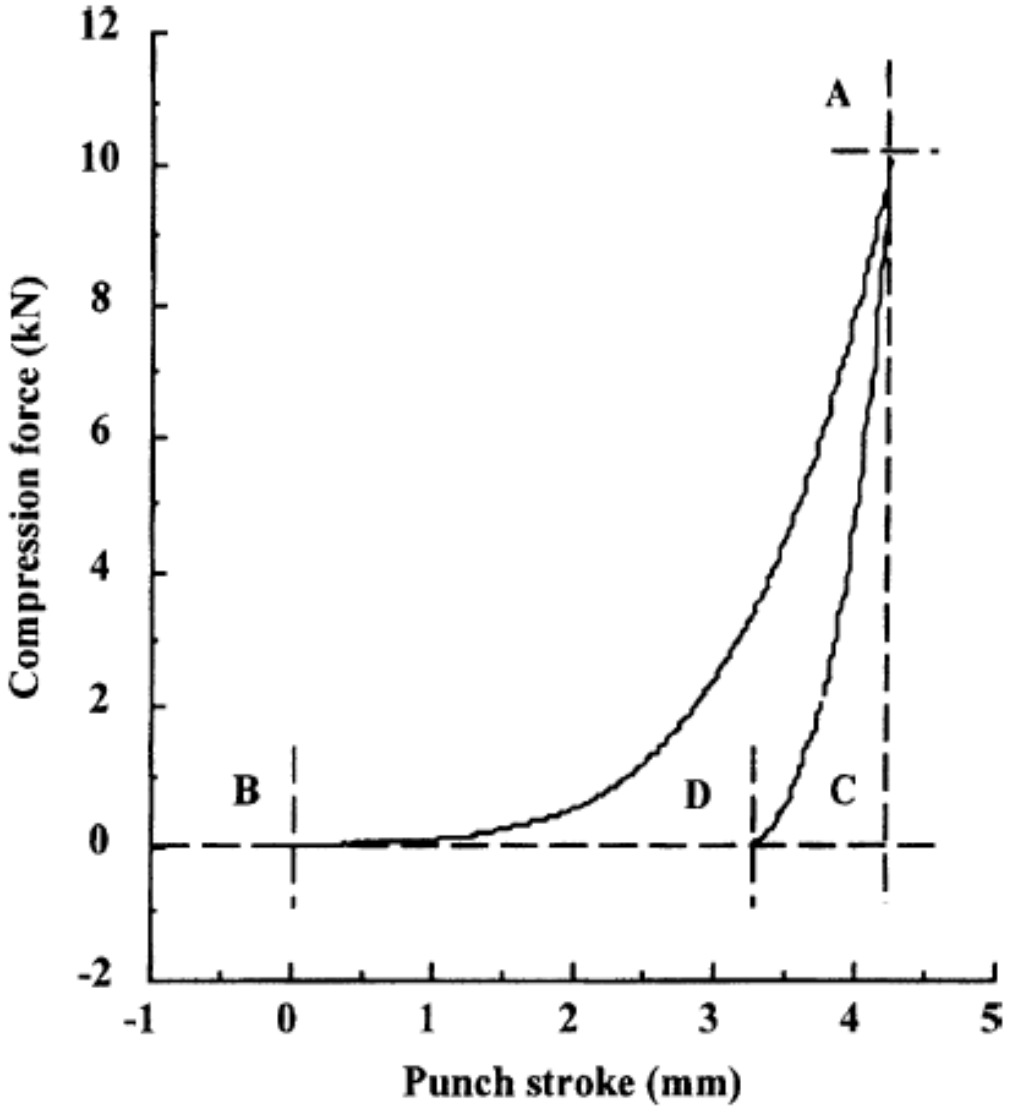

Figure 7: Typical force/ displacement curve generated by Caleva Compaction Studies press.

2.3.4. Analysis of the elastic recovery of the tablets

Elastic recovery E is defined as the fractional increase in tablet thickness after decompression due to immediate elastic relaxation of the tablet. The parameter E is calculated according to equation 4: (Armstrong and Haines-Nutt 1974).

$$E = (t_2 - t_1)/ t_1 \text{ X } 100 \qquad \text{Equation 4}$$

Where t_1 is the minimal thickness of the powder bed in the die and t_2 is the thickness of the recovered tablet. This parameter was calculated for the samples compacted.

2.3.5. Heckel analysis of compaction data

The thickness of the compact during the single compaction event was plotted as a function of the compression pressure applied by the upper punch. The obtained data was analyzed by the following equation (Heckel, 1961a and Heckel, 1961b).

$$\ln (1/ (1-D) = kP + A \qquad \text{Equation 5}$$

Where D is the relative density, the ratio of the compact density, at an applied pressure P, to true density of powder, and k and A are constants. Value of k and A were obtained from the linear portion of the Heckel plot, over a range of compression pressures from 20 to 50 MPa (Figure 8). The reciprocal of k is the yield pressure, the total densification of powder bed after particle rearrangement, D_A, was calculated from the extrapolated intercept (A), D_0 is the initial densification after filling of die, and D_B is calculated by subtracting D_0 from D_A.

The Heckel plot (Figure 8) describes five regions, namely:

Region 1 represents the densification phase in which the orientation of powder particles occurs.

Region 2 represent the true compression phase in which the bondings and the plastic deformation take place. The slope in this region is used to calculate the deformation of powder.

Region 3 starts at the maximum compression force and ends at the dead point of the upper punch in the die.

Regions 4 and 5 represent the decompression phase, where the upper punch loses its contact with the tablet at Region 5, and its force gets back to zero.

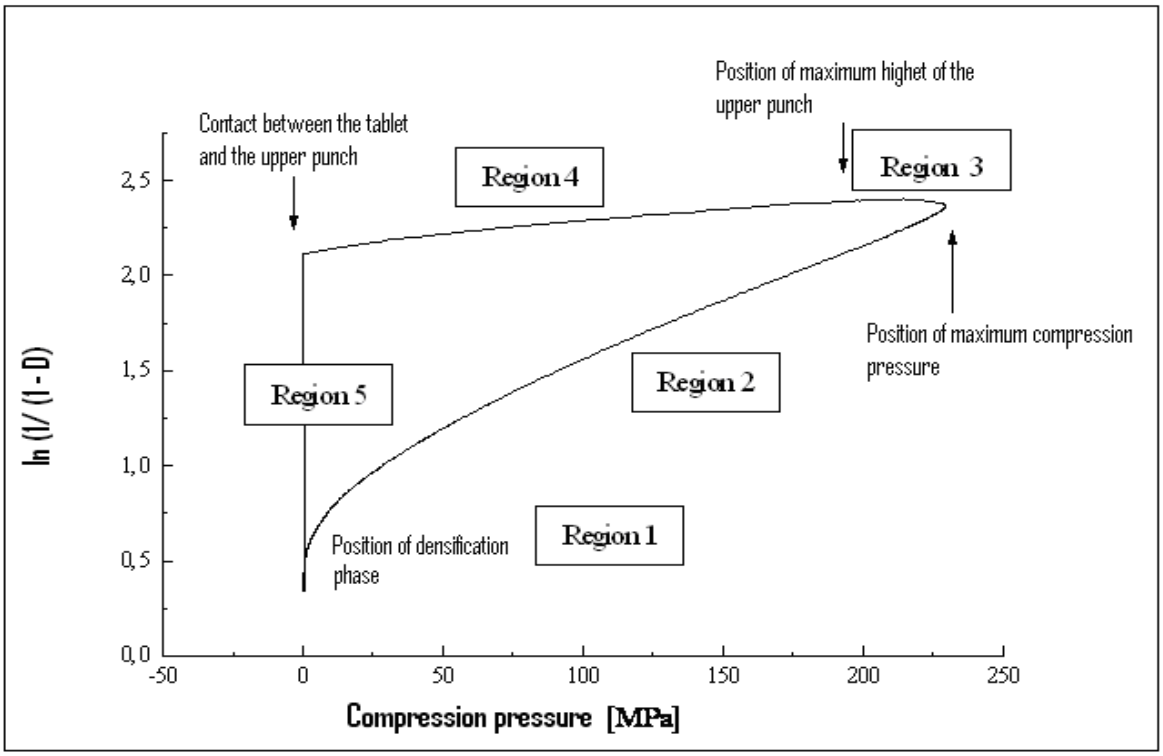

Figure 8: Densification regions in Heckel adapted from Morris L.E. and Schwartz, J. (1995).

2.4. Mixing procedures

2.4.1. Milling of Individual materials (urea, 2-MB, caffeine, and malonic acid)

7 g of each material was ground individually using a mortar and pestle for 30 min.

2.4.2. Particle size separation of individual materials by sieving

Sieving was performed using sieves from Endcotts Ltd., (London England). Each individual ground material was separated into three-size fractions 20- 45µ, 75- 125µ, and 180- 250µm using a sieve nest connected to a mechanical vibrator. Sieving time for each material was 35 min.

2.4.3. Mixing of urea/ 2-MB system (1:1 molar ratio)

0.8 g of each 20- 45µm, 75-125µm and 180- 250µm size fraction of 2-MB was added to 0.4g have 20- 45µm, 75-125µm, and 180- 250µm fractions of urea in glass vials, respectively. Each of the glass vials was sealed with tissues and put in a plastic container. The glass container was then placed on to the roll mixer (Pascall Engineering Co. Ltd. England). The samples for X-ray diffraction were taken after 30 min, 1h, 2h, 4h, 8h, 12h, 24h, 2 days, 4 days, 10 days and 14 days.

2.4.4. Mixing of caffeine/ malonic acid system (2:1 molar ratio)

1.43g of each 20- 45µ, 75-125µ, and 180- 250µm fractions of caffeine were added to 0.38g of 20- 45µ, 75-125µ and 180- 250µm size fractions of malonic acid in glass vials, respectively. The mixtures were sealed and treated as in the previous section (2.4.3).

Figure 9: Roll mixer (Pascall Engineering Co. Ltd. England).

2.5. Analytical techniques

2.5.1. X-ray Powder Diffraction (XRPD)

The Bruker D-8-X-ray diffractometer was used to obtain XRPD spectra for samples at room temperature. Powder samples were placed into a sample holder and leveled using a glass cover slide. Samples were scanned over 5-50° 2θ at a rate of 1° 2θ/ min by a copper Ka radiation source of wavelength 1.542Å with 1mm slits. The simulated patterns of the co-crystal have been calculated from CSD using CanQuest 1.10 software.

2.5.2. Fourier Transform Raman spectroscopy

Fourier-transform Raman spectroscopy was carried out using a Bruker IFS 66 instrument with an FRA 106 Raman module attachment and a Nd^{3+} /YAG laser operating at 1064 nm in the near infrared. The powdered specimens were examined in aluminum cups. The spectra were recorded at 4 cm^{-1} spectral resolution and 500 spectral scans accumulated to improve signal-to-noise ratio. Laser powers were maintained at 200 mW for the sample.

2.5.3. Thermo Gravimetric Analysis (TGA)

The TGA module (Q 5000, TA Instruments Iimited, Crowley, UK) was employed to study sample weight loss on heating. Samples weighing 5-20mg were placed onto an open platinum pan. This pan was weighed by the microbalance (accuracy ± 1µg), which is inside the instrument. Samples were heated over a predetermined temperature range at a heating rate of 10 ^{0}C/ min. and changes in sample weight were monitored by the microbalance. The temperature axis of the TGA was calibrated with a ferromagnetic standard.

2.5.4. Differential Scanning Calorimetry (DSC)

DSC profiles were obtained using a calorimeter (Q2000, TA Instruments limited, Crawley, UK) with a refrigerated cooling accessory. The instrument was calibrated with pure indium and zinc standards at the heating rates of interest. Samples weighing between 1-10mg were accurately weighed into an aluminum pan and an aluminum lid crimped onto the pan (closed system with a pin-hole). The samples were heated in an atmosphere of dry nitrogen at a heating rate of 10 ^{0}C/ min. over a predetermined temperature range. The energy (heat flow) required maintaining the contents of the sample pan (accuracy 0.1mW) at the same temperature as an identically prepared empty reference pan was measured.

2.5.5. Scanning Electron Microscopy (SEM)

Scanning electron microscopy of all samples was carried out using a Quanta 400 SEM (FEI Company, Cambridge, UK).

2.5.6. Hot-Stage Microscopy (HSM)

Microscopy was performed on a Zeiss Axioplan-2 microscope using a Linkam 44 hot stage (THMS600). Data were visualized using Axiovision (4.5) software with the linksys 32 patches for hot stage control. Contact thermal microscopy was conducted by heating from room temperature using a 1 °C/ min heating rate and discontinued on the melting of all material.

2.5.7. Moisture Sorption Isotherm

The samples were firstly prepared by milling the materials using a mortar and pestle. The freshly milled samples were then taken for the analysis of the moisture sorption isotherm. Moisture sorption isotherms were obtained using a Hiden IGAsorp Moisture sorption Analyzer HAS-036-080 (Hiden Analytical Limited. Warrington, Cheshire, UK). The temperature of the sample chamber was maintained at 25 °C using a R2 Hiden water bath (Grant Instruments, Cambridgeshire, UK.). The sample pans were tarred to zero before the sample was loaded. The isotherm programme analyzed the sample over the 0%RH to 95%RH range with steps of 10%RH for each equilibration and included a drying stage. For the desorption isotherm the experimental run was repeated in reverse.

3. Co-crystallization of urea/ 2-MB by co-grinding and co-precipitation methods: Evaluation of tableting properties

3.1. Introduction

Urea is known to form clathrates or host-guest complexes and can be regarded as a promising candidate to form co-crystals. As mentioned earlier in the first chapter, urea was found to form an equimolar complex with 2-methoxybenzamide (2-MB) as well as with other molecules such as α, ω-dinitriles, di- tricarboxylic acids (Videnova-Adrabinska 1996). The commonly used method to prepare urea/ 2-MB co-crystals is the co-precipitation methods. However, in this project, grinding methodology was also used because of its advantages over other techniques. It is an easier preparation method and the use of large amount of solvent can be avoided or minimized. In this study, we prepared urea/ 2-MB co-crystals by wet grinding at molar ratio 1:1 using mortar and pestle for 20 min. as well as co-precipitation at the same molar ratio (1:1).

In the urea/ 2-MB complex, the contribution of an intermolecular hydrogen bond between urea and 2-MB, as well as a hydrogen bond network between urea molecules, has been reported (Moribe et al. 2006). The characterization of the molecular arrangement of the compound has been carried out using the single crystal X-ray diffraction method, and the conformational change of guest molecules was tested in terms of intramolecular hydrogen bond length and the dihedral angles (Moribe et al. 2006).

In this chapter, the urea/ 2-MB co-crystal was prepared by grinding and co-precipitation (using the methods outlined in sections 2.2.1 and 2.2.2). The solid-state of this system was characterized using XRPD, Raman spectroscopy, DSC and SEM. After the

characterization, the effect of the co-crystallization on the tableting behaviour has been investigated.

3.2. Results and discussion

3.2.1. XRPD of a urea/ 2-MB co-crystal prepared by two methods

The XRPD patterns of urea/ 2-MB system are presented in Figure 10.

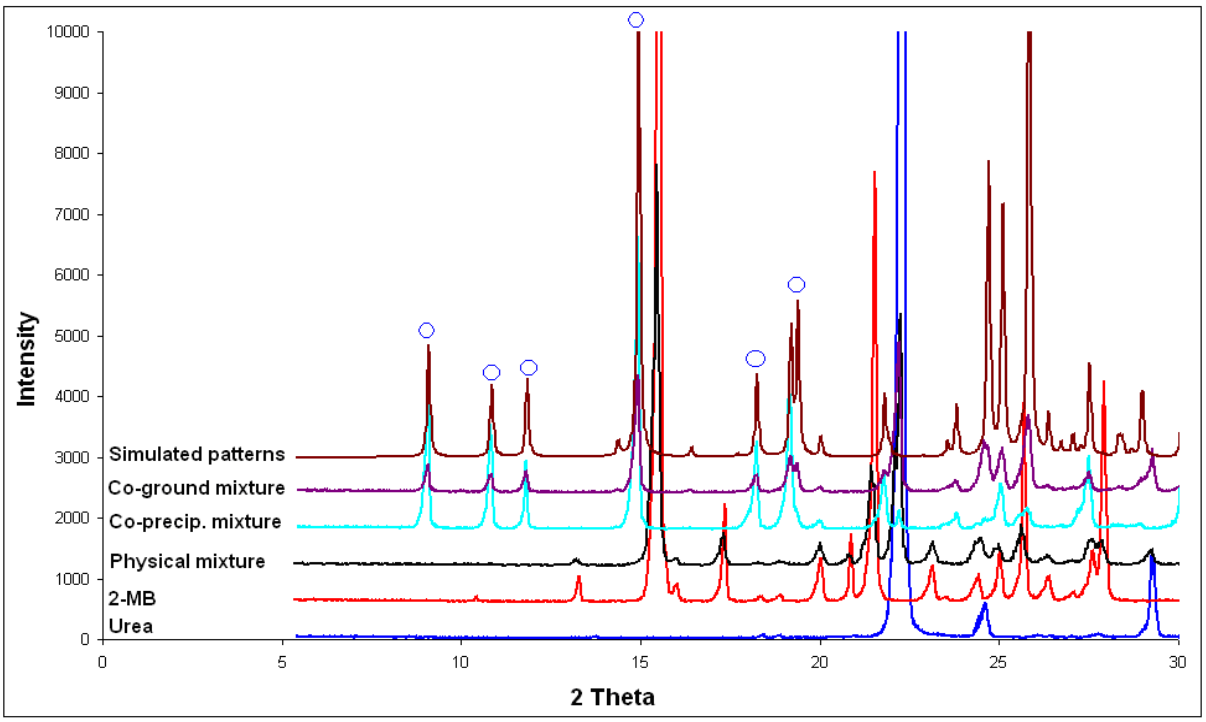

Figure 10: PXRD patterns of urea/ 2-MB systems (Simulated patterns = patterns calculated from CSD using CanQuest 1.10 software).

When urea was co-ground with 2-MB at a ratio of (1:1), new PXRD peaks at 2θ = 9.0 °, 10.8 °, 11.8 °, 14.9 °, 18.2° and 18.9 ° were observed as shown in (Figure 10). It is obvious that the peak positions of the new peaks are different from those of the physical mixture,

indicating that urea may have formed a co-crystal with 2-MB. For the co-precipitation of urea and 2-MB at molar ratio (1:1) with ethanol, the PXRD patterns (Figure10) show new peaks similar to those obtained from the co-ground mixture. These results are in agreement with results already published by Moribe and co-workers (2006) for the co-precipitated product. They found that 2-MB formed N3-H5…O3 intramolecular hydrogen bonding (2.66 Å) and interacted with urea through N3-H6…O1 (3.001 Å), N1-H1…O2 (3.022 Å) and N2-H3…O2 (3.032 Å) along the **a** axis. On the other hand, urea molecules interacted each other through N2 - H4…O1 (2.978 Å) and N1- H2…O1 (2.997 Å) hydrogen bondings to form extended polymeric structure using 8-membered hydrogen-bonded ring motifs (Moribe et al. 2006), as shown in Figure 11 and Figure 12.

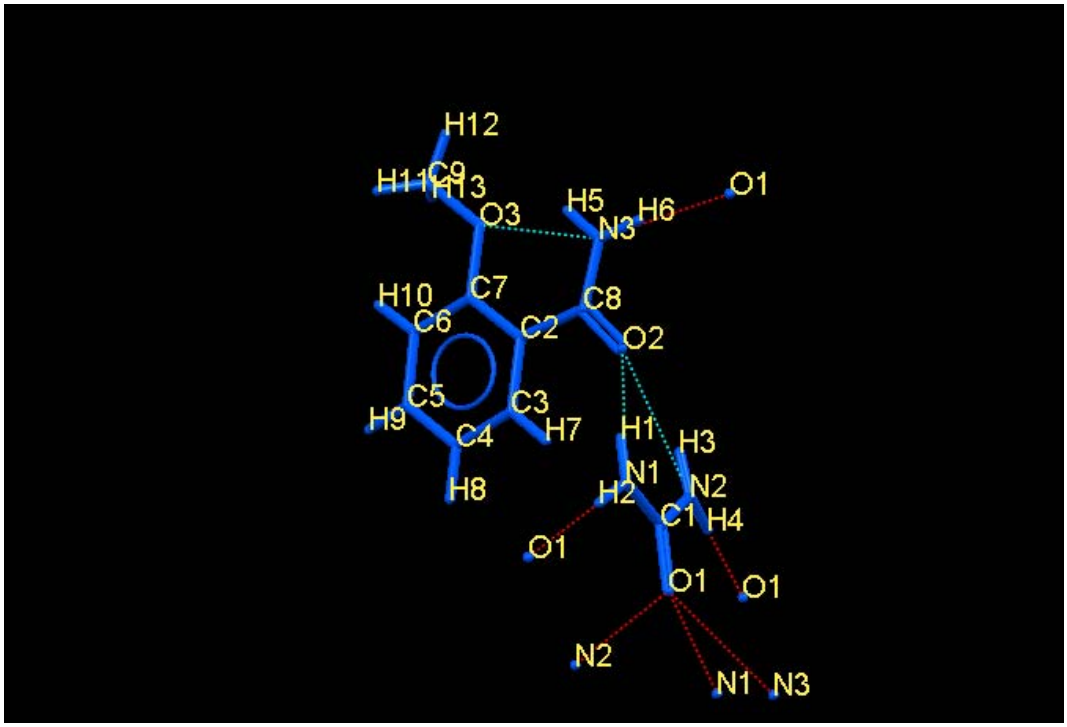

Figure 11: The molecular structure of the co-crystal of urea/ 2-MB produced using software (CanQuest 1.10) software permitted from CSD.

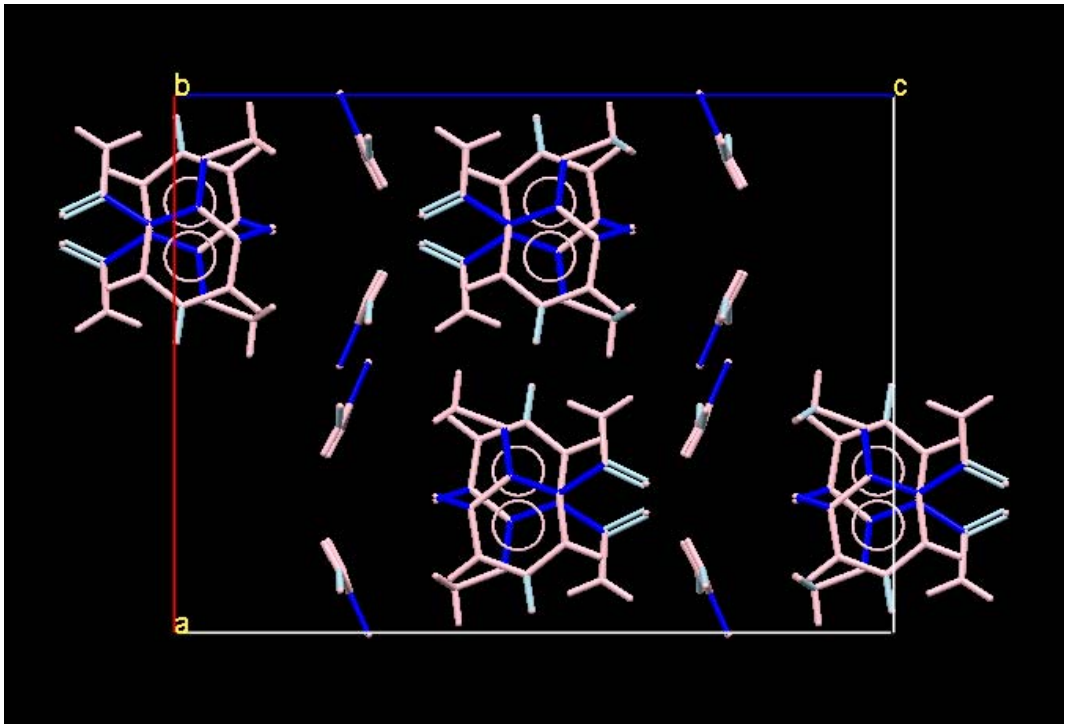

Figure 12: Crystal packing of urea/ 2-MB co-crystal in the crystal lattice.

3.2.2. Raman spectroscopy results of wet co-grinding and co-precipitation to produce urea/ 2-MB co-crystals

The Raman spectra of urea/ 2-MB system are shown in Figures 13a, 13b, 13c and 13d, respectively.

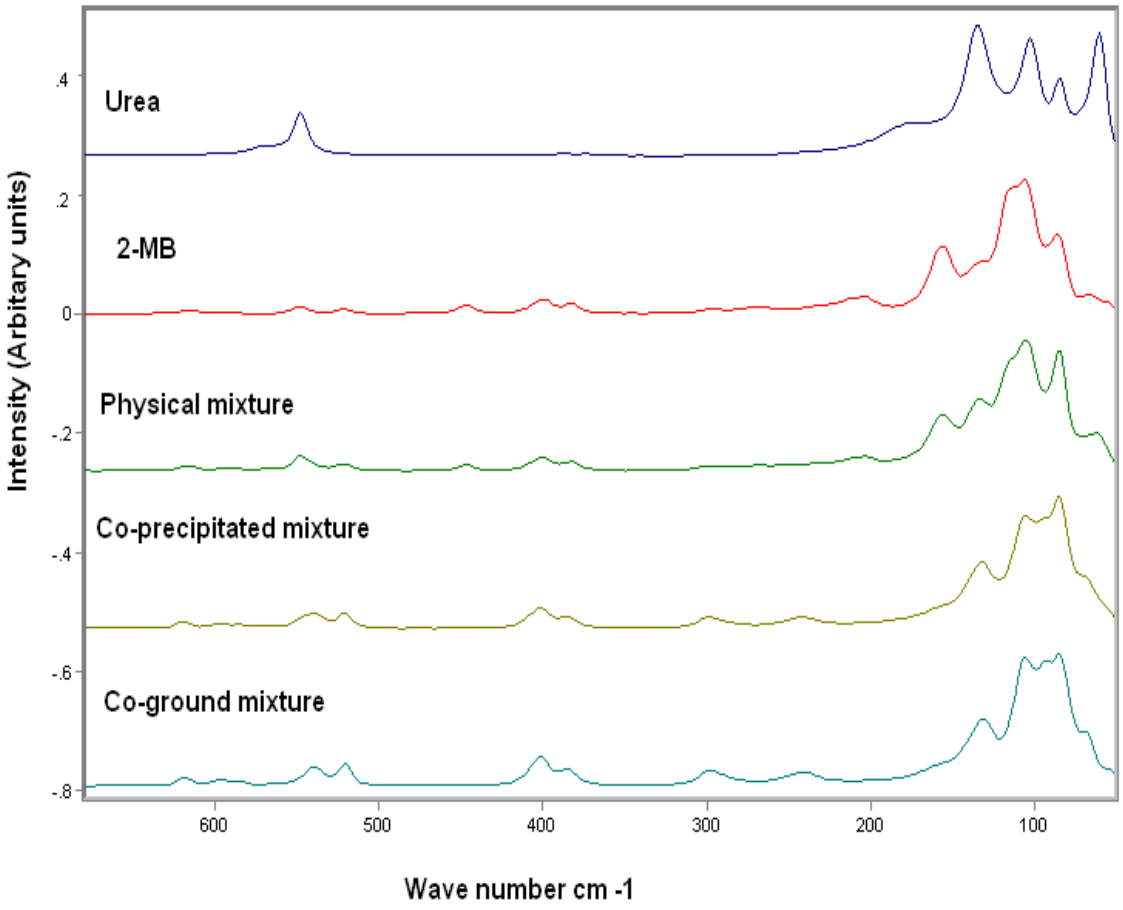

Figure 13a: F.T.Raman spectra of urea/ 2-MB-system (from 678 – 50 cm^{-1}).

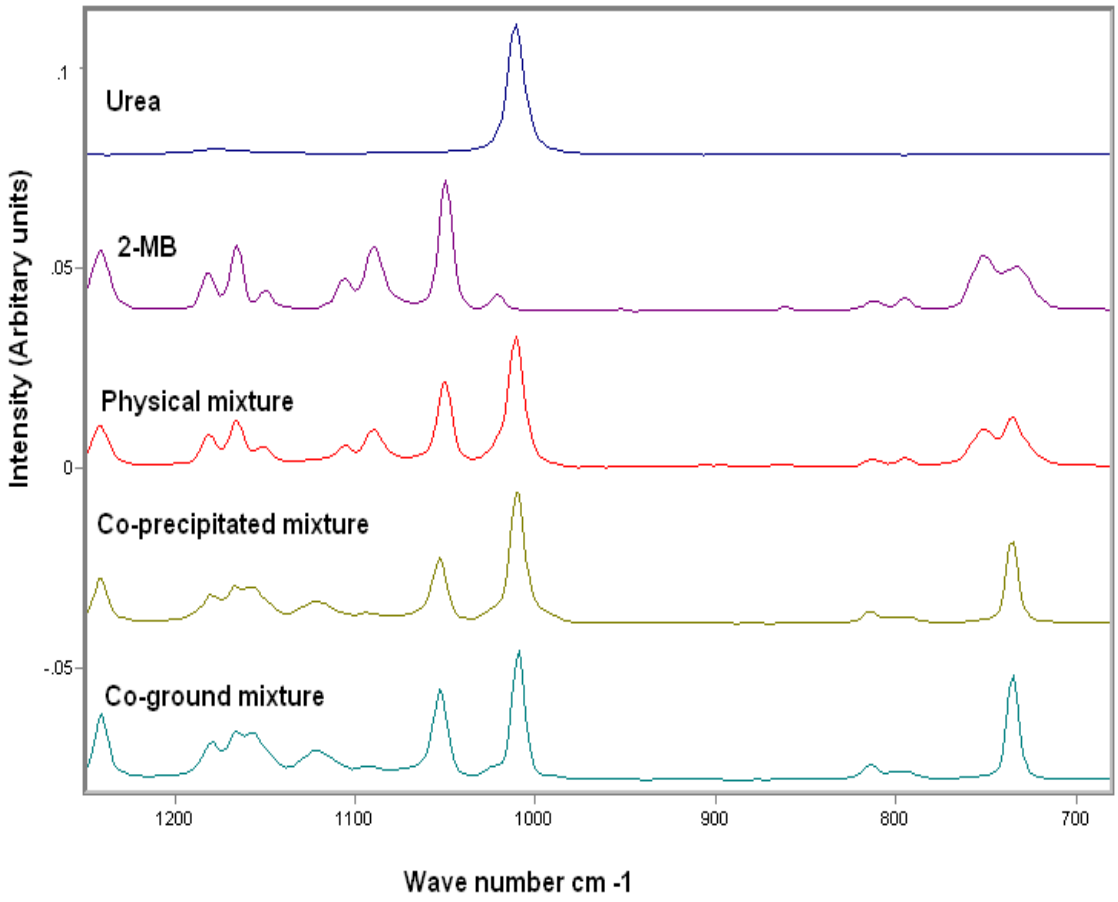

Figure 13b: F.T.Raman spectra of urea/ 2-MB-system (from 1275 – 678 cm^{-1}).

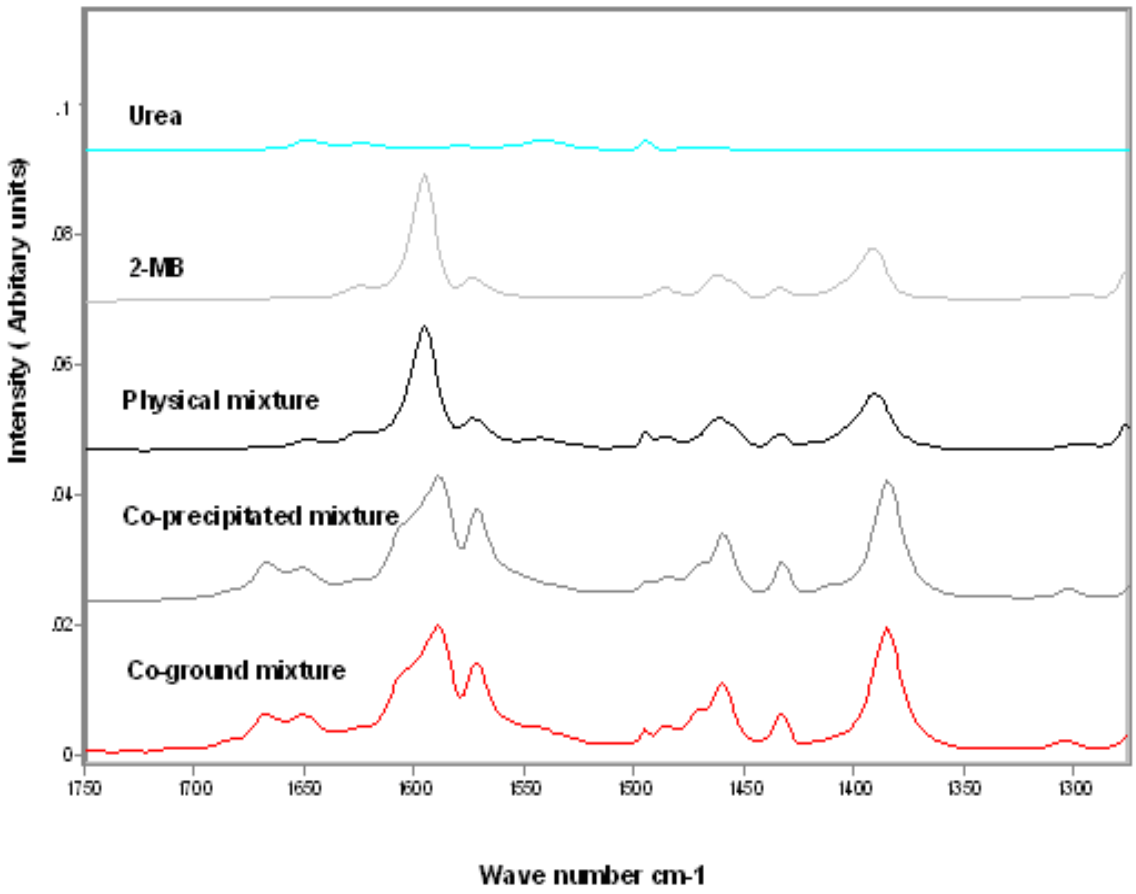

Figure 13c: F.T.Raman spectra of urea/ 2-MB-system (from 1750 – 1275 cm^{-1}).

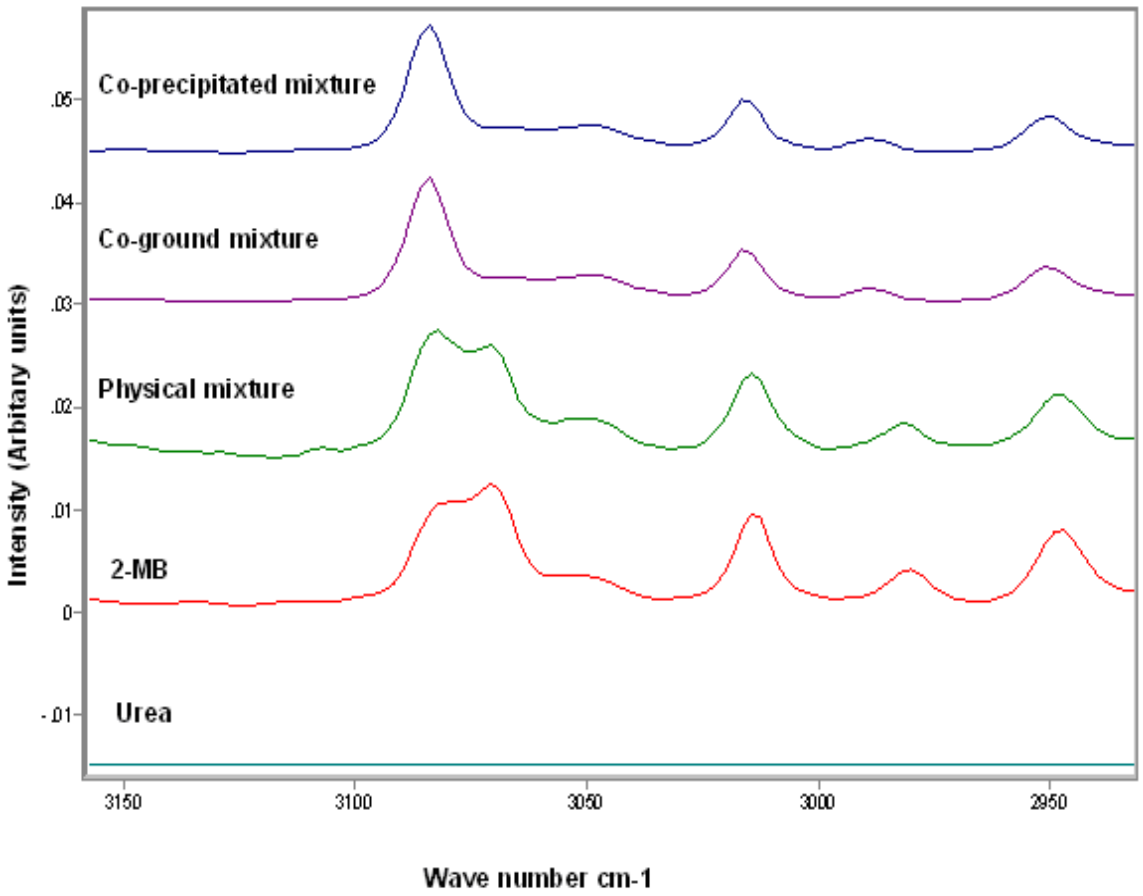

Figure 13d: Raman spectra of urea/ 2-MB system (3158- 2931 cm^{-1}).

It is believed that, this is the first reported study of Raman spectroscopy on the co-crystal. As shown in Figures 13a, 13b, 13c and 13d, both co-ground-and co-precipitated mixtures show spectra different from that of the physical mixture, in the wave number regions 678-50 cm^{-1}, 1275- 687 cm^{-1}, 1750- 1275 cm^{-1} and 3158-2931 cm^{-1}.

The bands at 115 cm^{-1} and 155 cm^{-1} disappeared, indicating a change in the lattice vibration (Figure 13a). In addition, the ring vibration bands of 2-MB at around 750 cm^{-1} disappeared (Figure 13b), while the amide 1-vibration bands of 2-MB at 1630 cm^{-1} and 1595 cm^{-1}, observed in the intact crystals, were shifted to higher wave numbers at 1660 cm^{-1} and 1606

cm^{-1} by both grinding and co-precipitation, respectively (Figure 13c). Furthermore, the position of N-H vibration band and C═O stretching of urea at around 1540 cm^{-1} and 1648 cm^{-1}, respectively, was changed by grinding and by co-precipitation. Furthermore, the ═CH2 stretches of 2-MB at 2980 and 3070 disappeared (Figure 13d). These results suggest that the 2-MB formed a co-crystal with the urea molecule.

3.2.3. SEM results of a urea/ 2-MB co-crystal prepared by two methods

Figure 14 illustrates the SEM micrographs of urea/ 2-MB system.

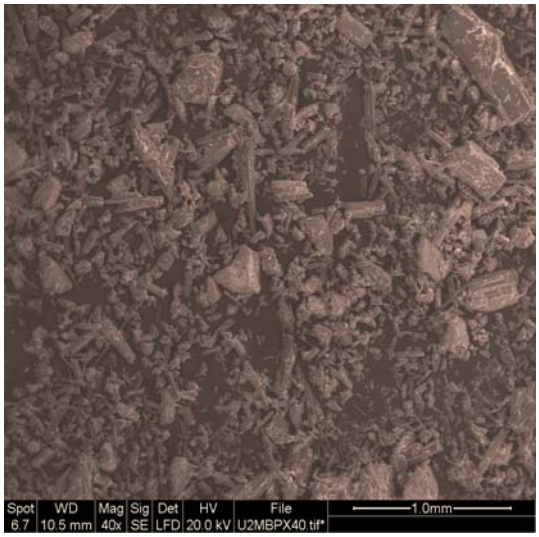

Physical mixture

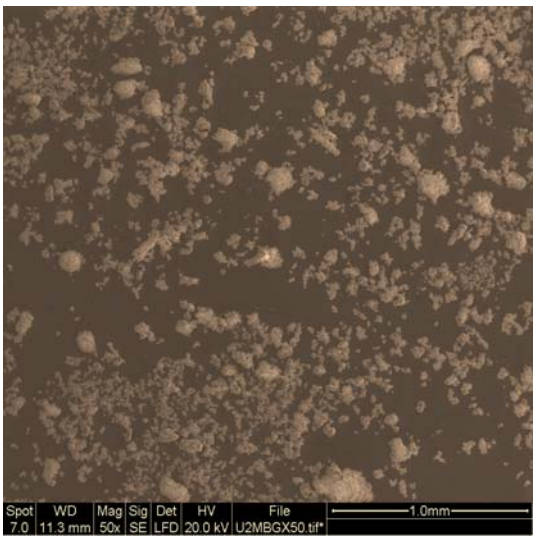

Co-ground mixture

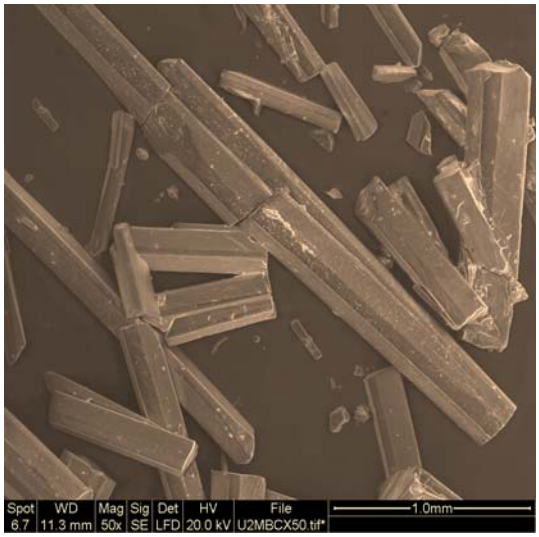

Co-precipitated mixture

Figure 14: The SEM micrographs of urea/ 2-MB system.

The co-precipitated- and co-ground mixtures show SEM micrographs different from that of the physical mixture as shown in Figure 14. The co-precipitated mixture possessed prism-like crystals, while the co-ground mixture showed rougher surface and aggregated particles,

indicating a phase transformation during grinding. These results are consistent with X-ray diffraction- and Raman results that a co-crystal formed between urea and 2-MB.

3.2.4. DSC results of a urea/ 2-MB co-crystal prepared by two methods

Figure 15 shows the DSC traces of the urea/ 2-MB system in its various forms.

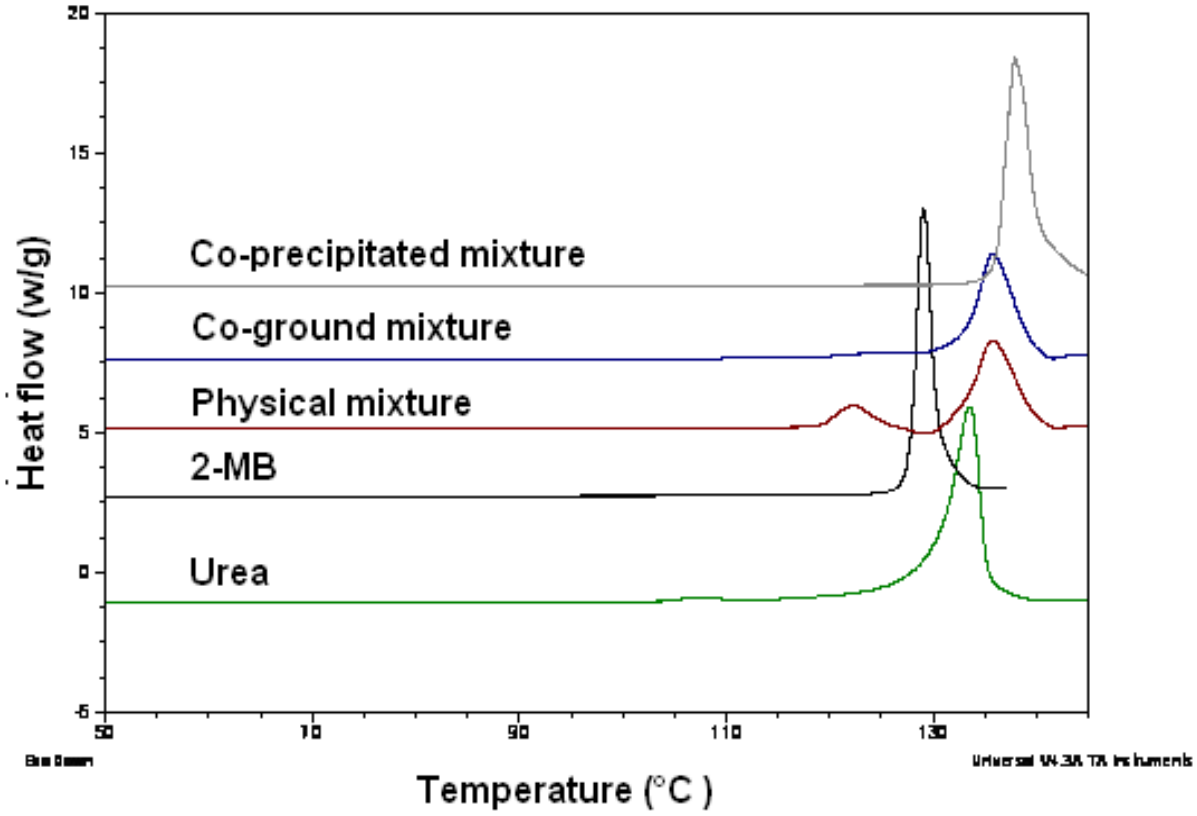

Figure 15: DSC curves of urea/ 2-MB system (sample weight 4-6mg, scan rate 10 °C/min).

The DSC traces of urea/ 2-MB systems are presented in Figure 15. The melting points (Peak temperatures) of urea and 2MB are 133 °C and 129 °C respectively. The physical mixture shows an endothermic peak at 127 °C, followed by an exothermic shift and an

endothermic peak at 136°C. Both the co-precipitated-and co-ground mixtures show melting points at 137°C and 136 °C respectively. These results indicated that urea formed a co-crystal with 2-MB by these methods. In the case of a physical mixture, the endothermic peak at 136°C, similar to that of the co-ground mixture is indicative of formation of some co-crystal during the heating process.

3.3. Effect of urea/ 2-MB co-crystal methods of preparation on compression properties

3.3.1. Compactibility

The compaction properties of three mixtures were compared, as shown in (Figure 16).

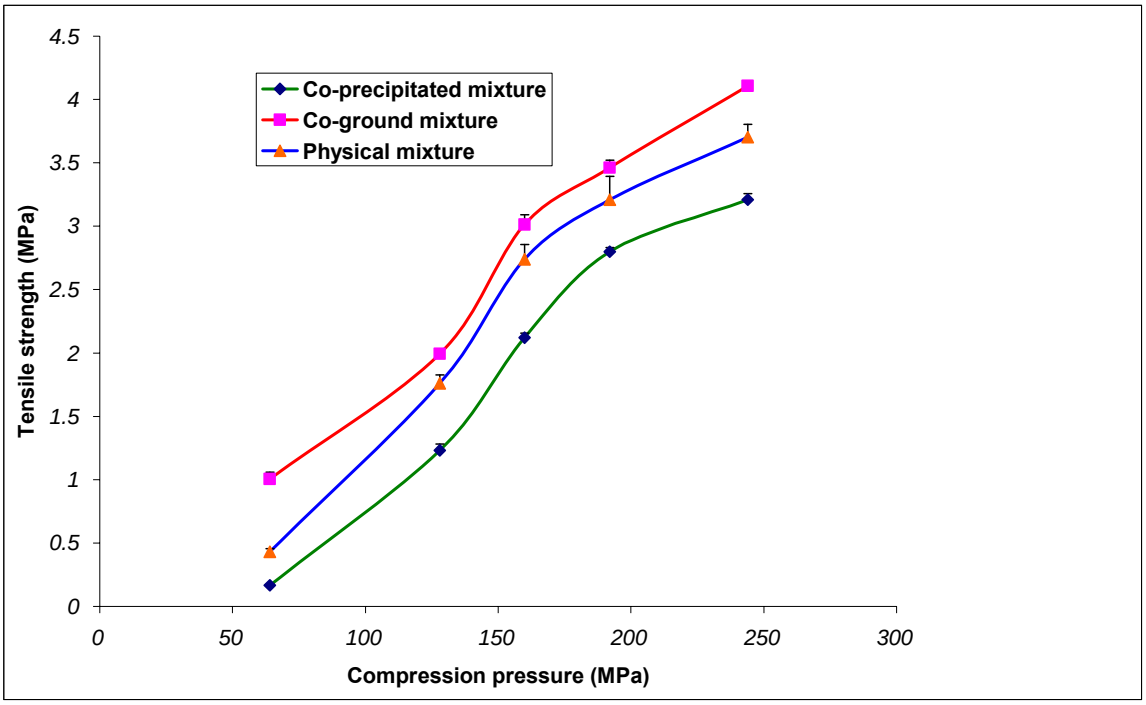

Figure 16: Tensile strength of urea/ 2-MB system obtained at a compression speed of 10 mm/s.

From the data presented in Figure 16, it is obvious that the tensile strength values of all mixtures increased with increasing compression forces. However, the co-ground mixture

showed the greatest values of tensile strength compared with those of co-precipitated or physical mixture, indicating a good tabletability of the co-ground mixture. All compacts were intact and showed no capping or lamination, either on ejection or before the crushing strength test. Good compact tensile strength may be due to the particle size reduction achieved by grinding, as the small size generally has good compactability. The tensile strength of compacts have been shown to increase as the particle size decreases (McKenna and McCafferty 1982; Morishima et al. 1994). It is also possible that the smaller crystals have more contact points between them, and can be compacted more densely than larger crystals.

From SEM micrographs (Figure 14), the co-precipitated mixture has needle-like crystals, which might result in poorer compactibility compared with other forms. In addition, good compactability of the co-ground mixture was in agreement with the theory that smaller particles produce a greater density and a greater number of contact points for interparticulate bonding (Rhines 1947). However, another reason for better compactibility of the co-ground mixture could result from its slightly smaller particle size and lower porosity, as the co-ground mixture showed the greatest bulk density (Table 2) compared with the co-precipitated mixture or physical mixture.

Table 2: Densities of the physical mixture, co-ground mixture and co-precipitated mixture of urea/ 2-MB system (mean ± SD, n =3).

Sample	True density (gm/cm^3)	Bulk density (gm/cm^3)
Physical mixture	1.324 ± 0.0037	0.2915 ± 0.0063
Co-ground mixture	1.335 ± 0.0146	0.5158 ± 0.0184
Co-precipitated mixture	1.378 ± 0.0133	0.323 ± 0.0103

3.3.2. Compressibility

The Heckel plots of urea/ 2-MB system are illustrated in Figure 17.

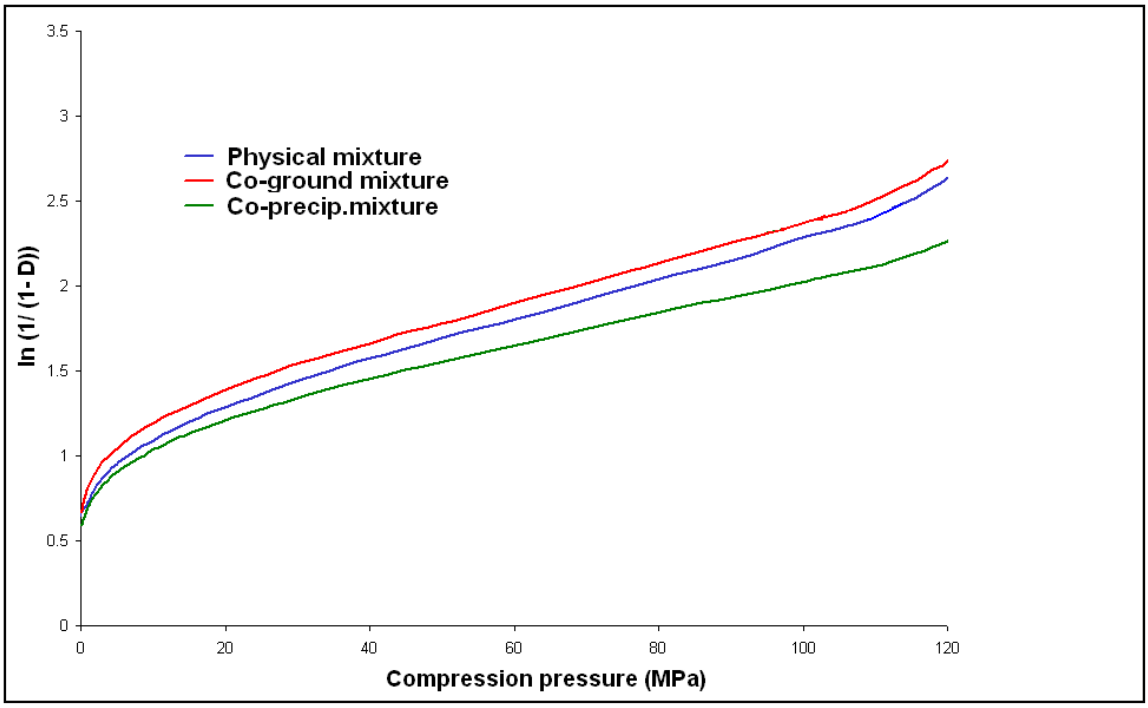

Figure 17: Heckel plots of urea/ 2-MB system obtained at a compression force of 10 KN and a compression speed of 10 mm/s.

Table 3: Heckel parameter of different mixtures of urea/ 2-MB system: (obtained at a compression speed of 10 mm/s and a compression force of 10 KN).

Sample	Yield pressure (MPa)	D_0	D_A	D_B
Physical mixture	74	0.477	0.642	0.165
Co-ground mixture	72	0.487	0.678	0.191
Co-precipitated mixture	85	0.446	0.626	0.180

D_0 = initial relative density, $D_A = 1 - e^{-A}$ is the extrapolated relative density from the intercept (A) of the linear portion of the Heckel plot, and D_B increase in relative density due to particle arrangement.

The relative volume changes during the early stage (0-120 MPa) of the compression event were recorded for each of the physical, co-ground and the co-precipitated mixtures.

The results of the Heckel data are presented in Figure 17 and Table 3. The Heckel plot profiles are classified into two types (Herssy et al. 1973). Type 1 describes powder that exhibits different initial bulk densities, depending on factors (e.g. particle size). Densification occurs under pressure due to particle slippage, and subsequently by plastic deformation. The initial curved portion followed by the parallel straight lines represents the two stages. Type 2, on the other hand, describes materials, in which consolidation occurs by fragmentation. The initial structure is progressively destroyed, so that above a certain pressure, coincident linear portions are obtained for all particle size fractions (Duberg and Nyström 1982).

The data shown in Figure 17 and Table 3 suggest that the Heckel plots of urea/ 2-MB systems are Type 1 materials, as the yield pressures of all mixtures are nearly similar. Furthermore, an extensive linearity during compression is indicative of a plastic

deformation mechanism, as the linear portion started below 20 MPa. However, the co-precipitated mixture possessed the greatest value of yield pressure, which indicates that the densification process by particle deformation is poorer than in other mixtures. In addition, the co-precipitated mixture exhibited the smallest particle slippage ($D_0 = 0.446$) compared with those of the co-ground or physical mixture (Table 3). This indicates that the co-precipitated mixture was the least compressible, as the plastic deformation decreases with increasing yield pressure. On the other hand, the co-ground mixture was the most compressible. These results were consistent with the compaction results reported for mannitol grades as the most compactible was the most compressible (Yoshinari et al. 2003).

Table 4: Elastic recovery of tablets produced from urea/ 2-MB systems obtained at a compression speed of 10 mm/s and a compression force of 10 KN.

Sample	t_1 (mm)	t_2 (mm)	Elastic recovery E (%)
Co-precipitated mixture	3.50	3.76	7.42
Co-ground mixture	3.54	3.78	6.77
Physical mixture	3.53	3.79	7.30

t_1 = minimal thickness of the powder bed in the die, and t_2 = is the thickness of the recovered tablet.

From the data given in Table 4, it is obvious that the elastic recovery of the co-precipitated mixture was greater than that of the co-precipitated mixture or physical mixture. This contributes to the lower compressibility of the co-precipitated mixture, as the greater elastic

recovery increases the tablet porosity during decompression phase (Roberts and Rowe 1987).

3.3.3. General Discussion

In this chapter, we have shown that the methods of preparation of urea/ 2-MB co-crystals affected compaction properties. Both methods produced the same co-crystal structure as indicated by XRPD and Raman spectroscopy.

In the next chapter, we evaluate a more representative drug-like model: caffeine and malonic acid.

4. Co-crystallization of caffeine/ malonic acid via both co-grinding and co-precipitation: Evaluation of compaction properties

4.1. Introduction

As it has been mentioned in the first chapter, caffeine was found to form co-crystals with dicarboxylic acids, e.g. oxalic acid, malonic acid, maleic acid and glutaric acids (Trask et al. 2005a). The co-crystallization was performed by both co-precipitation- and co-grinding techniques. Based on its basicity, caffeine may be suitable for co-crystallization in its neutral form. The pharmaceutical acceptability of malonic acid as a pharmaceutical salt former has already been confirmed (Stahl and Wermuth 2002).

It has been reported that in the co-crystals of caffeine with dicarboxylic acid, including malonic acid, the desired supramolecular interaction was the acid-base heterodimer synthon (Scheme 2) in order to allow stronger O─H···N and weaker C─H···O hydrogen bonding (Desiraju and Steiner 1999).

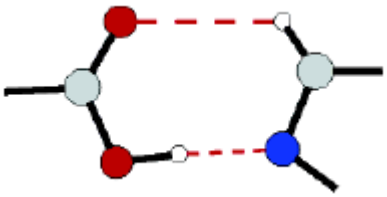

Scheme 2: Heteromemeric synthon showing stronger O─H···N and weaker C─H···O hydrogen bond interaction.

Like all caffeine/ acid materials, in the caffeine/ malonic acid system, the location of the acidic proton is of importance in differentiation between salts (ionic complexes) and co-crystals (neutral complexes). In all caffeine/ acid co-crystal structures, the location of acidic

protons on the acid in the X-ray difference maps has been observed, indicating, that the salt formation has not occurred. However, typical O─H bond distances were observed in all cases (Trask et al. 2005a).

In this chapter, XRPD, Raman spectroscopy, DSC and SEM techniques were used to characterize the co-crystal of caffeine/ malonic acid that prepared using the methods outlined in sections 2.2.7 and 2.2.8 and after the characterization, their tableting properties were compared.

4.2. Results and discussion

4.2.1. XRPD of a caffeine/ malonic acid co-crystal prepared by two methods

Figure 18 illustrated the X-ray powder diffraction patterns of caffeine/ malonic acid system.

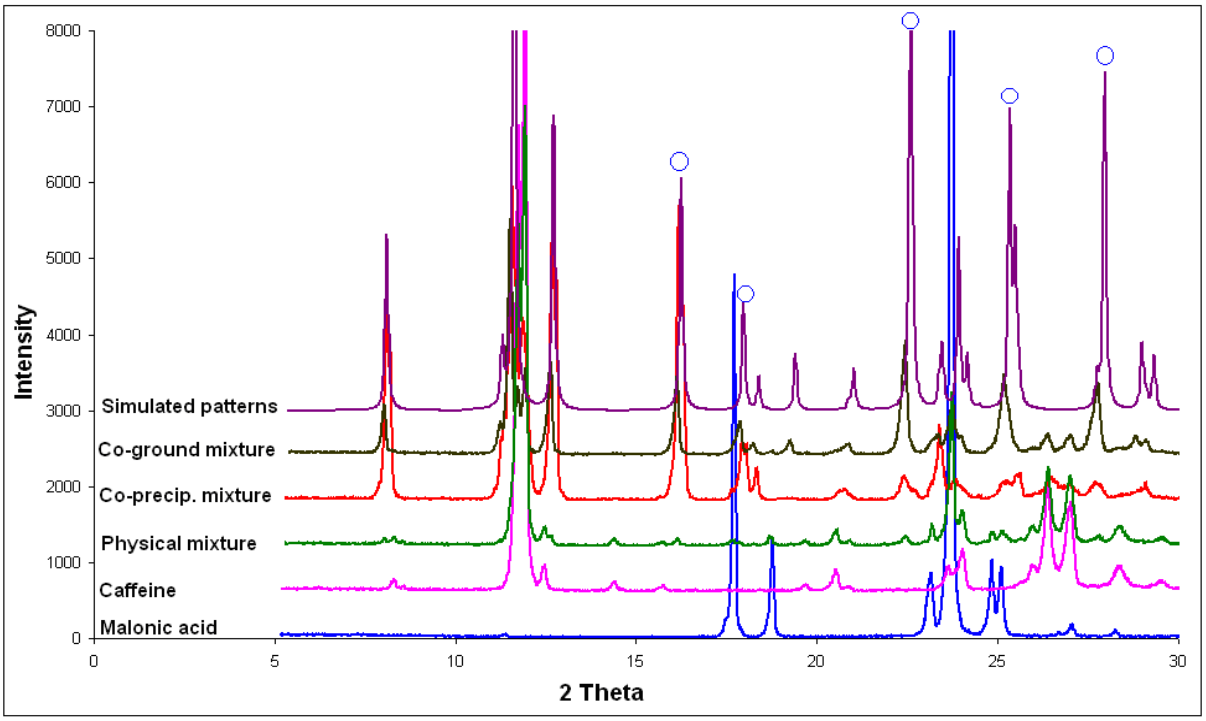

Figure 18: PXRD patterns of the caffeine/ malonic acid system (Simulated patterns = patterns calculated from CSD using CIF format).

When caffeine was co-ground or co-precipitated with malonic acid at a ratio of (2:1), new PXRD peaks at $2\theta = 16.2^{0}$, 18.28^{0}, 22.45^{0}, 25.34^{0} and 28^{0} were observed (Figure 18). The peak positions of new peaks were different from those of the physical mixture, indicating that caffeine may have formed a co-crystal with malonic acid. These results are in agreement with results already published by Trask et.al (2005). They reported that caffeine/ malonic acid co-crystal crystallizes in the orthorhombic Fdd2 space group and its calculated crystal density is 1.472 g cm^{-3}.

The co-crystal of caffeine/ malonic acid exhibited stacks of trimeric intermolecular hydrogen bonded units. The central sp^3 carbon of malonic acid imposes a V- shaped geometry to the trimeric unit (Trask et al. 2005a)(Figure 19) and (Figure 20).

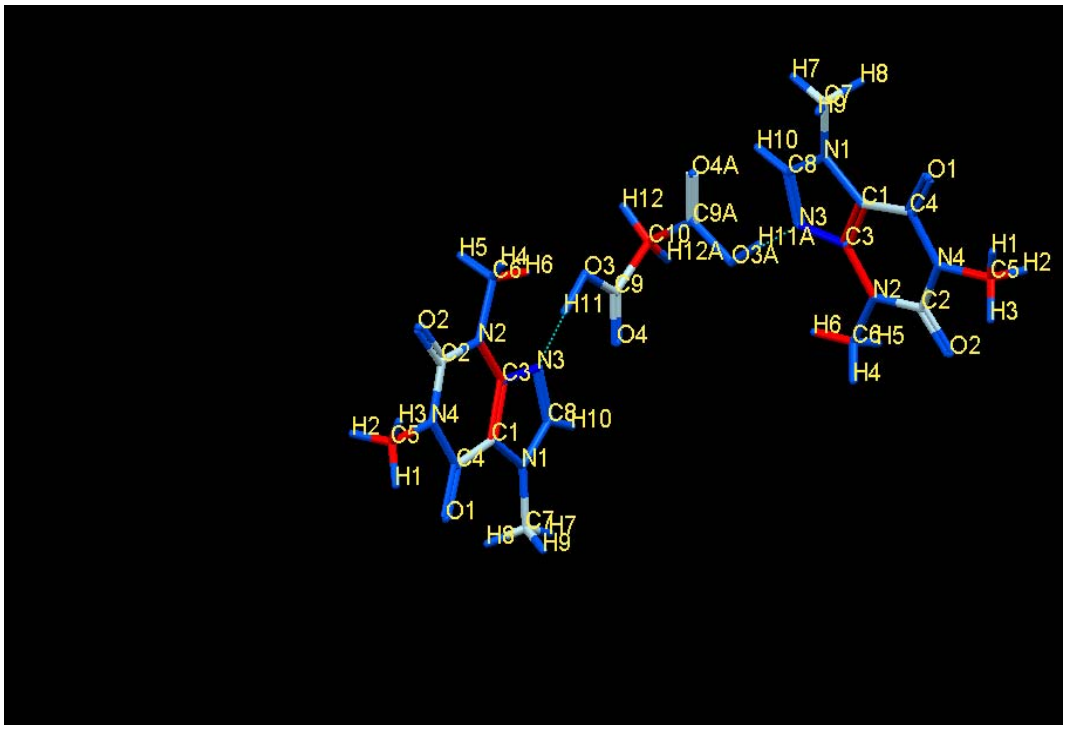

Figure 19: The molecular structure of the co-crystal of caffeine/ malonic acid produced using software permitted from Cambridge crystallographic database using CIF format.

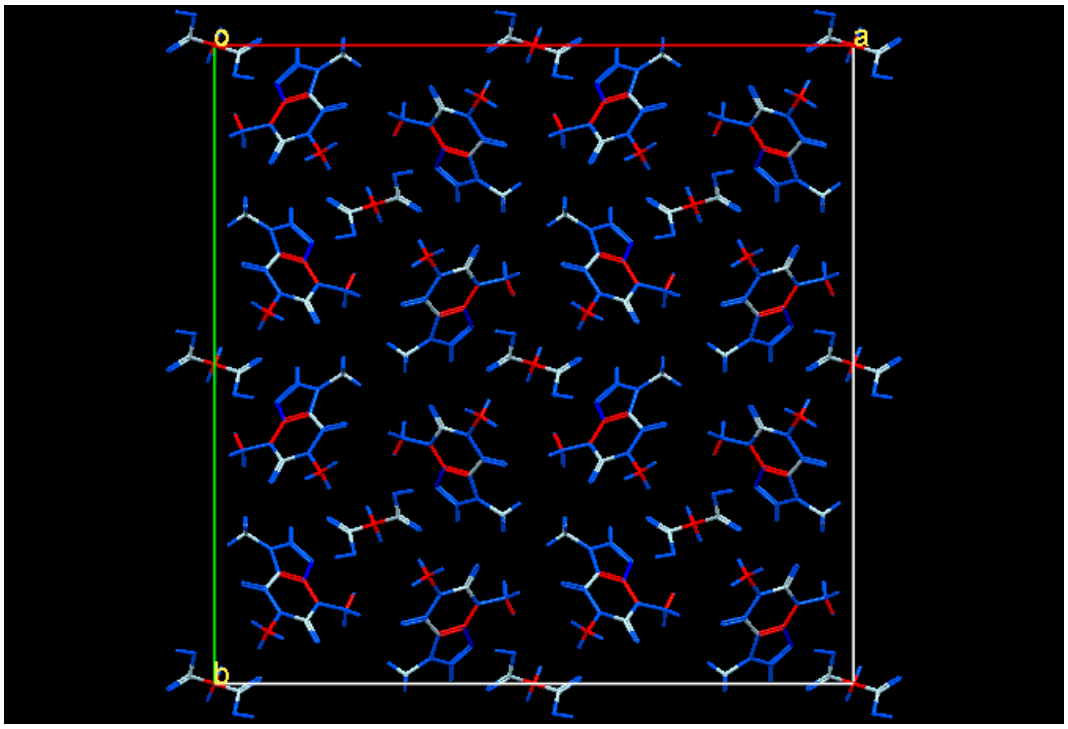

Figure 20: Crystal packing of caffeine/ malonic acid co-crystal in the crystal lattice.

4.2.2. Raman spectroscopy

Figures 21a, 21b and 21c illustrate the Raman spectra of caffeine/ malonic acid system.

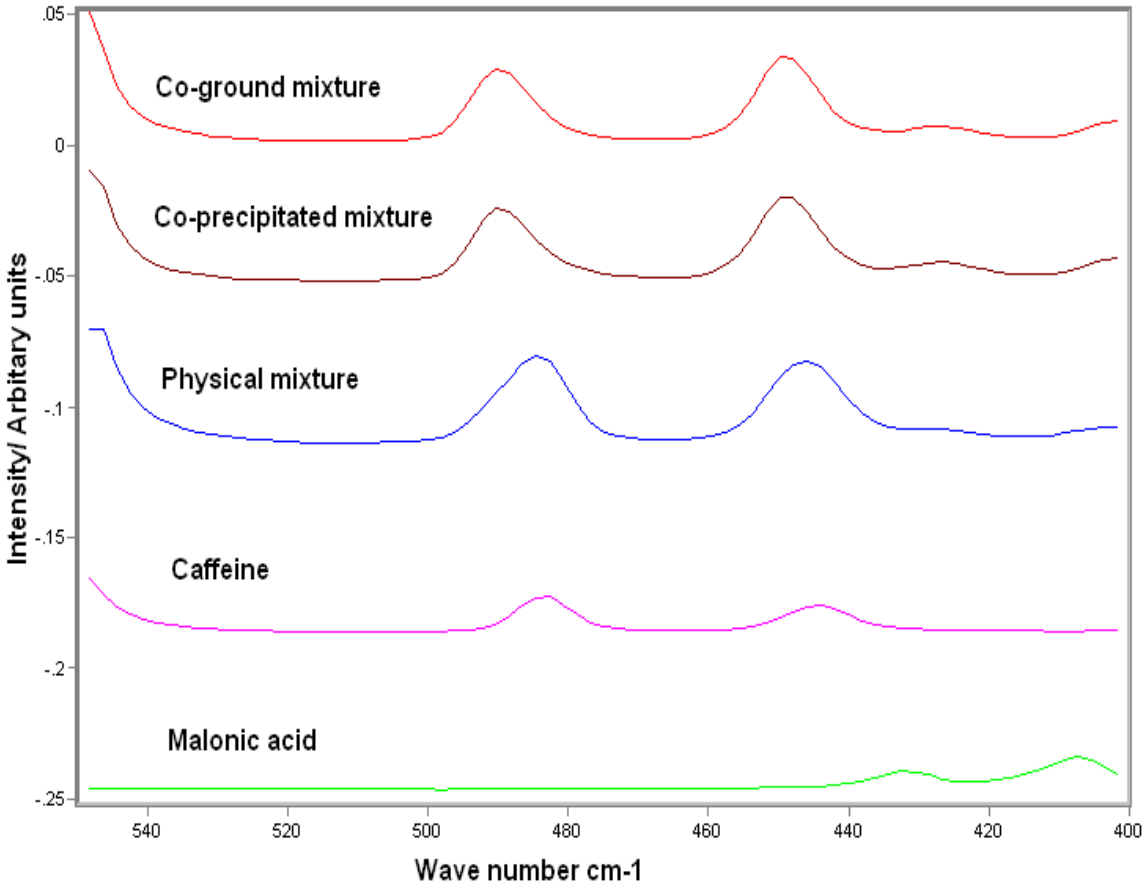

Figure 21a: Raman spectra of the caffeine/ malonic acid system (550- 400 cm^{-1}).

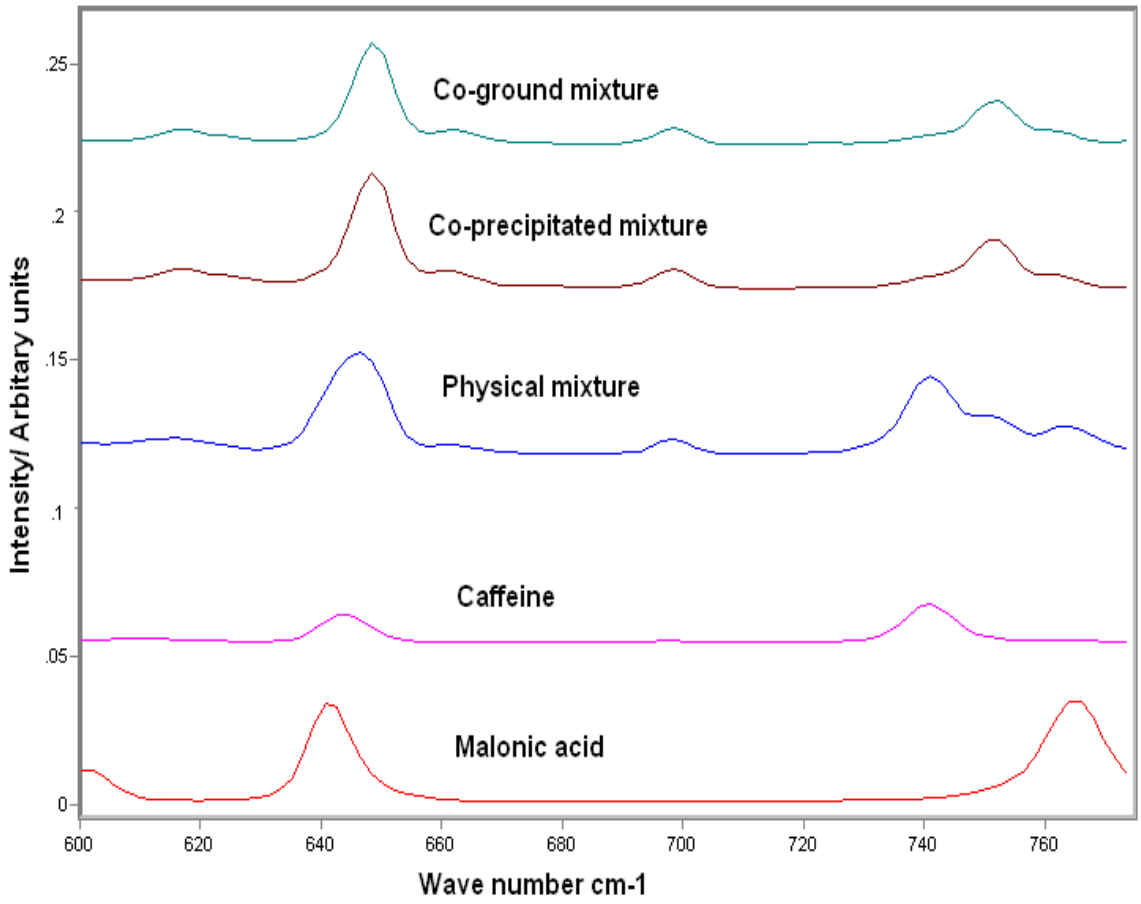

Figure 21b: Raman spectra of the caffeine/ malonic acid system (775- 600 cm^{-1}).

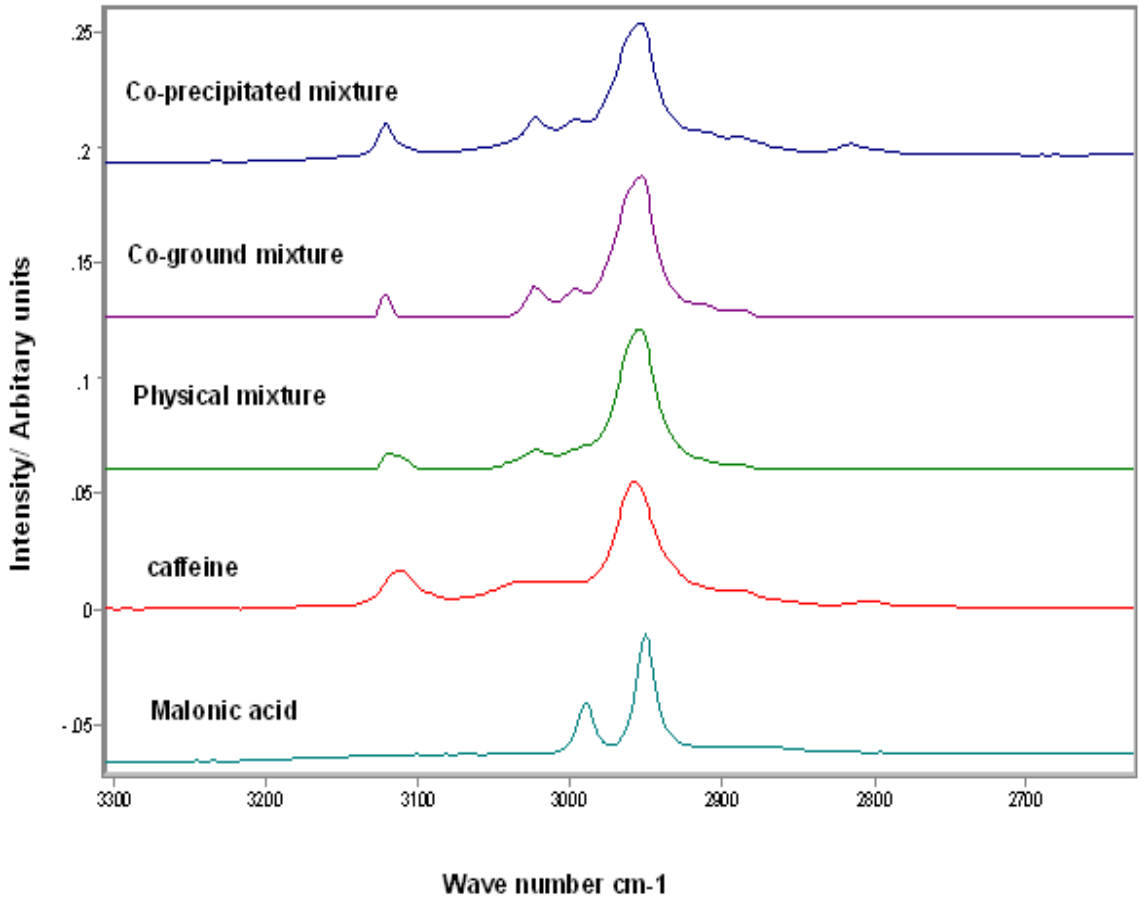

Figure 21c: Raman spectra of the caffeine/ malonic acid system (3175- 3050 cm^{-1}).

From Figures 21a, 21b and 21c, it can be seen that there were no differences observed between the peak positions for the pure drugs and the physical mixture. However, the data clearly show noticeable differences between the physical mixture and both co-ground- and co-precipitated mixtures in the wave number regions 550- 400 cm^{-1}, 775- 600 cm^{-1} and 3175- 3050 cm^{-1}as shown in Figure 21a, 21b and 21c, respectively.

The δ-pyrimidine ring vibrational bands of caffeine at around 442cm^{-1} and 484 cm^{-1} found in the intact crystal were shifted to higher wave numbers at 448 and 490 cm^{-1}, respectively.

In addition, the δ-pyrimidine imidazole ring vibrational bands of caffeine at 644 cm^{-1} and 740cm^{-1} were shifted to higher wave numbers at 649 cm^{-1} and 752 cm^{-1}, respectively. Furthermore, The OH stretch of malonic acid at 2989 cm^{-1} and the C=CH stretch of caffeine at around 3115 cm^{-1} were shifted to higher wave numbers at 2998 cm^{-1}.and 3122 cm^{-1}, respectively. This suggests that caffeine may have formed hydrogen bonds with malonic acid.

4.2.3. SEM results of caffeine/ malonic acid co-crystal prepared by two methods

The SEM micrographs of caffeine/ malonic acid system are presented in Figure 22.

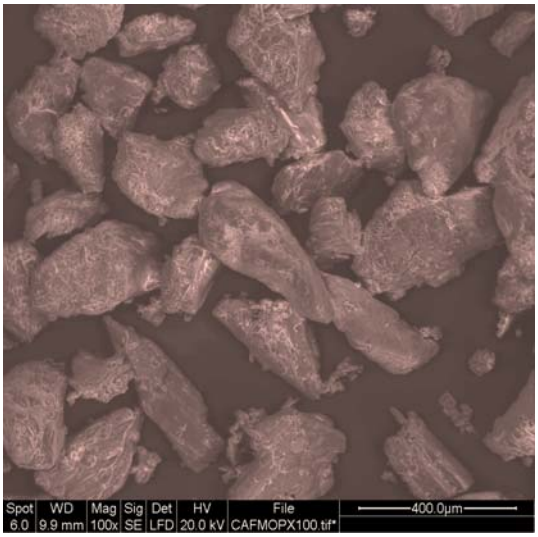

Physical mixture

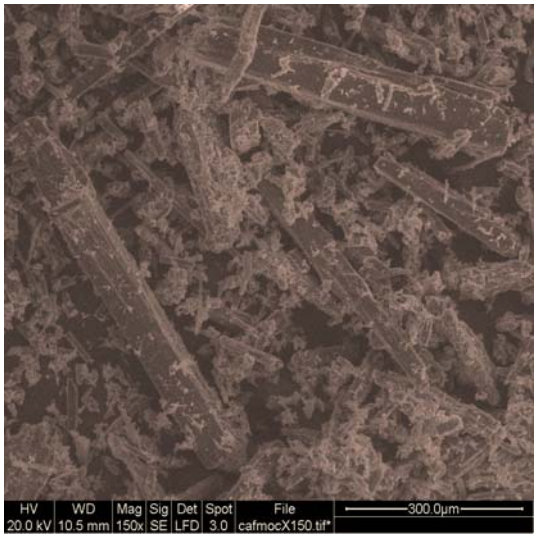

Co-precipitated mixture

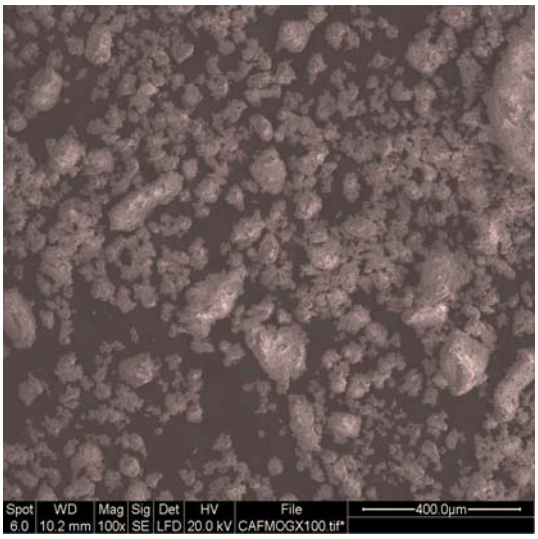

Co-ground mixture

Figure 22: SEM micrographs of caffeine/ malonic acid system.

Figure 22 shows that the particles of starting materials were unchanged, as seen in the physical mixture, while the co-precipitated mixture exhibited prism-like crystals. The co-ground mixture, on the other hand, showed aggregated particles that may result from milling of the powder with the solvent. These results were consistent with X-ray and Raman results and indicated that caffeine may have formed a co-crystal with malonic acid.

4.2.4. Thermal Analysis

Figure 23 illustrates the DSC traces of caffeine/ malonic acid system.

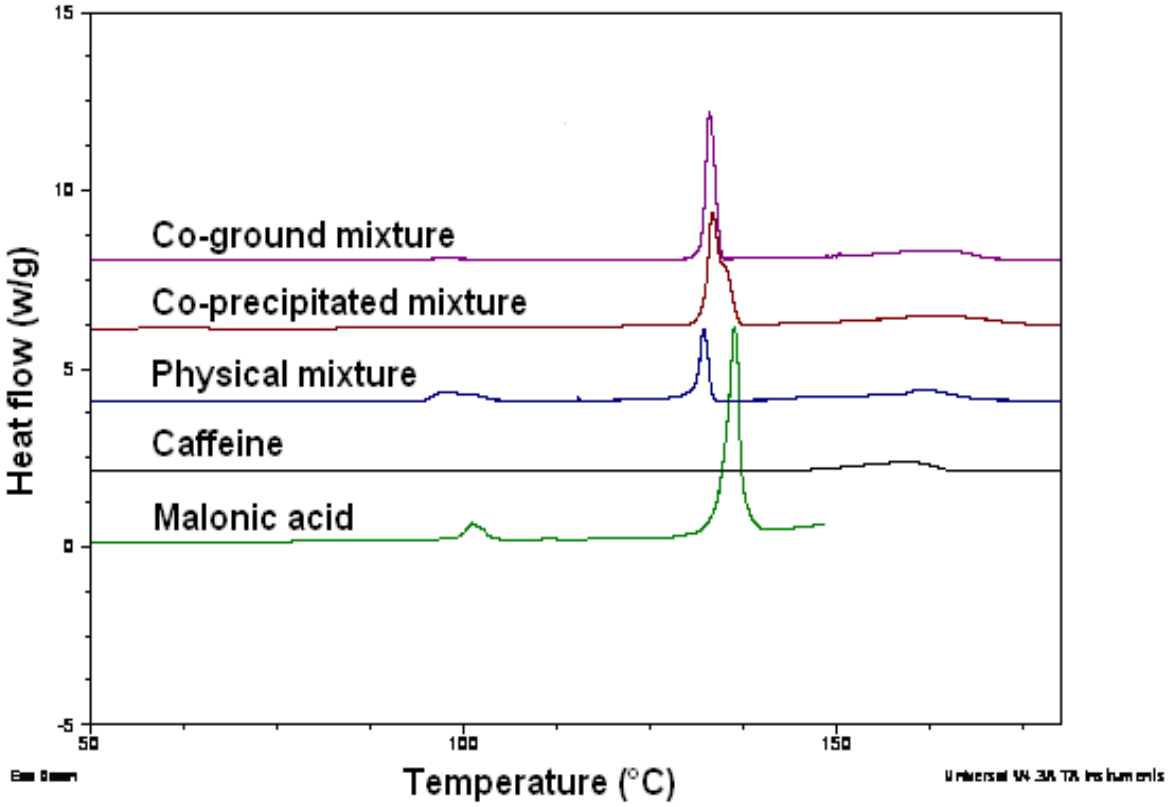

Figure 23: DSC traces of the caffeine/ malonic acid system (sample weight 4-6mg, scan rate 10 °C/ min).

The melting points (peak temperatures) of caffeine and malonic acid are 160 °C and 136 °C respectively. However, malonic acid shows an endothermic peak at 100°C. Both co-ground- and co-precipitated mixtures show melting points at 132.7 °C and 133.4°C respectively. The physical mixture shows small endothermic peak at 100 °C, corresponding to malonic acid, followed by endothermic peak at 132.3 °C. The endothermic peak of the physical mixture at 132.3°C, similar to that of the co-ground mixture, is possibly co-crystal

due to formation during the heating process in the calorimeter. These results indicate that caffeine might have formed a co-crystal with malonic acid.

4.3. Mechanical properties of tablets and deformational behaviour of powders: Caffeine/ Malonic acid system

4.3.1. Compactibility

Figure 24 presents the tensile strength of caffeine/ malonic acid systems.

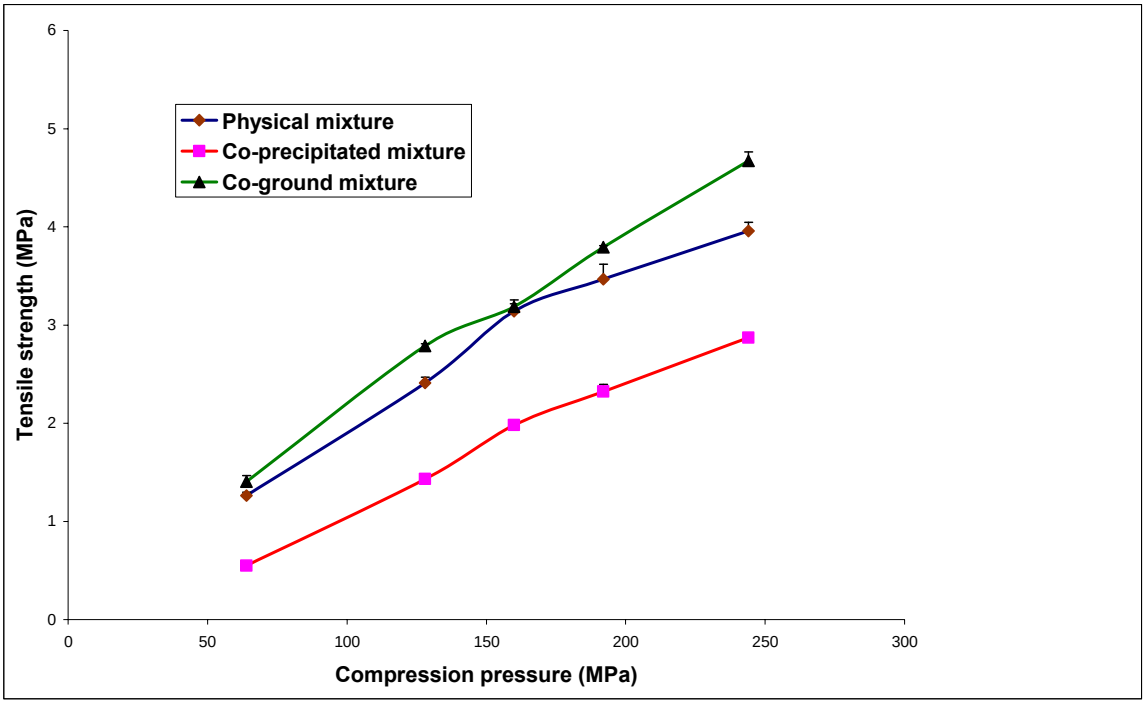

Figure 24: Tensile strength of the caffeine/ malonic acid system obtained at a compression speed of 10 mm/s.

As shown in Figure 24, the tensile strength values of compacts of all caffeine/ malonic acid systems increased with increasing compression force. This is consistent with fact that the mean contact area between the particles increases in proportion to the compaction pressure

(Rumpf 1962). However, the proportional increase of tensile strength with compaction pressure was higher for the co-ground mixture than for co-precipitated mixture, indicating better compactibility of the co-ground mixture. The data show a dramatic difference in compactibility between co-ground and co-precipitated mixture. This is because, on one hand, the co-precipitated mixture possessed needle-like or prism particles, which may result in smaller compactibility, compared with other mixtures. On the other hand, the particles of co-ground mixture were reduced in size during milling of the components, which may result in higher compactibility. Furthermore, the lower porosity of a co-ground mixture, as it showed the highest bulk density (Table 5), may contribute to its better tabletability, compared with the co-precipitated mixture or physical mixture.

These results were in agreement with the assumption that smaller particles generally have better compactibility than larger ones (Morishima et al. 1994), (McKenna and McCafferty 1982).

Table 5 Densities of physical mixture, co-ground mixture and co-precipitated mixture of caffeine/ malonic acid systems (mean ± SD, n =3).

Sample	True density (gm/cm^3)	Bulk density (gm/cm^3)
Physical mixture	1.4739 ± 0.0068	0.393 ± 0.008679
Co-ground mixture	1.4651 ± 0.0105	0.427 ± 0.012137
Co-precipitated mixture	1.4441 ± 0.0010	0.317 ± 0.00626

4.3.2. Compressibility

Figure 25 illustrates the Heckel plots of the caffeine/ malonic acid system.

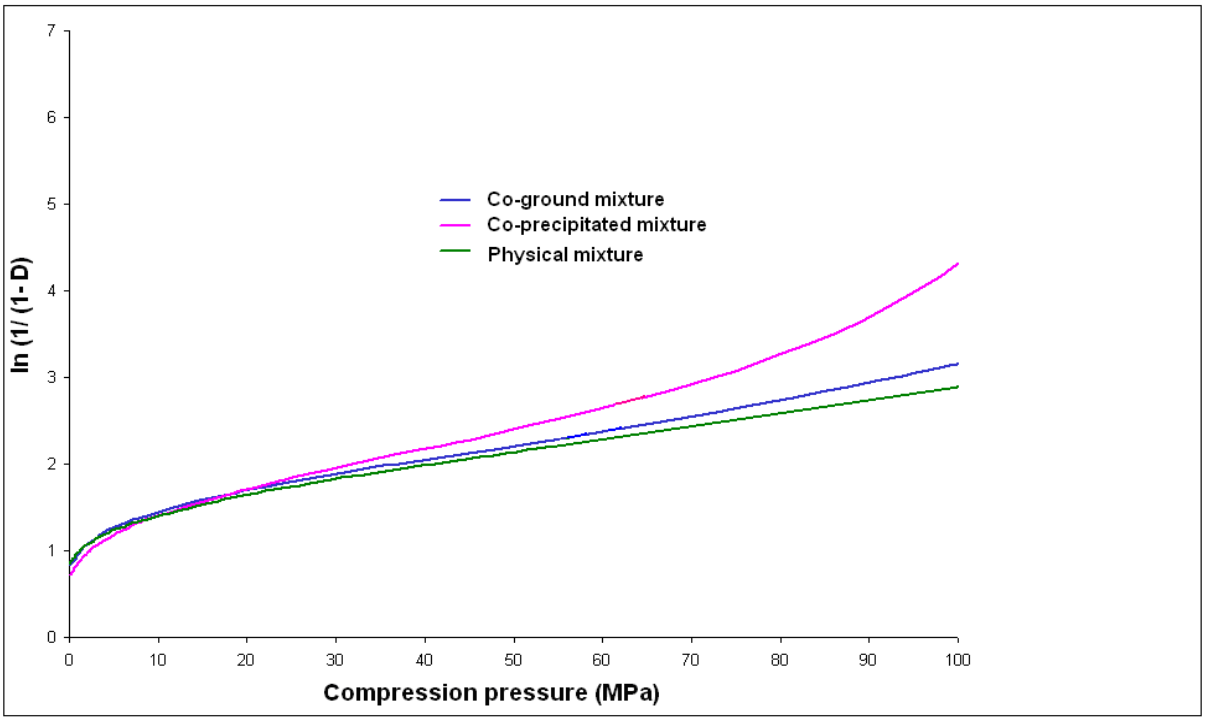

Figure 25: Heckel plots of the caffeine/ malonic acid system obtained at a compression force of 10 KN and a compression speed of 10 mm/s.

The linear portion of the Heckel plots below 20 MPa (Figure 25) clearly indicates that the caffeine/ malonic acid systems undergo plastic deformation, similar to Type 1 materials. The compaction processes were proceeded by deformation rather than fragmentation of particles as observed for sodium chloride (McKenna and McCafferty 1982).

However, the co-precipitated mixture showed the best compressibility compared with both the co-ground- and physical mixtures, as indicated by the highest slope of the Heckel plot

(Figure 25) and the smallest yield pressure (Table 6). Although the co-ground mixture was the most compactible among all mixtures, the co-precipitated mixture showed the best ductility. This indicates that the yield strength is more a material property for this system and it is not affected greatly by the morphology of the crystals. However, crystal morphology was found to have an impact on the tableting behaviour of the compacts in other studies (Shell 1963; Staniforth et al. 1981). The compressibility (using the Heckel-plot) of different crystal forms (polyhedral and thin plate-like crystals were compared. It was found that polyhedral crystals produced the greater slope in the Heckel plot (Garekani et al. 1999). In the present study, the physical mixture showed compressibility, which was closely akin to that of the co-ground mixture. This is consistent with the compaction results, where the tensile strengths of both were very similar.

Table 6 Heckel parameters of the caffeine/ malonic acid system obtained at a compression speed of 10 mm/s and a compression force of 10 KN.

Sample	Yield pressure (MPa)	D_0	D_A	D_B
Physical mixture	62.9	0.569	0.728	0.158
Co-ground mixture	60	0.568	0.750	0.182
Co-precipitated mixture	44	0.512	0.719	0.207

D_0 = initial relative density, $D_A = 1 - e^{-A}$ is the extrapolated relative density from the intercept (A) of the linear portion of the Heckel plot, and D_B = increase in relative density due to particle arrangement.

Table 7: Elastic recovery of tablets produced from the caffeine/ malonic acid systems obtained at a compression speed of 10 mm/s and a compression force of 10 KN.

Sample	t_1 (mm)	t_2 (mm)	Elastic recovery E (%)
Co-precipitated mixture	3.10	3.32	7.28
Co-ground mixture	3.05	3.33	9.21
Physical mixture	3.02	3.35	11.34

t_1 = minimal thickness of the powder bed in the die, t_2 = is the thickness of the recovered tablet.

Furthermore, the data presented in Table 7 show that the co-precipitated mixture exhibited the smallest elastic recovery compared to that of co-precipitated or physical mixture. This was may be due to the higher compressibility of the co-precipitated mixture, because the greater elastic recovery acts to increase the compact porosity during decompression phase (Roberts and Rowe 1987).

4.3.3. General Discussion

In this chapter, we have shown that the methods of preparation of caffeine/ malonic acid co-crystals affected the tableting behaviour. Both methods produced the same co-crystal structure as indicated by Raman and XRPD.

In the next chapter, we evaluate a more representative drug-like model: caffeine and oxalic acid.

5. Co-crystallization of caffeine/ oxalic acid using both co-grinding and co-precipitation: Evaluation of compaction properties

5.1. Introduction

Similar to caffeine/ malonic acid co-crystal, a stoichiometry of 2:1 has been observed for caffeine/ oxalic acid co-crystal from the solved crystal structure. In addition, the trimeric caffeine-acid-caffeine motif is demonstrated in both co-crystal structures (Figure 27). However, the different geometries of oxalic acid and malonic acid require differences in crystal packing (Trask et al. 2005a).

Caffeine/ oxalic acid that crystallizes in the $P2_1/c$ space group was found to have the highest calculated density (1.542 g cm^{-3}) of all the solved co-crystal structures (Trask et al. 2005a). The planarity of the oxalic acid molecule allows a flat trimeric motif to stack along the a axis.

Similar to caffeine/ malonic acid co-crystal, in the caffeine/ oxalic acid co-crystal the supramolecular interaction was the acid-base heterodimer synthon (see Scheme 2) in order to permit stronger O─H···N and weaker C─H···O hydrogen bonding (Desiraju and Steiner 1999).

In this chapter, the solid-state characterization of the caffeine/ oxalic acid co-crystals (prepared using the methods outlined in sections 2.2.4 and 2.2.5) was carried out using XRPD, Raman spectroscopy, DSC and SEM. Furthermore, the impact of the co-crystal formation on the tableting behaviour and deformation properties has been investigated.

5.2. Results and discussion

5.2.1. XRPD of a caffeine/ oxalic acid co-crystal prepared by co-grinding and co-precipitation methods

The XRPD spectra of caffeine/ oxalic acid systems are presented in Figure 26.

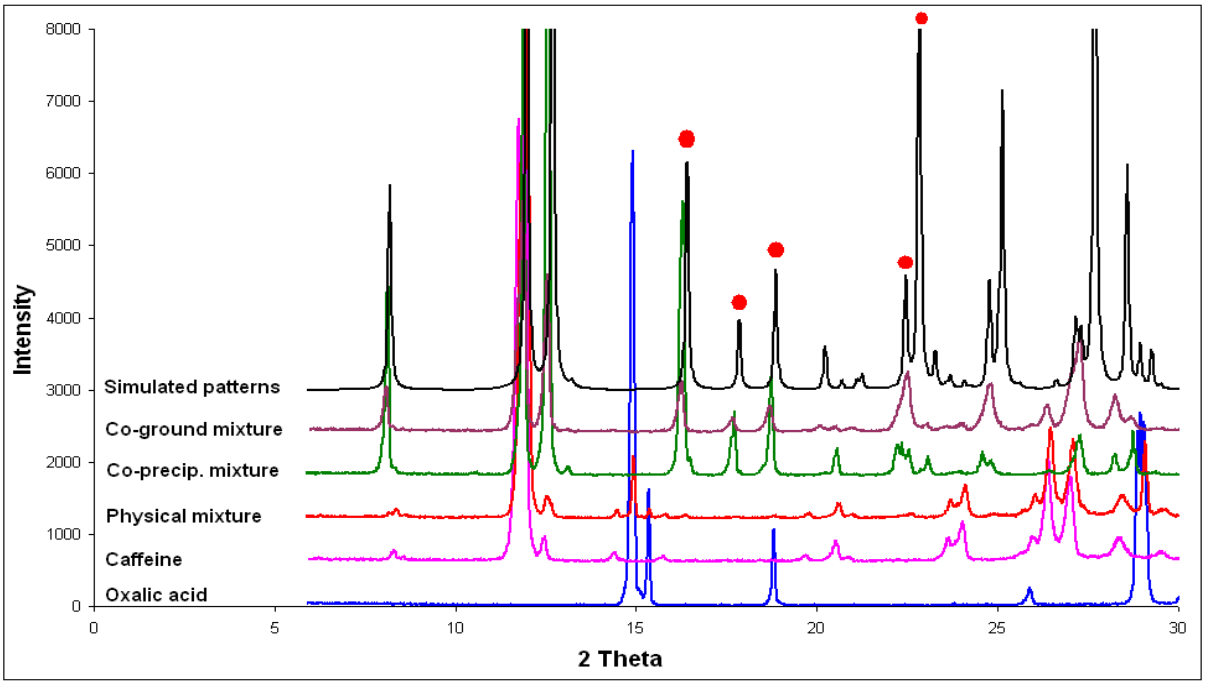

Figure 26: XRPD spectra of the caffeine/ oxalic acid system (Simulated patterns = patterns calculated from CSD using CIF format).

When caffeine was co-ground or co-precipitated with oxalic acid at a ratio of (2:1), new PXRD peaks at 2θ = 16.31°, 17.67 °, 22.53 ^{0} and 24.84° were observed (Figure 26). The peak positions of new peaks were different from those of the physical mixture and similar to those of the simulated patterns, indicating that caffeine may have formed a co-crystal with oxalic acid. These results are in agreement with results already published by Trask et

al. (2005), as they reported that caffeine/ oxalic acid co-crystal formed by both co-grinding and co-precipitation methods.

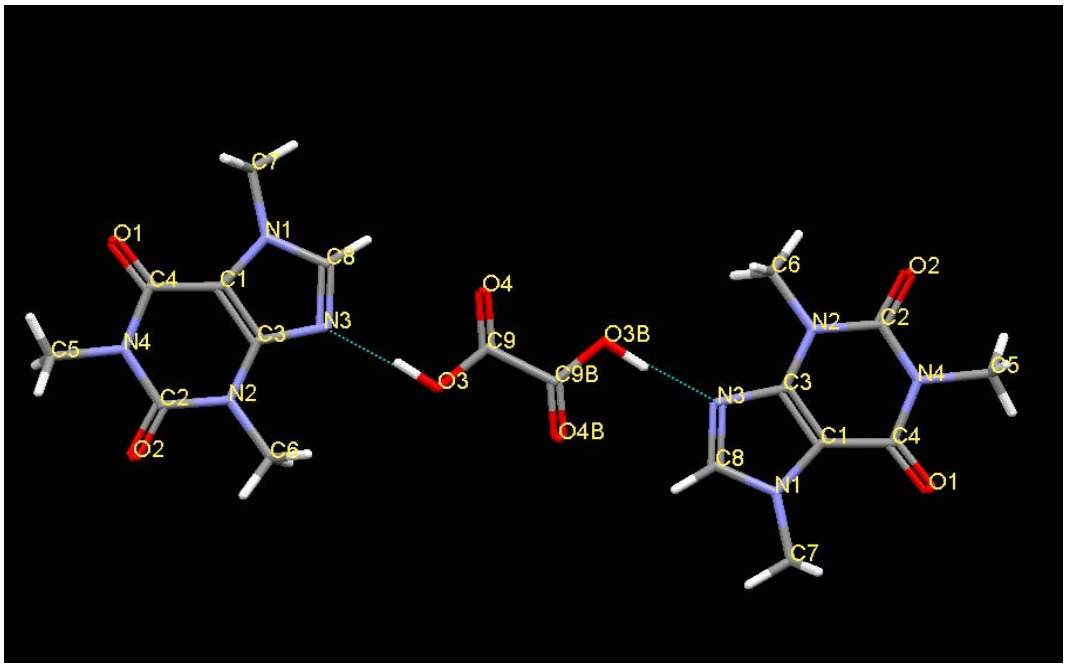

Figure 27: Molecular structure of the co-crystal of caffeine/ oxalic acid produced using software permitted from Cambridge crystallographic database using CIF format.

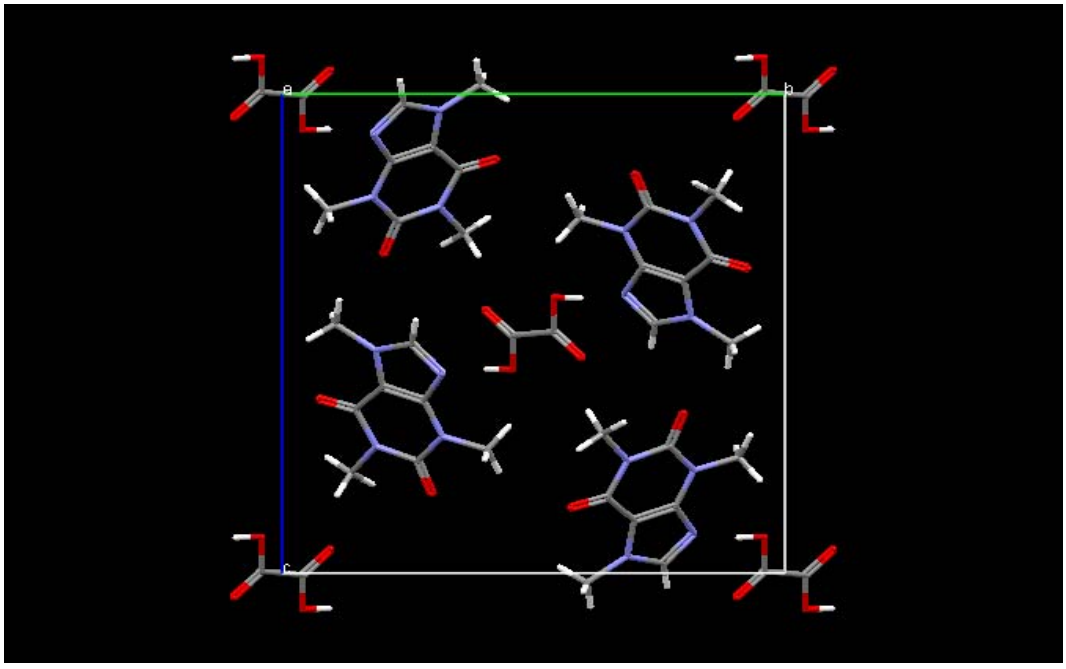

Figure 28: Crystal packing of caffeine/ oxalic acid co-crystal in the crystal lattice.

5.2.2. Raman spectroscopy results of wet co-grinding and co-precipitating physical mix induced caffeine/ oxalic acid acid co-crystal

Figures 29a, 29b, 29c and 29d illustrate the Raman spectra of caffeine/ oxalic acid system.

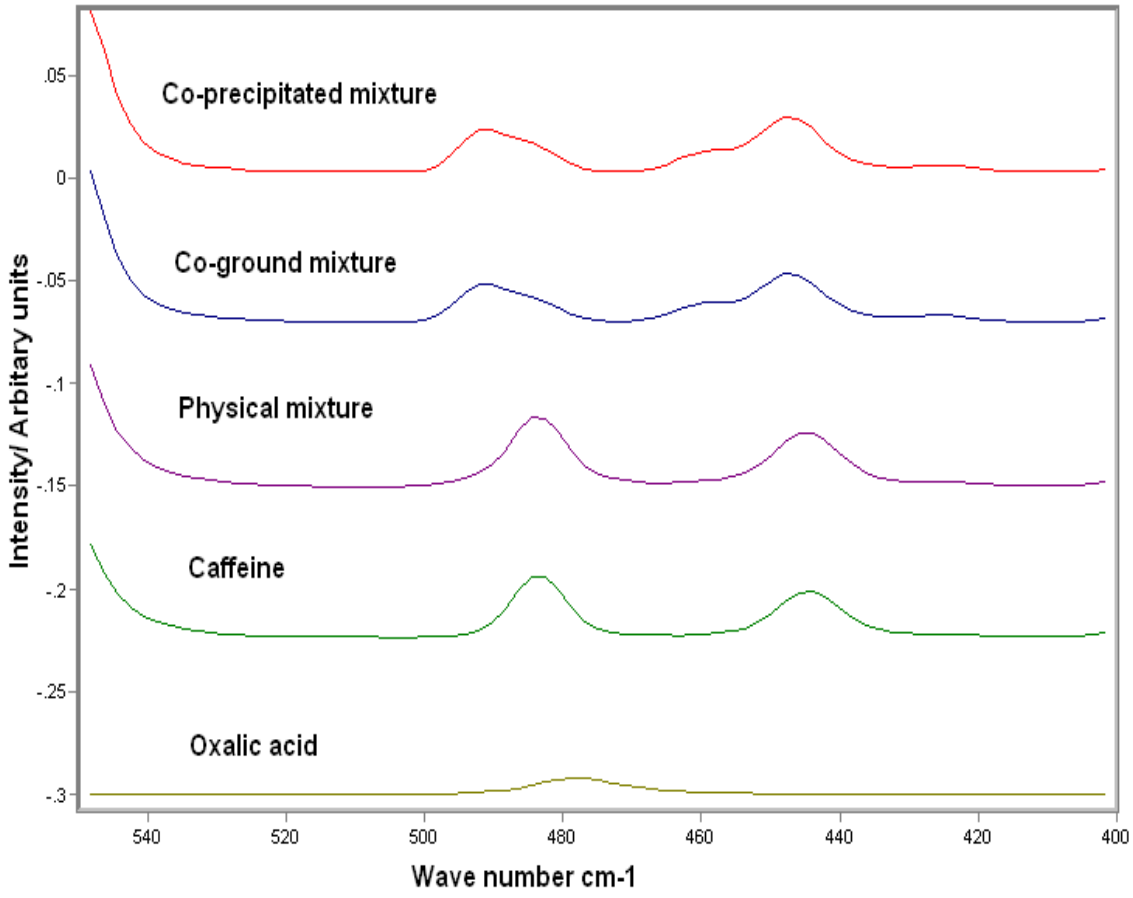

Figure 29a: Raman spectra of the caffeine/ oxalic acid system (550-400 cm^{-1}).

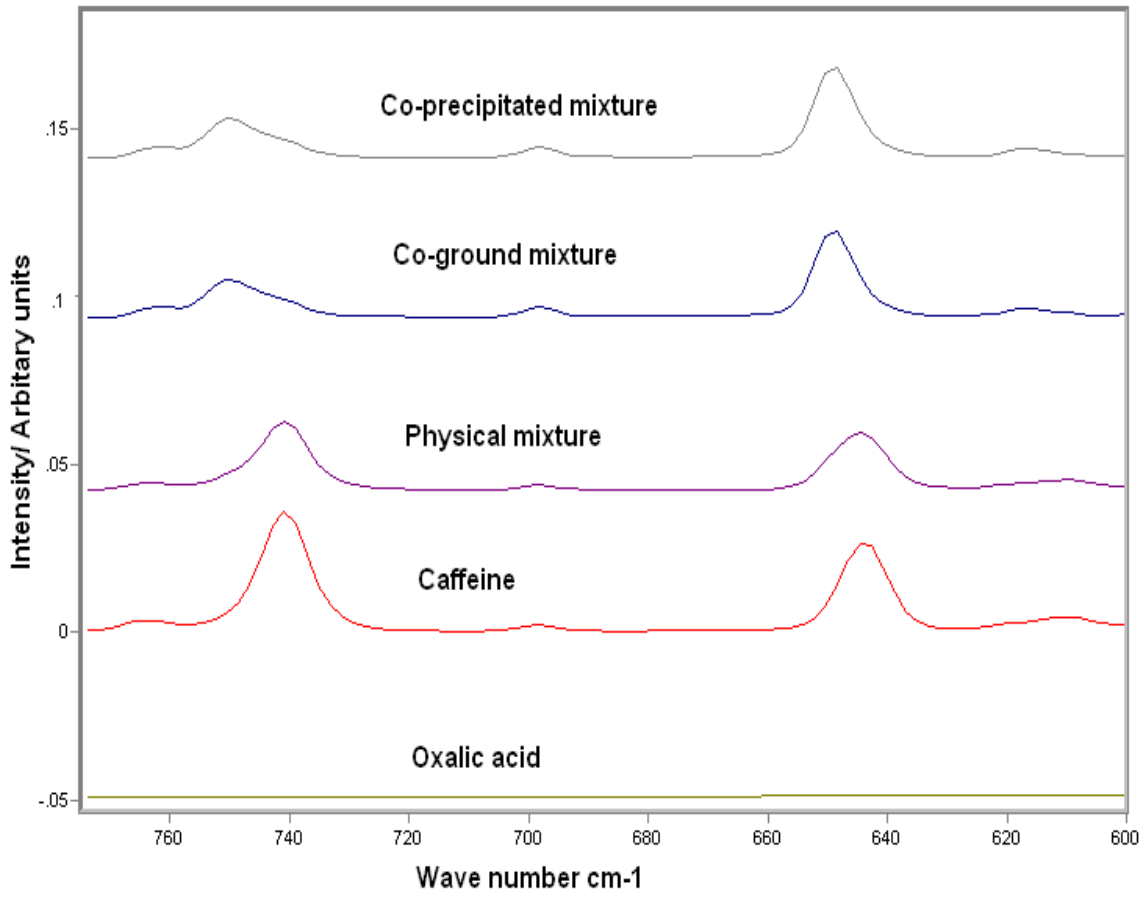

Figure 29b: Raman spectra of the caffeine/ oxalic acid system (775- 600 cm^{-1}).

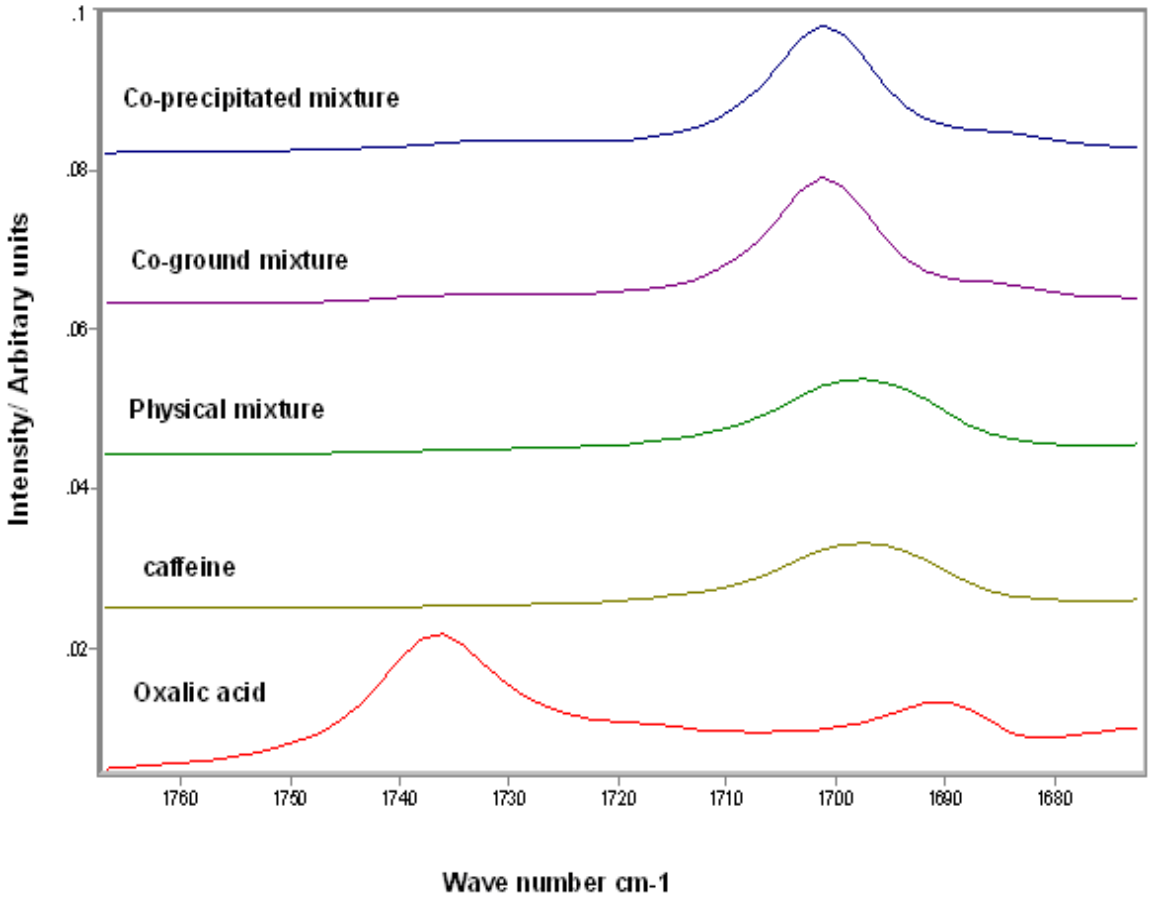

Figure 29c: Raman spectra of caffeine/ oxalic acid system (1767-1671 cm^{-1}).

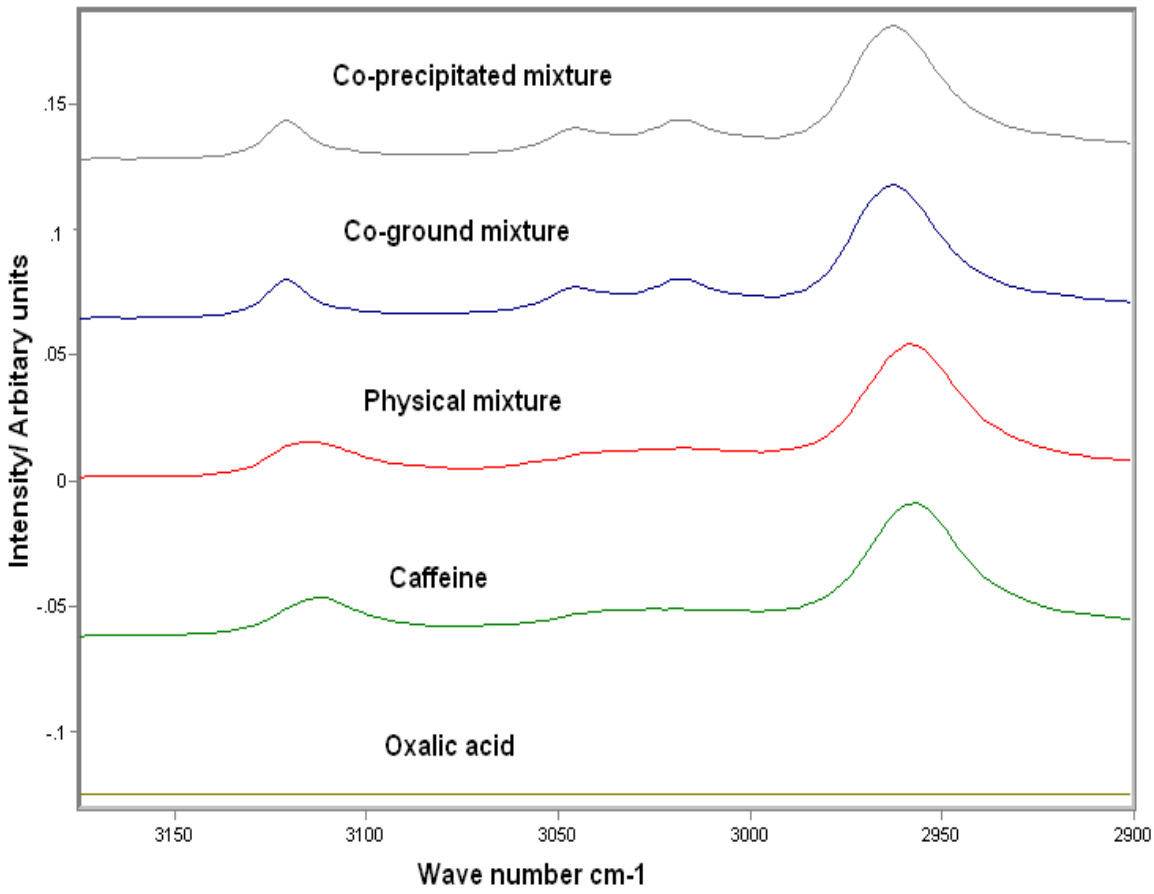

Figure 29d: Raman spectra of the caffeine/oxalic acid system (3175- 2900 cm^{-1}).

As shown in Figures 29a, 29b, 29c and 29d, there were no differences observed between the peak positions for the pure drugs and the physical mixture. However, the data clearly show noticeable differences between the physical mixture and both co-ground- and co-precipitated mixtures in the wave number regions 550- 400 cm^{-1}, 750-600 cm^{-1}, and 3175-2900 cm^{-1}.

The δ-pyrimidine ring vibrational bands of the caffeine at around 482 cm^{-1} and 641 cm^{-1} found in the caffeine crystal was shifted to higher wave numbers at around 489 cm^{-1} and

649 cm^{-1}, respectively in the co-crystals (Figure 29a). In addition, the δ-pyrimidine imidazole ring vibrational band of caffeine at around 741cm^{-1} was shifted to higher wave number at 749 cm^{-1}, respectively for the co-crystals (Figure 29b). In addition, the C═O stretch of oxalic acid at 1684 cm^{-1} disappeared (Figure 29c).

Furthermore, the CH3 and C=CH2 stretches of caffeine at 2957 cm^{-1} and 3114cm^{-1} were shifted to higher wave numbers at 2963 cm^{-1} and 3120 cm^{-1}, respectively (Figure 29d). These results are consistent with the XRPD results and suggest that caffeine may have formed a co-crystal with oxalic acid.

5.2.3. SEM results of caffeine/ oxalic acid co-crystal prepared by two methods

Figure 30 illustrates the SEM of the caffeine/ oxalic acid systems.

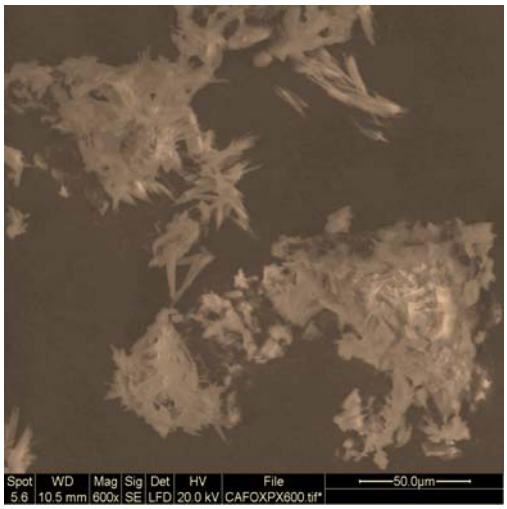

Physical mixture

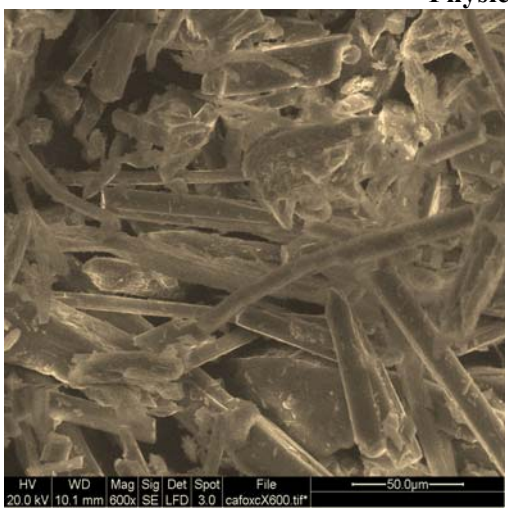

Co-precipitated mixture

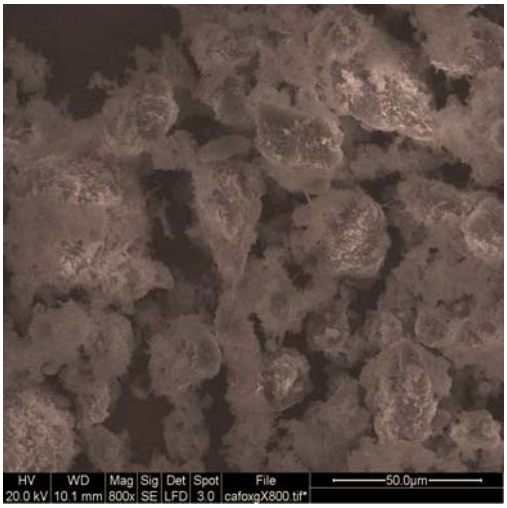

Co-ground mixture

Figure 30: SEM micrographs of caffeine/ oxalic acid system.

The SEM micrographs presented in Figure 30, clearly show that the physical mixture possesses particles different from that of the co-precipitated or co-ground mixture. On one hand, the co-precipitated mixture exhibited well-defined needle-like crystals that are

believed to be due to solvent crystallization. On the other hand, fully aggregated particles can be seen in the co-ground mixture. This suggests a phase transformation during both co-precipitation and co-grinding and indicates that caffeine may have formed a co-crystal with oxalic acid.

5.2.4. DSC results of the caffeine/ oxalic acid co-crystal prepared by two methods

The DSC traces of the caffeine/ oxalic acid system are presented in Figure 31.

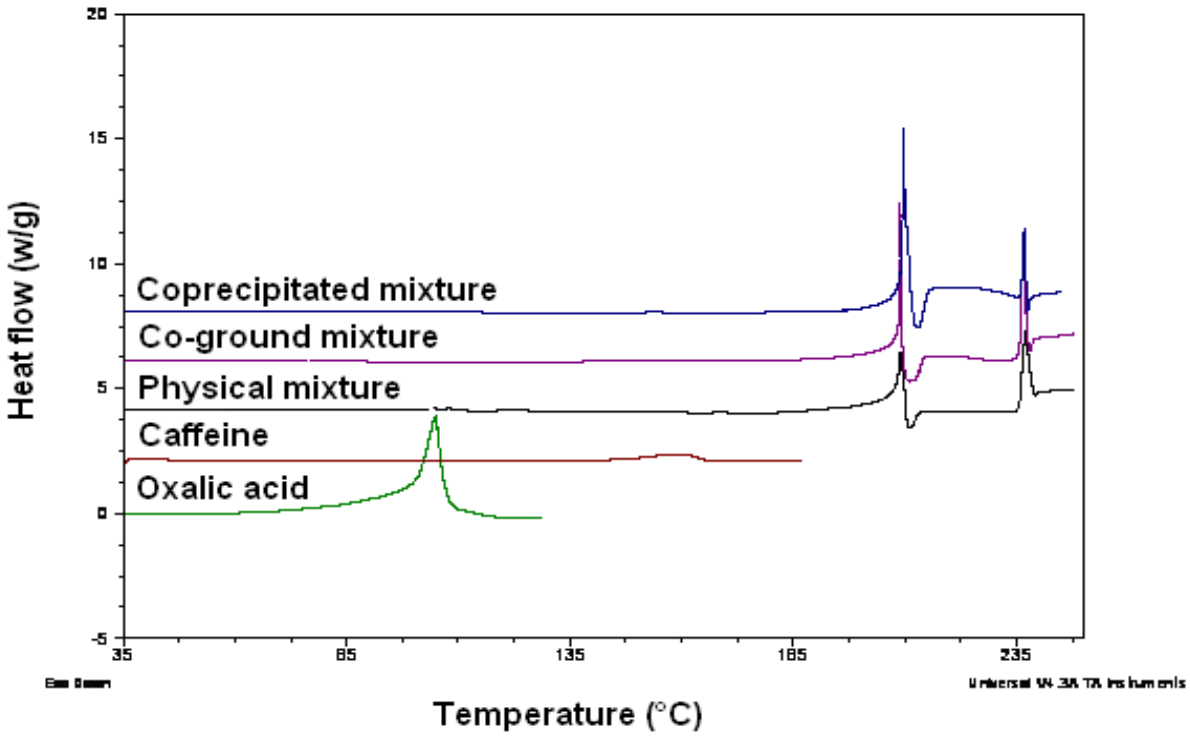

Figure 31: DSC traces of the caffeine/ oxalic acid system (sample weight 4-6mg, scan rate 10 °C/min).

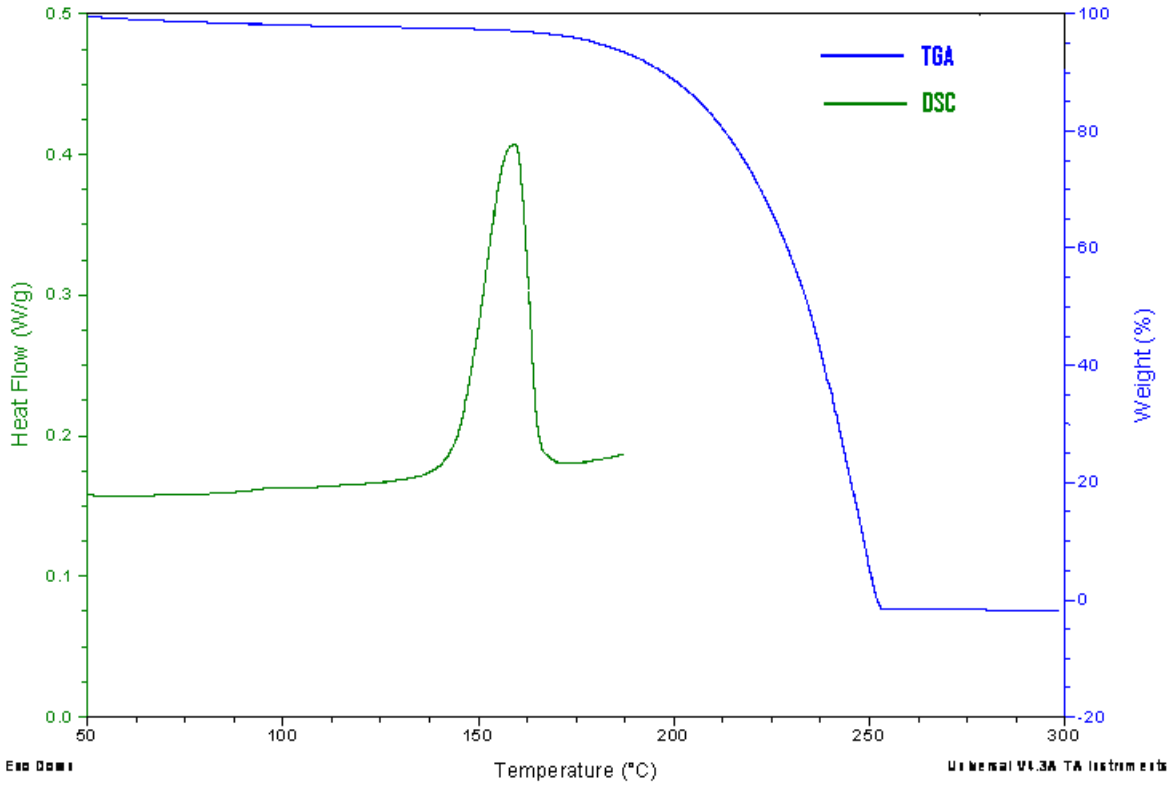

Figure 32: TGA and DSC curves of caffeine (sample weight 4-6mg, scan rate 10 °C/min).

As shown in Figure 31, the melting points (peak temperature) of caffeine and oxalic acid are 160 °C and 105 °C, respectively. Both the co-ground- and co-precipitated mixtures show an endothermic peak at 209 °C, followed by exothermic peak at 211°C and endothermic peak at 236°C. The first endothermic peak of both mixtures at 209°C is the suggested melting point of the caffeine/ oxalic acid co-crystal, however, the second endothermic peak at 237°C is supposed to be due to degradation and not the melting point of the caffeine (TGA and DSC of caffeine in Figure 32). This is in agreement with the literature, as it has been reported that the endotherms of caffeine between 225°C- 320°C are

due to fusion and evaporation respectively (Colacio-Rodriguez et al. 1983). On the other hand, the physical mixture shows an endothermic peak at 209 °C, followed by exothermic peak at 211°C and endothermic peak at 236°C, similar to those of co-ground and co-precipitated mixtures is indicative of some co-crystal formation during the heating process.

5.3. Effect of the co-crystallization of caffeine/ oxalic acid on mechanical properties of tablets and deformational properties of powders

5.3.1. Compactibility

Figure 33 presents the tensile strength of caffeine/ oxalic acid systems.

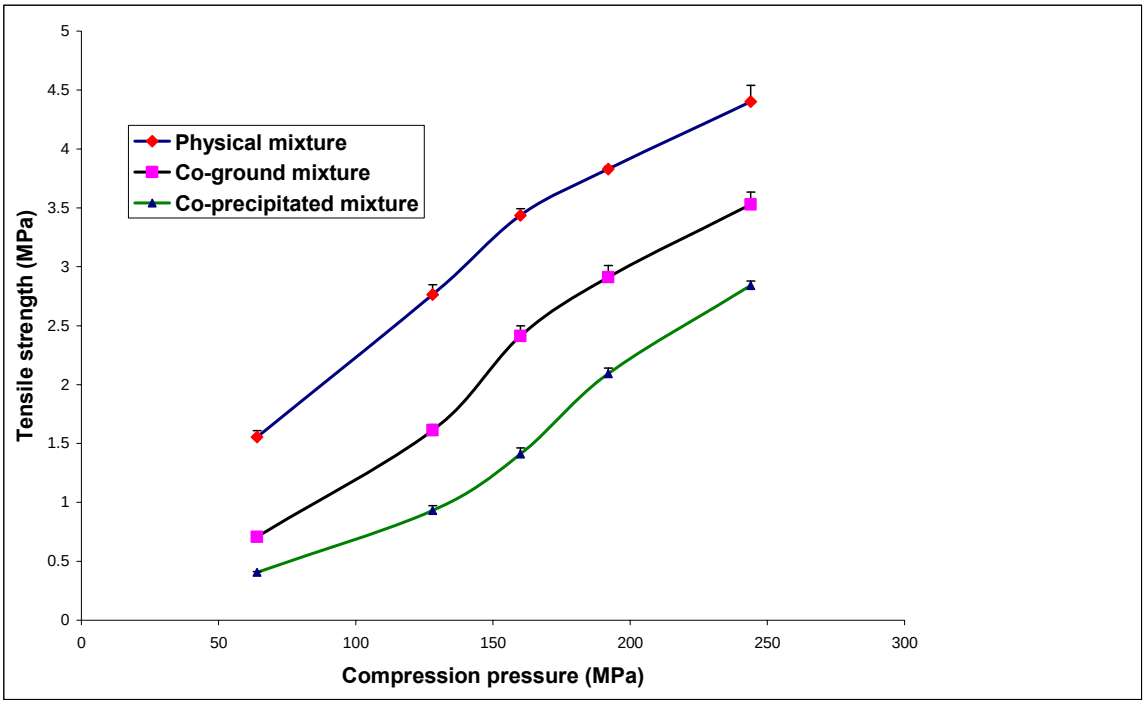

Figure 33: Tensile strength of the caffeine/ oxalic acid system obtained at a compression speed of 10 mm/s.

As shown in Figure 33, the tensile strength values of compacts produced from all mixtures increase proportionally with increasing compression force. However, tablets produced from

the physical mixture show the highest values of tensile strength, and thus the greatest compactibility among all tablets produced from other mixtures. On the other hand, tablets of the co-precipitated mixture show the lowest values of tensile strength and thus the smallest compactibility. The reason for this is understandable, as the needle-like crystals (Figure 30) are less dense (Table 8) and possess less contact points between them, which may result in smaller compactibility compared to other mixtures. The good compactibility of the physical mixture was possibly due to its lower porosity, as it possessed the highest bulk density (Table 8) compared with the co-ground or co-precipitated mixtures. It is unexpected that the compactibility of compacts of the co-ground mixture is smaller than that of the physical mixture as the tensile strength of compacts have been shown to increase with decreasing particle size (McKenna and McCafferty 1982; Morishima et al. 1994). However, this could result from the irregularity of particle of the physical mixture, which may have enhanced its compactibility.

Table 8: Densities of physical mixture, co-ground mixture and co-precipitated mixture of caffeine/ oxalic acid systems (mean ± SD, n =3).

Sample	True density (gm/cm^3)	Bulk density (gm/cm^3)
Physical mixture	1.5458 ± 0.0071	0.428 ± 0.025534
Co-ground mixture	1.7319 ± 0.0402	0.408 ± 0.00802
Co-precipitated mixture	1.6057 ± 0.0253	0.367 ± 0.01527

5.3.2. Compressibility

Figure 34 and Table 9 illustrate the Heckel plots and Heckel parameter of the caffeine/ oxalic acid system, respectively.

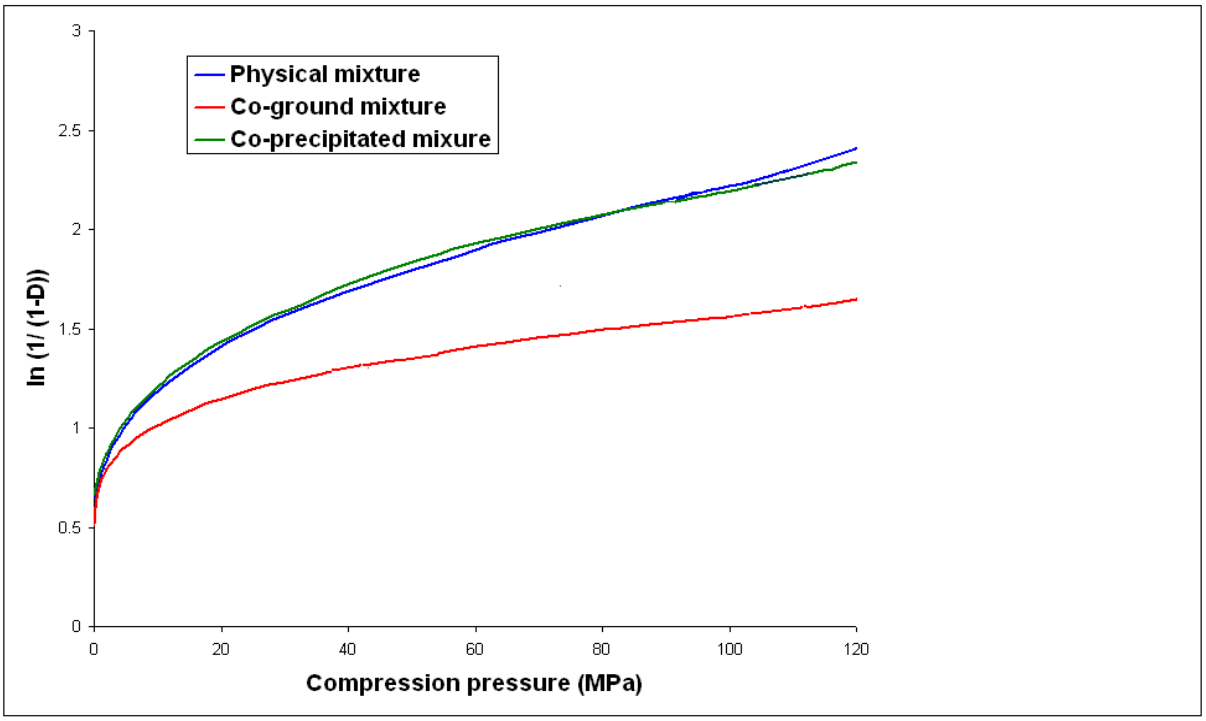

Figure 34: Heckel plots of the caffeine/ oxalic acid system at a compression force of 10 KN and a compression speed of 10 mm/s.

The results shown in Figure 34 and Table 9 clearly demonstrate that the patterns of Heckel plots of caffeine/ oxalic acid system are typical of Type 2 materials. In contrast to the caffeine/ malonic acid system (Figure 26 and Table 6), this system exhibited higher values of yield pressure. In addition, below 30 MPa, all mixtures show significant deviation from linearity, which indicates that the densification, up to this value of compression pressure

(30 MPa), occurs by fragmentation, while beyond this point, the particles will deform plastically, as indicated by perfect linearity.

However, the data presented in Figure 34 and Table 9, obviously show that the co-ground mixture possess the highest value of yield pressure and thus the smallest compressibility among all mixtures. In addition, the co-ground mixture was found to have the smallest particle slippage (D_0 = 0.397) compared with those of the co-ground or physical mixture. This indicates that the co-ground mixture was the least compressible, as the plastic deformation decreases with increasing yield pressure. The co-precipitated mixture, on the other hand, shows the best compressibility as indicated by the lowest value of the yield pressure. This may result from its crystal shape (Figure 30), as it has been reported by Garekani and co-workers (1999) that the compressibility (using the Heckel-plot) of polyhedral crystal was greater than that of thin plate-like crystal.

The data presented in Table 10 are consistent with the Heckel results, as the elastic recovery was greater for the co-ground mixture compared with those of the co-precipitated or the physical mixture. Both the physical and co-precipitated mixtures show similar yield pressure values and similar relative densities (Table 9), which may indicate similar densification behaviour of the powder during compression.

Table 9: Heckel parameters of caffeine/ oxalic acid system obtained at a compression speed of 10 mm/s and a compression force of 10 KN.

Sample	Yield pressure (MPa)	D_A	D_0	D_B
Physical mixture	76.9	0.595	0.478	0.117
Co-ground mixture	166	0.640	0.397	0.243
Co-precipitated mixture	74	0.692	0.483	0.209

D_0 = initial relative density, D_A = 1- e $^{-A}$ is the extrapolated relative density from the intercept (A) of the linear portion of the Heckel plot, and D_B = increase in relative density due to particle arrangement.

Table 10: Elastic recovery of tablets produced from the caffeine/ oxalic acid systems obtained at a compression speed of 10 mm/s and a compression force of 10 KN.

Sample	t_1 (mm)	t_2 (mm)	Elastic recovery E (%)
Co-precipitated mixture	2.99	3.14	5.0
Physical mixture	3.09	3.26	5.5
Co-ground mixture	3.11	3.28	5.5

t_1 = minimal thickness of the powder bed in the die, and t_2 = is the thickness of the recovered tablet.

5.3.3. General Discussion

In this chapter, we have shown that the methods of preparation of caffeine/ oxalic acid co-crystals affected the tableting properties. Both methods produced the same co-crystal structure as indicated by Raman, XRPD, DSC and SEM.

In the next chapter, we evaluate a more representative drug-like model: theophylline and malonic acid.

6. Solid-state characterization of theopylline/ malonic acid; Evaluation of compaction properties

6.1. Introduction

The availability of good hydrogen bond donors and acceptors is of considerable consequence for the design of co-crystals (Etter 1990). It has been documented, from systematic studies of co-crystals that all hydrogen bond donors and acceptors are utilized in hydrogen bond formation. In addition, for the design of a co-crystal, hydrogen bond donors will be inclined to interact with good hydrogen acceptors in a given crystal structure (Etter 1990). From a formulation perspective, theophylline represents a challenge, as is known to interconvert between crystalline hydrate and monohydrate forms as a function of relative humidity (RH) (Trask et al. 2006). It has been reported that the crystalline hydrate formation, could probably confuse the design of a reliable, reproducible formulation process of an API in the drug development process (Kahnkari and Grant 1995). The study of theophylline as a model API is of a great interest, as its hydrate/ anhydrate interconversion is demonstrated by many researchers (Agbada and York 1994; Duddu et al. 1995; Hermann et al. 1988; Otsuka and Kaneniwa 1988; Phadnis and Suryanayanan 1997; Puttipipatkhachorn et al. 1990; Rodriguez-Hornedo et al. 1992; Shefter et al. 1973; Suihko et al. 1997; Suzuki et al. 1989; Ticehurst et al. 2002).

By comparing theophylline with its chemical analogue caffeine, co-crystal design of theophylline is more complex. The hydrogen bonding competence of theophylline includes the numerous hydrogen bond acceptors it shares with caffeine; in addition, it has one less methyl group than caffeine, and possesses a good N-H hydrogen bond donor. Theophylline

is regarded as both weakly acidic and weakly basic, with pK_a and pK_b values of 8.6 and 11.5, respectively (Cohen 1975).

Suihko and co-workers intensively investigated the impact of solid-state transformations of theophylline on tableting properties, as they reported that the densification and compact properties were linked with its dynamic solid-state transformation (Suihko et al. 2001).

However, in the current study, the solid-state of theophylline/ malonic acid co-crystal (prepared using the methods outlined in sections 2.2.10 and 2.2.11) was characterized. In addition, the impact of the co-crystallization on the subsequent tableting behaviour has been intensively investigated.

6.2. Results and discussion

6.2.1. XRPD of a theophylline/ malonic acid co-crystal prepared by two methods

Figure 35 illustrates the XRPD spectra of the theophylline/ malonic acid system.

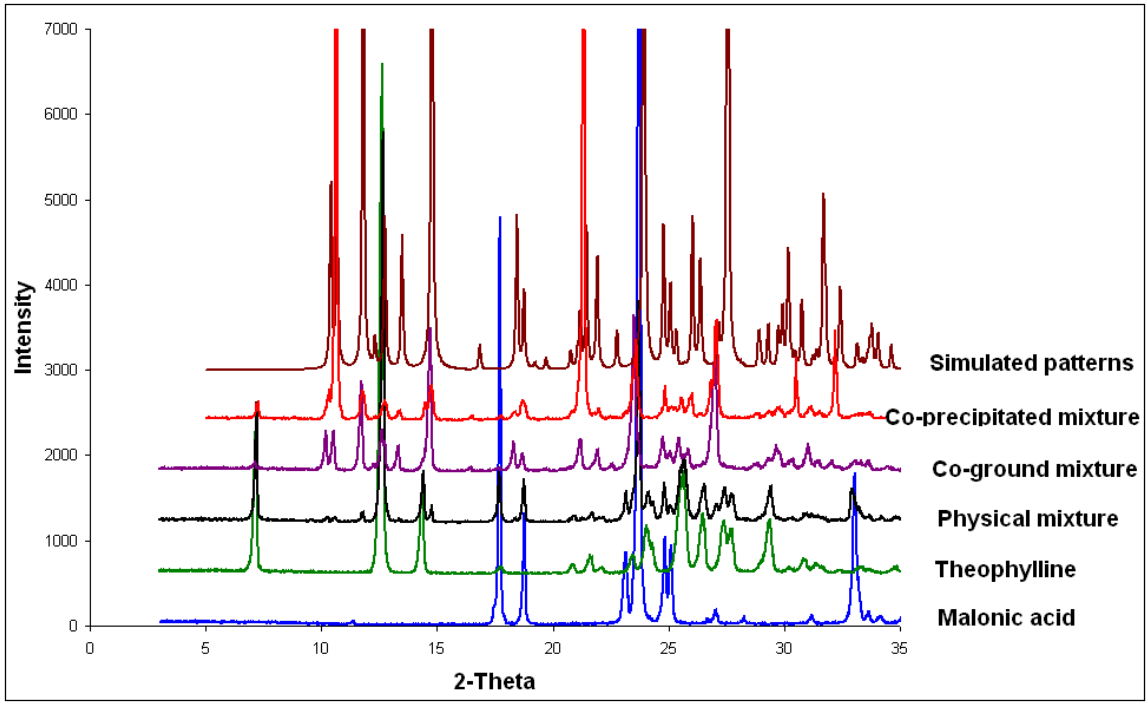

Figure 35: XRPD spectra of the theophylline/ malonic acid system.

As shown in Figure 35, when theophylline was co-ground or co-precipitated with malonic acid, new XRPD peaks at 2θ= 10.42°, 11.84°, 18.35°, and 21.25° were observed. The peak positions of the new peaks were different from those of the physical mixture, indicating that theophylline may have formed a co-crystal with malonic acid. However, a small peak at 2θ= 7.3°, appears in the co-precipitated mixture corresponding to theophylline hydrate, is indicative of a co-crystal formation with unconverted theophylline hydrate. These results are in agreement with results already published by Trask and co-workers (2006). They reported that the packing of theophylline/ malonic acid co-crystal demonstrates the primary intermolelcular O─H···N bonds as well as the theophylline dimmer formation via secondary N─H···O bonds (Figure 36). Further, the 1:1 stoichiometry was observed, which means that

only one of the acid groups bonds of the theophylline leaving the other to participate in a bifracted hydrogen bond with the two carbonyls of a neighbouring acid (Figure 37).

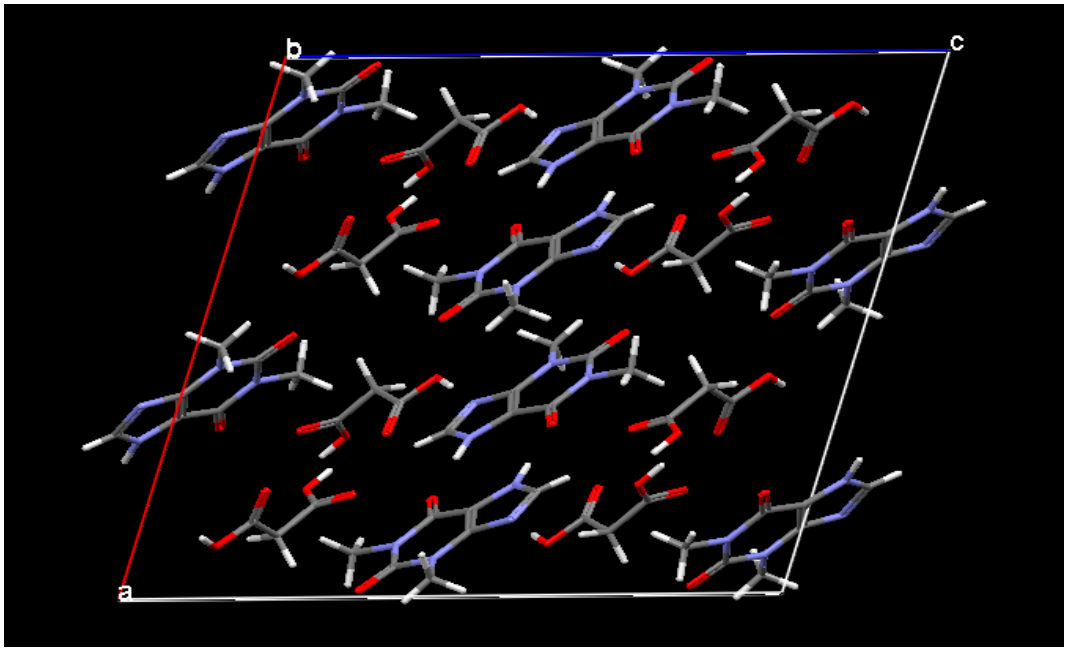

Figure 36: Crystal packing of theophylline/ malonic acid system.

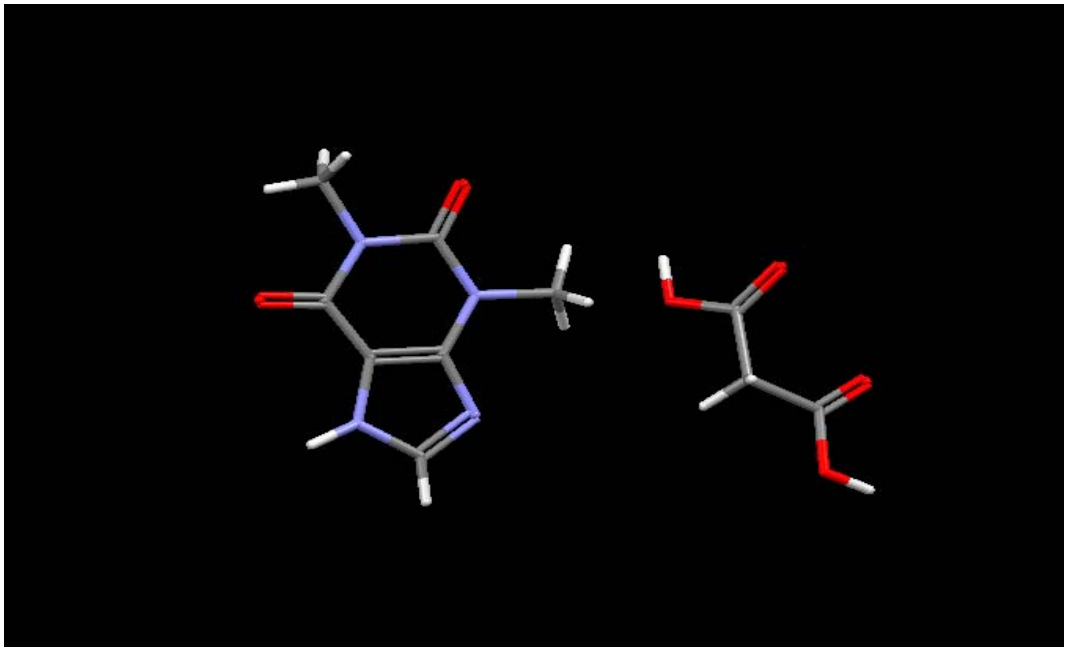

Figure 37: Molecular structure of theophylline/ malonic acid system.

6.2.2. Raman spectroscopy results of co-grinding and co-precipitating physical mix induced theophylline/ malonic acid co-crystal

Figures 38a, 38b, 38c and 38d illustrate the Raman spectra of theophylline/ malonic acid system.

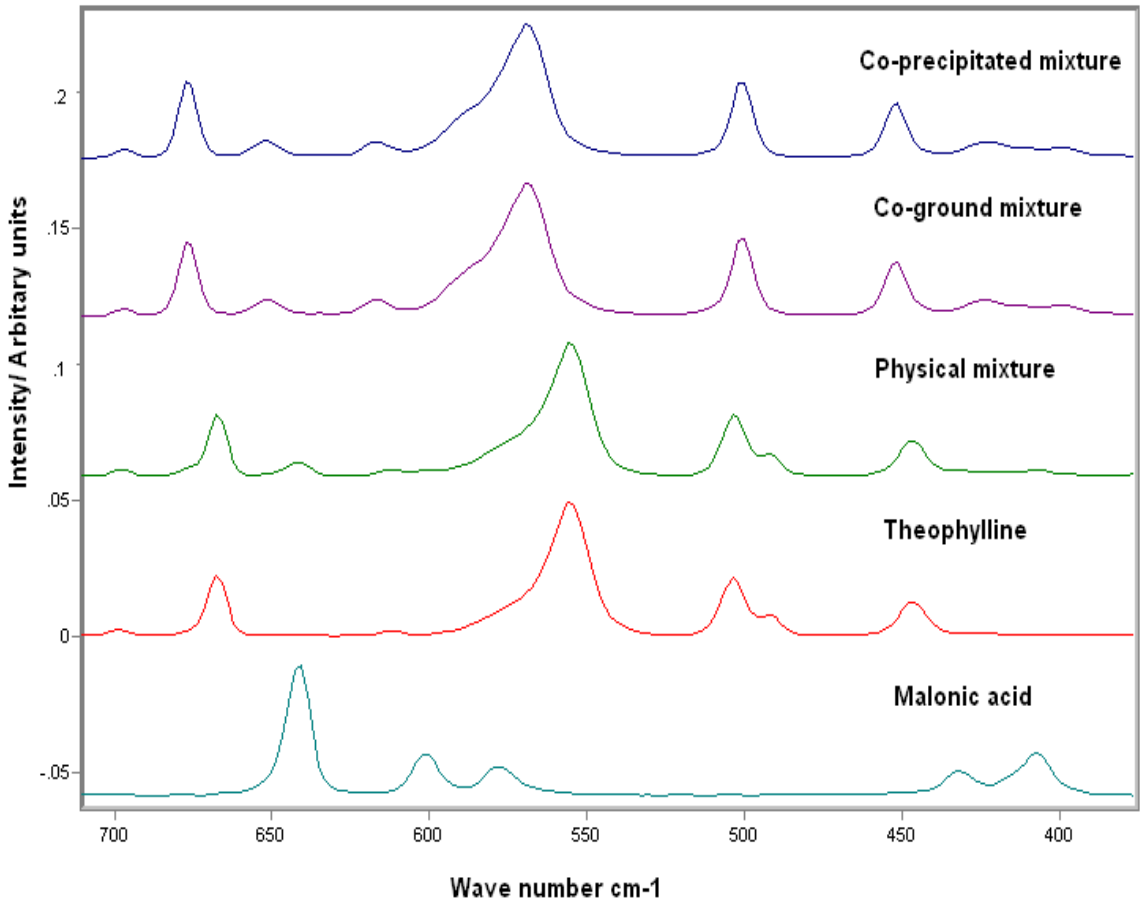

Figure 38a: Raman spectra of the theophylline/ malonic acid system (712-330 cm^{-1}).

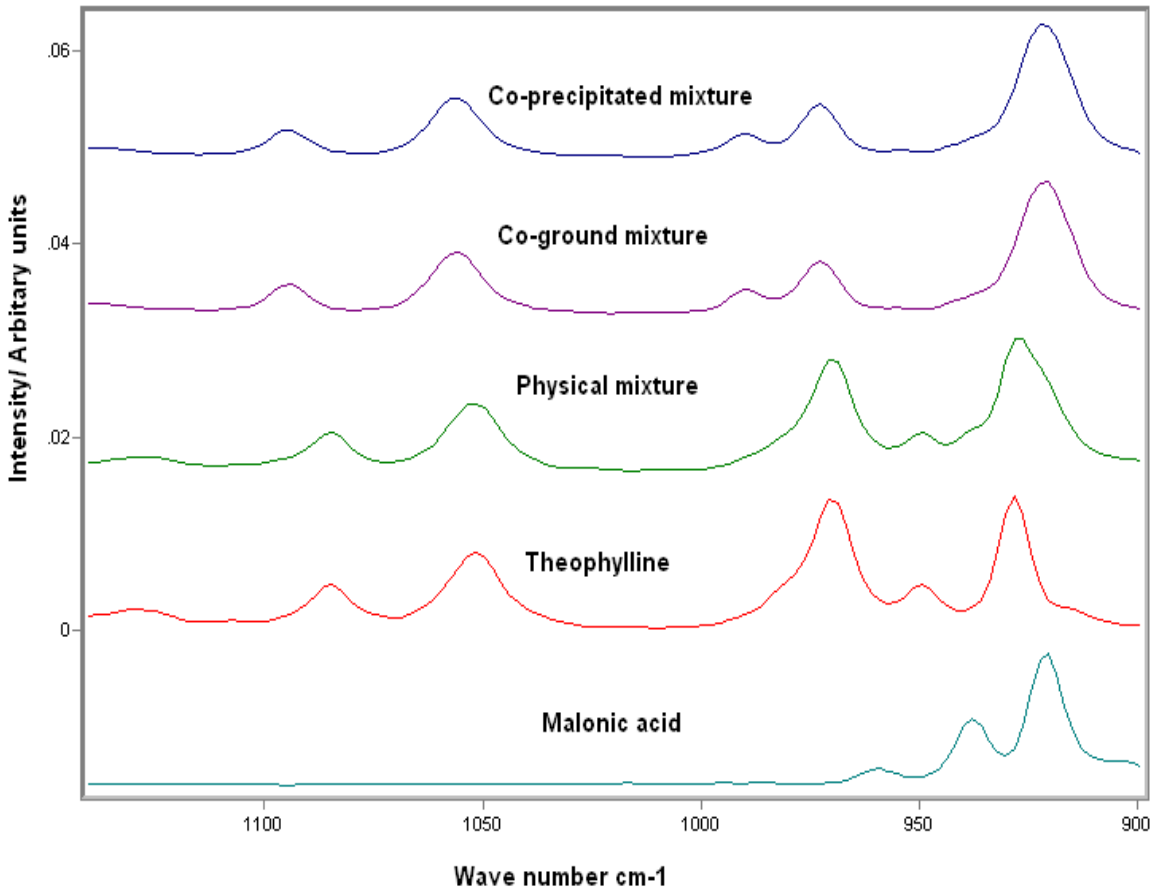

Figure 38b: Raman spectra of the theophylline/ malonic acid system (1141-897 cm^{-1}).

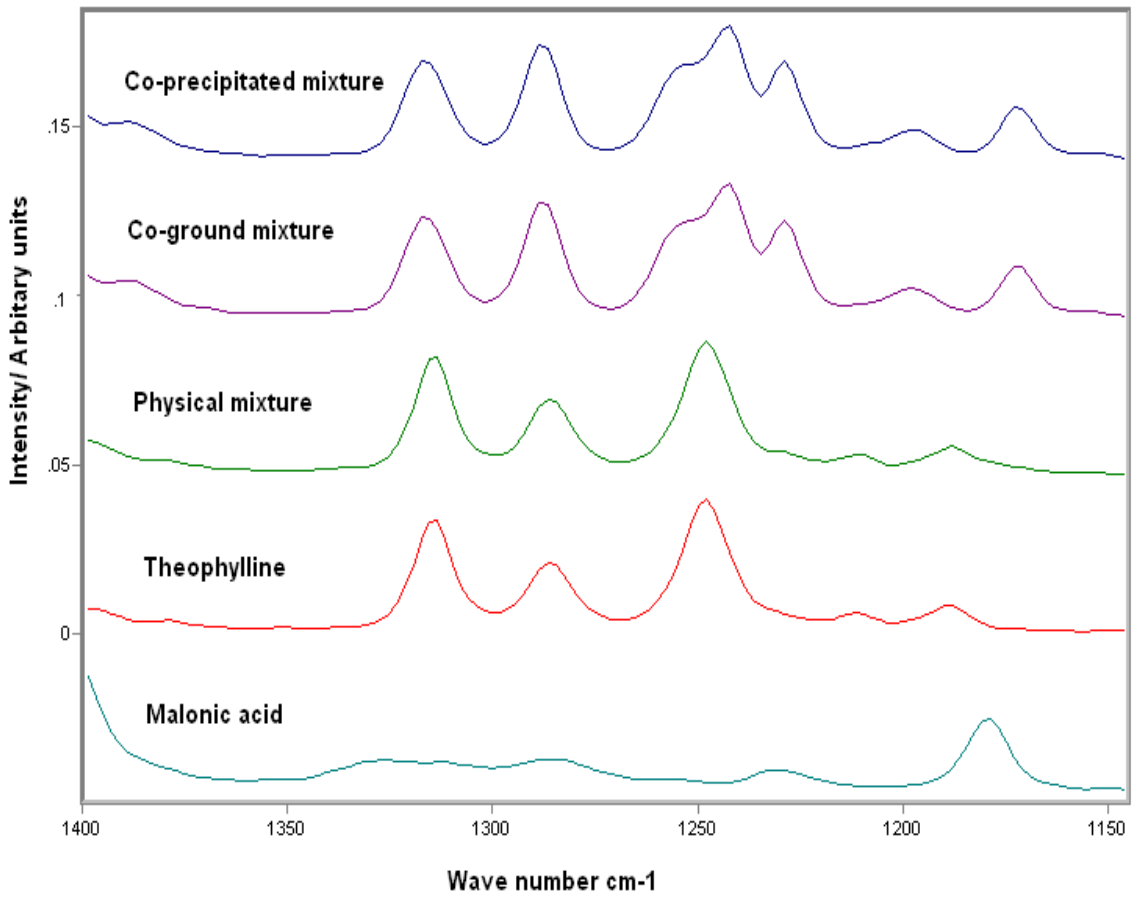

Figure 38c: Raman spectra of the theophylline/ malonic acid system (1400- 1145 cm^{-1}).

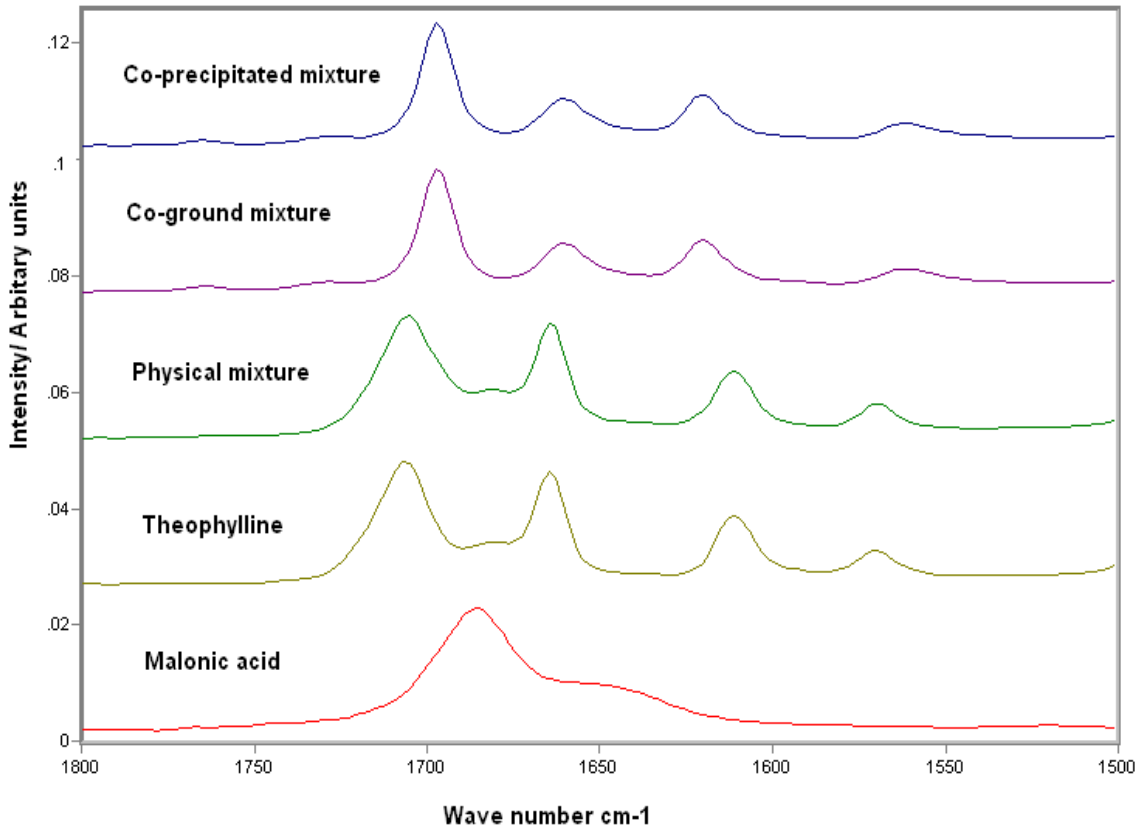

Figure 38d: Raman spectra of the theophylline/ malonic acid system (1800- 1500 cm^{-1}).

The Raman data presented in Figure 38a, 38b, 38cand 38d, clearly show noticeable differences between the physical mixture and both co-ground- and co-precipitated mixtures in the wave number regions (712-380 cm^{-1}), (1355-858 cm^{-1}) and (1740-1526 cm^{-1}). The δ-pyrimidine ring vibrational bands of theophylline at around 447 cm^{-1}, 493 cm^{-1}, 555 cm^{-1}, and 668 cm^{-1}, found in the intact crystal were shifted to higher wave numbers at 451 cm^{-1}, 500 cm^{-1}, 569 cm^{-1}, and 676 cm^{-1}, respectively. In addition, the δ-pyrimidine imidazole ring vibrational band of caffeine at around 741cm^{-1} was shifted to higher wave number at 749 cm^{-1}. In addition, the CH─N bands of theophylline at 1052 cm^{-1} and 1085 cm^{-1} were shifted to higher wave numbers at 1056 cm^{-1} and 1094 cm^{-1}, respectively. Furthermore, the C═C stretch of theophylline at 1611 cm^{-1}, was shifted to higher wave number at 1620 cm^{-1}. Further, the C═O stretch of malonic acid at 1684 cm^{-1} disappeared, while the C═O of

theophylline at 1707 cm^{-1} was shifted to lower wave number at 1697 $cm^{-1.}$ These results suggested that theophylline might have formed a co-crystal through both grinding and co-precipitation.

6.2.3. SEM results of theophylline/ malonic acid co-crystal prepared by two methods

Figure 39 presents the SEM micrographs of the theophylline/ malonic acid system.

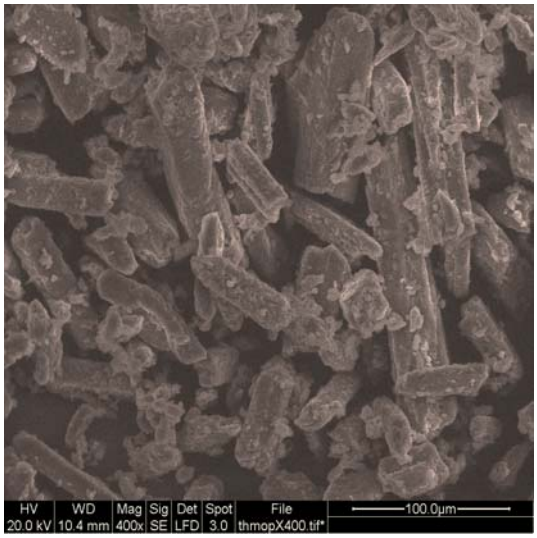

Physical mixture

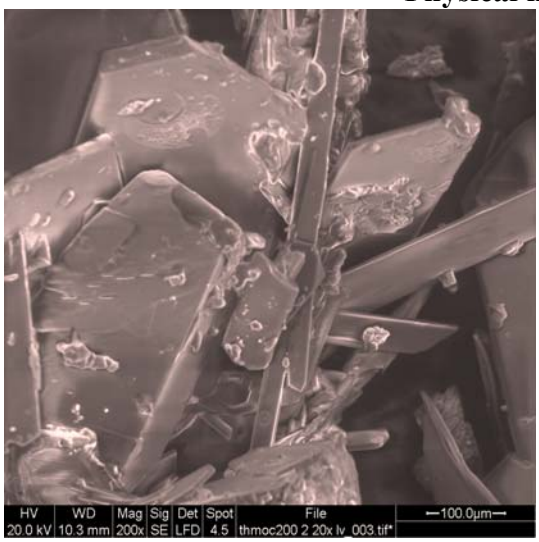

Co-precipitated mixture

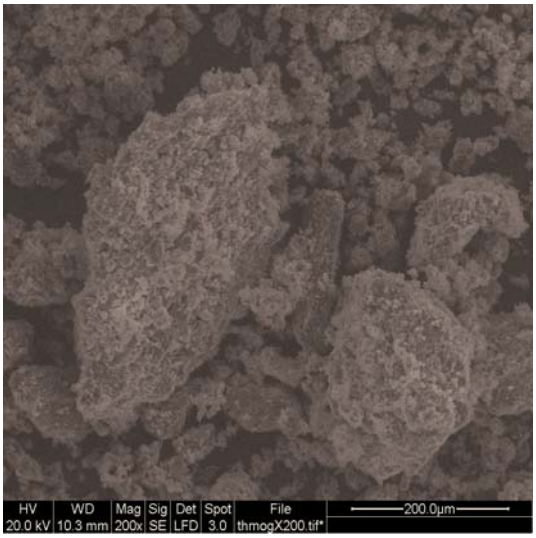

Co-ground mixture

Figure 39: The SEM micrographs of the theophylline/ malonic acid system.

From Figure 39, it can be seen that physical mixture possesses SEM micrograph, very different from either co-ground or co-precipitated mixtures. The SEM micrograph of the co-precipitated mixture possesses relatively thick plate-like crystals with flat surfaces, while SEM micrograph of the co-ground mixture exhibits aggregated particles with rough surfaces. These results are consistent with XRPD and Raman, and confirm a phase transformation via both co-grinding and co-precipitation.

6.2.4. DSC results of a theophylline/ malonic acid co-crystal prepared by two methods

Figure 40 shows the DSC traces of the theophylline/ malonic acid system in its various forms.

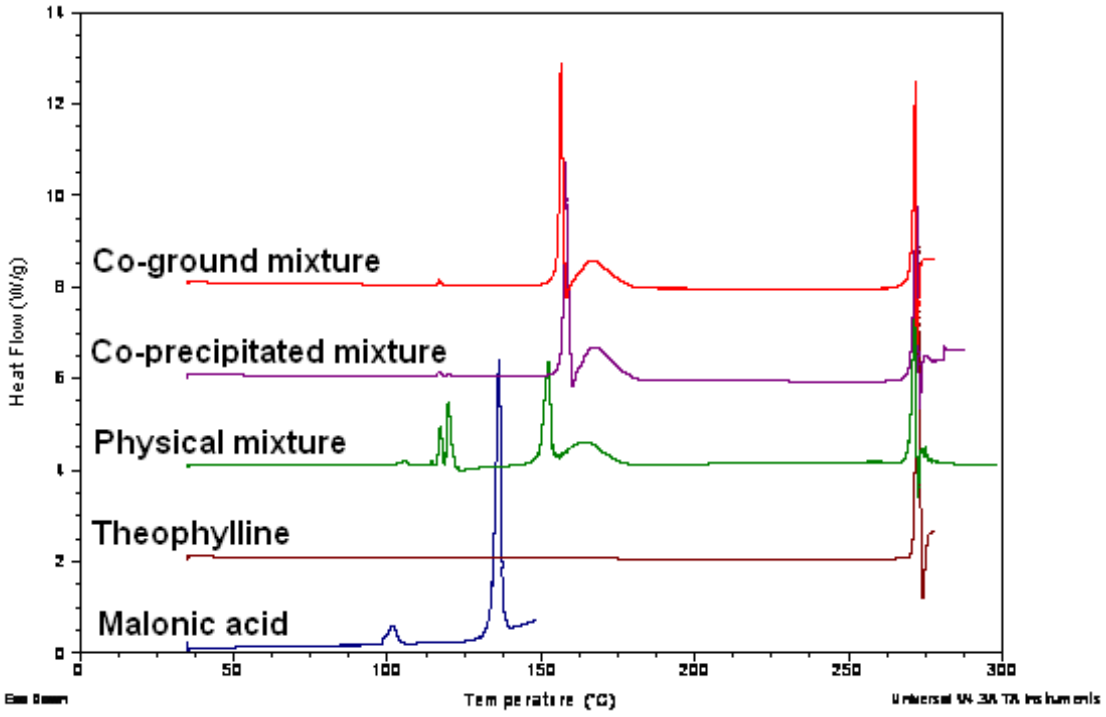

Figure 40: DSC traces of the theophylline/ malonic acid system (sample weight (4-6mg, scan rate =10 °C/min.).

As presented in Figure 40, the melting points (peak temperature) of theophylline and malonic acid are 272°C and 136°C, respectively. The physical mixture firstly shows two small endothermic peaks at 117°C and 120°C, followed by an endothermic peak at 152°C. Both the co-precipitated and co-ground mixtures show melting points at 157°C and 156°C respectively. These results indicated that theophylline formed a co-crystal with malonic acid by these methods. In the case of a physical mixture, the endothermic peak at 152°C, nearly similar to that of the co-ground mixture is indicative of formation of co-crystal during the heating process. However, the first two small peaks of the physical mixture at 117°C and 120°C are thought to be due to evaporation and in agreement with the TGA curve (Figure 41), and the endothermic reaction at 170°C can be related with further water loss as reported by Picker (Picker 2001).

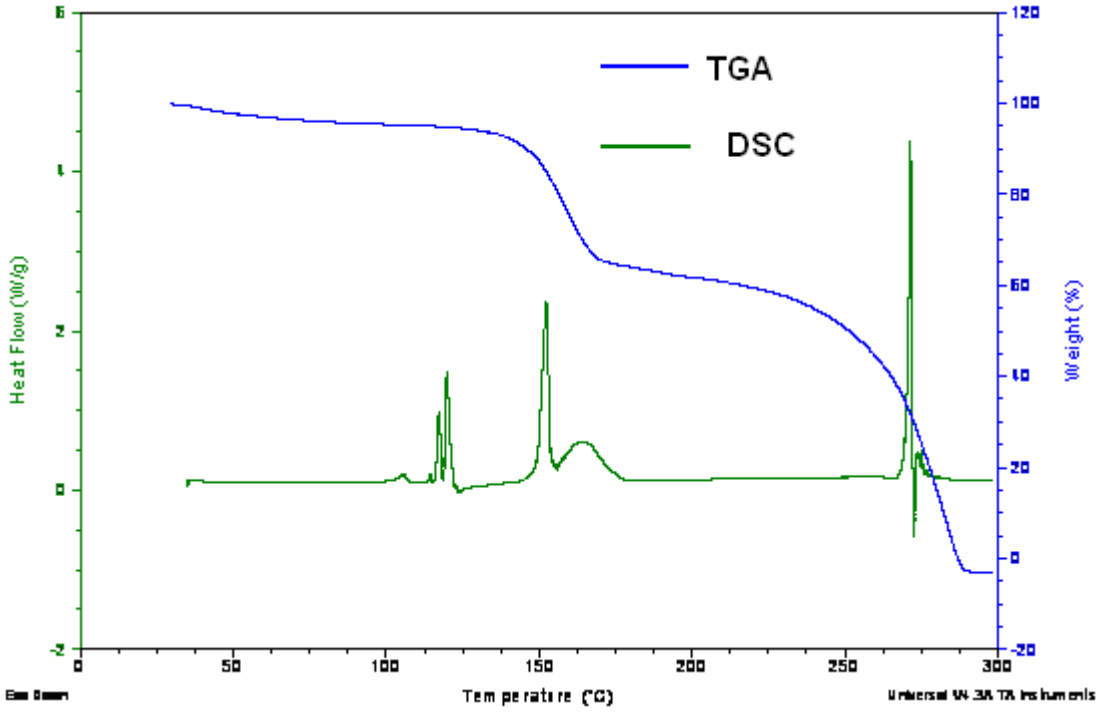

Figure 41: TGA and DSC of the physical mixture of theophylline/ malonic acid.

6.3. Effect of co-crystallization of theophylline with malonic acid on tableting properties

6.3.1. Compactibility

The tensile strengths of compacts of the theophylline/ malonic acid system are illustrated in Figure 42.

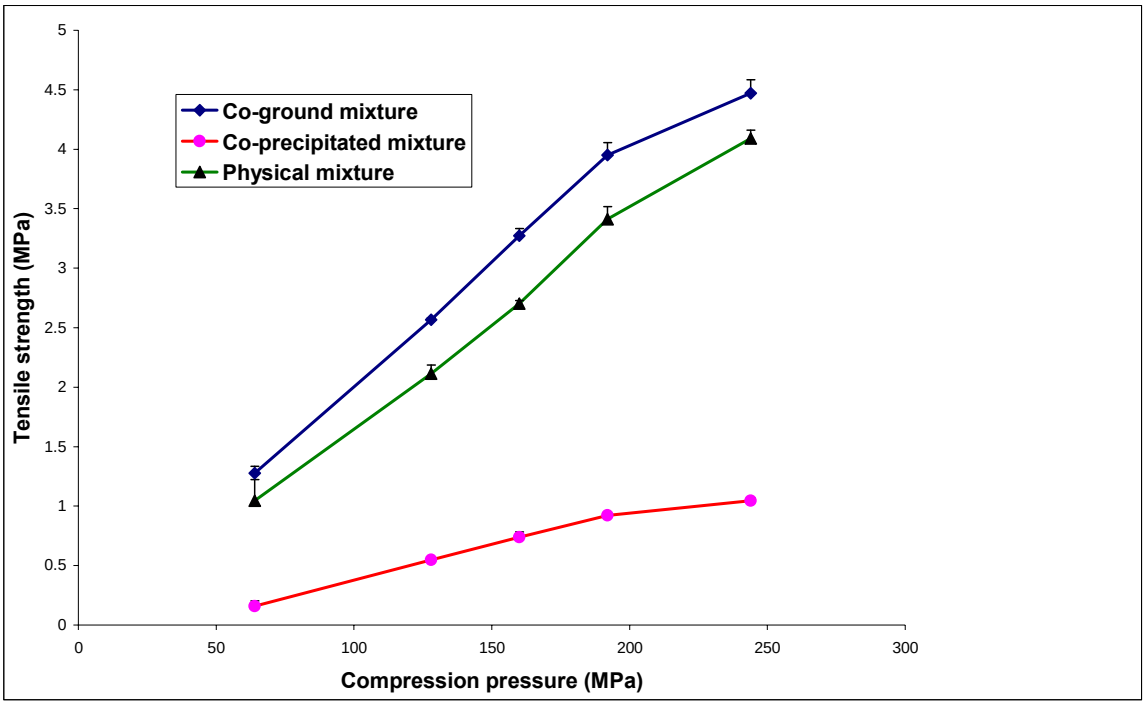

Figure 42: Tensile strength of the theophylline/ malonic acid system obtained at a compression speed of 10mm/ s.

The compaction properties of the co-precipitated, co-ground and physical mixtures of theophylline/ malonic acid system were compared, as presented in Figure 42. It can be seen that the tensile strength values of tablets produced from all mixtures increased with increasing compression force. Tablets produced from the co-ground mixture showed higher values of tensile strength compared to those of co-precipitated and physical mixtures. The

tablets were intact and showed no capping or lamination, either on ejection or during crushing strength test. This was may be due to the small particle size of the co-ground mixture that results from grinding, as the small size generally has good compactability. It has been reported that the tensile strength of compacts increases as the particle size decreases (McKenna and McCafferty 1982; Morishima et al. 1994). It is also possible that the smaller crystals have more contact points between them, and can be compacted more tightly than larger crystals. The lower porosity of the co-ground mixture may have contributed to its better compactibility, as it showed the highest bulk density among all other mixtures (Table 11). However, the difference in tensile strength values between the mixtures may result from crystal morphology, as the plate-like crystals of the co-precipitated mixture shows the least compressibility (Figure 39). The good compactability of the co-ground mixture is in agreement with the theory that smaller particles produce a greater density and a greater number of contact points for inter-particulate bonding (Rhines 1947).

Table 11: Densities of physical mixture, co-ground mixture and co-precipitated mixture of theophylline/ malonic acid system (mean ± SD, n =3).

Sample	True density (gm/cm^3)	Bulk density (gm/cm^3)
Physical mixture	1.4988 ± 0.0079	0.2860 ± 0.0010
Co-ground mixture	1.4823 ± 0.0031	0.4767 ± 0.0030
Co-precipitated mixture	1.5111 ± 0.0039	0.3763 ± 0.0025

6.3.2. Compressibility

The Heckel plots of theophylline/ malonic acid system are presented in Figure 43.

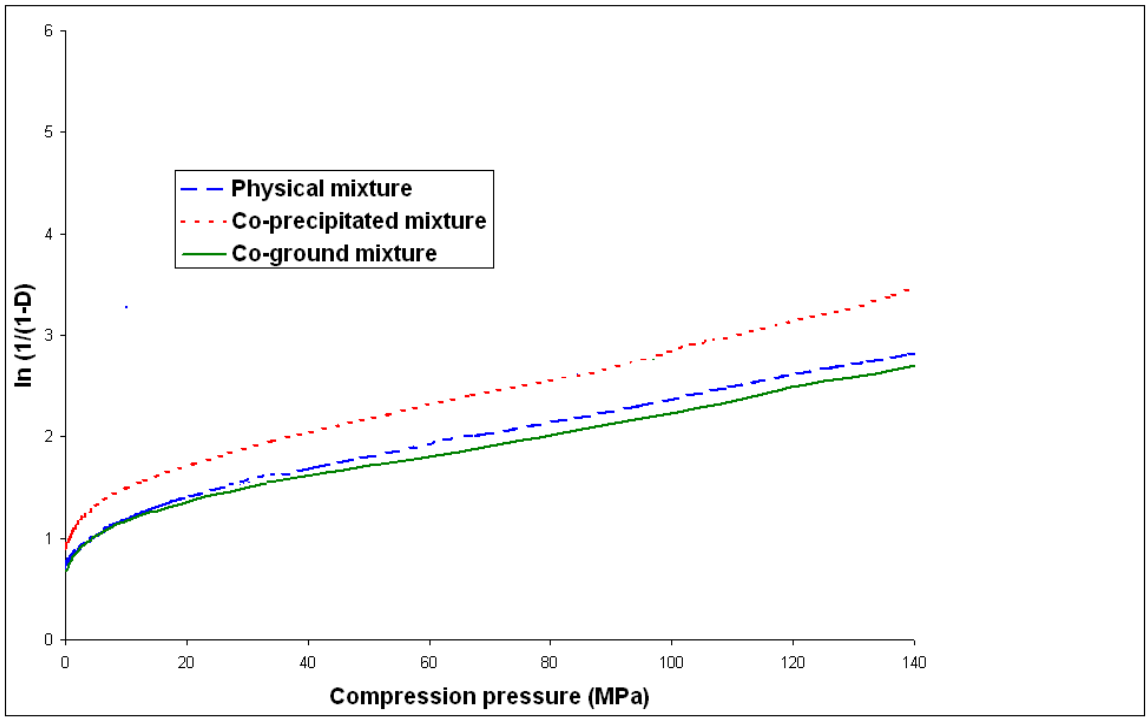

Figure 43: Heckel plots of the theophylline/ malonic acid system obtained at a compression force of 12.5 KN and a compression speed of 10mm/ s.

Table 12: Heckel parameter of different mixtures of theophylline/ malonic acid system: (obtained at a compression speed of 10 mm/s and a compression force of 10 KN).

Sample	Yield pressure (MPa)	D_A	D_0	D_B
Physical mixture	83	0.698	0.489	0.209
Co-ground mixture	87	0.686	0.492	0.194
Co-precipitated mixture	80	0.757	0.587	0.17

D_0 = initial relative density, $D_A = 1 - e^{-A}$ is the extrapolated relative density from the intercept (A) of the linear portion of the Heckel plot, and D_B increase in relative density due to particle arrangement.

The relative volume changes during the early stage (0-120 MPa) of the compression event were recorded for each of the physical, co-ground and the co-precipitated mixtures.

The results of the Heckel data are presented in Figure 43 and Table 12 suggest that the Heckel plots of the theophylline/ malonic acid systems are Type 1 materials, as the yield pressures of all mixtures are nearly similar. Furthermore, an extensive linearity during compression is indicative of a plastic deformation mechanism, as the linear portion started below 20 MPa. However, the co-ground mixture possessed the greatest value of yield pressure, which indicates that the densification process by particle deformation is poorer than in other mixtures. In addition, the co-ground mixture exhibited the smallest particle slippage (D_0 = 0.489) compared to those of the co-precipitated or physical mixture (Table 12). This indicates that the co-ground mixture was the least compressible, as the plastic deformation decreases with increasing yield pressure, despite the fact that the most compactible is the most compressible (Yoshinari et al. 2003). However, the co-precipitated mixture was the most compressible among all other mixtures. This indicates that the crystal morphology of the co-precipitated mixture contributed to its better compressibility (Garekani et al. 1999).

Table 13: Elastic recovery of tablets produced from theophylline/ malonic acid systems obtained at a compression speed of 10 mm/s and a compression force of 10 KN.

Sample	t_1 (mm)	t_2 (mm)	Elastic recovery E (%)
Co-precipitated mixture	2.909	3.100	6.56
Co-ground mixture	3.014	3.226	7.03
Physical mixture	2.976	3.195	7.35

t_1 = minimal thickness of the powder bed in the die, and t_2 = is the thickness of the recovered tablet.

The data shown in Table 13 are in agreement with the Heckel results in Figure 88 and Table 16, as the co-precipitated mixture possesses the smallest value of elastic recovery compared to either co-ground or physical mixture. This indicates that the lower elastic recovery of the co-precipitated mixture contributes to its better compressibility, as the greater elastic recovery increases the tablet porosity during decompression phase (Roberts and Rowe 1987).

6.3.3. General Discussion

In this chapter, we have shown that the methods of preparation of theophylline/ oxalic acid co-crystals affected the tableting properties. Both methods produced the same co-crystal structure as indicated by Raman, XRPD, DSC and SEM.

In the next chapter, we evaluate the impact of additives, namely MCC and α-lactose monohydrate on phase transformation, crystal structure of an in situ co-crystals formation and subsequent tableting properties of urea/ 2-MB and caffeine/ malonic acid systems.

7. Effect of additives (microcrystalline cellulose & α-lactose monohydrate) on phase transformation and molecular structure of in situ co-crystal formation and subsequent tableting behaviour

7.1. Introduction

The inclusion of fillers in tablet formulation is required, especially for drugs presented in low doses. However, these types of excipients may have an impact on other properties, including, for example crystallinity changes, tablet compactibility and the compressibility of powders. Microcrystalline cellulose (MCC) is widely used as a filler, disintegrant, and binder of oral tablets. Several studies and reviews on the tableting properties of MCC indicate some limitation to its use as direct compression excipient. These limitations include low bulk density, poor flow, high sensitivity to lubricant and moisture content, excessive mechanical strength of tablets and other physical properties (Bolhuis and Chowan 1996). On the other hand, lactose is a disaccharide, which can exist in different forms in the solid-state. These various forms of lactose show different compaction behaviour (Bolhuis et al. 1985; Fell and Newton 1970). Lactose was chosen for our study because it is one of the most extensively used excipients in pharmaceutical dosage forms. Many researchers (De Boer et al. 1986; Van Kamp et al. 1986a) have studied the tableting properties of lactose.

It has been shown in the previous chapters (Chapter 3 and Chapter 4) that the co-crystals of urea/ 2-MB and caffeine/ malonic acid systems have successfully been prepared by both grinding and precipitation. It has also been shown that the co-crystallization has clearly affected the tableting properties and deformation characteristics of both systems.

In this chapter, we combined MCC and α-lactose monohydrate as diluents to investigate their impact on the structure and on the formation of urea/ 2-MB and caffeine/ malonic acid co-crystals. Furthermore, the effect of these fillers on the mechanical properties of tablets produced from co-crystals and physical mixtures was also studied.

Details of the composition of the blends are given in sections 2.2.13 to 2.2.18.

7.2. Results and discussion

7.2.1. Effect of additives (MCC & α-lactose monohydrate) on the structure of co-crystal of urea/ 2-MB produced by grinding before and after compression

The X-ray powder diffraction patterns of the urea/ 2-MB system are presented in Figure 44.

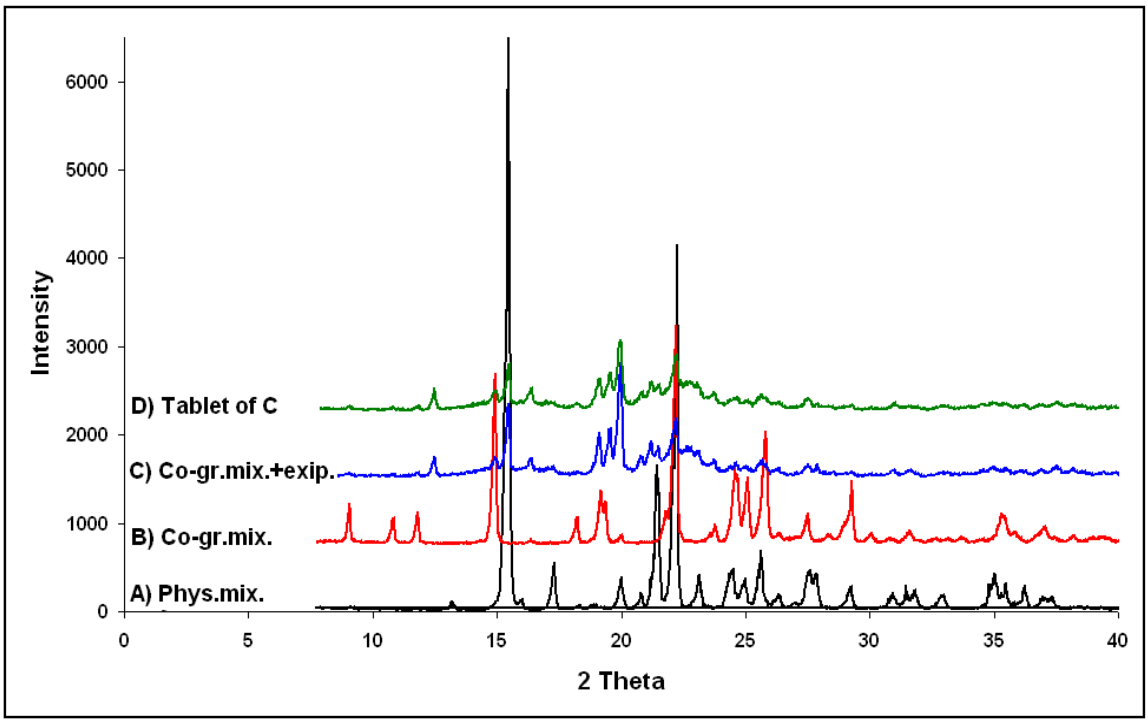

Figure 44: PXRD patterns of the urea/ 2-MB system: (A) the physical mixture, (B) the co-ground mixture, (C) the co-ground mixture with excipients, and (D) crushed tablet of the co-ground mixture with excipients.

The effect of MCC and α-lactose on the crystallinity of urea/ 2-MB co-crystal produced by grinding was investigated using XRPD, as shown in Figure 44.

After the addition of MCC and α-lactose monohydrate to the co-ground mixture, the intensities of the diffraction peaks of the intact co-crystal, that were observed at 2θ = 9.0°, 10.8°, 11.8°, 14.9°, 18.2° and 18.9° disappeared, indicating a lowering of crystallinity and an increasing amorphous state of the co-crystal. The SEM images presented in Figure 45 are in good agreement with the XRPD, as the rough surface of the co-ground mixture was completely changed into a smooth surface. On the other hand, the tablet of the co-ground mixture with excipients shows the same XRPD spectra, similar to those of the same mixture before tableting. This indicates that the interference of excipients between co-crystal particles has affected the crystallinity of the co-crystal by weakening the hydrogen bonds. Furthermore, the new diffraction peaks with small intensities at 2θ = 12.14°, 20.88° and 21.24°, are consistent with lactose(Gombas et al. 2003). These results suggest a change in the molecular structure of the urea/ 2-MB co-crystal.

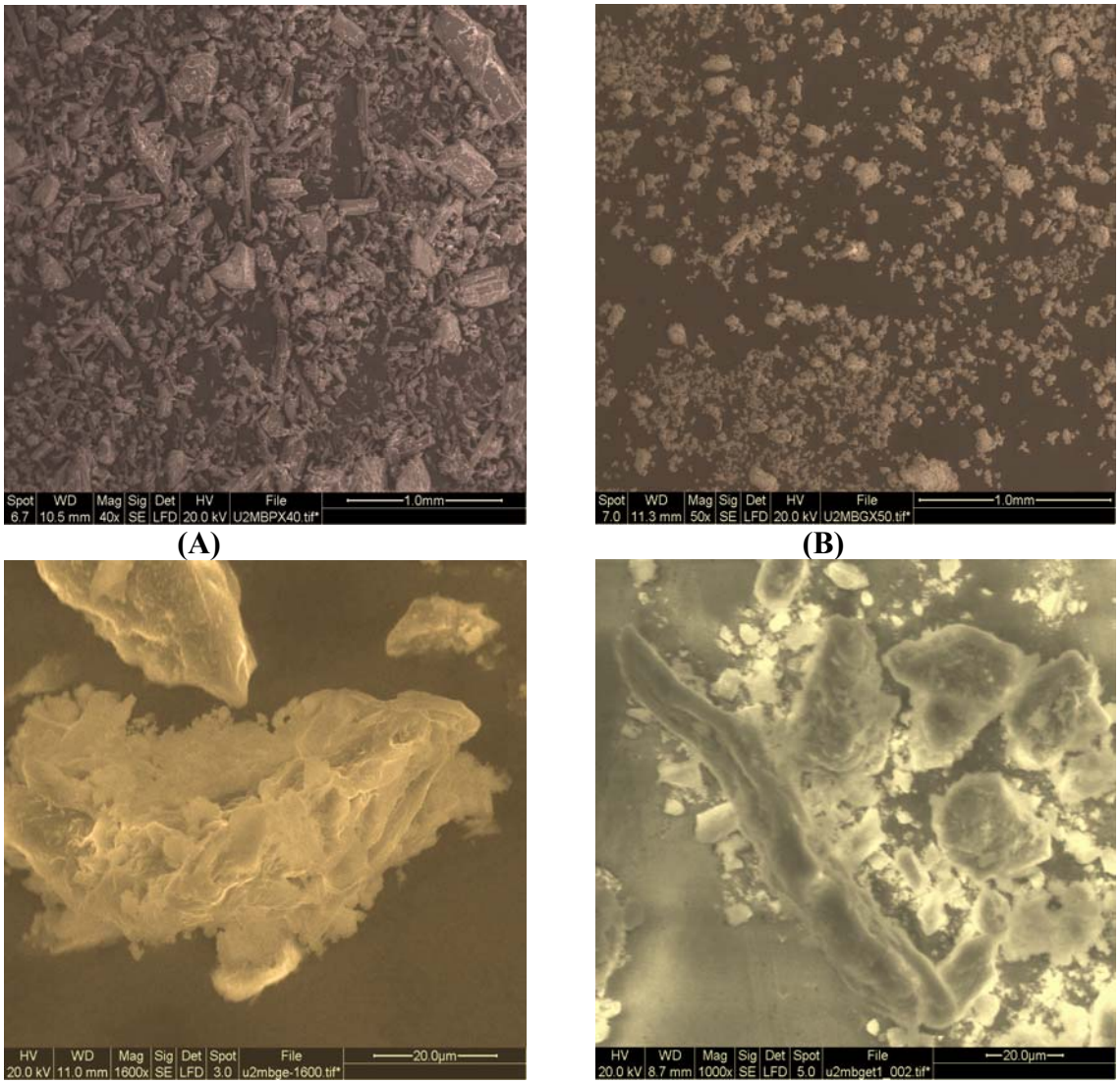

Figure 45: SEM of the uea/2-MB system: (A) the physical mixture, (B) the co-ground mixture, (C) the co-ground mixture with excipients, and (D) crushed tablet of the co-ground mixture with excipients.

7.2.2. Effect of additives (MCC & α-lactose monohydrate) on the structure of co-crystal of urea/ 2-MB produced by co-precipitation before and after compression

Figure 46 illustrates the X-ray powder diffraction patterns of urea/ 2-MB system.

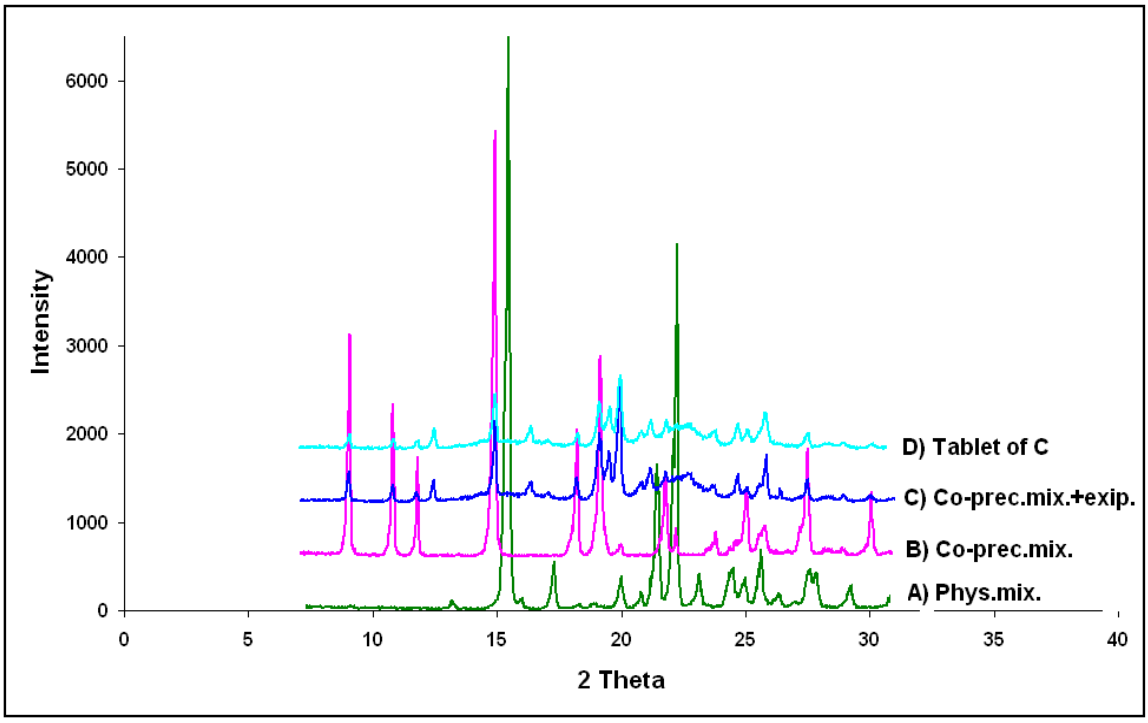

Figure 46: PXRD patterns of the urea/ 2-MB system: (A) the physical mixture, (B) the co-precipitated mixture, (C) the co-precipitated mixture with excipients, and (D) crushed tablet of the co-precipitated mixture with excipients.

The effect of MCC and α-lactose on the crystallinity of urea/ 2-MB co-crystal produced by co-precipitation was investigated using XRPD, as shown in Figure 46.

After the addition of MCC and α-lactose monohydrate to the co-precipitated mixture, the diffraction peaks of the co-crystal, at $2\theta = 9.0^{0}$, 10.8^{0}, 11.8^{0}, 14.9^{0}, 18.2^{0} and 18.9^{0} could still be seen with a dramatic decrease in their intensities. However, new peaks with

small intensities, similar to those observed in the co-ground mixture, at 2θ = 12.14°, 20.88° and 21.24° were also formed. The SEM micrographs presented in Figure 47, were consistent with the XRPD results, as the needle-like crystals of co-precipitated mixture have transformed into plate-like crystals after the addition excipients. On the other hand, the tablet of the co-precipitated mixture with excipients showed the same XRPD spectra, similar to those of the same mixture before tableting. These results show, on one hand, that the crystallinity of the co-crystal decreased, as indicated by the decreased intensities of the diffraction peaks. On the other hand, the new peaks formed due to lactose, suggest that these excipients have been able to interrupt the feature of the co-crystal and change its molecular structure.

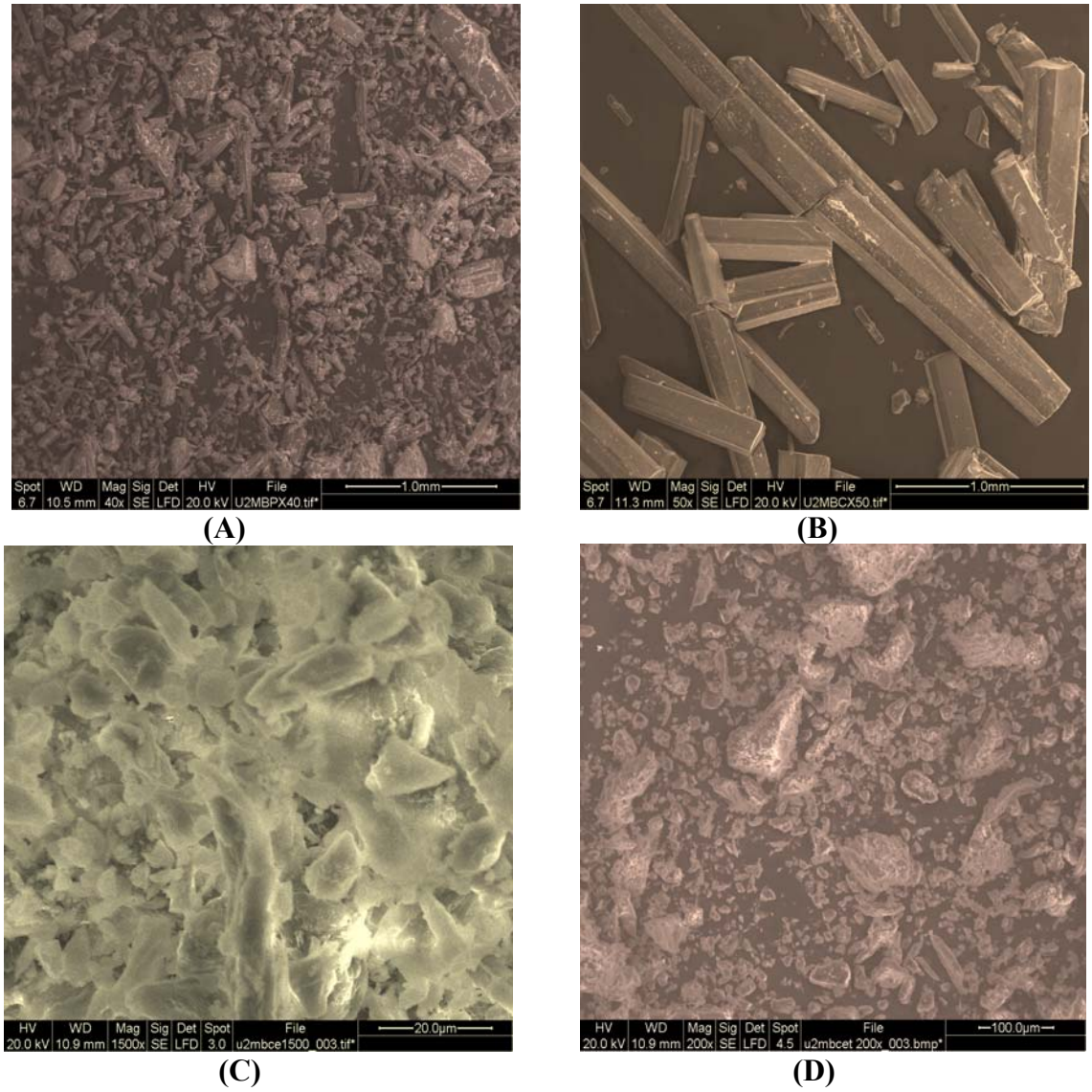

Figure 47: SEM of the urea/ 2-MB system: (A) the physical mixture, (B) the co-precipitated mixture, (C) the co-precipitated mixture with excipients, and (D) crushed tablet of the co-precipitated mixture with excipients.

7.2.3. Effect of additives (MCC & α-lactose monohydrate) on the structure of co-crystal of caffeine/ malonic acid produced by co-grinding before and after compression

Figure 48 shows the PXRD patterns of the caffeine/ malonic acid system.

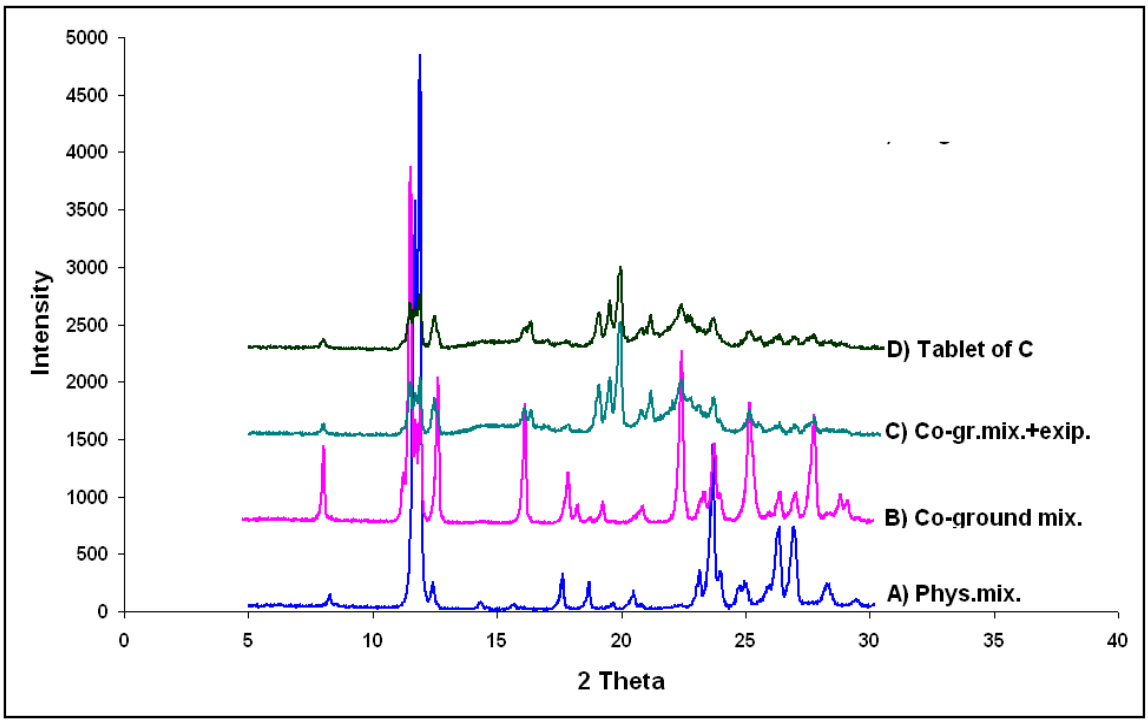

Figure 48: PXRD patterns of the caffeine/malonic acid system: (A) the physical mixture, (B) the co-ground mixture (C) the co-ground mixture with excipients, and (D) crushed tablet of the co-ground mixture with excipients.

The effect of MCC and α-lactose on the crystallinity of the caffeine/ malonic acid co-crystal produced by co-grinding was investigated using XRPD, as shown in Figure 48.

The diffraction peaks intensities of the intact co-crystal at 2θ = 8 ^{0}, 16.2 ^{0}, 18.28 ^{0}, 22.45 ^{0}, 25.34° and 28 ^{0}, dramatically decreased after the addition of MCC and α-lactose monohydrate, indicating a lowering of crystallinity. This assumption is supported by the SEM micrographs in Figure 49, as the agglomerated particles of the co-ground mixture

transformed into a smooth surface after the addition of excipients. In addition, new peaks at 2θ = 20° and 19.5°, were due to lactose, indicating a change in the molecular structure of the co-crystal.

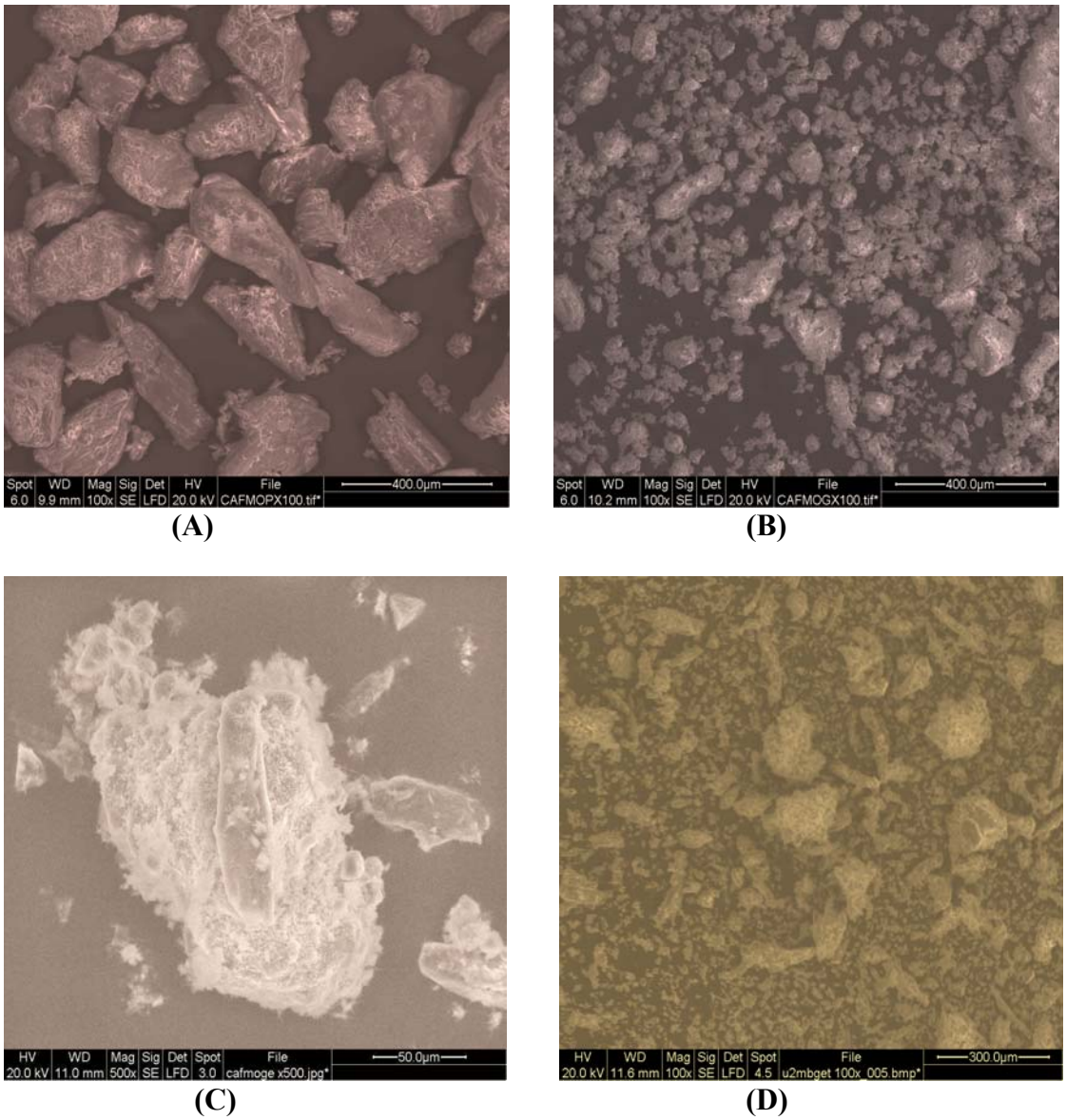

Figure 49: SEM of the caffeine/ malonic acid system: (A) the physical mixture, (B) the co-ground mixture, (C) the co-ground mixture with excipients, and (D) the crushed tablet of the co-ground mixture with excipients.

7.2.4. Effect of additives (MCC & α-lactose monohydrate) on the structure of co-crystal of caffeine/ malonic acid produced by co-precipitation before and after compression

Figure 50 illustrates the XRPD patterns of the caffeine/ malonic acid system.

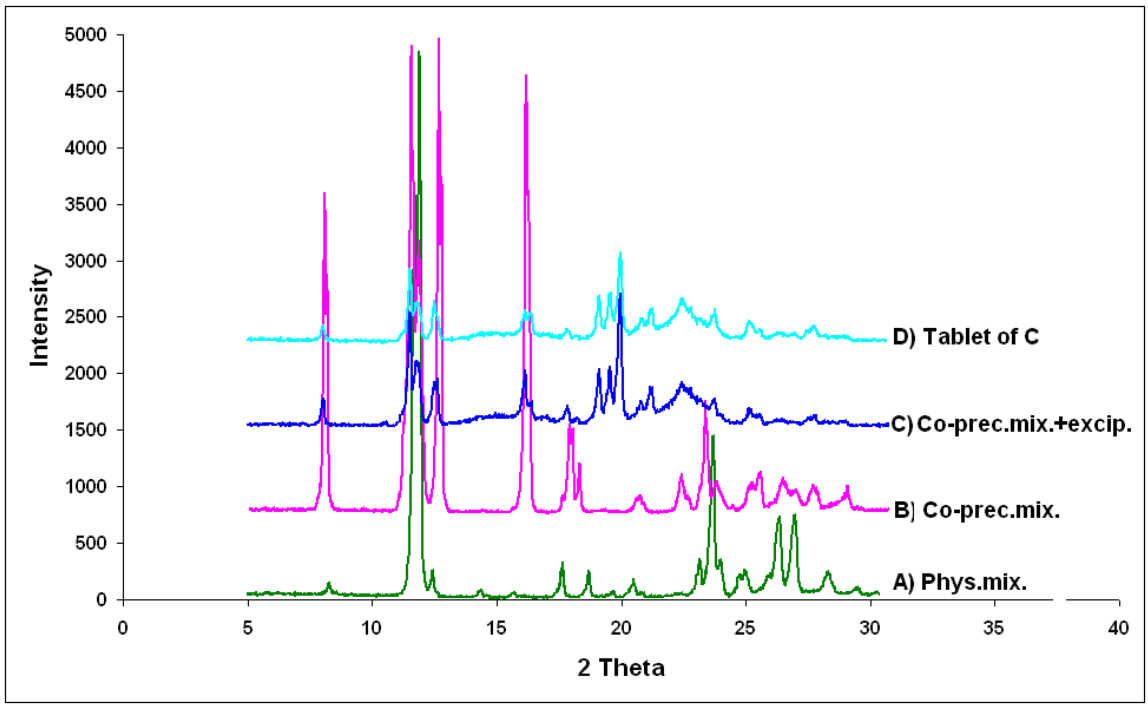

Figure 50: PXRD patterns of the caffeine/ malonic acid system: (A) the physical mixture, (B) the co-precipitated mixture (C) the co-precipitated mixture with excipients, and (D) the crushed tablet of the co-precipitated mixture with excipients.

When MCC and α-lactose monohydrate were added to the co-precipitated mixture, diffraction peaks intensities of the co-crystal at 2θ = 8 ^{0}, 16.2 ^{0}, 18.28 ^{0}, 22.45 ^{0}, 25.34 ^{0} and 28 ^{0} decreased, indicating a lower of crystallinity, as well as an increase in the amorphous portion of the co-crystal (Figure 50). In addition, new peaks were found at 2θ = 20° and 19.5°, due to lactose (Gombas et al. 2003), indicating a change in the molecular

structure of the co-crystal. Furthermore, the SEM micrographs illustrated in Figure 51 were consistent with the PXRD results, as the prism-like crystals of the co-precipitated mixture changed into random shapes after the addition of excipients.

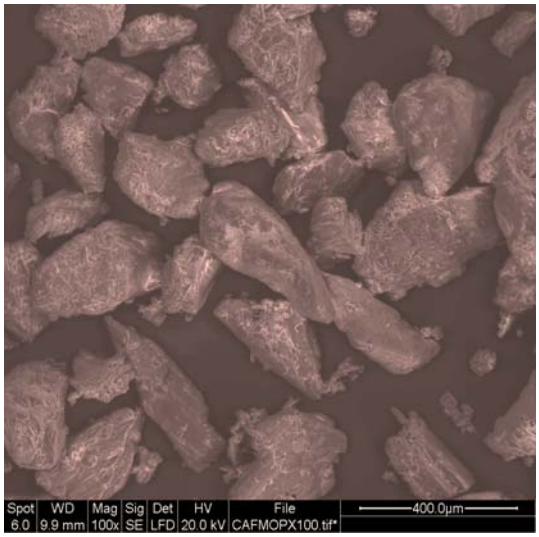

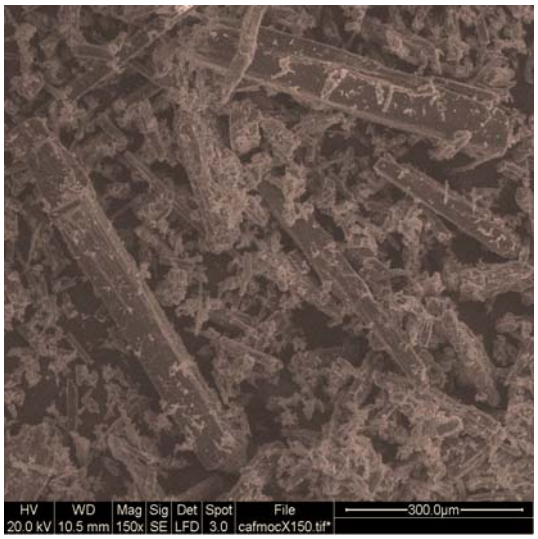

(A)

(B)

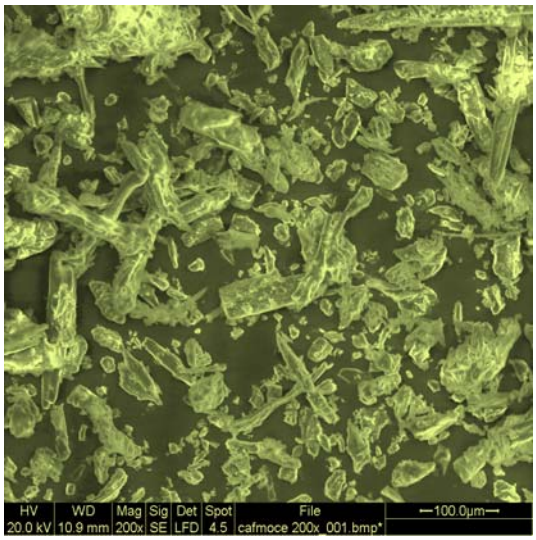

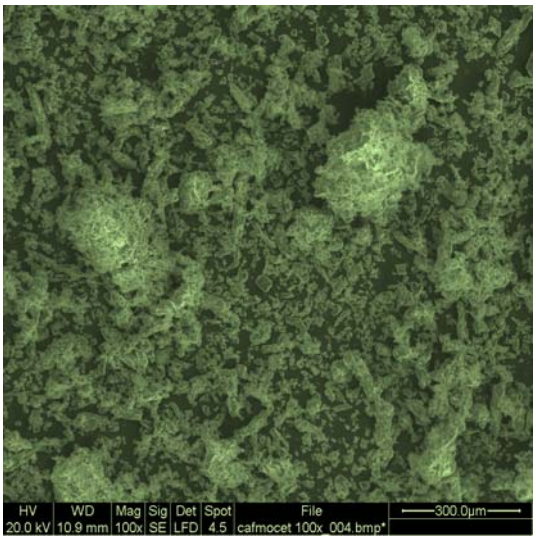

(C) **(D)**

Figure 51: SEM of the caffeine/ malonic acid system: (A) the physical mixture, (B) the co-precipitated mixture, (C) the co-precipitated mixture with excipients, and (D) the crushed tablet of the co-precipitated mixture with excipients.

7.2.5. Effect of additives (MCC & α-lactose monohydrate) on the tableting behaviour of urea/ 2-MB co-crystal

7.2.5.1. Compactibility

The tensile strength values of the urea/ 2-MB system, with excipients are given in Figure 52.

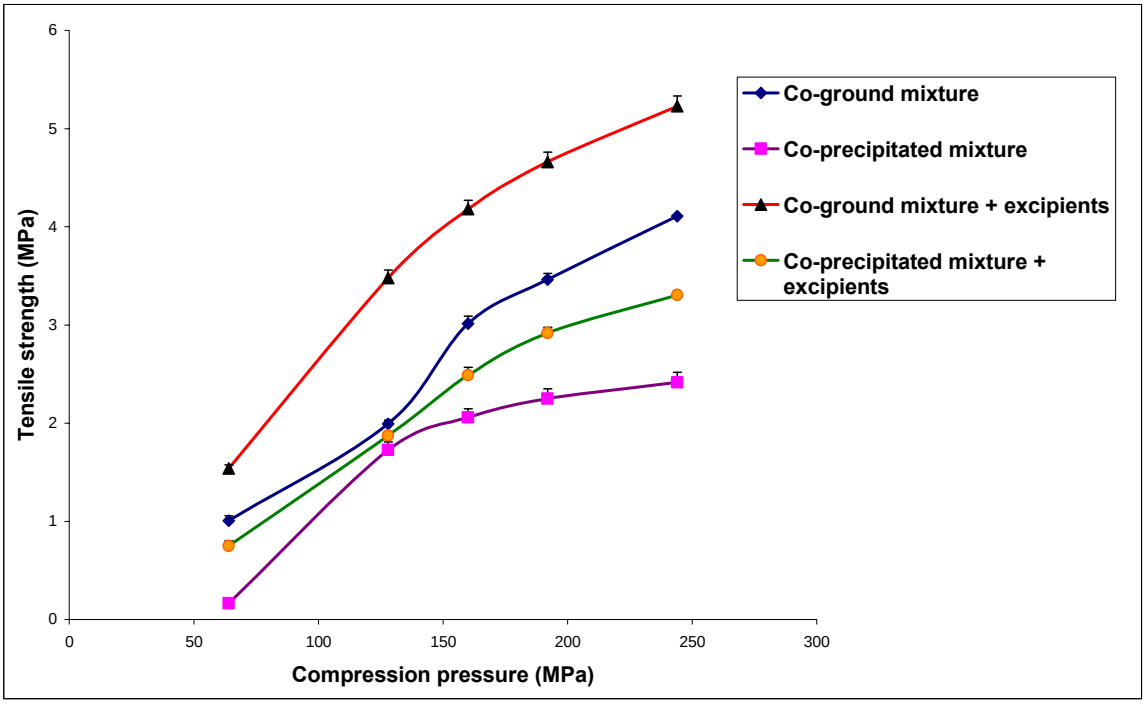

Figure 52: Tensile strength of the urea/ 2-MB system with excipients obtained at a compression speed of 10 mm/s.

As presented in Figure 52, for all mixtures, the tensile strength values of compacts increased with increasing compaction force. The pure co-ground mixture showed good compactibility compared with the pure co-precipitated mixture, which was indicated by the higher tensile strength values of compacts of the co-ground mixture. This was possibly due

to the particle size reduction achieved by grinding, as the small size generally has good compactibility. The tensile strength of compacts increases as the particle size decreases (McKenna and McCafferty 1982; Morishima et al. 1994). It is also possible that the smaller crystals have more contact points between them, and can be compacted more tightly than larger crystals. The difference in crushing strength between the co-ground mixture and the co-precipitated mixture may result from crystal morphology and crystal size, which possibly was caused by the method of crystallization and the type of crystallization solvents.

After the addition of MCC and α-lactose monohydrate to each of the pure co-ground or co-precipitated mixtures, the tensile strength values of compacts of both mixtures containing the excipients dramatically increased, indicating a good compactibility on the addition of MCC and α-lactose monohydrate. However, the compactibility of the co-ground mixture was still greater than that of the co-precipitated mixture after the addition of excipients. This resultant change in the mechanical strength of tablet was, on one hand, related to the fine particles of α-lactose monohydrate as the small sizes have generally good compactibility (McKenna and McCafferty 1982; Morishima et al. 1994). On the other hand, the combination of α-lactose monohydrate with MCC, which is known as a moisture sensitive excipient, might result in good compactibility. This is consistent with results published by Ferrari and co-workers as they reported that the interparticle bonding of the final component containing α-lactose monohydrate with MCC resulted in the overall inter-particle area of contact (Ferrari et al. 1995; Mashadi and Newton 1987). Furthermore, the surface properties of MCC may have contributed to good tabletability of either co-ground or co-precipitated mixtures, as it has been reported that microcrystalline celluloses possess highly desirable compaction characteristics (Fox et al. 1963).

7.2.5.2. Compressibility

The Heckel data of the urea/ 2-MB system with excipients are presented in Figure 53 and Table 14, respectively.

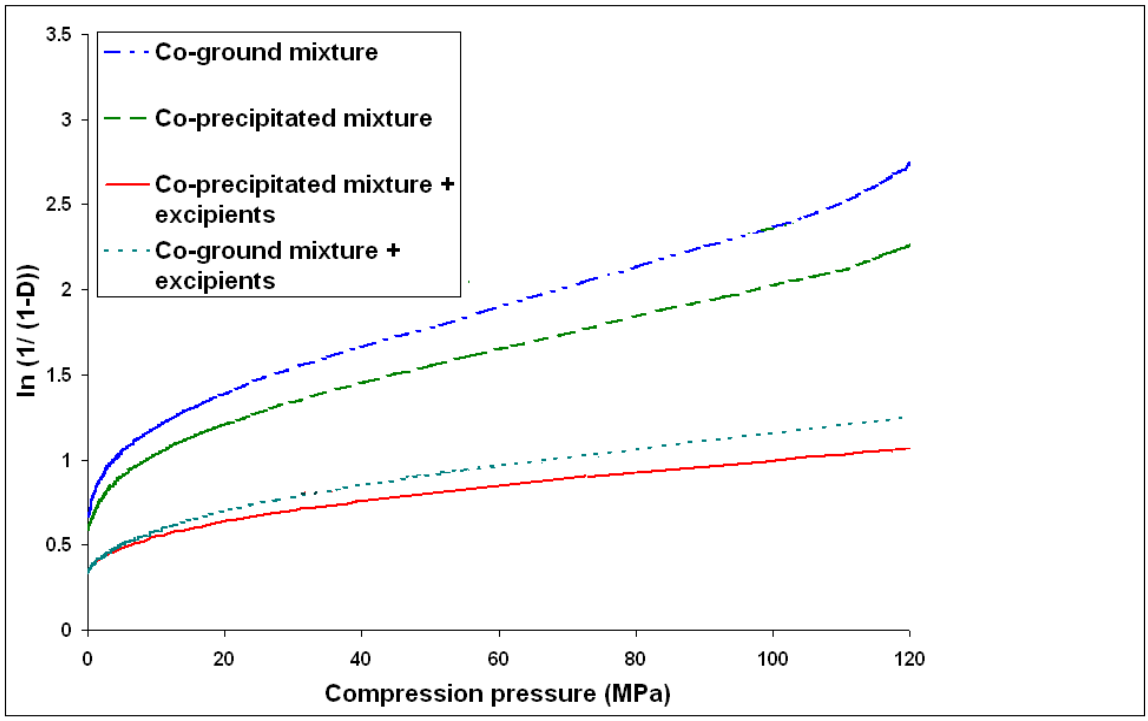

Figure 53: Heckel plots of the urea/ 2-MB systems with excipients obtained at a compression speed of 10 mm/s.

Table 14: Heckel parameter of different mixtures of the urea/ 2-MB system, with excipients, at a compression speed of 10 mm/s, and a compression force of 10 KN.

Sample	Yield pressure (MPa)	D_A	D_0	D_B
Co-ground mixture	72	0.678	0.487	0.191
Co-ground mixture + excipients	149	0.434	0.282	0.152
Co-precipitated mixture	85	0.626	0.446	0.180
Co-precipitated mixture + excipients	185	0.416	0.295	0.121

D_0 = initial relative density, $D_A = 1 - e^{-A}$ is the extrapolated relative density from the intercept (A) of the linear portion of the Heckel plot, and D_B increase in relative density due to particle arrangement.

It is clear that the yield pressures of the both co-ground and co-precipitated mixtures dramatically increased after the addition of excipients. For both mixtures containing MCC and α-lactose monohydrate, the yield pressure values were two times higher than those of pure mixtures were. This is an indication of a decrease in compressibility, as it increases with decreasing yield pressure. The changes in the inter-particle bonding caused by excipients were possibly behind the dramatic collapse in compressibility of both mixtures. As the combination of MCC and α-lactose monohydrate was found to affect the inter-particle bonding of final component and resulted in the overall inter-particle area of contact (Ferrari et al. 1995; Mashadi and Newton 1987). On the other hand, the co-ground mixture with excipients still has higher compressibility than the co-precipitated mixture with excipients. Another reason for the decrease in compressibility of pure mixtures after the

addition of MCC and α-lactose monohydrate was possibly due to moisture induced by MCC that affected the plastic deformation of powders.

The data presented in Table 15 are consistent with the Heckel data in Figure 53 and Table 14, as the elastic recovery of pure mixtures increased with addition of MCC and α-lactose monohydrate.

Table 15: Elastic recovery of tablets produced from the urea/ 2-MB systems with excipients at a compression speed of 10 mm/s and a compression force of 10 KN.

Sample	t_1 (mm)	t_2 (mm)	Elastic recovery E (%)
Co-precipitated mixture	3.50	3.76	7.42
Co-ground mixture	3.54	3.78	6.77
Co-precipitated mixture + excipients	3.12	3.45	10.7
Co-ground mixture + excipients	3.07	3.35	9.12

t_1 = minimal thickness of the powder bed in the die, and t_2 = is the thickness of the recovered tablet.

7.2.6. Effect of additives (MCC & α-lactose monohydrate) on the tableting behaviour of caffeine/ malonic acid co-crystal

7.2.6.1. Compactibility

Figure 54 illustrates the tensile strength of the caffeine/ malonic acid system with excipients.

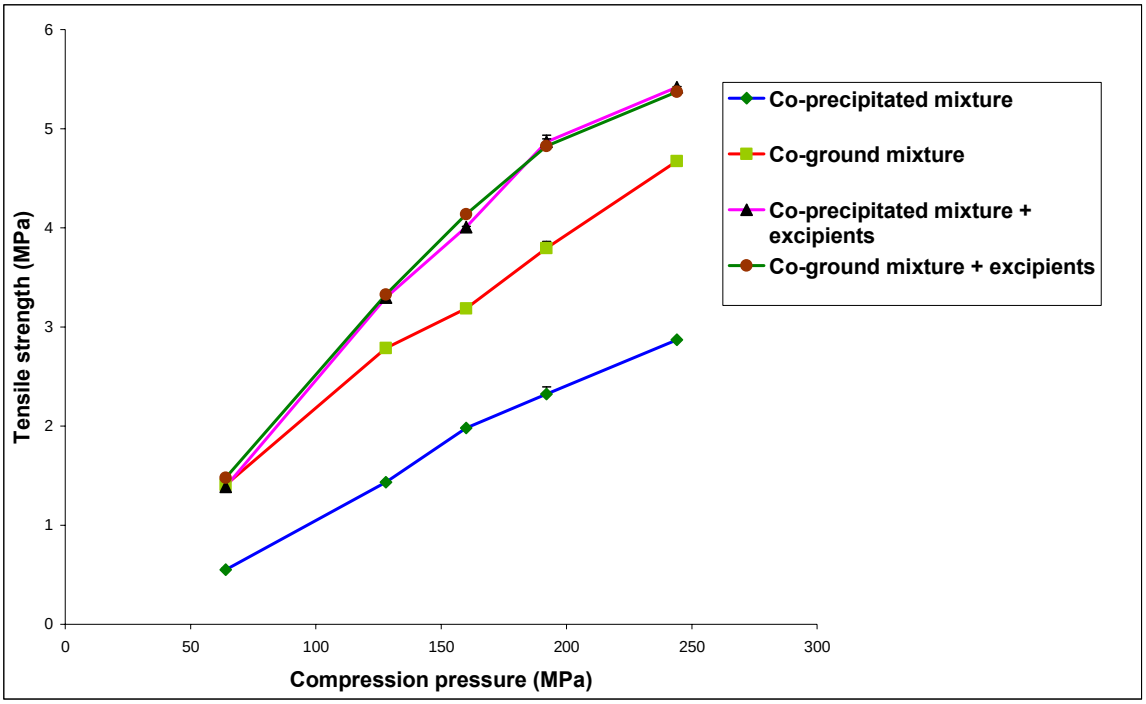

Figure 54: Tensile strength of the caffeine/ malonic acid system with excipients obtained at a compression speed of 10 mm/ s.

For all mixtures, the tensile strength values increased with increasing compaction force. The pure co-ground mixture was more compactible than the pure co-precipitated mixture. The difference in tensile strength values between the co-ground and the co-precipitated mixtures may have resulted from crystal morphology and crystal size, as the co-precipitated mixture exhibited needle-like crystals, while the co-ground mixture consisted of relatively fine particles. These differences in sizes and shapes very possibly be caused by the method

of crystallization and the type of crystallization solvents (Kachrimanis et al. 2003). After the addition of MCC and α-lactose monohydrate to the pure mixtures, the tensile strength values of both mixtures containing excipients increased, indicating good tabletability on the addition of MCC and α-lactose monohydrate.

7.2.6.2. Compressibility

The Heckel data of the caffeine/ malonic acid system are given in Figure 55 and Table 16, respectively.

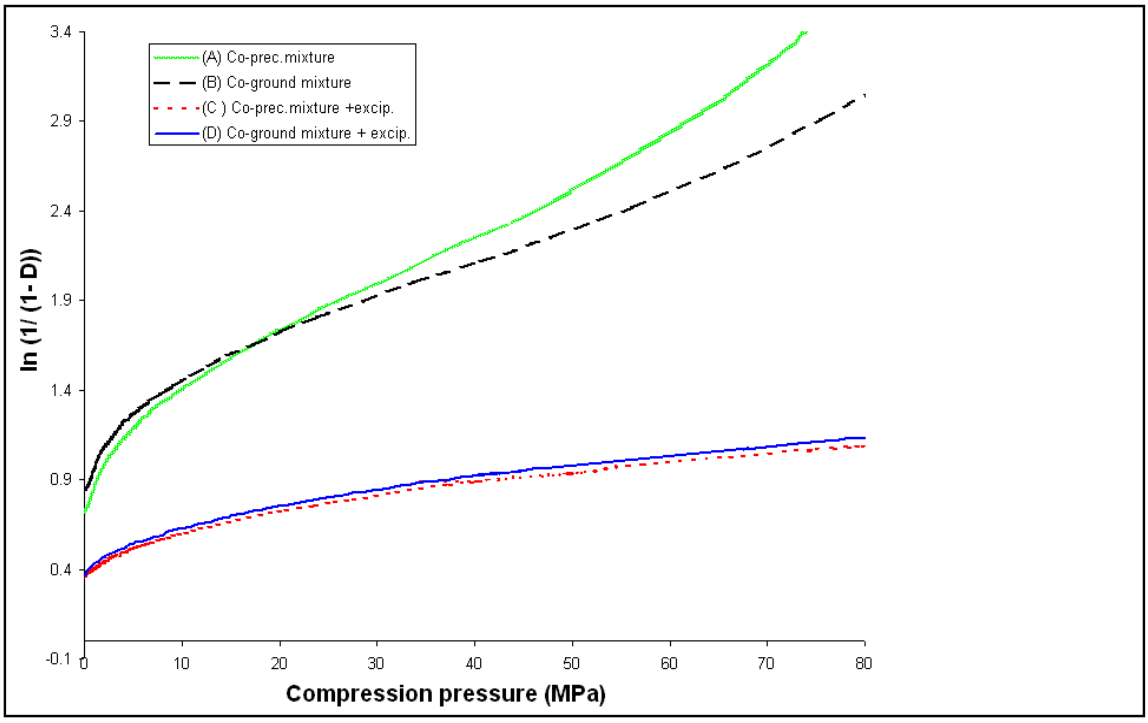

Figure 55: Heckel plots of the caffeine/ malonic acid system: (A) the co-precipitated mixture, (B) the co-ground mixture, (C) the co-precipitated mixture with (MCC and α-lactose monohydrate), and (D) the co-ground mixture with (MCC and α-lactose monohydrate.

Table 16: Heckel parameter of different mixtures of the caffeine/ malonic acid system with excipients at a compression speed of 10 mm/s and a compression force of 10 KN.

Sample	Yield pressure (MPa)	D_A	D_0	D_B
Co-ground mixture	60	0.750	0.568	0.182
Co-ground mixture + excipients	133	0.456	0.317	0.139
Co-precipitated mixture	44	0.719	0.512	0.207
Co-precipitated mixture + excipients	129	0.436	0.293	0.143

D_0 = initial relative density, $D_A = 1 - e^{-A}$ is the extrapolated relative density from the intercept (A) of the linear portion of the Heckel plot, and D_B increase in relative density due to particle arrangement.

The data presented in Figure 55 and Table 16 showed nearly similar slopes of Heckel plot for both co-ground and co-precipitated mixtures, indicating similar compressibility, with slightly higher plastic deformation for the co-ground mixture. As with the urea/ 2-MB system, the addition of MCC and α-lactose monohydrate to the pure mixtures of the caffeine/ malonic acid system was found to exert a significant increase in the yield pressures of both mixtures. As a result, the compressibility decreased. As mentioned above, the combination of MCC and α-lactose monohydrate might affect the interparticle bonding of final component and resulted in the overall inter-particle area of contact (Ferrari et al. 1995; Mashadi and Newton 1987).

On the other hand, the elastic recovery data in Table 17 were consistent with the Heckel data in Figure 46 and Table 13. The elastic recoveries of both pure mixtures were higher than those containing excipients.

Table 17: Elastic recovery of tablets produced from the caffeine/ malonic acid systems with excipients at a compression speed of 10 mm/s and a compression force of 10 KN.

Sample	T_1 (mm)	t_2 (mm)	Elastic recovery E (%)
Co-precipitated mixture	3.10	3.32	7.28
Co-ground mixture	3.05	3.33	9.21
Co-precipitated mixture + excipients	2.95	3.27	10.84
Co-ground mixture + excipients	2.99	3.28	9.69

t_1 = minimal thickness of the powder bed in the die, and t_2 = is the thickness of the recovered tablet.

7.2.6.3. General Discussion

In general, the addition of MCC and α-lactose monohydrate affected the crystal structure of the co-crystals as well as phase transformation during compression of the physical mixtures of both systems. However, the co-precipitated mixtures had been less affected as indicated by XRPD patterns. In addition, the tableting properties of the co-crystals and the physical mixtures had been greatly influenced after the addition of these excipients.

In the next chapter, we demonstrate findings of the co-crystal formation of urea/ 2-MB and caffeine/ malonic acid by compaction as a novel method of preparation of co-crystals using the Compaction Studies Simulator and IR-Press.

8. Pharmaceutical co-crystal of urea/ 2-MB-and caffeine/ malonic acid systems formed during compaction; Relationship between the compression force and the degree of crystallinity.

8.1. Introduction

As mentioned in the previous chapters, co-crystals can be obtained quantitatively by different methods, such as manual grinding, or electromechanical ball milling (Boldyrev and Takacova 2000), kneading (Watano et al. 2002), and by seeding which is the growth of crystals from solution (Seiler and Dunitz 1982). Co-crystals are usually synthesized by slow evaporation from solutions that contain co-crystal formers, growth from melt, sublimation, or slurrying and grinding two solid co-crystal formers using a ball mill or mortar and pestle (Zaworotka 2005).

As it was shown earlier in Chapter 3 and Chapter 4, the co-crystals of urea/ 2-MB and caffeine/ malonic acid systems have been prepared via both co-precipitation and co-grinding methods and several techniques (e.g. XRPD, Raman spectroscopy, DSC and SEM) were used to characterize the co-crystals.

However, in this chapter, we present our findings of co-crystal formation during compaction using both a Compaction Simulator and an IR-Press, as this is not reported in the literature to date as a method for the preparation of pharmaceutical co-crystals. For this study, we investigated caffeine and urea as model APIs and malonic acid and 2-methoxybenzamide (2-MB) respectively, as co-crystal formers. Furthermore, the effect of compaction forces on the degree of crystallinity of co-crystals and the subsequent effect on

deformational characteristics of powders, as well as the mechanical properties of the tablets have been investigated. Compacts were prepared using the methods presented in section 2.3.

8.2. Results and discussion

8.2.1. XRPD results of a urea/ 2-MB co-crystal formed during tableting using Compaction Studies Simulator

Figure 56 illustrates the XRPD patterns of tablets produced from the urea/ 2-MB system.

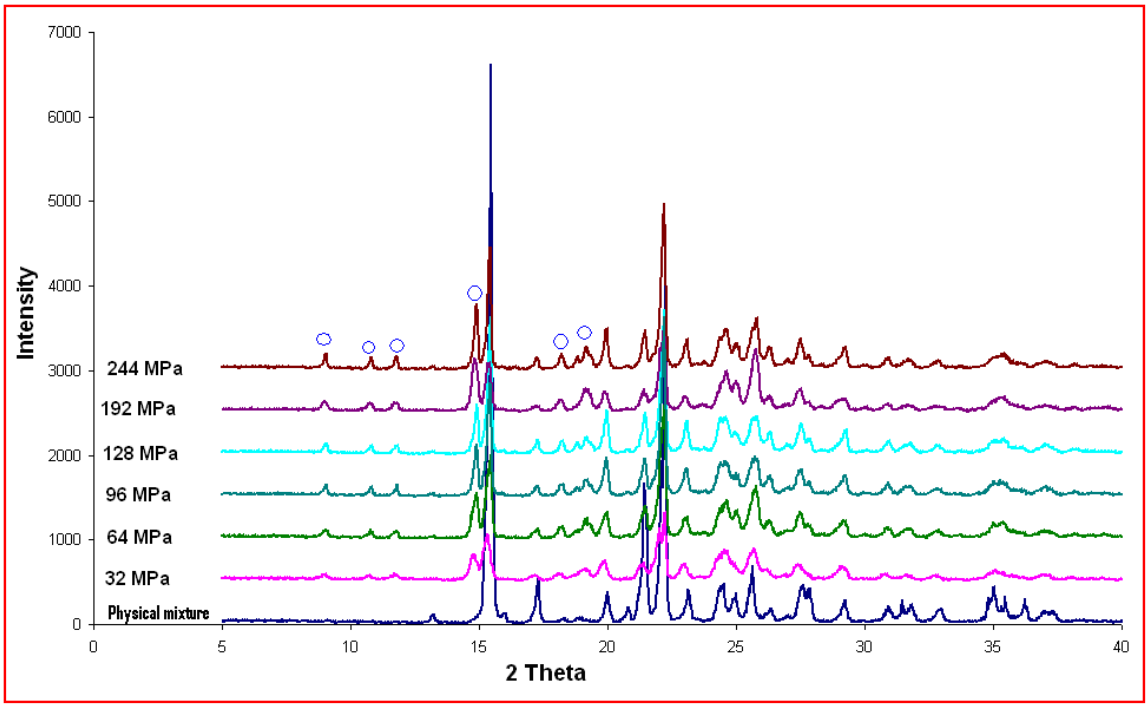

Figure 56: PXRD patterns of the urea/ 2-MB tablets prepared by the Compaction Studies Press at different compression forces.

As shown in Figure 56, the XRPD patterns show that all tablets possessed new peaks at 2θ = 9.0 ^{0}, 10.8 ^{0}, 11.8 ^{0}, 14.9 ^{0}, 18.2 ^{0} and 18.9 ^{0}, different from those of the physical mixture.

The co-crystal started to form at 2.5 KN. However, the intensity of the new peaks increased with increasing compression force, indicating higher crystallinity at higher compaction pressure. As shown in Chapter 3 the co-crystals of the urea/ 2-MB system have successfully been prepared via both co-precipitation and co-grinding and our recent findings are in line with both co-precipitation and co-grinding results. These findings demonstrate that compaction represents a novel means of obtaining co-crystals, as it is a fast and inexpensive route of production. Braga and co-workers (2002) have tried dry compression as a method of co-crystal formation. They pressed a mixture of 1,1 di-pyridyl-ferrocene and anthranilic acid using an IR-pellet maker. They showed no success, as no reaction had taken place. However, their trials were successful with wet compression of the same mixture and the addition of small amount of methanol.

Figure 57 presents the XRPD patterns of the urea/ 2-MB system for different methods of preparation, the simulated patterns, physical mixture and the starting materials.

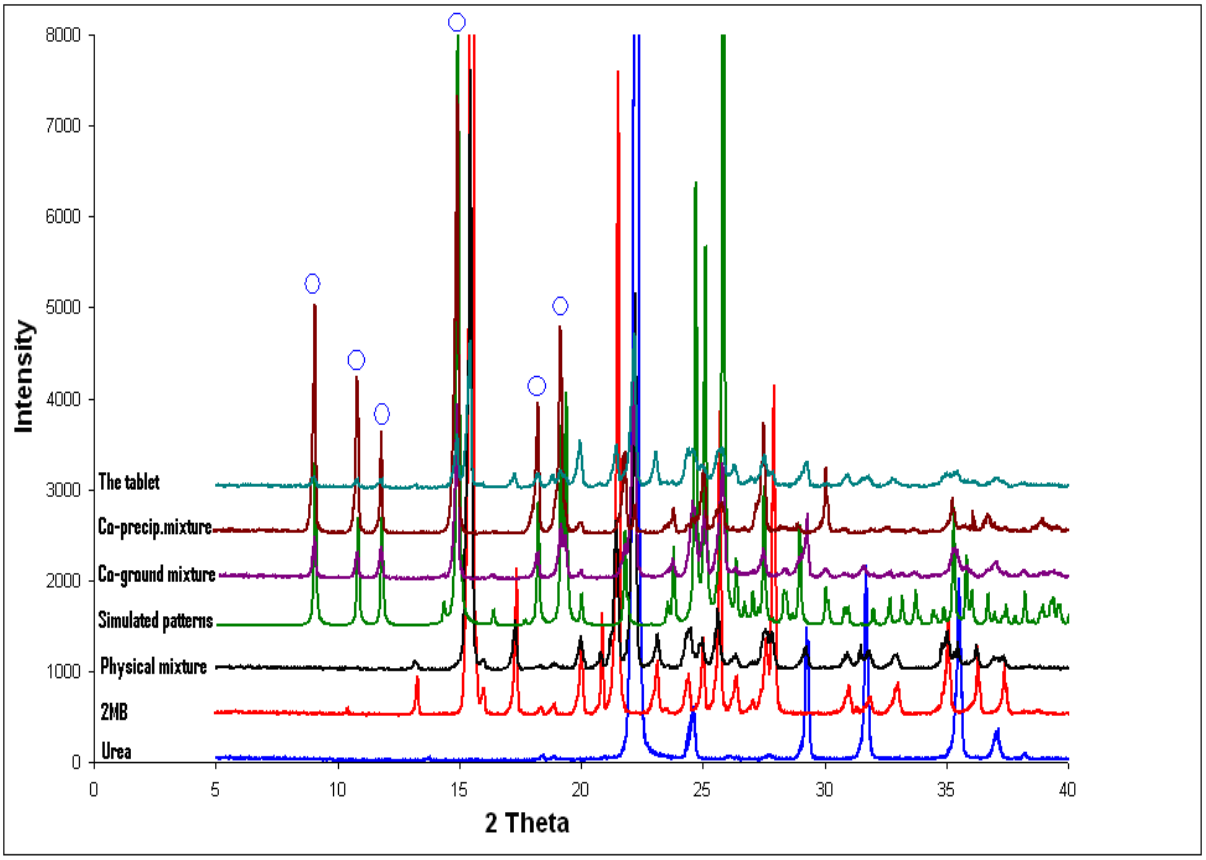

Figure 57: XRPD patterns of the urea/ 2-MB system: all methods of preparation, the simulated patterns, the physical mixture and the starting materials.

By comparing the X-ray powder diffraction patterns of urea/ 2-MB co-crystals prepared by the different methods (Figure 57), the positions of the new peaks are similar for all methods. However, the intensities of the new peaks are different. The co-precipitated mixture exhibited peaks of highest intensity compared with co-grinding or compaction. The small intensity of XRPD peaks of the co-ground mixture was possibly due to grinding, as it is known to decrease XRPD peaks intensity (Oguchi et al. 2000). As for compaction, it is possible that the reduction of the diffraction peak intensities may result from the collapse of the crystalline phase without reorganization into a new charge-transfer crystal phase.

Furthermore, during compaction, the particles were exposed to high mechanical energy for a short period of time, which may also tend to reduce the intensity of the peaks.

8.2.2. Quantitative (peak width) analysis of the crystallinity of urea/ 2-MB system by XRPD

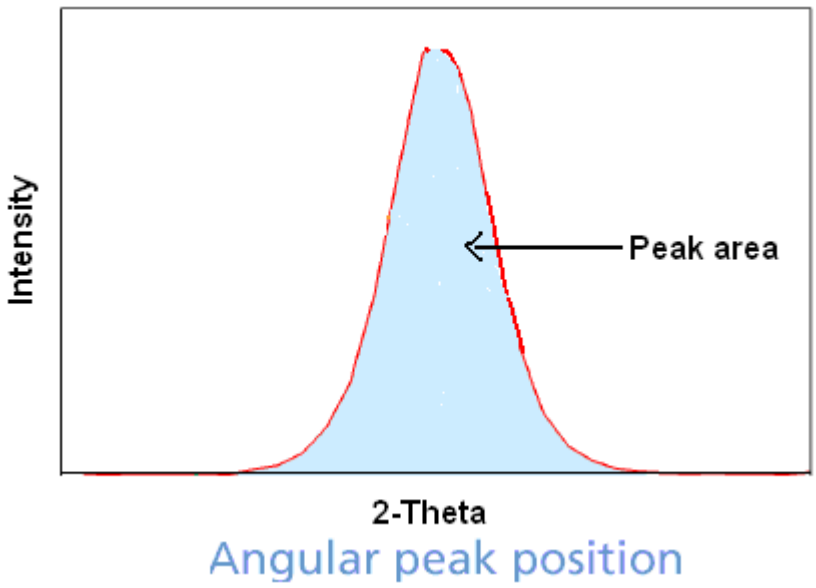

The analysis was carried out by calculating the net areas of the relevant peak for the co-crystal and one of the starting materials. Then, the ratio was obtained by dividing the area of the co-crystal by the area of the starting material (Area $_{co\text{-}crystal}$/ Area $_{st.material}$). Finally, the analysis is presented by plotting the ratio versus compression force (Klug and Alexander 1970).

The peak width analysis of the urea/ 2-MB system is given in Figure 58.

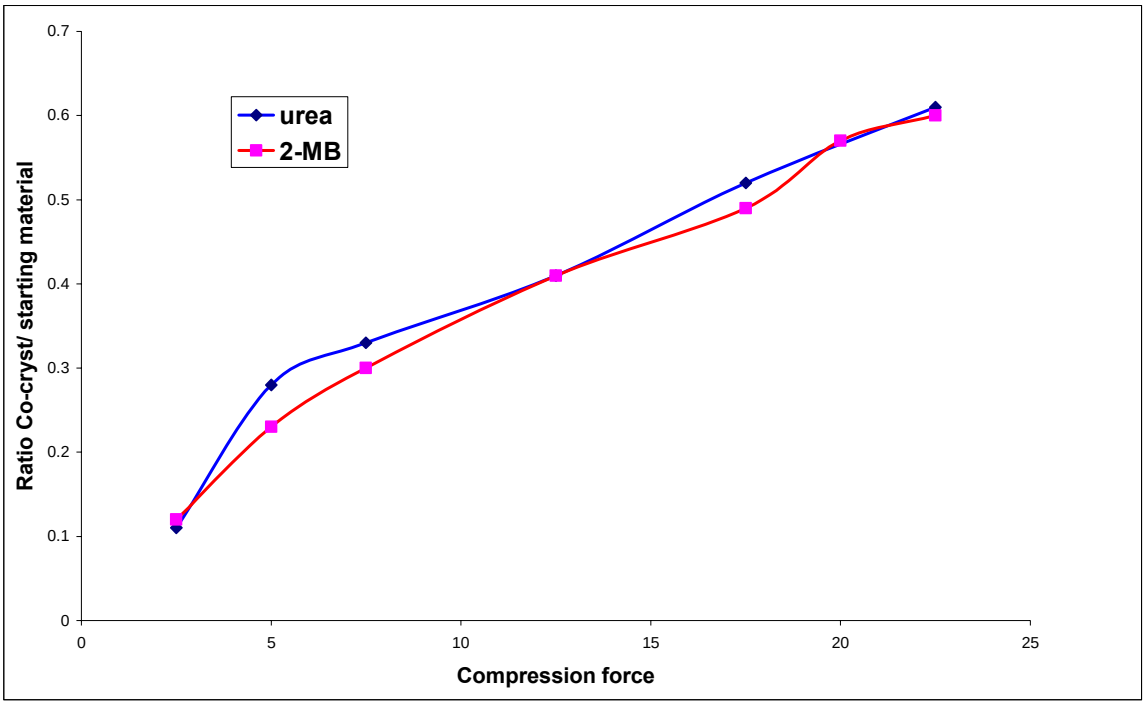

Figure 58: Quantitative representation of the urea/ 2-MB co-crystal produced by compaction at different compression forces.

From Figure 58, it can be seen that the ratio increases with increasing compression force, indicating higher crystallinity at a higher compression force. In addition, the ratios obtained from both starting materials are comparable, which indicates that the urea/ 2-MB co-crystal formed from 1:1 molar ratio of the starting materials.

The SEM micrographs of the urea/ 2-MB are illustrated in Figure 59.

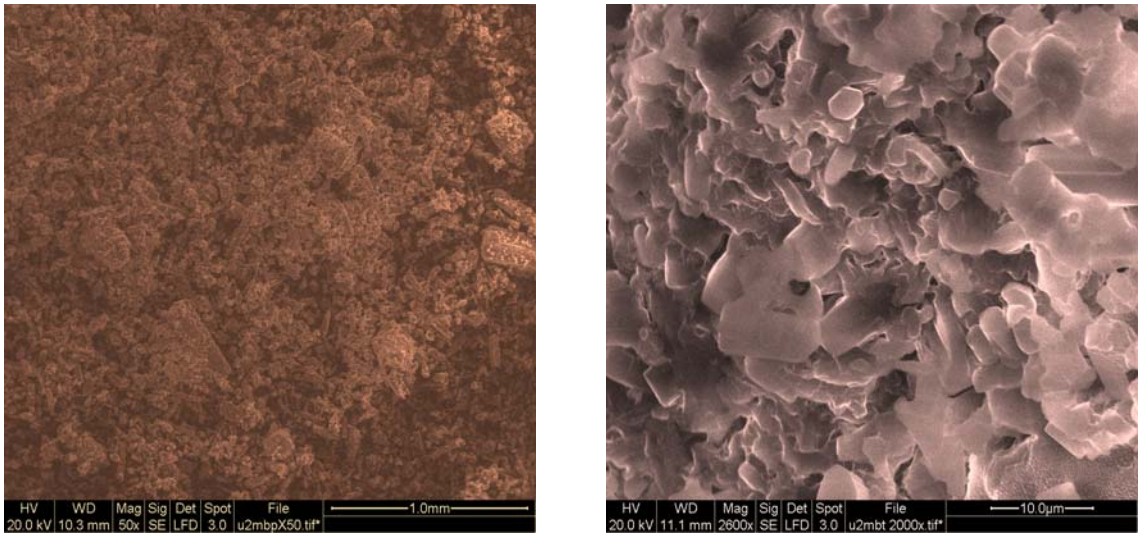

(A) **(B)**

Figure 59: SEM micrographs of the urea/ 2-MB system: (A) the physical mixture and (B) the crushed tablet of the physical mixture.

It is obvious from the SEM in Figure 59 that the tablet produced from the physical mixture is morphologically different from that of the intact particles of the physical mixture. The smooth surface of the particles has totally changed into plate-like crystals during compression, indicating a phase transformation of the components in the compacted product. These results are in agreement with XRPD results and confirm that urea may have formed a co-crystal with 2-MB during compaction.

8.2.3. XRPD results of a caffeine/ malonic acid co-crystal formed during tableting using Compaction Studies Simulator

Figure 60 presents the XRPD patterns of the caffeine/ malonic acid system.

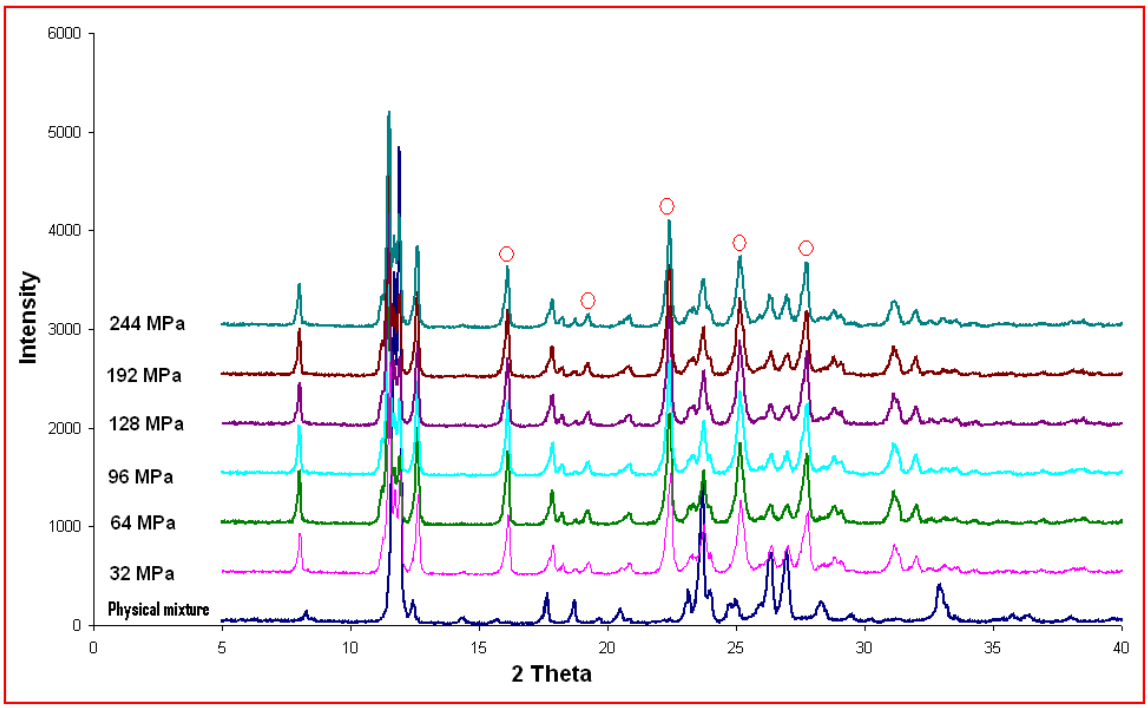

Figure 60: PXRD patterns of the caffeine/ malonic acid tablets prepared by the Compaction Studies Press at different compression forces.

As mentioned earlier in Chapter 4, caffeine successfully formed a co-crystal with malonic acid by both co-grinding and co-precipitation methods, The XRPD patterns presented in Figure 60 show new peaks at $2\theta = 16.2^{0}$, 18.28^{0}, 22.45^{0}, 25.34^{0} and 28^{0} similar to those observed in the co-ground- or co-precipitated mixtures, indicating a co-crystal formation during compaction. Similar to the urea/ 2-MB system, the co-crystal started to form at 2.5 KN and the intensity of the new peaks increased with increasing compression force, indicating higher crystallinity at higher compaction pressure.

The XRPD patterns of the caffeine/ malonic acid system for different preparation methods were compared in Figure 61.

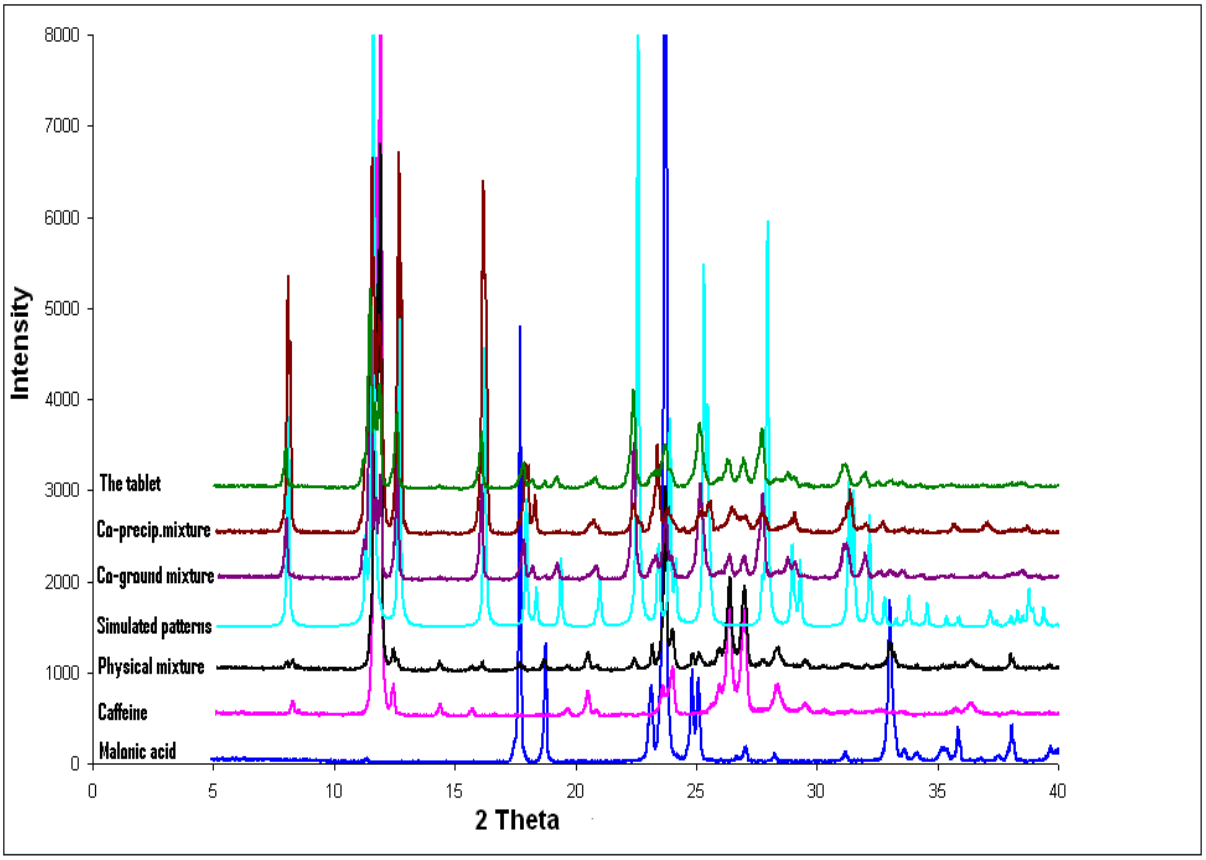

Figure 61: XRPD patterns of the caffeine/ malonic acid system (all methods).

It is apparent from Figure 61, that the peak positions of new peaks at $2\theta = 16.2^{0}$, 18.28^{0}, 22.45^{0}, 25.34^{0} and 28^{0} are similar to those of simulated patterns and that they are different from those of the physical mixture. However, the diffraction peak intensities were different. As with the urea/ 2-MB system, the co-precipitated mixture of this caffeine/ malonic acid system showed the highest peak intensities compared with co-grinding or compaction.

8.2.4. Quantitative (peak width) analysis of the crystallinity of caffeine/ malonic acid system by XRPD

The peak width analysis of the caffeine/ malonic acid system is presented in Figure 62.

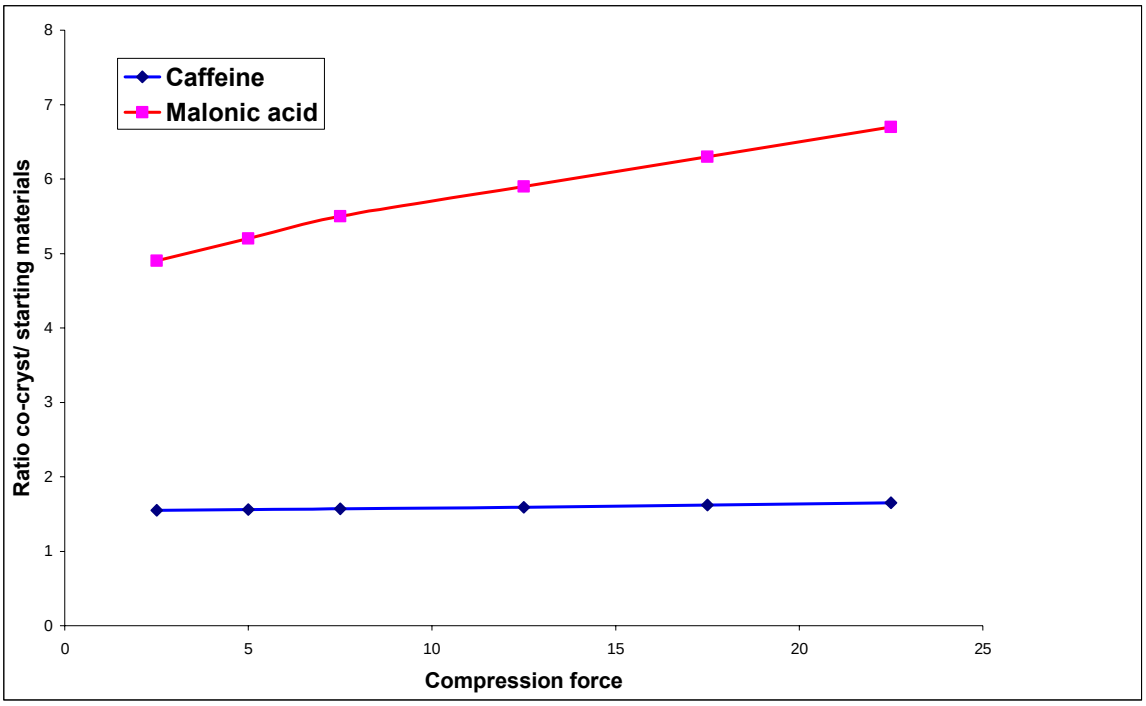

Figure 62: Quantitative representation of the caffeine/ malonic acid co-crystal produced by compaction at different compression forces.

It is apparent that the crystallinity of the caffeine/ malonic acid co-crystal increased with increasing compaction force, as reflected by the increased ratios at higher compression force. However, in contrast to the urea/ 2-MB co-crystal that formed in a molar ratio 1:1, the difference in the ratio of the starting materials is indicative of a co-crystal formation by a 2:1 molar ratio.

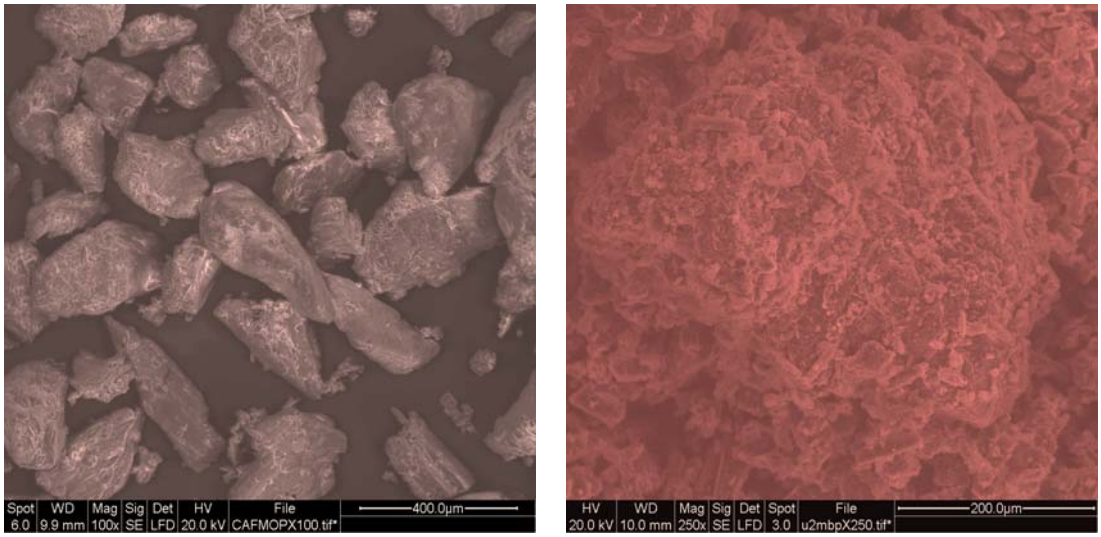

(A) **(B)**

Figure 63: SEM micrographs of the caffeine/ malonic acid system: (A) the physical mixture, and (B) the crushed tablet of (A).

Figure 63 clearly shows that the tablet possessed a surface morphology different from that of the physical mixture. The intact particles of starting materials changed into a fully aggregated single phase.

8.2.3. XRPD results of a urea/ 2-MB co-crystal formed during tableting using IR-Press

The XRPD patterns of tablets produced from the physical mixture of urea/ 2-MB are given in Figure 64.

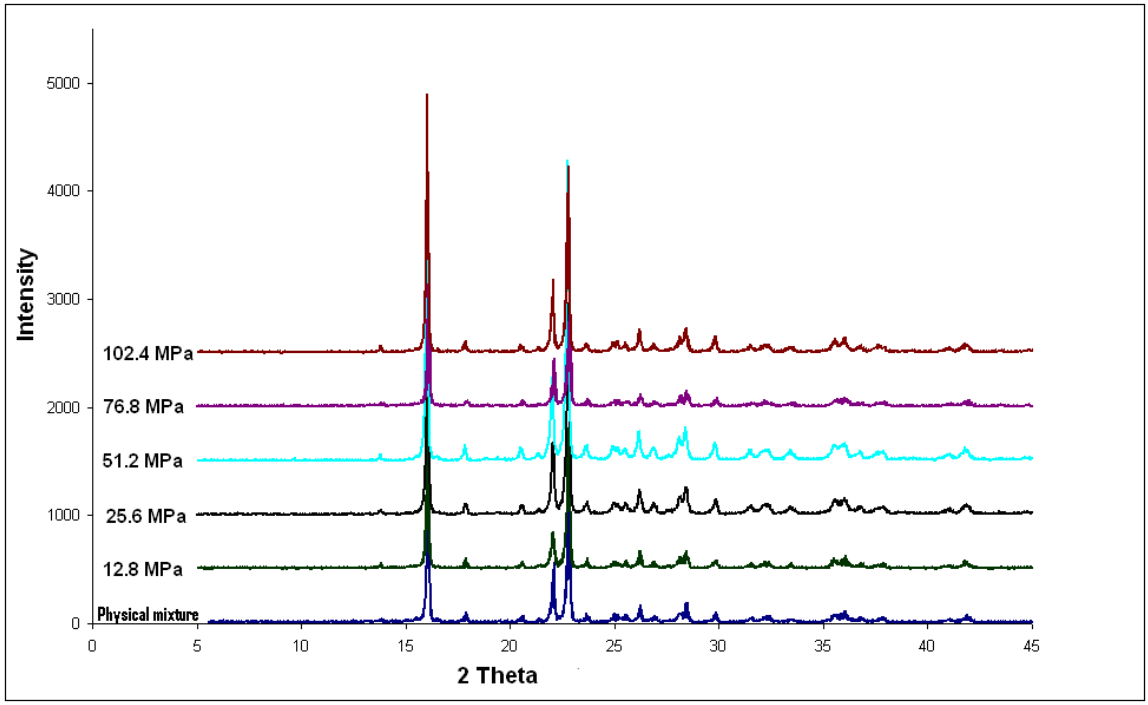

Figure 64: XRPD patterns of the physical mixture and tablets of urea/ 2-MB produced by IR-Press.

The data presented in Figure 64 showed no traces of co-crystal of urea with 2-MB, as the peak positions of XRPD spectra of tablets produced with different compression forces are the same as those of the physical mixture. Although the pressure was sufficient to bring particles in closer contact to each other, it is possible that the IR-press is not well calibrated.

8.2.4. XRPD results of a caffeine/ malonic acid co-crystal formed during tableting using IR-Press

The XRPD patterns of tablets produced from the physical mixture of caffeine/ malonic acid using IR-Press are given in Figure 65.

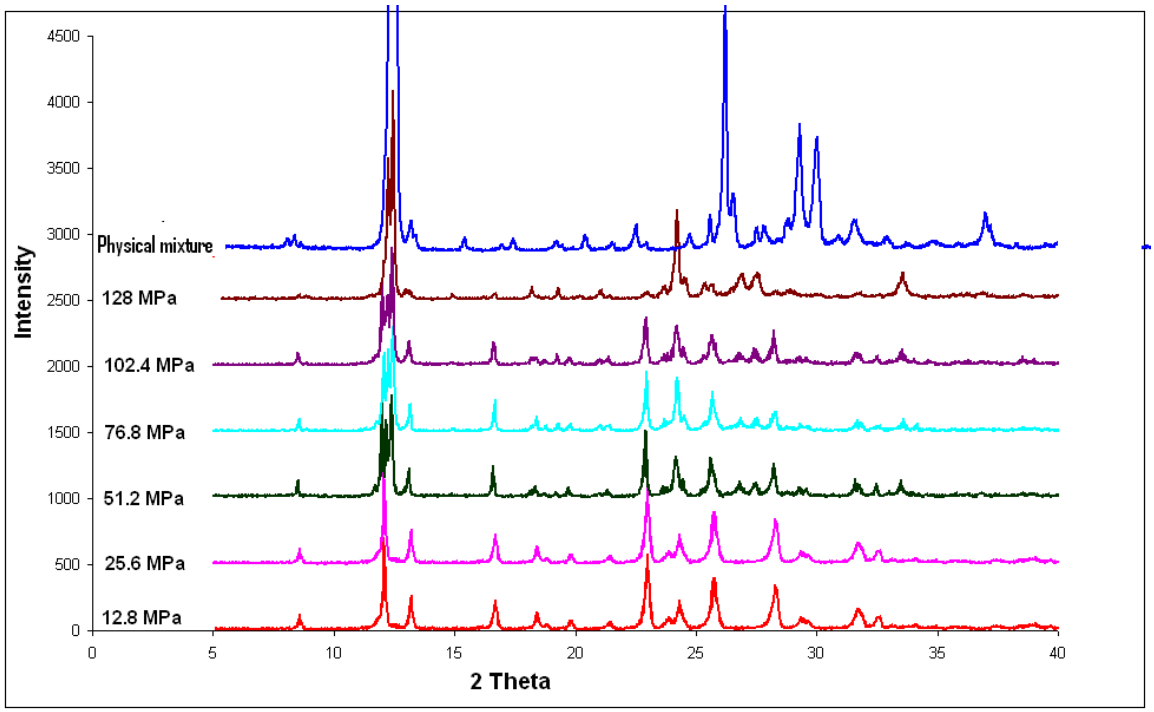

Figure 65: XRPD spectra of the physical mixture and tablets of caffeine/ malonic acid system produced by the IR-Press.

Whereas the XRPD spectra of tablets of pure mixture of urea / 2-MB produced by IR-Press (1min under pressure) showed no evidence of co-crystal formation, the caffeine/ malonic acid system, obviously showed co-crystal formation during compression by the IR-Press as shown in Figure 65. However, in contrast to tablets produced by the Compaction Studies Simulator from the same system, the diffraction peak intensities decreased with increasing compression load, indicating a lower degree of crystallinity at higher forces.

8.2.5. Effect of additives (MCC & α-lactose monohydrate) on the co-crystal formation of urea/ 2-MB during compaction

Figure 66 presents the XRPD patterns of the urea/ 2-MB system with excipients.

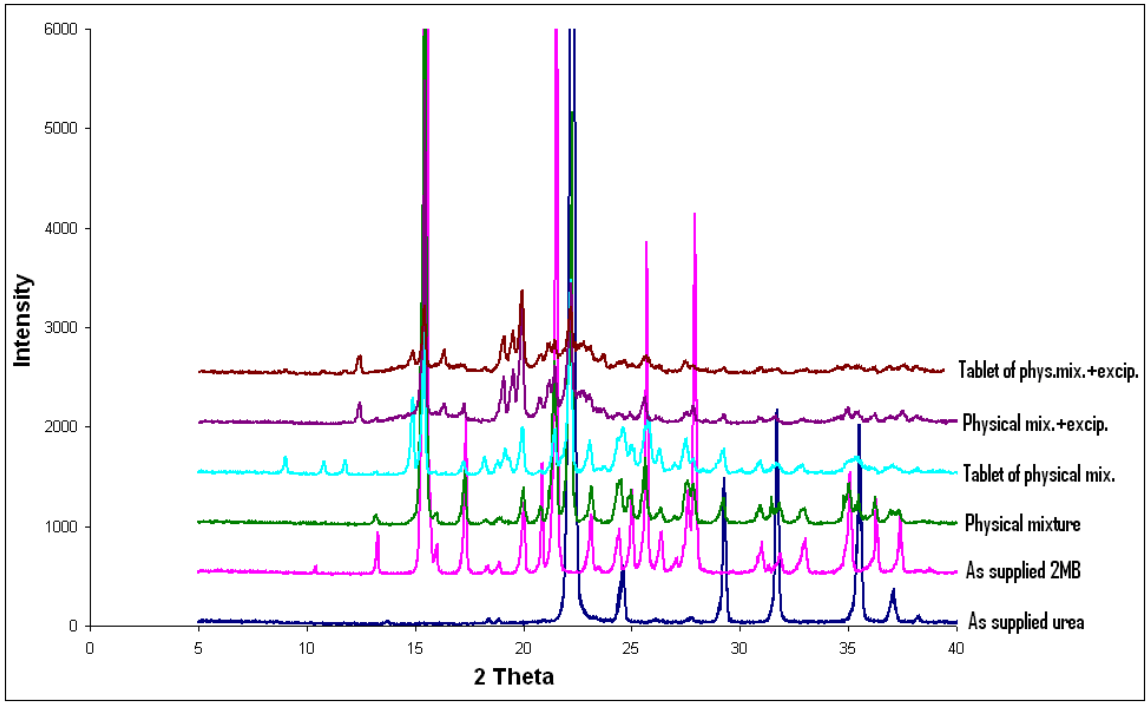

Figure 66: XRPD spectra of the urea/ 2-MB system.

As shown in this chapter (Section 8.2.1, Figure 56), urea formed a co-crystal with 2-MB during compaction. The new peaks observed at 2θ = 9.0 ^{0}, 10.8 ^{0}, 11.8 ^{0}, 14.9 ^{0}, 18.2 ^{0} and 18.9 ^{0}, were different from those of the physical mixture.

The data presented in Figure 66 show that after the addition of additives to the physical mixture, two peaks of the co-crystal at 2θ = 9°, 14.9° disappeared while one peak at 2θ = 18.9°, with a very small intensity, was preserved and new peak at 2θ = 12.14° was formed. When the same mixture was compressed, the two peaks of the co-crystal at 2θ = 14.9° and 18.9° disappeared while the peak at 2θ = 9°, with small intensity was observed. It is obvious that excipients interfered between the co-crystals particles, led to a breakdown of some hydrogen bonds, and may have stopped the co-crystal formation. However, the

molecular structure of the co-crystal has been affected greatly by the addition of additives before and after compression. Furthermore, a new peak at 2θ = 12.14°, due to the additives, explains that excipients not just delayed or stopped the co-crystal formation but also changed the nature of the co-crystal structure.

8.2.6. Effect of additives (MCC & α-lactose monohydrate) on the co-crystal formation of caffeine/ malonic acid during compaction

Figure 67 presents the XRPD patterns of the caffeine/ malonic acid system with excipients.

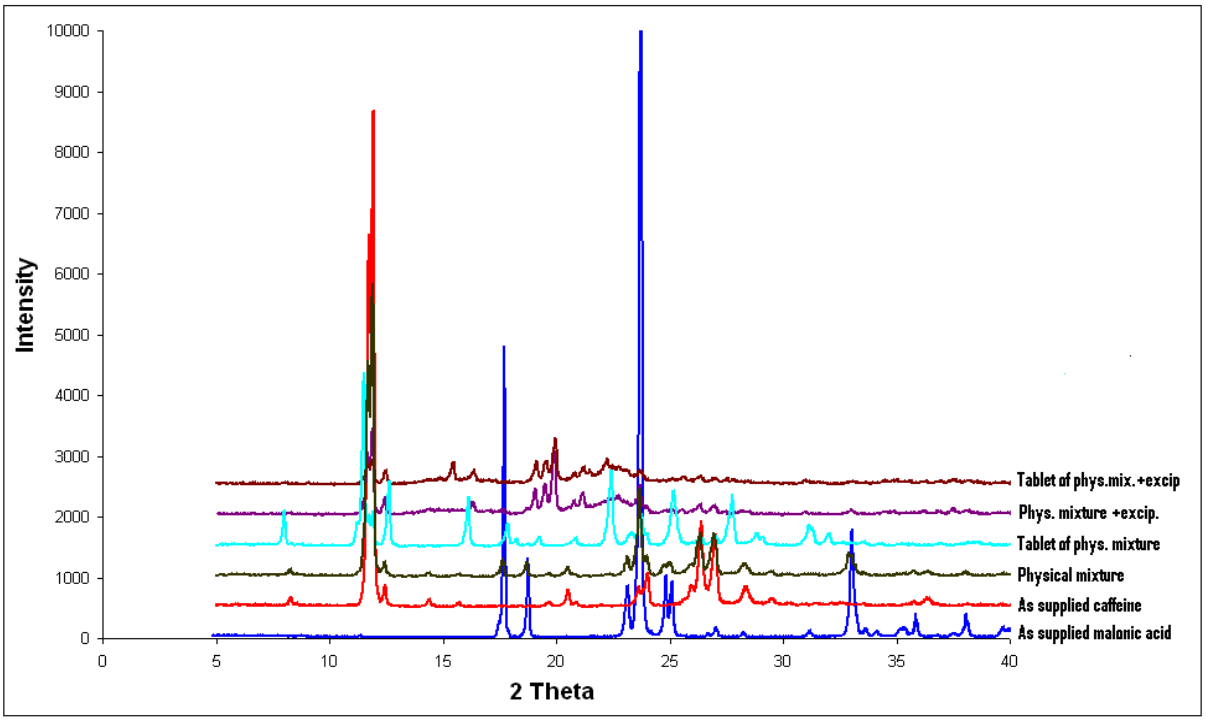

Figure 67: XRPD spectra of the caffeine/ malonic acid system.

As mentioned in this Chapter (Section 8.2.3, Figure 60), caffeine formed a co-crystal with malonic acid during compaction. The new peaks observed at 2θ = 16.2°, 18.28°, 22.45°

and 28° are similar to those of simulated patterns and that they are different from those of the physical mixture.

The data presented in Figure 67 show that after the addition of MCC & α-lactose monohydrate to the co-crystal, all new peaks of the co-crystal disappeared and the compound is likely to be amorphous. However, after tableting this mixture, there was no significant difference observed and spectra remained the same as before compression. These results indicated that the excipients not only stopped the formation of the co-crystal during tableting but also affected even the nature of the physical mixture by converting it into an amorphous form.

8.3. Conclusion

It can be concluded that it was possible to form co-crystal during compaction. For both of the urea/ 2-MB and caffeine/ malonic acid systems, the physical mixtures were found to form co-crystal by compression using a Compaction Studies Press. For both systems, the crystallinity increased with increasing compression force. By using The IR-Press, urea/ 2-MB system showed no evidence co-crystal formation, while caffeine/ malonic acid system was found to form a co-crystal. However, the crystallinity decreased with increasing compaction loads. Furthermore, the excipients stopped the co-crystal formation of both systems during compression as indicated by XRPD.

In the next chapter, we evaluate findings of the synthesis of the urea/ 2-MB and caffeine/ malonic acid co-crystals through convection mixing as a novel method of preparation of co-crystals.

9. Co-crystal synthesis through convection mixing

9.1. Introduction

Historically physical mixtures are prepared by combining of two or more solid compounds using adequate agitation without the addition of any liquid (Harnby et al. 1989). In the context of drug development, this process may involve the combination of one or more drugs with one or more excipients. This technique is straightforward and adaptable and is carried out using different mixing mechanisms, e.g. tubular mixer, mortar, etc. The use of physical mixes of carriers and drugs is required as standards or a control, against which formulation systems (i.e. solid dispersions) are measured for improvements in physicochemical properties (Tantishiyakul et al. 1996). Additionally, physical mixes of carriers and drug have also been shown to induce molecular conformation changes of the API and this would lead to an improvement in dissolution profile without any further treatment of the physical mixes.

Compared with melting, solvent depositions or co-grinding all of which induce strong molecular interaction between the active pharmaceutical ingredients (APIs) and carriers within delivery systems, mixing is less deemed energetic. In addition, processing using mixing systems has the advantages over solid dispersions in that the exposure of the drug molecules to mechanical stress, heat or solvent is avoided.

In the context of new phase formation between powder components, the previously reported methods involved in the preparation of co-crystals using co-grinding, co-precipitation, growth from the melt and slurry (Zaworotka 2005), all of which have combined mixing and attrition driven size reduction process.

In this study, we have separated the attrition size reduction step from the mixing step, and subsequently tracked the co-crystal formation during the physical mixing step. For this study, an investigation of the caffeine and urea drug co-crystal system and the APIs system, malonic acid and 2-methoxybenzamide (2-MB) was examined for co-crystal formation during a mixing step. For both molecular complexes, three different primary particle size fractions were employed of 20- 45μm, 75-125μm, and 180- 250μm. The impact of particle size of the components on co-crystal formation for both systems was monitored using XRPD, DSC, SEM, and Hot-stage microscopy.

9.2. Cross-Reference to the methods

For the methods relevant to this section, see Chapter 2, Section 2.4.

9.3. Results and discussion

The outcomes for both the urea/ 2-MB and caffeine/ malonic acid systems with regards co-crystal formation from mixing pre-milled samples will be presented for each system and will follow powder x-ray evidence, micrograph evidence including hot stage and sorption studies respectively.

9.3.1. XRPD Results of urea/ 2-MB co-crystal

A visual inspection of the resulting diffractograms was undertaken to track any conversion of the components to co-crystal showed the following observations: Figure 68 shows that there was no difference in XRPD spectra between the physical mixture and the starting materials. On the other hand, the co-ground- and co-precipitated mixtures showed new

XRPD peaks at 2θ = 9.0°, 14.9° and 18.9°, similar to those of the simulated patterns, and different from those of the physical mixture.

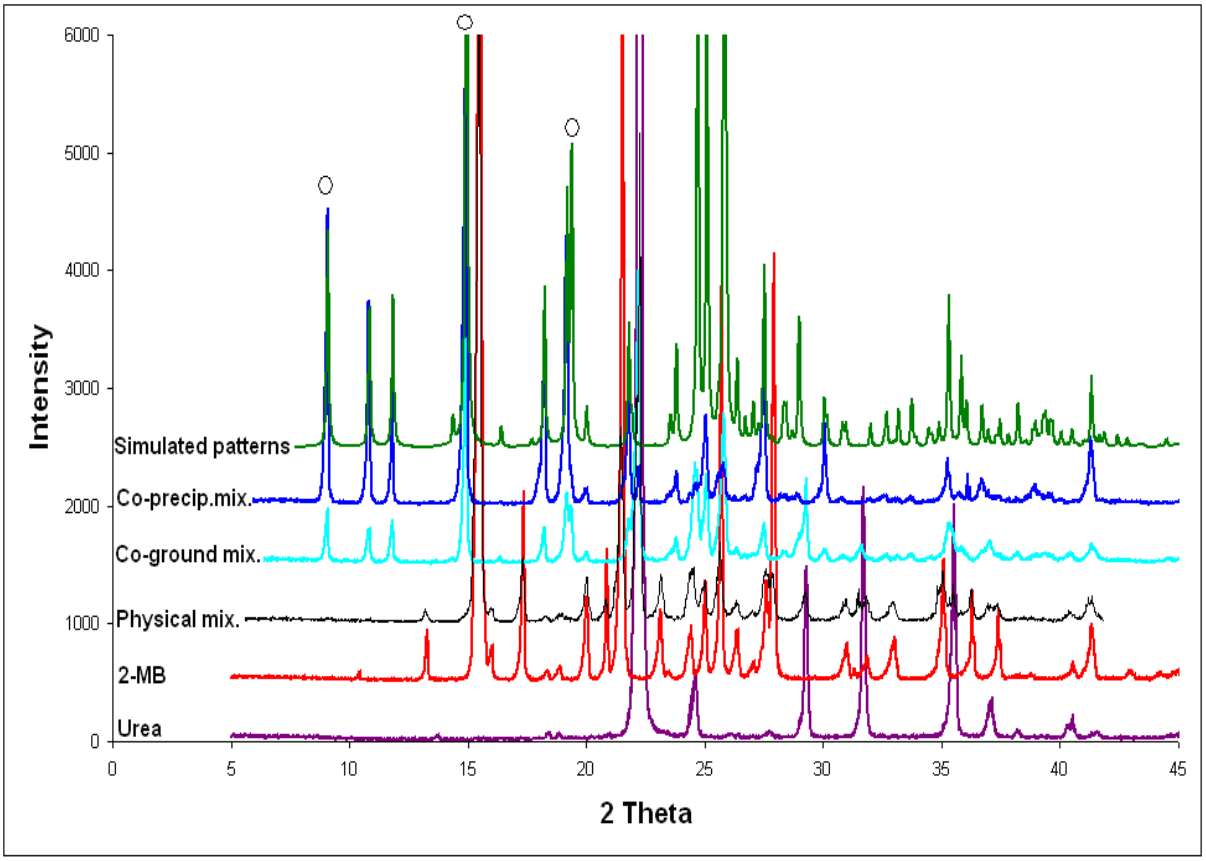

Figure 68: XRPD patterns of the urea/ 2-MB co-crystal prepared by different methods (2θ = 9.0°, 14.9° and 18.9°).

To ensure that only the particle size contributed to rate changes, the components were pre-ground and sieved to specific particle size and then low-energy convection mixing was used to introduce the components together.

The progression of the co-crystal formation, from the sieved starting components, was monitored using X-ray powder diffraction for particle size fraction of 45µm, 125µm and 250µm, as shown in Figures 69, 70 and 71, respectively.

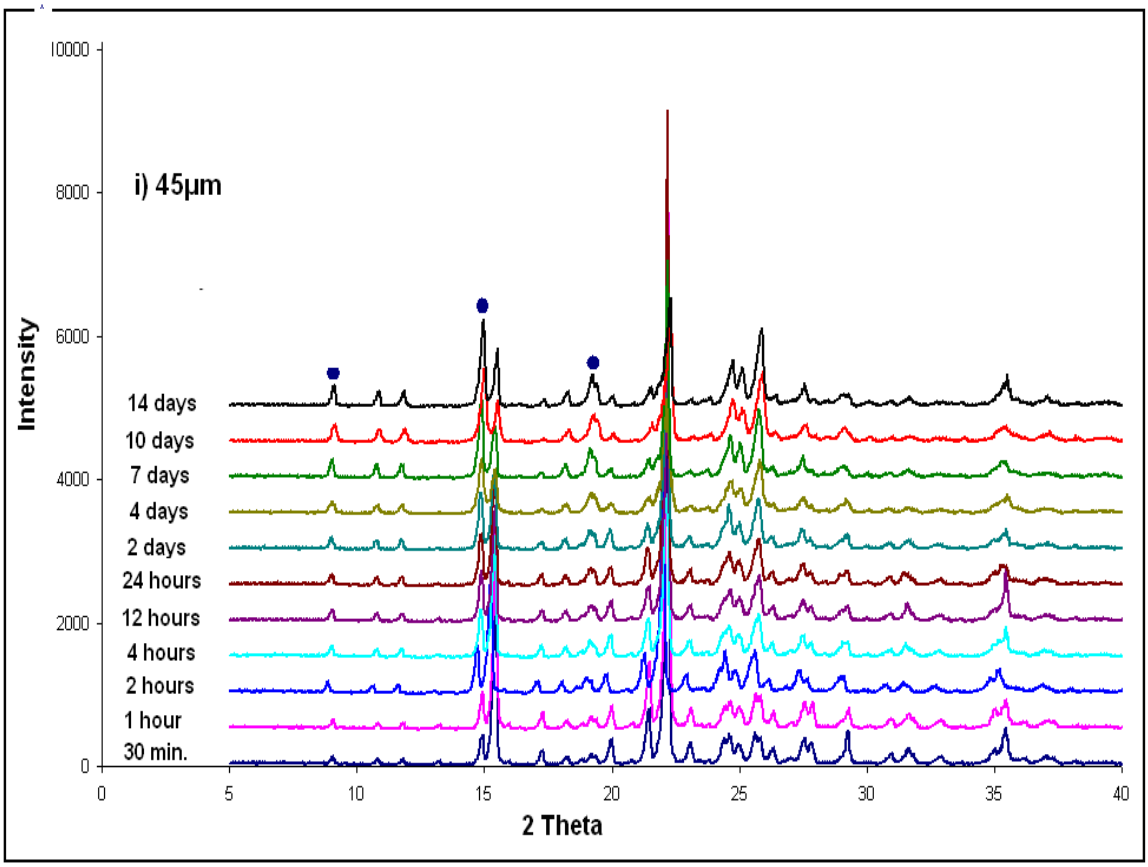

Figure 69: PXRD patterns of mixing system of the urea/ 2-MB for (20- 45µm) particle size fraction and different mixing times (30 min. to 14 days), (2θ = 9.0°, 14.9° and 18.9°).

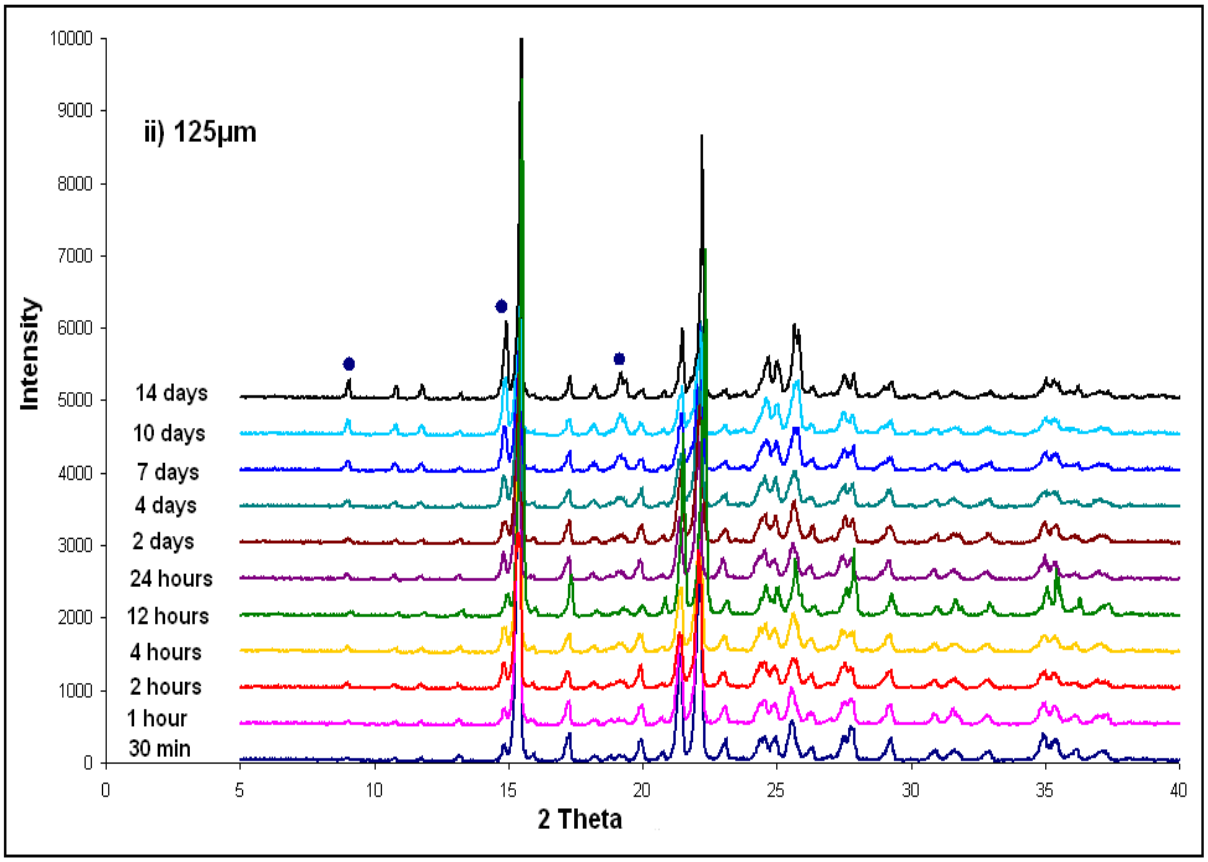

Figure 70: PXRD patterns of mixing system of the urea / 2-MB for (75- 125µm) particle size fraction and different mixing times (30 min. to 14 days), (2θ = 9.0°, 14.9° and 18.9°).

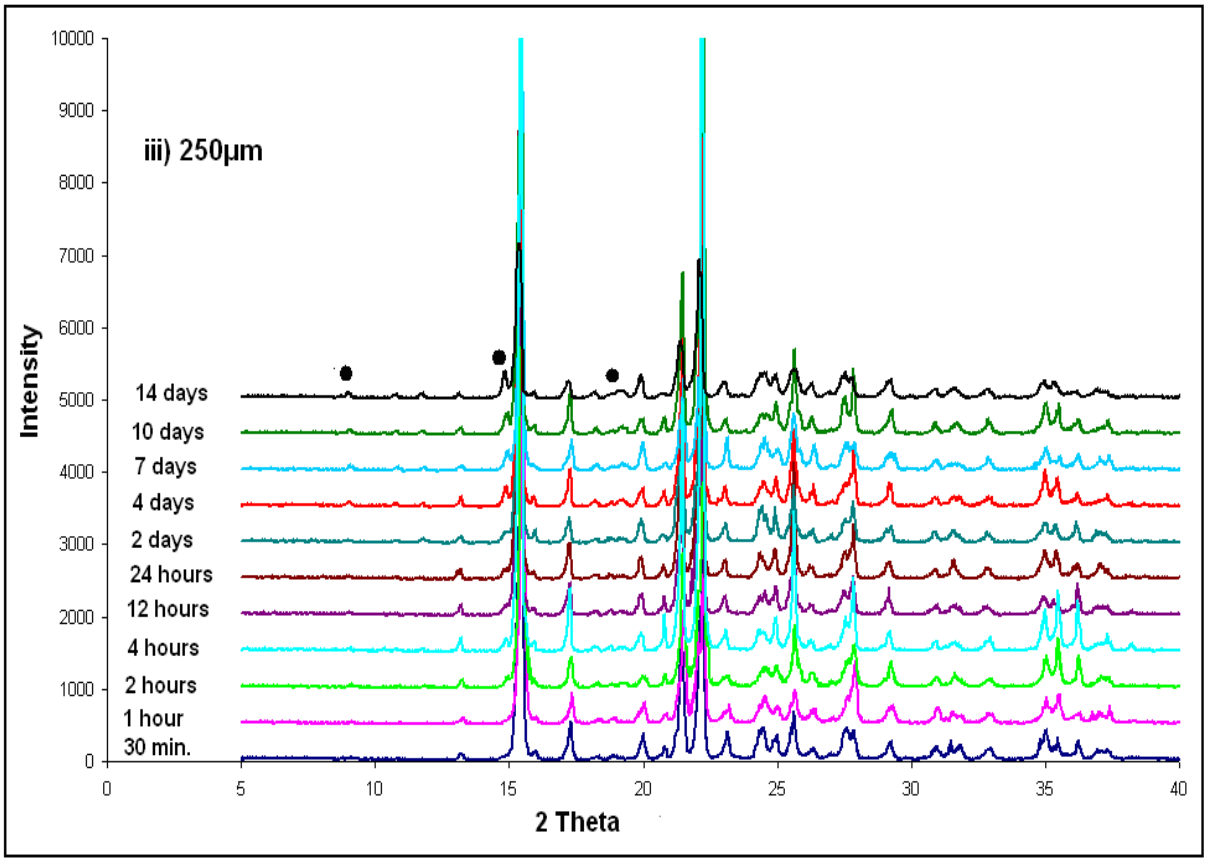

Figure 71: PXRD patterns of mixing system of the urea / 2-MB for (180- 250µm) particle size fraction and different mixing times (30 min. to 14 days), (2θ = 9.0°, 14.9° and 18.9°).

For all size fractions examined, overall transformation can be seen in the diffractograms, as the same new XRPD peaks at 2θ = 9.0°, 14.9° and 18.9° were observed; as indicated by the circles (Figures 69, 70, 71). It is obvious that the positions of new peaks were different from those of the physical mixture and similar to those of co-ground, co-precipitated mixtures and the simulated patterns (Figure 59), indicating that urea may have formed a co-crystal with 2-MB through mixing. The co-crystal started to form after 30 min. and the intensity of the new peaks increased with increasing mixing time for all size fractions.

However, the co-crystal formation for particle size fraction of 45μm was faster, compared with those for particle size fractions 125μm and 250μm. These findings reveal accelerated formation of the co-crystal upon convection mixing with decreasing initial particle size. Historically, systems with a submerged eutectic are found to have an accelerated formation as the particle size increases (Rastogi et al. 1963). This suggests that in our system the surface energetics of the particles are increased as particle size is reduced, thus favouring any surface aided processes. However, the possibilities with regards a mechanism driving the co-crystal formation may include submerged eutectics and the role of an amorphous state or uptake of water from the atmosphere (deliquescence) (Jayasankar et al. 2007), (Jayasankar et al. 2006), (Kuroda et al. 2004). However, in our system, not only amorphous state but also crystalline behaviour and polymorphic transition were present. . From observations of single crystal contact that will be discussed in Section 8.5, Figure 70 (components held together for 48 h at 25 °C on a hot-stage microscope) no conversion to the co-crystal phase was seen.

9.3.2. XRPD results of caffeine/ malonic acid co-crystals

Visual inspection of the resulting diffractograms was undertaken to track any conversion of the components to co-crystal and showed the following observations: Figure 72 shows that there was no difference in XRPD spectra between the physical mixture and the starting materials. On the other hand, the co-ground- and co-precipitated mixtures showed new XRPD peaks at 2θ = 16.2°, 22.4°, 25.6 and 28°) similar to those of the simulated patterns, and different from those of the physical mixture.

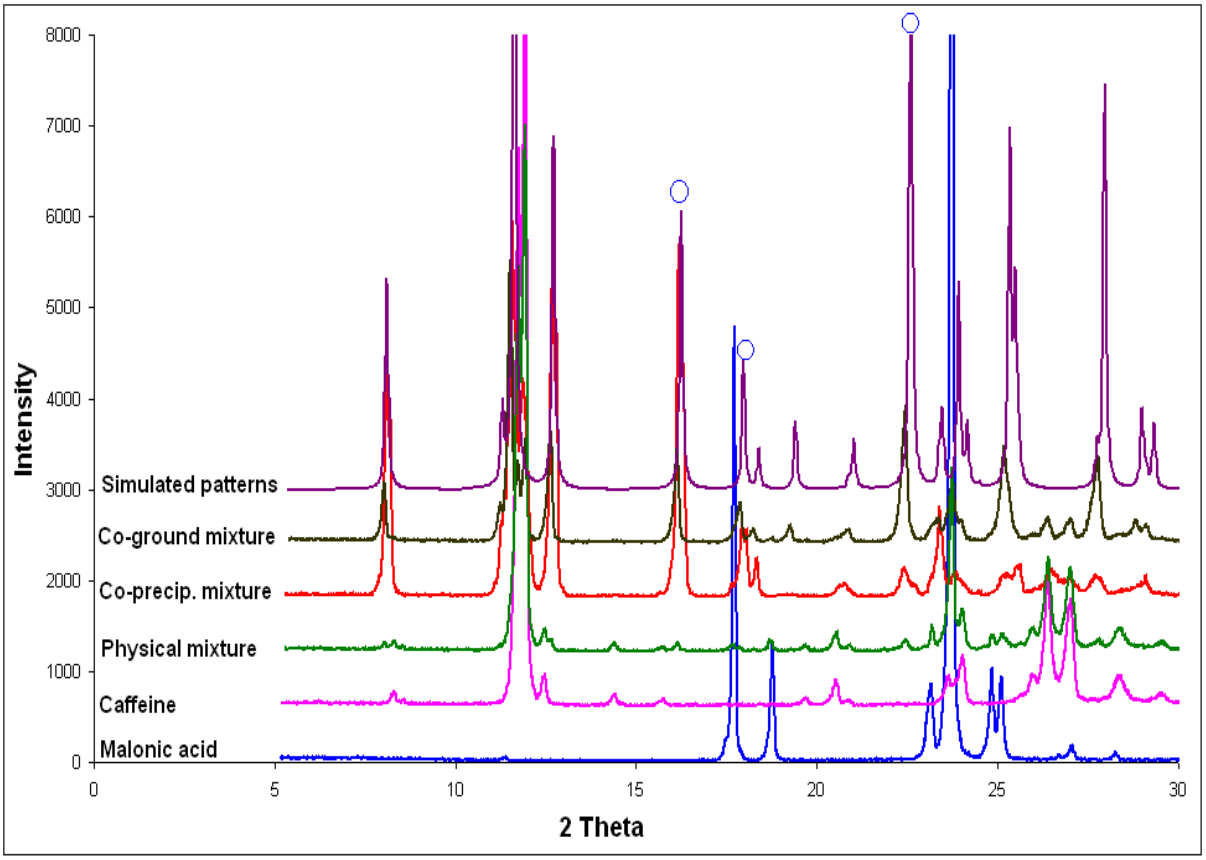

Figure 72: XRPD patterns of the caffeine/ malonic acid co-crystal prepared by different methods (2θ = 16.2°, 22.4°, 25.6° and 28°).

To ensure that only the particle size contributed to rate changes, the components were pre-ground and sieved to specific particle size and then low-energy convection mixing was used to introduce the components together.

The progression of the co-crystal formation, from the sieved starting components, was monitored using X-ray powder diffraction for particle size fraction of 45µm, 125µm and 250µm, as shown in Figures 73, 74 and 75, respectively.

The 45µm particles converted within two days, the 125µm particles within 4 days and the 250µm particles after 14 days. Overall transformation can be seen in the diffractograms as the physical mixture possesses a pair of peaks with a 2θ value of 27° whereas the co-crystal shows a single peak at 28°. The transformation is further characterized by the evolution of peaks at 16.2°, 22.4° and 25.6°.

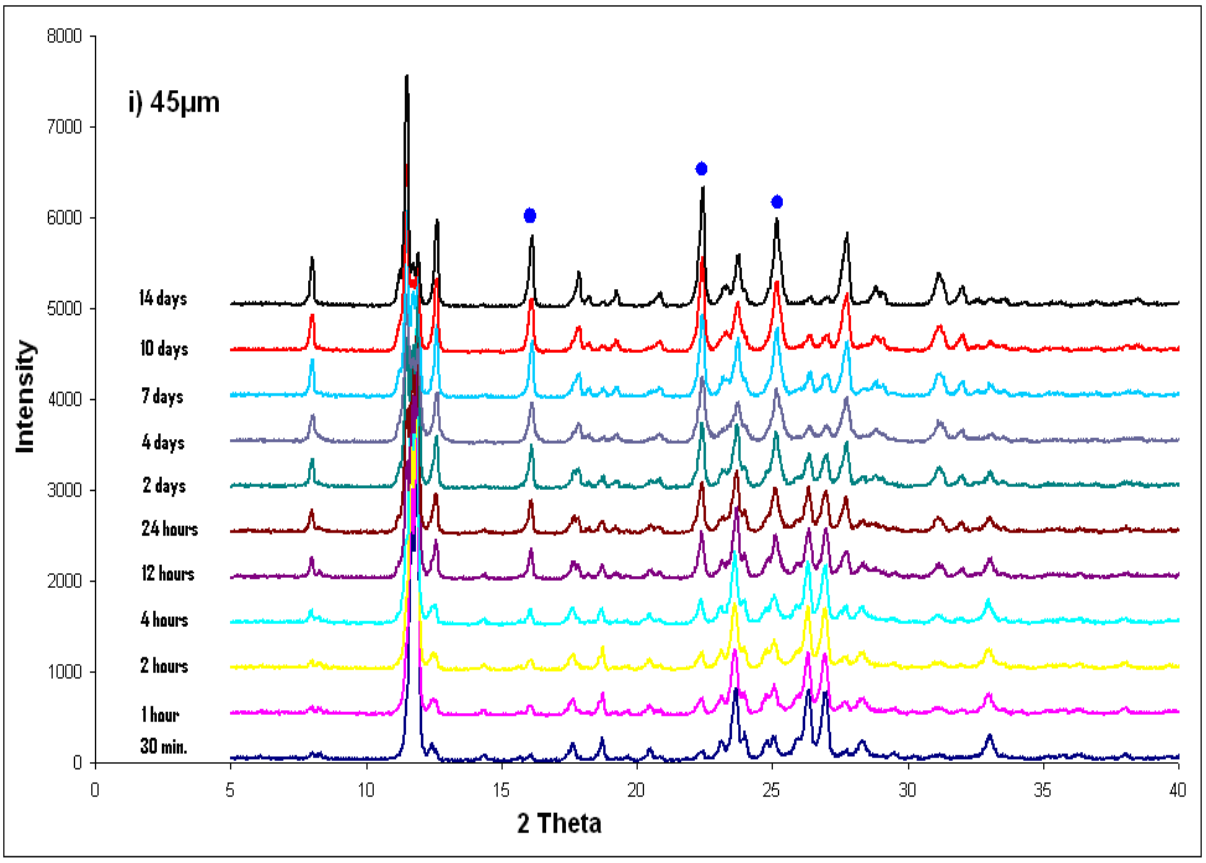

Figure 73: XRPD patterns of mixing system of the caffeine/ malonic acid for (20-45µm) particle size fraction and different mixing times (30 min. to 14 days), (2θ = 16.2°, 22.4°, 25.6° and 28°).

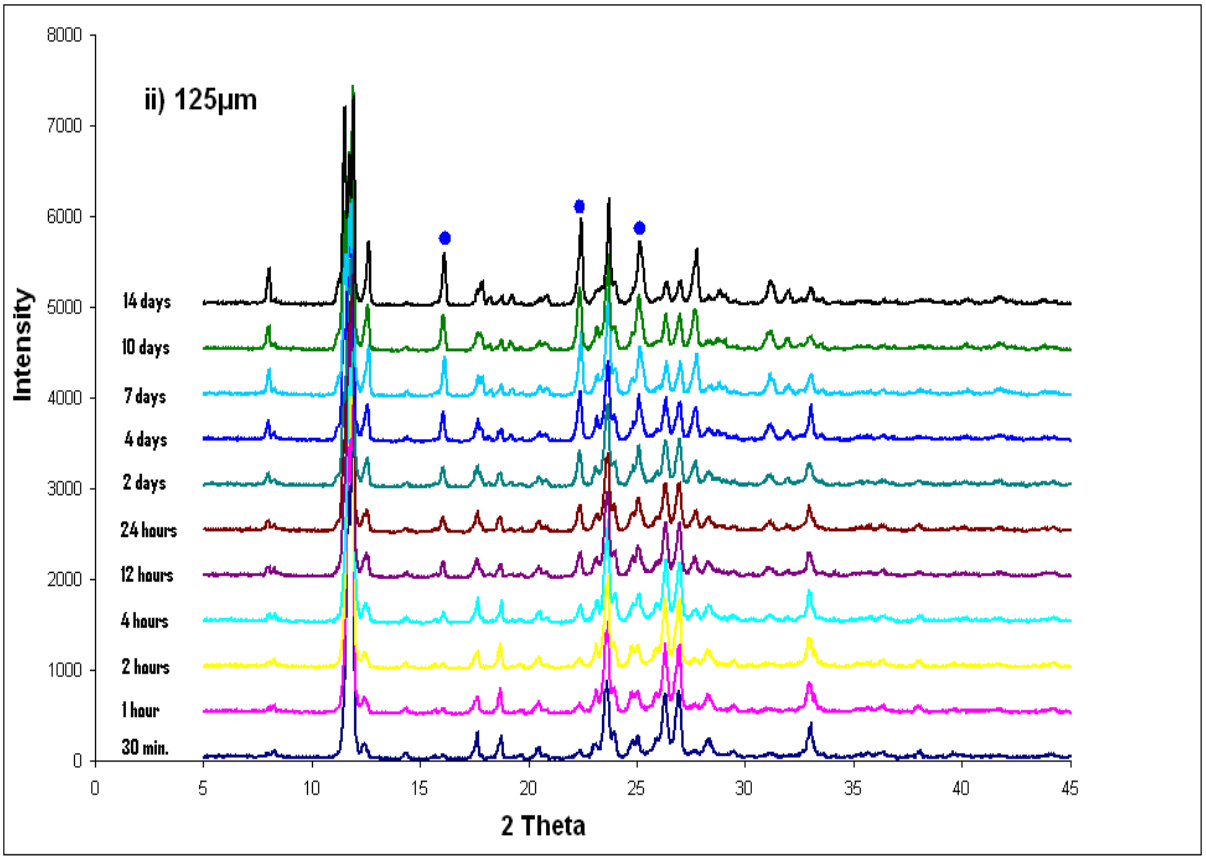

Figure 74: XRPD patterns of mixing system of the caffeine/ malonic acid for (75-125µm) particle size fraction and different mixing times (30 min. to 14 days), (2θ = 16.2°, 22.4°, 25.6° and 28°).

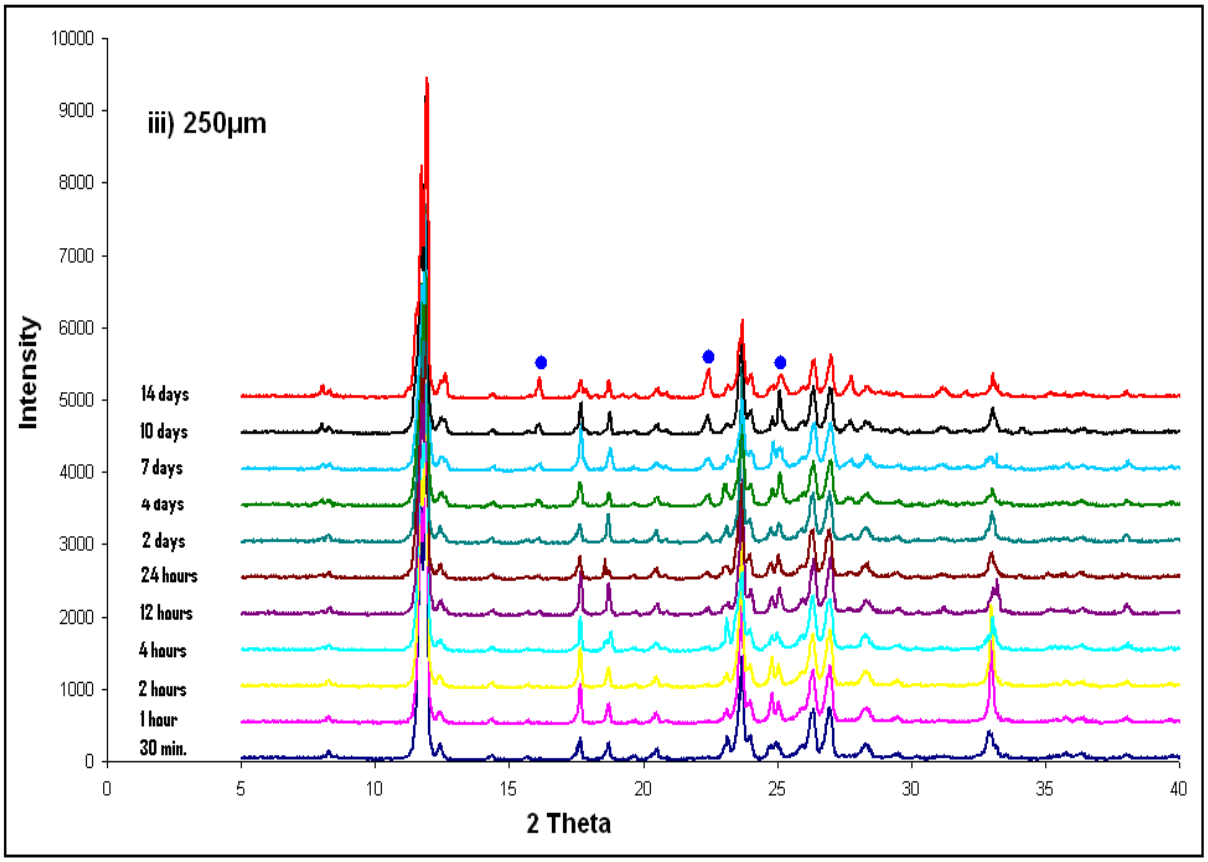

Figure 75: XRPD patterns of mixing system of the caffeine/ malonic acid for (180-250µm) particle size fraction and different mixing times (30 min. to 14 days), (2θ = 16.2°, 22.4°, 25.6° and 28°).

It is already established that caffeine formed a co-crystal with malonic acid by both co-grinding and co-precipitation (Trask et al. 2005b). Similar to the urea/ 2-MB system, the caffeine/ malonic acid system has successfully formed co-crystal during mixing. As shown in Figure 72, there was no difference in XRPD spectra between the physical mixture and the starting materials. On the other hand, the co-ground- and co-precipitated mixtures

showed new XRPD peaks at 2θ =16.2°, 22.4°, 25.6° and 28°, different from those of the physical mixture and similar to those of simulated patterns.

For all particle size fractions of 45μm, 125μm and 250μm (Figures 73, 74, and 75), the same new PXRD peaks at 2θ = 16.2°, 22.4°, 25.6° and 28° were observed as indicated by the circles. It is obvious that peak positions of new peaks were different from those of the physical mixture, indicating that caffeine may have formed a co-crystal with malonic acid during mixing. Similar to the urea/ 2-MB system, the co-crystal started to form after 30 min, and the intensity of the new peaks increased with increasing mixing time for all size fractions.

However, the rate of co-crystal formation for size fraction of 45μm increased rapidly with time compared to those for size fractions of 125μm and 250μm. Even though, historically, systems with a submerged eutectic are found to have an accelerated formation as the particle size increases (Rastogi et al. 1963), the current findings suggest that on mixing, it is the resulting particle contact of the pre-milled crystals that contributes to co-crystal formation and with the observation that the rate of the process increases as the particle size decreases.

9.4. Quantitative (peak width) analysis

Having investigated the possible mechanism for co-crystal formation, the extent (kinetics) was examined using quantitative XRPD (Klug and Alexander 1970).

The analysis was carried out by calculating the net areas of the relevant and significant resolvable peaks for the co-crystal and for the starting materials. Transformation was tracked using the ratio was obtained by dividing the area of the co-crystal by the area of the starting material ($\text{Area}_{\text{co-crystal}}$/ $\text{Area}_{\text{st.material}}$). Finally, the trajectory of transformation using

this peak area approach was presented by plotting the calculated ratio versus time (Klug and Alexander 1970).

9.4.1. Quantitative (peak width) analysis of urea/ 2-MB mixing systems

The quantitative peak width analysis of the mixing system of urea/ 2-MB using the co-crystal/ 2-MB and the co-crystal/ urea are given in Figure 76 and Figure 77 respectively.

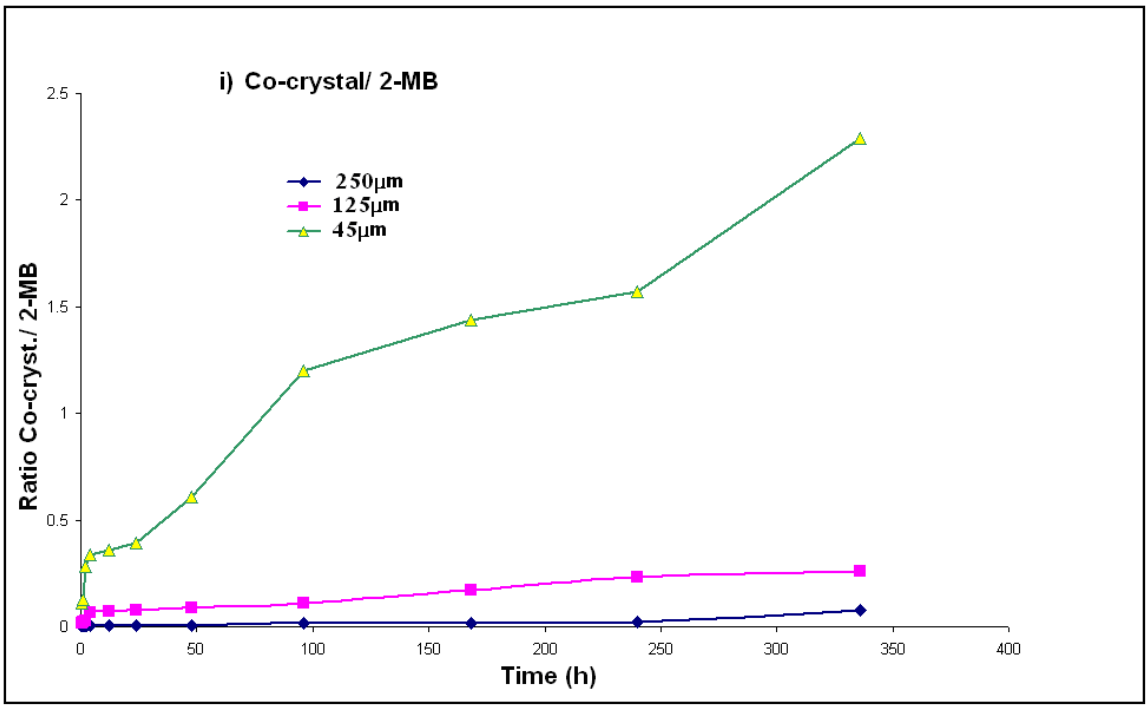

Figure 76: Quantitative representation peak width analysis of the mixing system of urea/ 2-MB for different particle size fractions (time versus ratio of the co-crystal and the 2-MB).

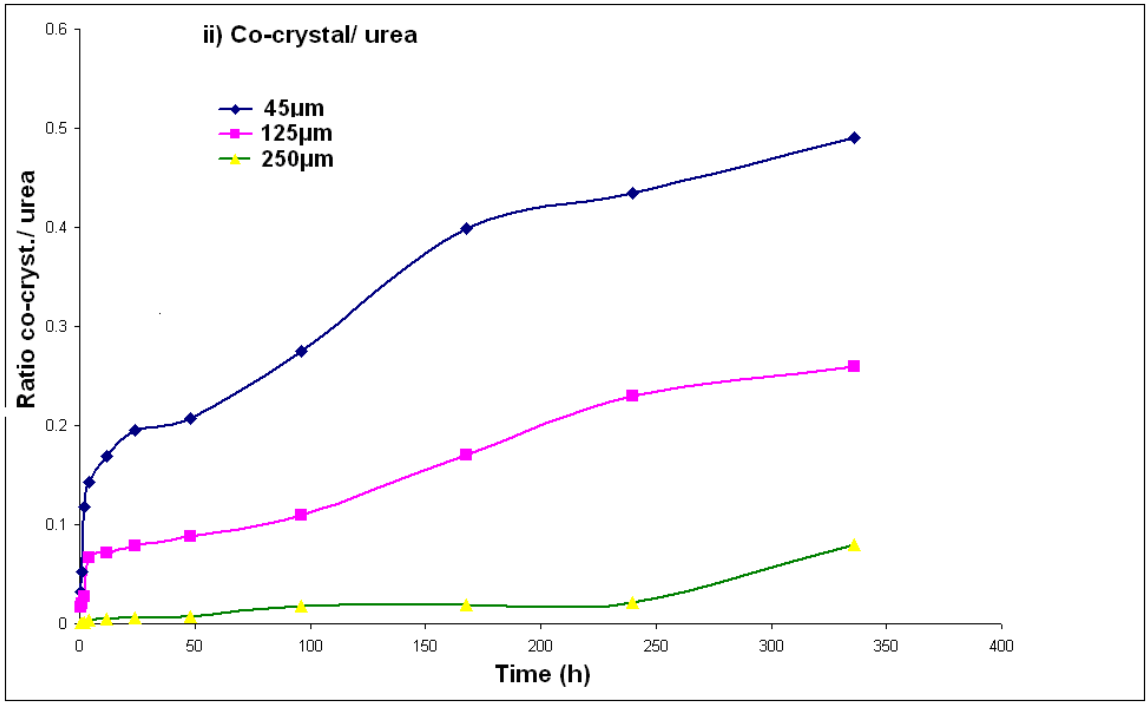

Figure 77: Quantitative representation peak width analysis of the mixing system of urea/ 2-MB for different particle size fractions (time versus ratio of the co-crystal and the urea).

To further explore the effect of particle size on the formation of co-crystals via contact in the solid-state, the ratio was higher for particle size fraction of 45µm than for particle size fractions 125µm and 250µm. On the other hand, by plotting mixing time versus ratio calculated from the peak areas of the co-crystal and the urea, the same result has been observed, and the ratio increases as the particle size decreases. This indicates that the smaller the size of the particles the greater the inter-particle contact and the faster the intermolecular interaction. In addition, the attractive forces between the particles increased with time during mixing; hence, an intermolecular interaction and hydrogen bonding between guest and host compounds were supposed to form in this manner.

9.4.2. Quantitative peak width analysis of caffeine/ malonic acid mixing systems

The quantitative peak width analysis of the mixing system for caffeine/ malonic acid using the co-crystal/ caffeine and the co-crystal/ malonic acid are given in Figure 78 and Figure 79, respectively.

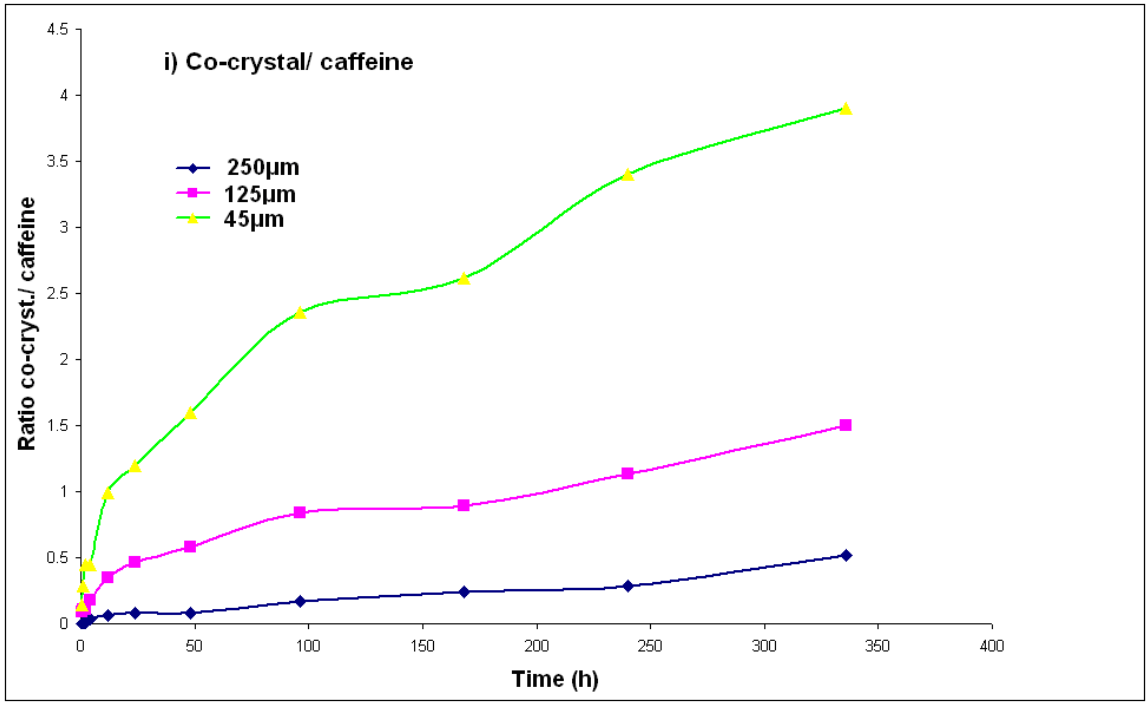

Figure 78: Quantitative representation peak width analysis of the mixing system of caffeine/ malonic acid for different particle size fractions (time versus ratio of the co-crystal and the caffeine).

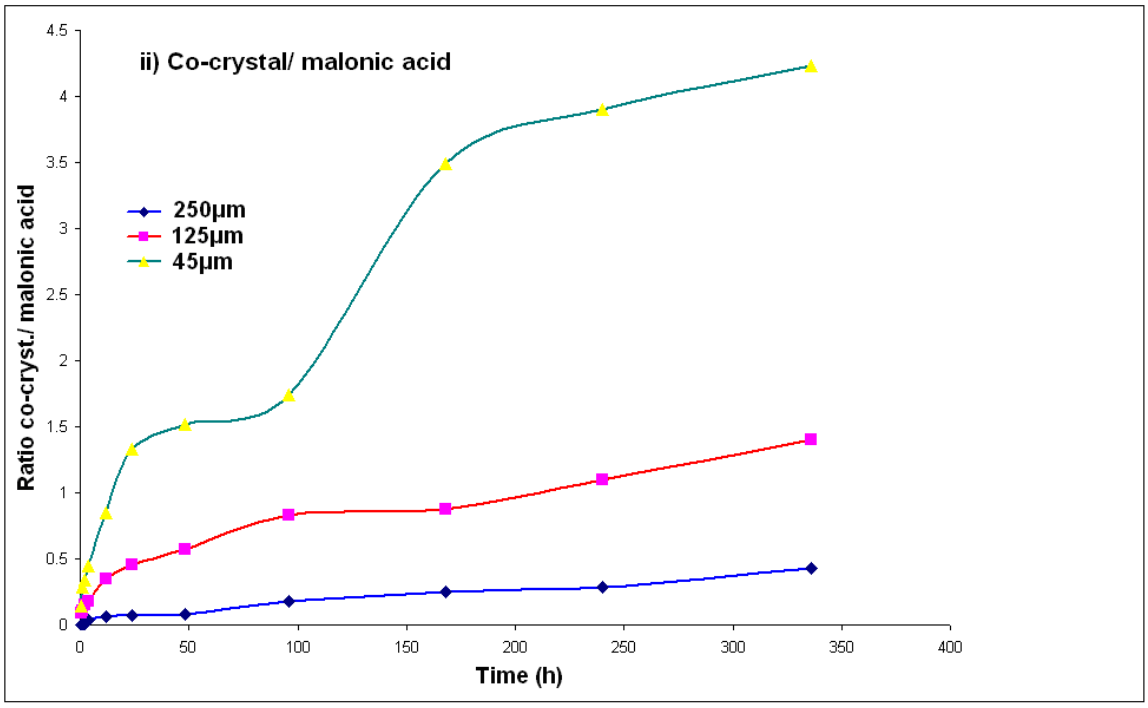

Figure 79: Quantitative representation peak width analysis of the mixing system of caffeine/ malonic acid for different particle size fractions (time versus ratio of the co-crystal and the malonic acid).

As show in Figures 78 and 79, the mixing time is plotted versus the ratio calculated from the peak areas of the co-crystal/caffeine, and the co-crystal/ malonic acid, respectively. The ratios of all particle size fractions increase proportionally with time. However, the increase was found to be faster for particle size fraction 45µm, than for particle size fractions 125µm and 250µm. This again, explains the effect of particle size on phase transformation in the solid-state, and in turn, on the hydrogen bond formation.

9.5. Results of hot-stage microscope of urea/ 2-MB system

The hot-stage microscope has been developed as a technique for compound identification, molecular weight determination, purity testing, polymorphic analysis and determination of composition diagrams (Kofler and Kofler 1952), as well as to determine the co-crystalline phases that may form between two components (Davis et al. 2004). In this study, we used controlled heating microscope to explore the features of co-crystalline systems and the melting point diagram of binary mixtures.

In order to identify phase behaviour between two components and rule out the effect of thermodynamic properties on co-crystal formation, mixed fusion or contact method was used to this end.

As shown in Figure 80, when putting two particles of the host and the guest compounds (urea and 2-MB) close to each other under hot-stage microscope at room temperature, the micrograph of the system, after 30 min was similar to that after 48 h., which indicates that no conversion of the system into co-crystal has taken place after 48 h. These results suggest that the conversion via convection mixing favours any aided processes.

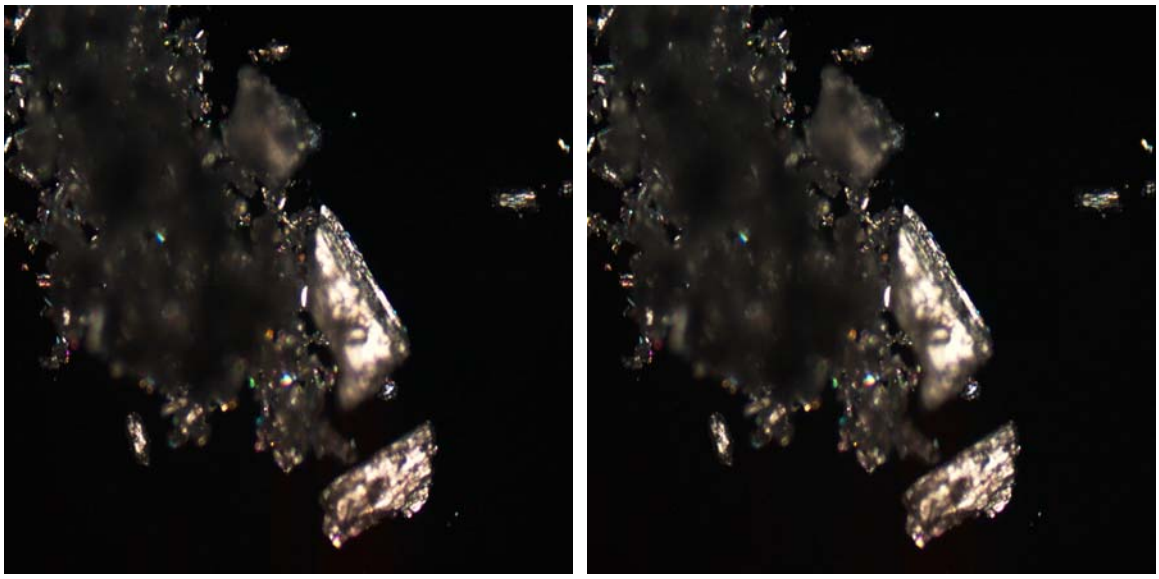

(A) **(B)**

Figure 80: Hot-stage micrographs at room temperature of urea/ 2-MB system: (A) after 30 min. and (B) after 48 h.

The hot-stage micrographs at different temperatures of urea/ 2-MB system are presented in Figure 81.

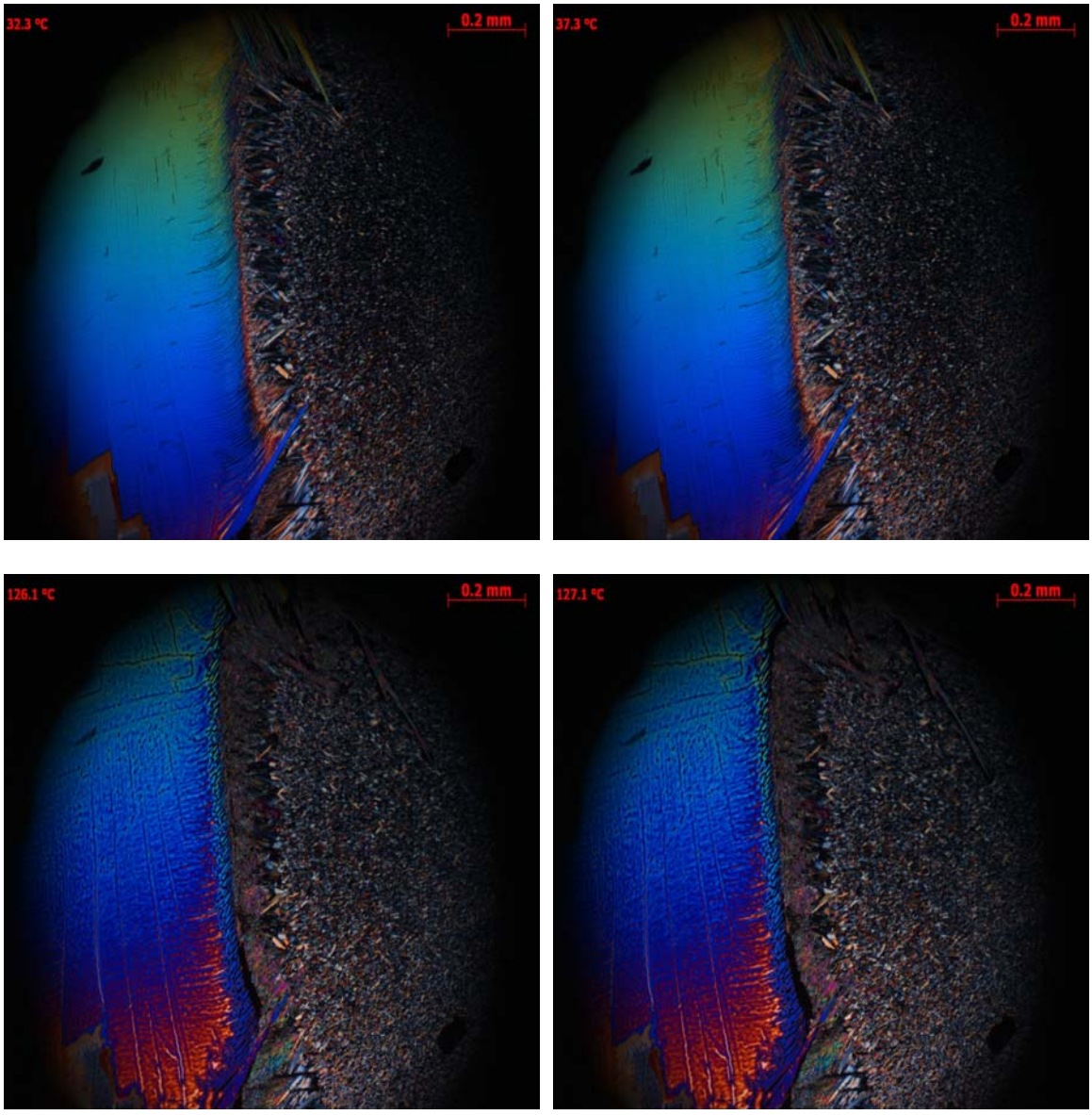

Continue

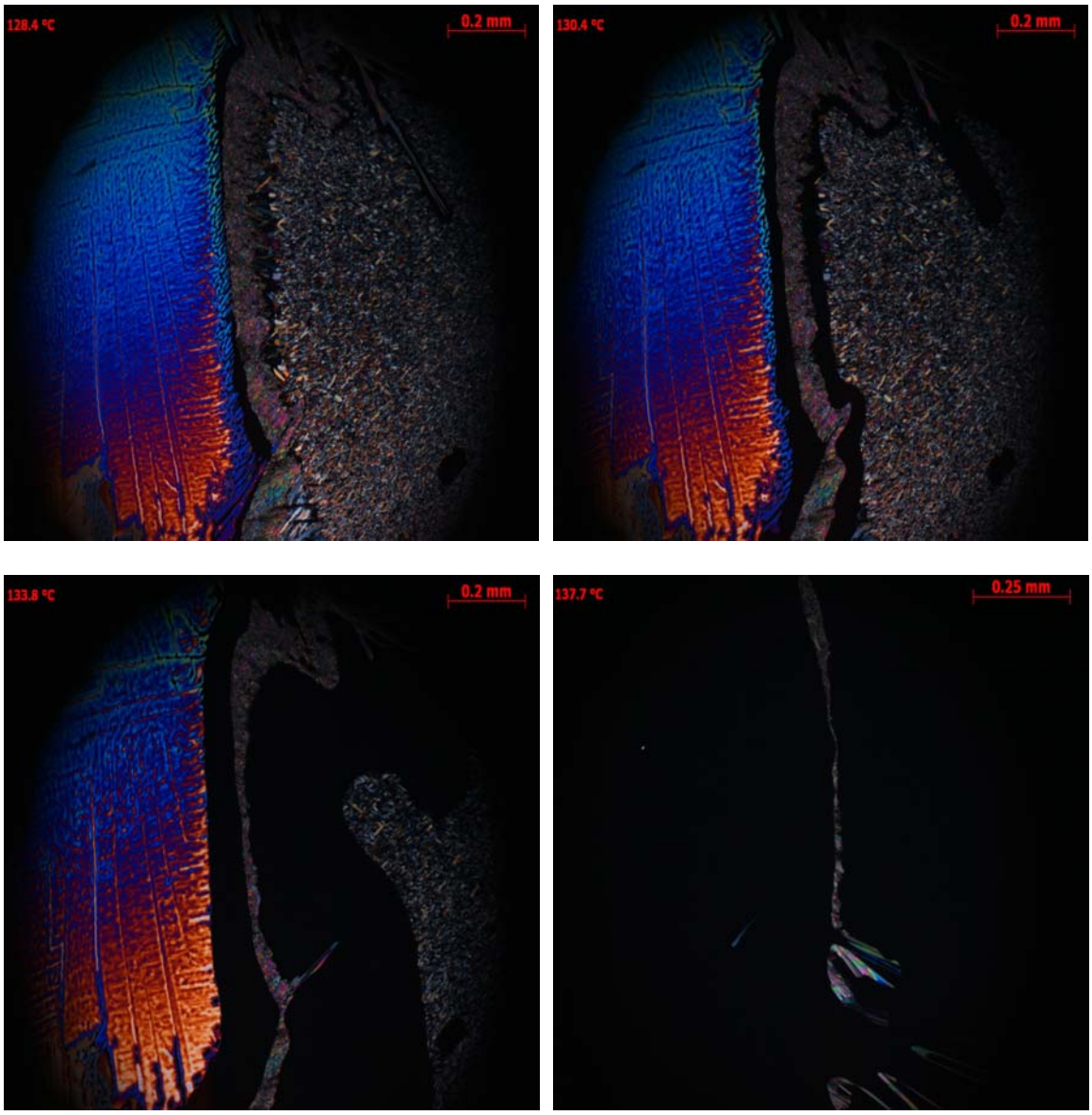

Figure 81: Hot-stage micrographs of urea/ 2-MB system: Snapshots at different temperatures.

From Figure 81, it can be seen that there are only solid phases at the temperatures 33.3 °C and 37.3°C. When the temperature was raised to 126.1 °C and 127.1 °C, the 2-MB started to melt, as it has the lowest melting point. At the temperatures 128.4 °C and 130.4 °C, the two eutectics are just visible as narrow black stripes near the center of the diagram with the

co-crystal phase between them. At increasing temperature by 137.3 °C, the two solid phases of the pure components are completely melted and the co-crystal is still solid. This shows that the urea/ 2-MB co-crystal has the higher melting point than either pure component.

9.6. Results of hot-stage microscope of caffeine/ malonic acid system

Similar to the urea/ 2-MB system, Figure 82 shows that both the hot-stage micrographs of the caffeine/ malonic acid system after 30 min. and 48 h. were the same and no change has occurred. This confirms that just a contact of coarse particles of host and guest compound did not bring about conversion into co-crystals; hence, mixing of size reduced particles through convection is the mechanism for transformation.

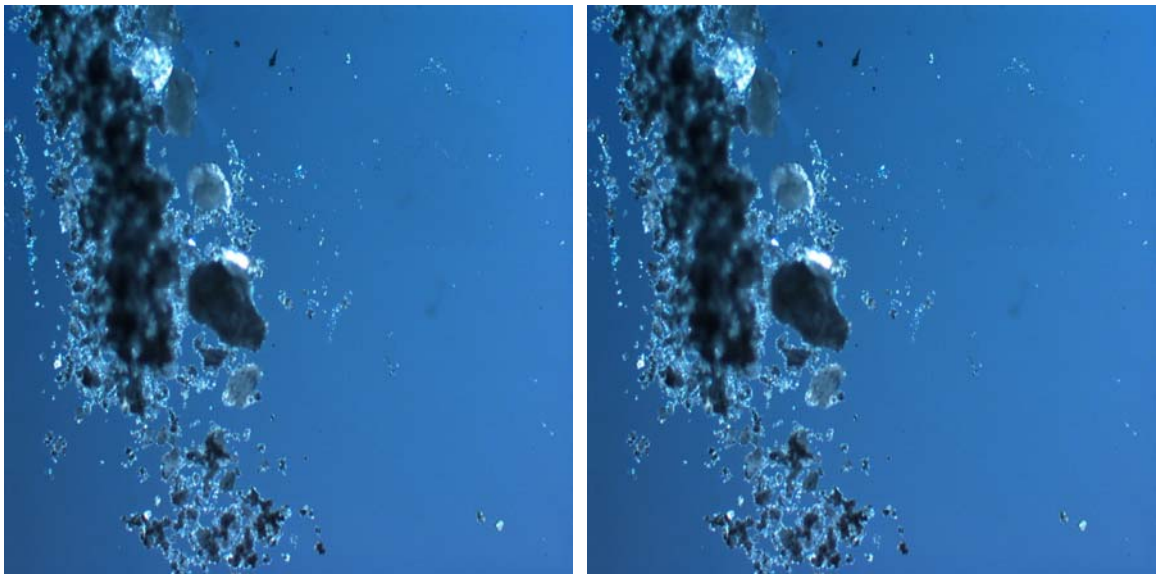

(A) **(B)**

Figure 82: Hot-stage micrographs of the caffeine/ malonic acid system: (A) after 30 min. and (B) after 48 h.

By using a controlled heating microscope to explore the features of co-crystalline systems and the melting point diagram of binary mixtures, the schematic representation of the hot-stage microscope in Figure 83 shows that at the temperatures 45.5 °C and 50.5 °C, only solid phases are detectable. Then, the malonic acid, which has the lowest melting point, started to melt at 103.7 °C. By raising the temperature to 120.1°C, the malonic acid was completely melted and the co-crystal is still visible as a narrow white stripe across the edge of the caffeine. At 136.7 °C, the co-crystal melted, while the caffeine was still solid. This situation shows that melting point of the co-crystal is an intermediate between the two starting materials.

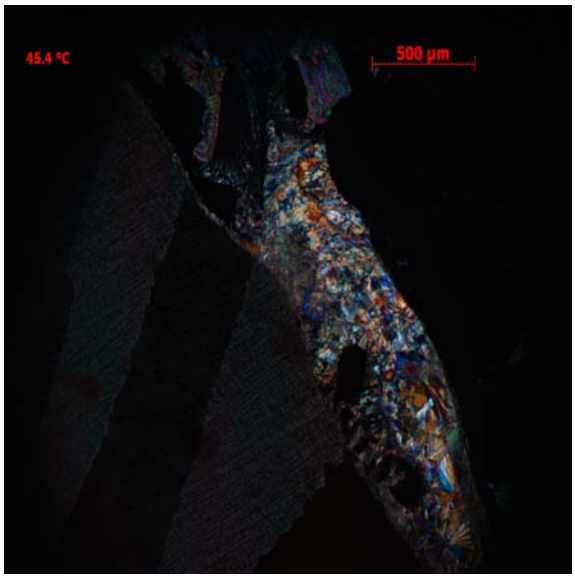

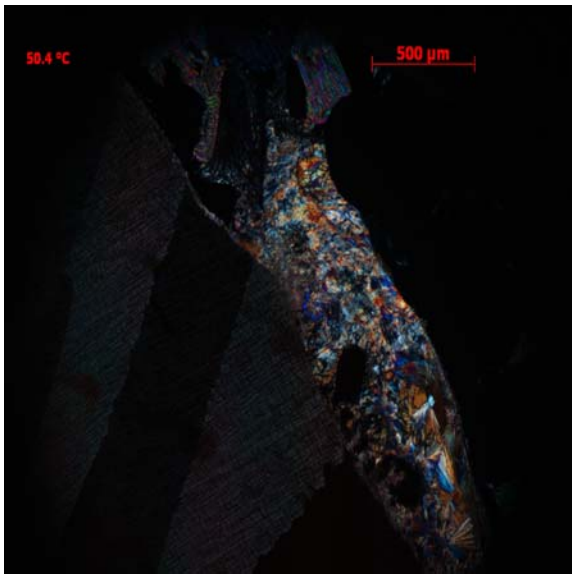

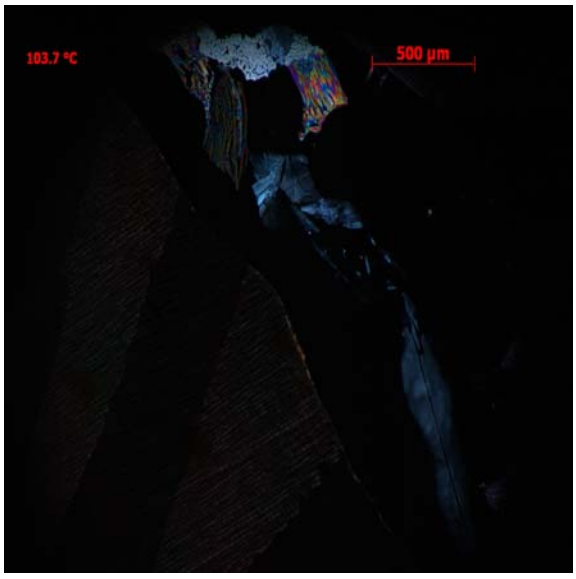

Continue

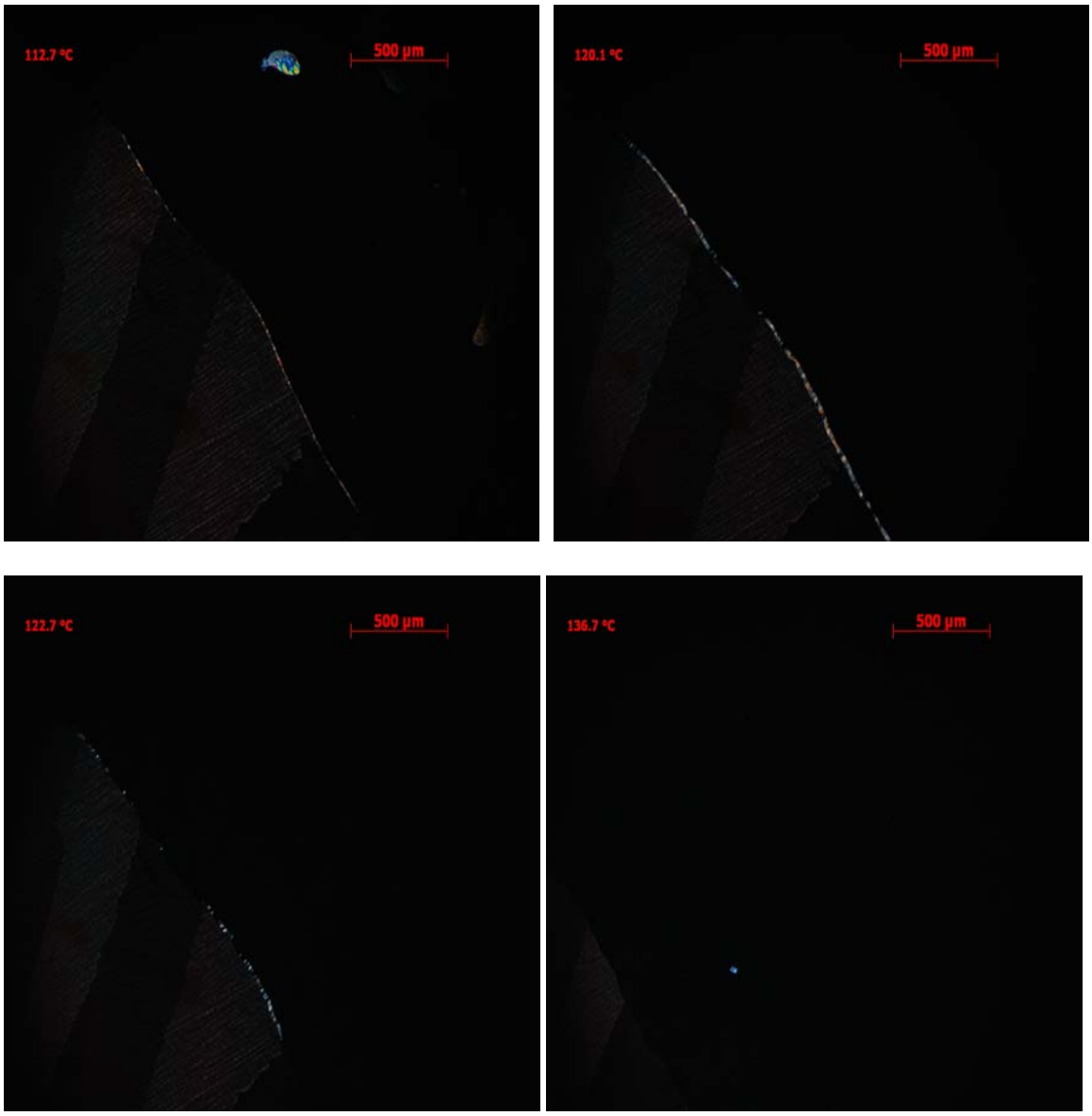

Figure 83: Hot-stage micrographs of the caffeine/ malonic acid: Snapshots at different temperatures.

9.7. Scanning electron microscopy (SEM)

To further explore the transformation and rule out the thermodynamic relationship between the co-crystal formation and the particle size, the SEM has been used for the starting materials and the mixing systems of urea/ 2-MB and caffeine/ malonic acid as shown in Figure 84 and Figure 85, respectively.

9.7.1. Scanning electron microscopy (SEM) of urea/ 2-MB mixing system

Figure 84 shows that the particles of starting materials were unchanged, as seen in the physical mixture. This is because in the physical mixture, the particles of the starting materials were pure and unmilled, and no phase transformation has occurred. On the other hand, all mixing systems that containing pre-milled particles show SEM micrographs different from that of the physical mixture. For all systems, the intact particles converted into rough and aggregated surfaces. These results suggest that a phase transformation has taken place during convection mixing, as the sizes of the particles are decreased.

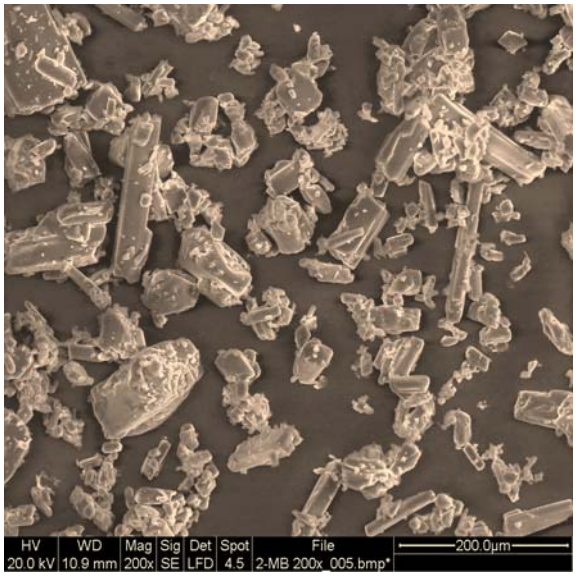

(A)

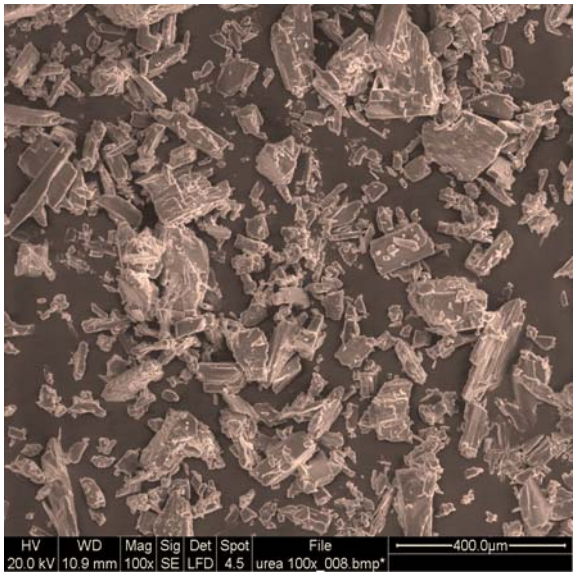

(B)

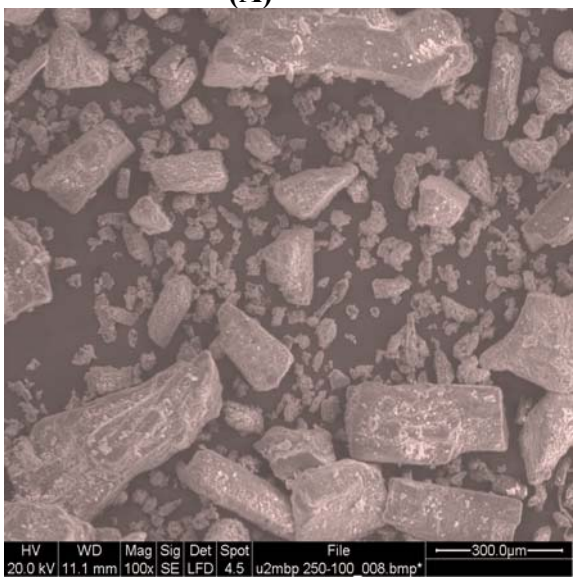

(C)

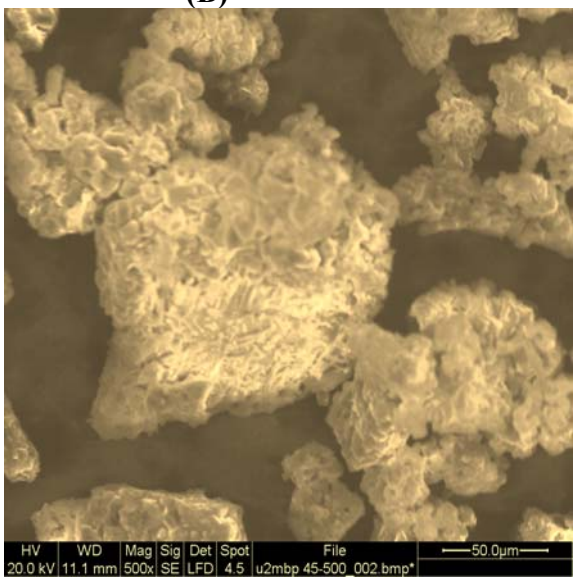

(D)

Continue

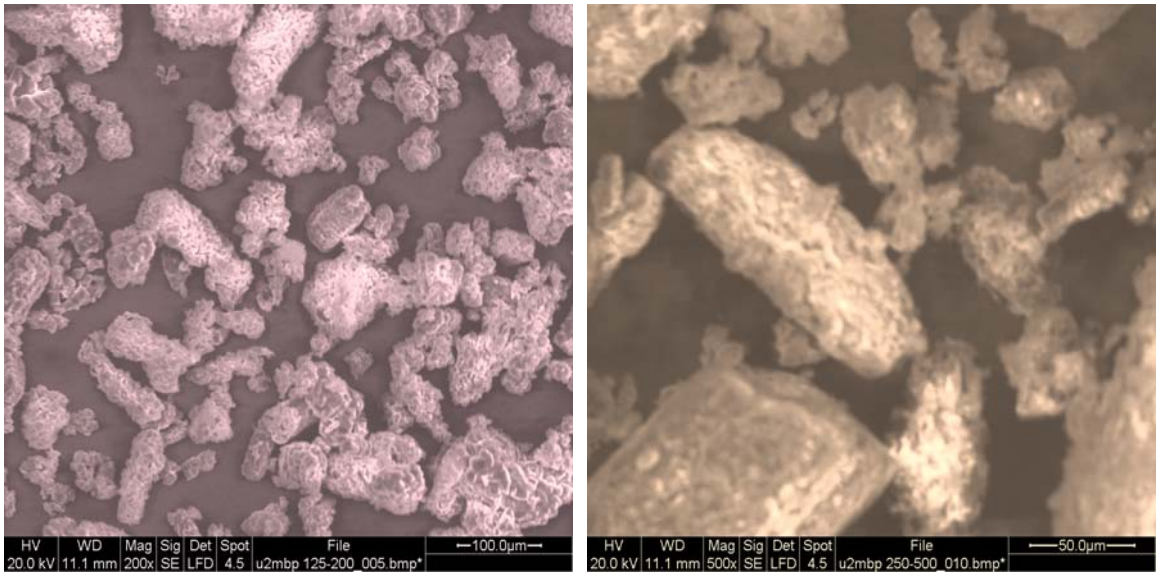

(D) **(F)**

Figure 84: SEM micrographs of the urea/ 2-MB system: (A) pure 2-MB, (B) pure urea, (C) the physical mixture, (D) mixing system 20- 45µm, (E) mixing system 75-125µm, and (F) mixing system 180-250µm.

9.7.2. Scanning electron microscopy (SEM) of caffeine/ malonic acid mixing systems

Figure 85 shows that the particles of pure and unmilled components were unchanged, as seen in the physical mixture. On the other hand, all mixing systems, exhibited SEM micrographs different from that of the physical mixture. The particles were converted into fully aggregated surfaces, indicating that caffeine may have formed a co-crystal during mixing of the pre-milled components.

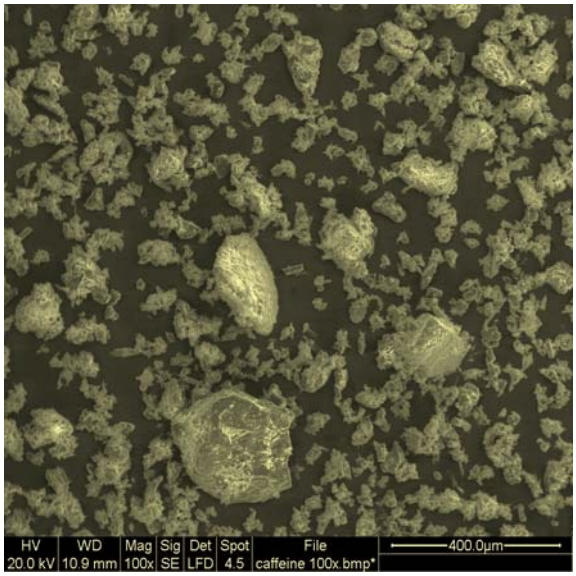

(A)

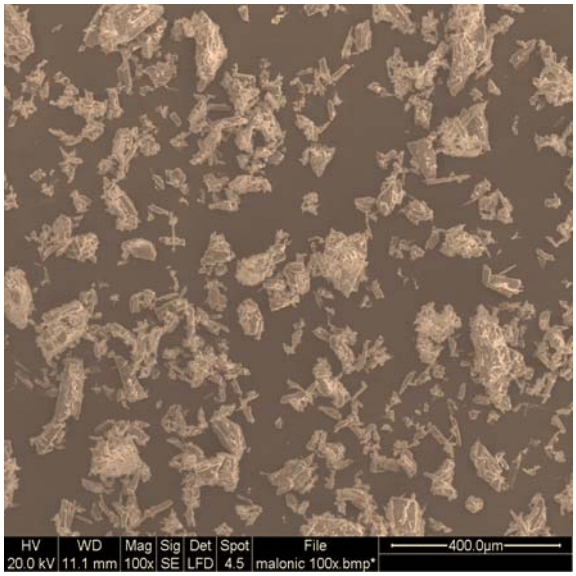

(B)

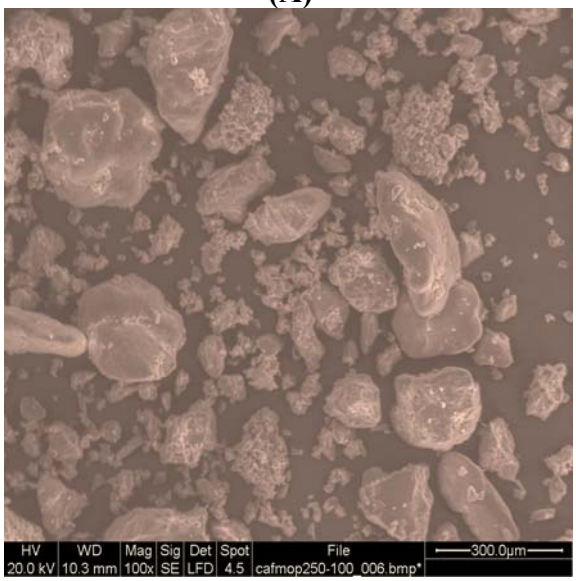

(C)

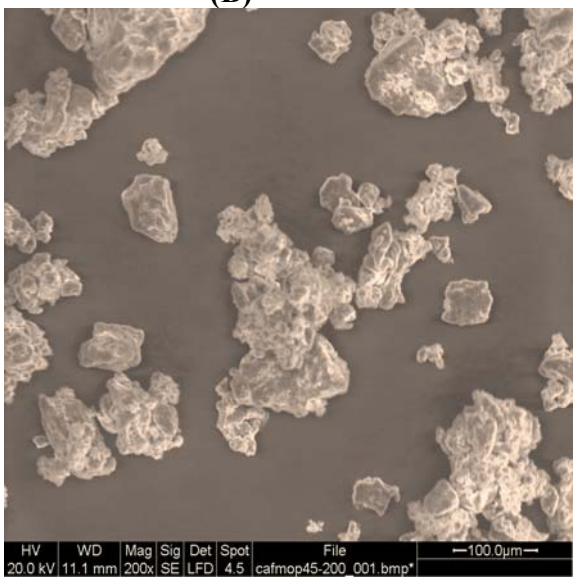

(D)

Continue

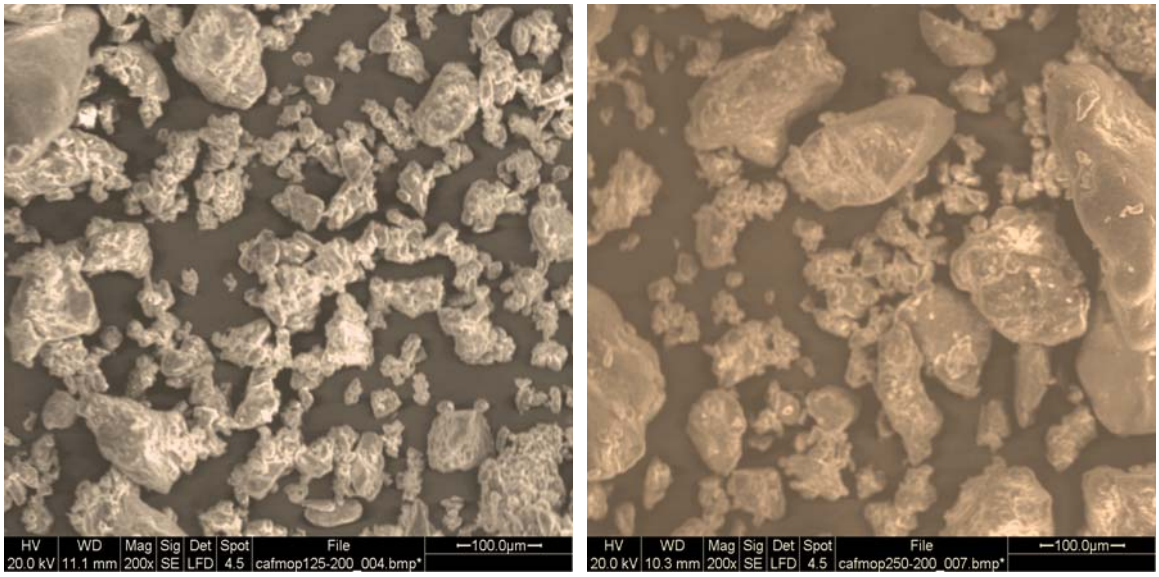

(D) **(F)**

Figure 85: SEM micrographs of the caffeine/ malonic acid mixing system: (A) pure caffeine, (B) pure malonic acid, (C) the physical mixture, (D) mixing system (20-45µm, (E) mixing system 75-125µm, and (F) mixing system 180-250µm.

9.8. Moisture sorption isotherms of the starting materials

Moisture sorption isotherms are essential thermodynamic tools for the investigation of moisture sensitive materials; they relate the equilibrium water content of the sample material to the water activity by exposing the sample to a range of relative humidities while monitoring the change in mass. Sorption isotherms can be used to identify the solid-state difference in chemically identical substances or to study important structural changes such as recrystallisation. Moisture sorption is one of the most sensitive techniques for the investigation of amorphous content with a detection cut off of 1% w/w. Moisture sorption isotherms can be obtained by static gravimetric methods using saturated salt solutions, which generate the desired relative humidity.

Concerning the role of an amorphous phase in co-crystal formation through mixing the pre-milled materials, the XRPD and DSC did not show the presence of such a phase. To this end, the moisture sorption isotherm has been determined for the starting materials to rule out the presence of sub-micron surface domains of amorphous material due to milling.

The current findings suggest that on mixing it is the resulting particle contact of the pre-milled crystals that contributes to the co-crystal formation with the observation that the rate of the process increases as the particle size decreases. This also suggests that the sub-micron detail of the surface would yield an insight into the driver of solid-state co-crystal formation. This approach does not rule out contributions from surface defects arising from milling, which generate amorphous or polymorphic surface zones, or water droplets on the surface of a drug particle, which can then contribute to conversion. The issue of localized surface phases have been previously reported with regards physical transformation of pharmaceutical ingredients through drug surface conversion, from amorphous, hydrate and polymorph sites generated by milling (Price and Young 2005).

For these reasons, the analysis of starting materials (caffeine, malonic acid, urea and 2-MB) through sorption has been carried out to determine the rate enhancement associated with these classes of sites as presented in Figures 86, 87, 88, and 89, respectively.

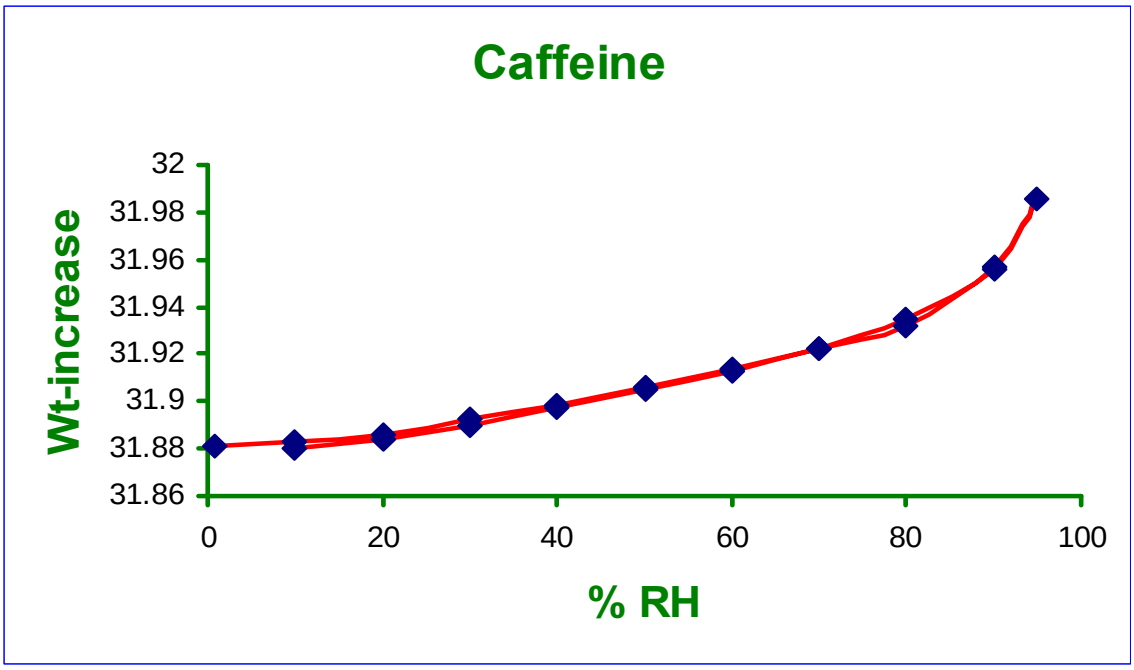

Figure 86: Sorption isotherms for a freshly milled sample of caffeine.

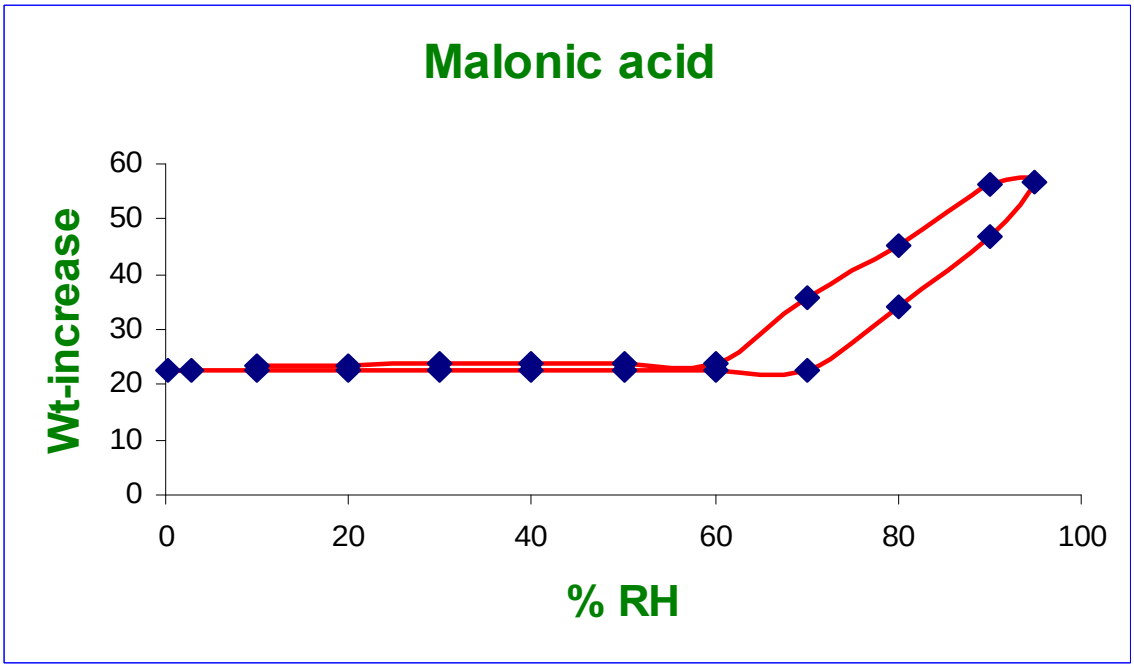

Figure 87: Sorption isotherms for a freshly milled sample of malonic acid.

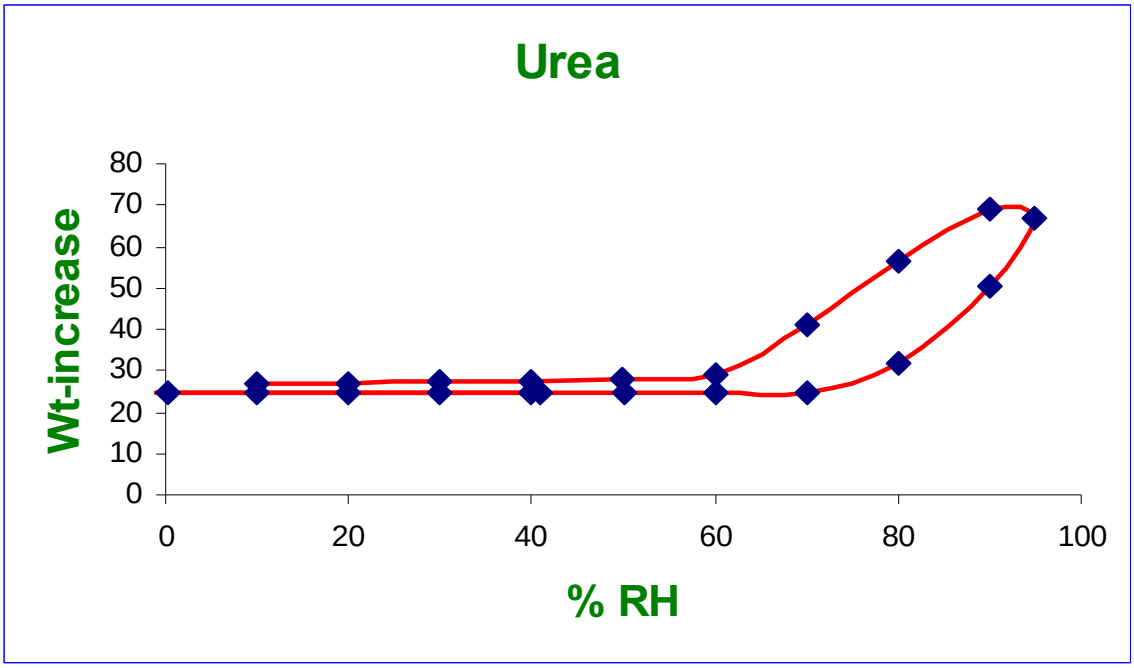

Figure 88: Sorption isotherms for a freshly milled sample of urea.

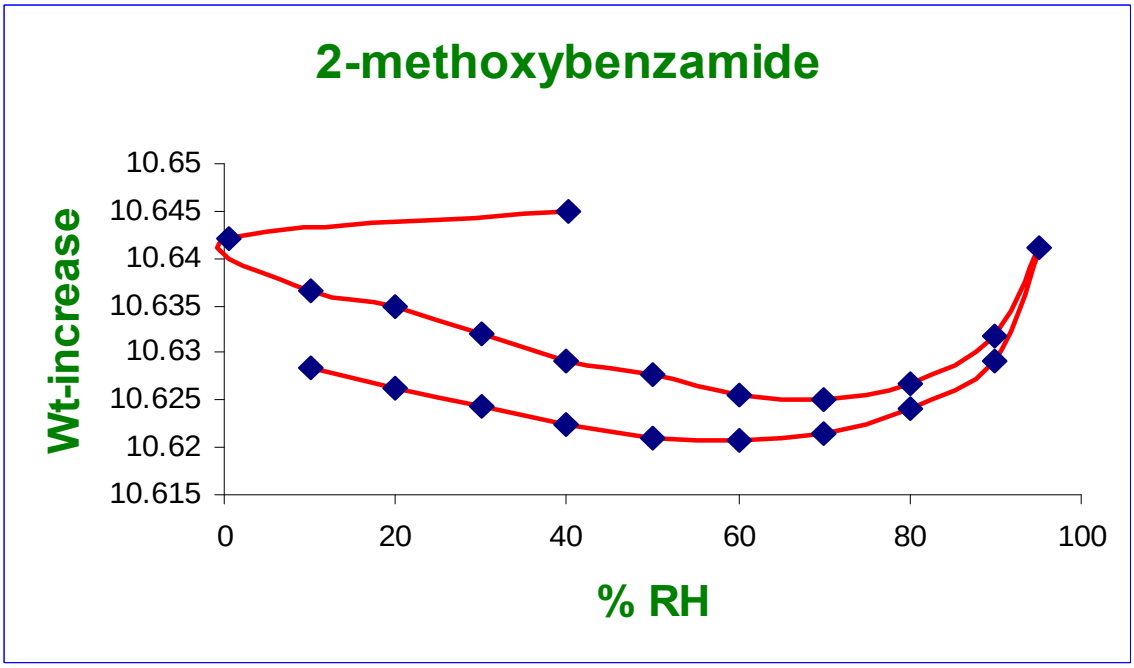

Figure 89: Sorption isotherms for a freshly milled sample of 2-MB.

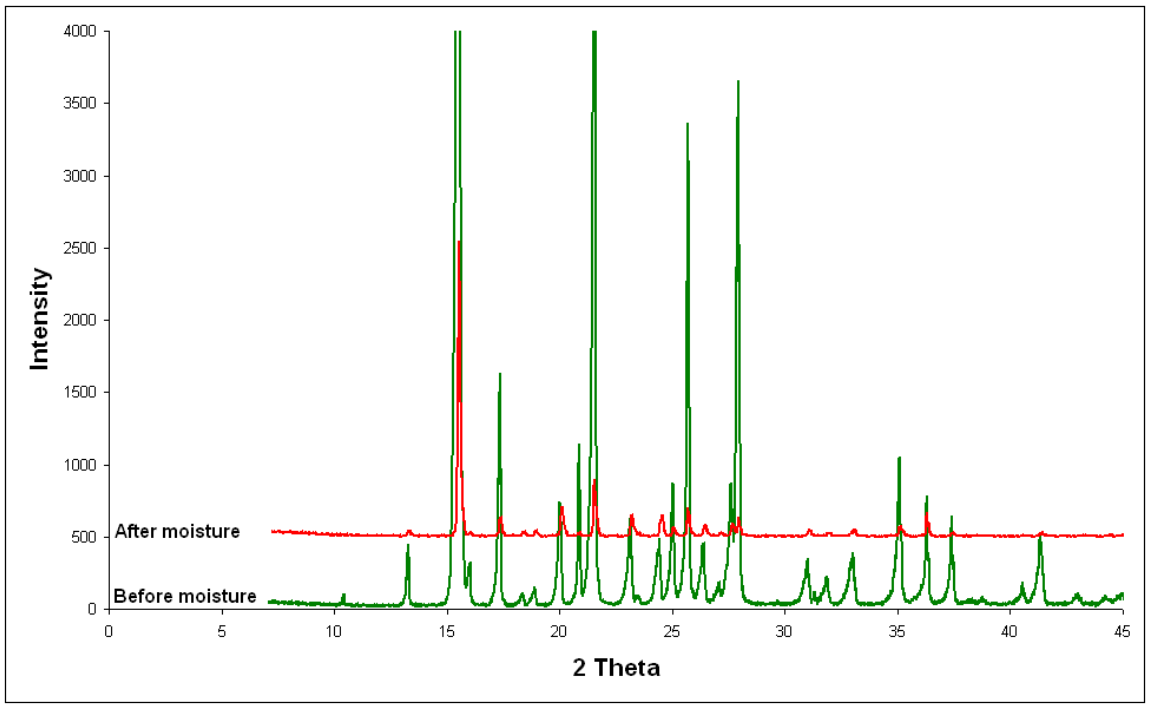

Figure 90: XRPD of 2-MB, before and after moisture sorption.

As presented in Figures 86, caffeine shows crystalline behaviour, as the weight increase against relative humidity, was very small. On the other hand, both urea and malonic acid (Figure 87 and Figure 88, respectively) exhibit some amorphous behaviour, as the weight of both dramatically increased above 60%RH. Finally, the isotherm of the 2-MB (Figure 89) is indicative of polymorphic transition with atmospheric moisture (Figure 90). This explains the role of surface phases arising from milling with regards to physical transformation of pharmaceutical ingredients through drug surface conversion, from amorphous, hydrate and polymorph sites generated by milling (Price and Young 2005).

However, in the case of caffeine, milling of the particles has not brought about any phase transformation.

9.9. Discussion and conclusion

This study demonstrated our finding of co-crystal synthesis through convection mixing. We investigated caffeine and urea as model APIs, and malonic acid and 2-methoxybenzamide (2-MB) respectively, as co-crystal formers. In both systems, three different size fractions 20- 45μm, 75-125μm, and 180- 250μm have been selected. Assessment of the transformation indicated that, typically, the co-crystals started to form after 30 min., as reflected in the intensity of the new peaks of XRPD spectra and increased with time. However, the co-crystal formation rapidly increased for size fraction 20- 45μm as the initial particle size accelerates the formation of co-crystal during convection mixing. Further investigations have been made to explore and rule out the thermodynamic relationship between co-crystal formation and particle size. In the SEM, there was no conversion observed for the pure mixture while conversion was observed for mixtures that contained pre-milled particles. The results of the hot-stage microscope study using Koffler and Koffler method indicated that for single crystal contact (components held together 48 h at 25 °C) no conversion to the co-crystal was seen, while conversion occurred at higher temperatures. The moisture sorption isotherm has also been used for the starting materials to rule out the presence of sub-micron surface domain of amorphous or polymorphic properties due to milling. The possibilities with regards a mechanism driving the co-crystal formation may include submerged eutectics, role of an amorphous state or uptake of water from the atmosphere (deliquescence) (Jayasankar et al. 2007), (Jayasankar et al. 2006), (Kuroda et al. 2004). However, in our system, not only amorphous state but also crystalline

behaviour and polymorphic transition were present. Additionally, in both systems, the DSC data show that physical mixtures form co-crystal during the heating process, indicating the presence of sub-micron surface domains of amorphous material due to milling, as previously reported to these factors to contribute (Jayasankar et al. 2006), (Jayasankar et al. 2007), (Rastogi et al. 1963).

It is concluded that the thermodynamic picture of the co-crystallization process and optimization of the kinetic effect are linked to the phase transformation during mixing. These kinetic factors were significantly important for the co-crystal formation by solid-state grinding. The data demonstrated that the acceleration of co-crystal formation accompanied a reduction in particle size, if pre-milling and low energy mixing of the component is undertaken.

The current findings suggest that on mixing it is the resulting particle contact of the pre-milled crystals that contribute to co-crystal formation. However, initial particle size accelerated the formation of co-crystal upon convection mixing and the surface energetics of the particles are increased as particle size is reduced. The data revealed a link between the polymorphic behaviour of the components and the co-crystallization process. Further, the kinetics factors were found to play a significant role in co-crystal formation by solid-state grinding, as the investigation has shown that the acceleration of co-crystal formation accompanies a reduction in particle size, if pre-milling and low-energy mixing of the components is undertaken.

10. General discussion and suggestion for future work

10.1. Discussion

Pharmaceutical co-crystallization is emerging as an attractive alternative to polymorphs, salts and solvates in the modification of an active pharmaceutical ingredient (API) during dosage form design. The physicochemical properties of the API and the bulk material properties can be modified, whilst maintaining the intrinsic activity of the drug molecule. The aim of this thesis was to study in depth the impact of the co-processing of drugs and co-crystal formers on the pharmaceutical performance of a medicinal agent. Pharmaceutical co-crystals have been studied by other researchers in the perspective of crystal engineering but have not been widely investigated in detail for drug formulation. In the first stage, the model drugs and the co-crystal formers were chosen, and the preparation of co-crystals was carried out using different methods of preparation (e.g. co-grinding, co-precipitation and hot stage temperature). In addition, other novel methods (e.g. convection mixing and compaction) have been tried to produce co-crystals. After the preparation of the co-crystals, intensive investigations had been carried out to characterize the new compounds using different techniques such as X-ray powder diffraction, Raman spectroscopy, DSC, TGA, SEM, and hot-stage microscopy.

Furthermore, intensive investigations had been carried out to evaluate the effect of co-crystallization of different systems on the pharmaceutical performance of a drug material, using different tableting parameters. These included the calculations of tensile strength of compacts to determine the compactibility. In addition, the raw compaction data and Heckel plots have been processed to calculate the yield pressure values and elastic recovery for evaluation of the compressibility of powders. All these parameters have been compared for

the different methods of preparation of the co-crystals and the physical mixtures. As a result, detailed information was made on the tableting behavior of the different mixtures and the different systems.

The objectives of this thesis were thus:

1. To study the effect of co-processing two drugs or a drug-excipient mix on the crystallographic and solid- state properties and behaviour using model drug substances and different co-crystal formers.

2. To study the manipulation of the solid-state properties of drugs through different methods such as dry-and wet grinding and co-precipitation.

3. To find out other methods of co-crystallization such as compression and mixing).

4. To evaluate the impact of the additives microcrystalline cellulose (MCC) and α-lactose monohydrate on crystallinity of co-crystals, the delay of formation of co-crystals during tableting and subsequent tableting behaviour.

5. To investigate the subsequent effect of the modification of the solid-state properties of the model drug on the overall mechanical and deformational characteristics.

Chapter 3 examined the solid-state characterization of urea/ 2-MB co-crystals prepared by co-grinding and co-precipitation methods. In addition, the tableting properties of different mixtures of the system were evaluated. All analytical techniques utilized in this research confirmed the formation of urea/ 2-MB co-crystal via both co-grinding and co-precipitation methods. However, the co-ground mixture exhibited a small intensity of the new peaks in the X-ray powder diffraction compared with the co-precipitated mixture. This was due to grinding, as it is known to decrease the XRPD peaks intensity (Oguchi et al. 2000). Further, the DSC traces showed that the physical mixture exhibited an endothermic peak at 136°C,

similar to that of the co-ground mixture, which was indicative of formation of a co-crystal during the heating process. The co-precipitated mixture had prism-like crystals, while the co-ground mixture exhibited aggregated particles as shown in the SEM micrographs. This is believed to be due to crystallization conditions, as they were found to have an impact on the crystal morphology (Hiestand et al. 1981).

The compaction data revealed that the tensile strength of compacts produced from the co-ground mixture was greater compared with either the co-precipitated or the physical mixture. However, good compact tensile strength may be due to the particle size reduction achieved by grinding, as the small size generally has good compactibility (McKenna and McCafferty 1982; Morishima et al. 1994).

The Heckel data suggested that the urea/ 2-MB systems are Type 1 materials, as an extensive linearity during compression is indicative of a plastic deformation mechanism. However, the co-precipitated mixture possessed the greatest value of yield pressure, which indicated that the densification process by particle deformation is poorer than in other mixtures. This indicated that the co-precipitated mixture was the least compressible, as the plastic deformation decreased with increasing yield pressure. On the other hand, the co-ground mixture was the most compressible. These results were consistent with the compaction results as the most compactible was the most compressible (Yoshinari et al. 2003).

In Chapter 4, caffeine was co-crystallized with malonic acid through both co-grinding and co-precipitation. The co-crystals were characterized using XRPD, Raman spectroscopy, DSC, and SEM. Similar to the urea/ 2-MB system, the co-ground mixture XRPD spectra showed small intensities compared with those of the co-precipitated mixture, resulting from grinding. The Raman spectra of the co-ground mixture were the same as those of the co-

precipitated mixture. On the other hand, the DSC traces of the system showed that the physical mixture formed co-crystals during the heating process, as indicated by endothermic peak at 132.3°C, similar to that of the co-ground mixture. Further, the SEM images revealed that the co-precipitated mixture possessed prism-like crystals, while aggregated particles had been shown in the co-ground mixture.

The tableting results of the caffeine/ malonic acid system showed that the co-ground mixture was the most compactible among all other mixtures, as reflected by higher values of the tensile strength. The Heckel plots clearly indicated that this system had undergone plastic deformation, similar to Type 1 materials. The compaction processes were proceeded by deformation rather than fragmentation of particles, as observed for sodium chloride (McKenna and McCafferty 1982). However, the co-precipitated mixture showed the best compressibility compared with both co-ground and physical mixtures, as indicated by the highest slope of the Heckel plot and the smallest yield pressure. Although the co-ground mixture was the most compactible among all the mixtures, the co-precipitated mixture showed the best ductility. This indicated that the yield strength was more a material property for this system and it was not affected greatly by the morphology of the crystals.

Chapter 5 presents the co-crystallization of caffeine/ oxalic acid system and its subsequent effect on tableting properties. The XRPD, Raman spectroscopy, SEM, and DSC confirmed the formation of the co-crystal by both co-precipitation and co-grinding methods. However, the DSC traces of the caffeine/ oxalic acid system showed that both co-ground- and co-precipitated mixtures exhibited two endothermic peaks at 209 °C and 236°C, respectively. This suggested that the melting point caffeine/ oxalic acid co-crystal is 209 °C. The second endothermic peak at 236°C is thought to be due to degradation and not the melting point of

the caffeine (see TGA and DSC of caffeine in Figure 32). This is in agreement with the literature, as it has been reported that the endotherm of caffeine between 225°C-320°C is due to fusion and evaporation, respectively (Colacio-Rodriguez et al. 1983). Similar to the urea/ 2-MB and caffeine/ malonic acid systems, which have been discussed in Chapter 3 and Chapter 4 respectively, the physical mixture of caffeine/ oxalic acid was found to form a co-crystal during the heating process, as indicated by the same melting point of both co-ground-and co-precipitated mixtures (209 °C).

In contrast to the caffeine/ malonic acid system (Chapter 4), the physical mixture of the caffeine/ oxalic acid system showed the best compactibility compared with either the co-ground or co-precipitated mixture. On the other hand, tablets of the co-precipitated mixture showed the lowest values of tensile strength and thus the smallest compactibility. The reason for this is understandable, as the needle-like crystals of the co-precipitated mixture are less dense and possess less contact points between them, which may have resulted in smaller compactibility compared with other mixtures. The Heckel plots clearly indicated that the caffeine/ oxalic acid system is similar to Type 2 materials, as the densification up to a value of 30 MPa compression pressure occurred by fragmentation. Beyond this point, the particles deformed plastically, as indicated by perfect linearity. However, the co-ground mixture possessed the highest value of yield pressure and thus the smallest compressibility among all mixtures. In addition, the co-ground mixture was found to have the smallest particle slippage ($D_0 = 0.397$) compared with those of the co-ground or physical mixture. This indicated that the co-ground mixture was the least compressible, as the plastic deformation decreased with increasing yield pressure. The co-precipitated mixture, on the other hand, showed the best compressibility as indicated by the lowest value of the yield pressure. This may have resulted from its needle-like crystals, as it has been reported by

Garekani and co-workers (1999) that the compressibility (using the Heckel-plot) of polyhedral crystal was greater than that of thin plate-like crystal.

Chapter 6 presents findings of solid-state characterization of theophylline/ malonic acid co-crystal and the impact of the co-crystallization of this system on the tableting properties. The XRPD, Raman spectroscopy, DSC and SEM revealed a co-crystal formation via both co-grinding and co-precipitation. However, the co-precipitated mixture showed a small peak at $2\theta = 7.3°$, corresponding to theophylline hydrate, was indicative of a co-crystal hydrate formation. These results are in agreement with results already published by Trask and co-workers (2005). Tablets produced from the co-ground mixture showed higher values of tensile strength compared to those of co-precipitated and physical mixture. However, the co-ground mixture possessed the greatest value of yield pressure, which indicates that the densification process by particle deformation is poorer than in other mixtures. In addition, the co-ground mixture exhibited the smallest particle slippage ($D_0 = 0.489$) compared to those of the co-precipitated or physical mixture.

The effect of excipients (MCC & α-lactose monohydrate) on the structure, formation of urea/ 2-MB & caffeine/ malonic acid co-crystals, and subsequent tableting behaviour were investigated in Chapter 7. It was obvious that MCC and α-lactose monohydrate exerted a significant change in the crystal structure of co-crystals of urea/ 2-MB and caffeine/ malonic acid systems, as shown in the XRPD and the SEM micrographs. The crystallinity of both co-crystal systems dramatically decreased with the addition of these excipients, as reflected in the reduced intensities of the peaks of XRPD patterns. However, the rate of decrease in the intensities was higher for the co-ground mixtures of both systems compared

with that of the co-ground mixtures. Furthermore, the compactibility of compacts produced from all mixtures of the two systems was found to increase dramatically after the addition of MCC and α-lactose monohydrate, however, the compactibility of the co-ground mixture containing excipients was always greater than that of the co-precipitated mixture containing excipients. On the other hand, the compressibility of all mixtures decreased after the addition of MCC and α-lactose monohydrate.

Chapter 8 presents findings of co-crystal formation for the urea/ 2-MB and caffeine/ malonic acid systems. It concluded that it was possible to form a co-crystal during compaction, as demonstrated by XRPD. For both the urea/ 2-MB and caffeine/ malonic acid systems, the physical mixtures were found to form co-crystals by compression using a Compaction Studies Press. The peak positions of the new peaks were similar to those obtained by co-grinding and co-precipitation methods, as discussed in Chapter 3 and Chapter 4. For both systems, the crystallinity increased with increasing compression force. When using the IR-Press, the urea/ 2-MB system showed no evidence co-crystal formation, while the caffeine/ malonic acid system was found to form co-crystal. However, the crystallinity decreased with increasing compaction loads, as reflected in the intensity of the new peaks that decreased with increasing the compression force.

Chapter 9 presents findings of co-crystal synthesis through convection mixing. For this study, we investigated caffeine and urea as model APIs, and malonic acid and 2-methoxybenzamide (2-MB) respectively, as co-crystal formers. In both systems, three different size fractions 20- 45μm, 75-125μm, and 180- 250μm have been selected. Assessment of the transformation indicated that, typically, the co-crystals started to form

after 30 min., as reflected in the intensity of the new peaks of XRPD spectra, increasing with time. However, the co-crystal formation increased rapidly for the size fraction 20-45μm, as the initial particle size accelerated the formation of the co-crystal during convection mixing. Further investigations have been made with the hot stage microscope using the Koffler and Koffler method. The results of this were consistent with the DSC results in Chapter 3 and Chapter 4 for urea/ 2-MB and caffeine/ malonic acid systems, respectively.

It can be concluded that the thermodynamic picture of the co-crystallization process and optimization of the kinetic effect are linked to the phase transformation during mixing. These kinetic factors were significantly important for the co-crystal formation by solid-state grinding. The data demonstrated that the acceleration of co-crystal formation accompanied a reduction in particle size, if pre-milling and low energy mixing of the component was undertaken.

In conclusion, within this thesis, XRPD, Raman spectroscopy, DSC, TGA, SEM, and hot stage microscope revealed excellent means of solid-state characterization of urea/ 2-MB, caffeine/ malonic acid, caffeine/ oxalic acid and theophylline malonic acid co-crystals. The co-crystallization of these systems showed a significant impact on the tableting behaviours. However, each system revealed different compression properties. In addition, the addition of MCC and α-lactose monohydrate exercised a significant effect on the crystal structure, compaction behaviour, and deformational characteristics of the co-crystals. Furthermore, novel methods of synthesis of pharmaceutical co-crystals through convection mixing and via compaction seem to be a promising and may open a new avenue in the pharmaceutical industry. However, more investigation of these novel types of co-crystal synthesis may be required.

10.2. Suggestions for future work

1. Perform dissolution testing on tablets produced from the co-crystals to evaluate the effect of co-crystallization on the dissolution rate of a drug material.
2. Investigation of other model drugs and co-crystal formers, for the preparation of co-crystals during compaction. Different particle size fractions could be used to explore the effect of particle size on intermolecular interaction and hydrogen bond formation. Furthermore, the surface energetic properties of the starting components could be investigated to explore its effect on the rate of conversion and co-crystal synthesis through compaction.
3. The ability of physical mixtures to form co-crystals during a heating process could be intensively investigated, using a modulated Differential Scanning Calorimetery (DSC).
4. Convection mixing gave good results in synthesizing co-crystals, depending on particle size and mixing time. Further investigation of the degree of crystallinity and determination of the amorphous content is required. This can be performed by using moisture sorption temperature and/ or DSC.
5. The co-processing of the produced co-crystals with microcrystalline cellulose and α-lactose monohydrate revealed interesting results in decreasing the crystallinity and delaying the formation of co-crystals during compaction. Further investigation would be required to evaluate this effect. Different percentages of these excipients or other excipients could be used for this study.
6. For direct compression, the homogeneity of mixing of pharmaceuticals and excipients is crucial in the manufacturing processes. This will affect quality,

efficacy and safety of a drug material. Therefore, evaluation of the mix is required to avoid fluctuation of crystal shapes, as this will affect compatibility of the tablets and compressibility of co-crystallized powders.

7. The compaction conditions such as reproducibility of the tableting machines, filling of powders and the setting of tableting parameters during compaction should be optimized, as these may affect the quality of products.

References

Aakeröy, C. B. (1997). "Crystal engineering: Strategies and architecture." *Acta Cryst.*, B53, 569-586.

Aakeröy, C. B., Beatty, A. M., Helfrich, B. A., and Nieuwenhuyzen, M. (2003). "Do polymorphic compounds make good co-crystals, importance of synthon flexibility." *Cryst. Growth Des.*, 3, 159-165.

Aakeröy, C. B., Beatty, A. M., Niewenhuyzen, M., and Zou, M. (2000). "Organic assemblies of 2-pyridones with dicarboxylic acid." *Tetrahydron*, 56, 6693-6699.

Aakeröy, C. B., Beatty, A. M., and Zou, M. (1998). "Building organic assemblies with 2-pyridone and dicarboxylic acid: Relating molecular conformation and synthon stability to co-crystal structure." *Mater.Res.Bull.*, 225-241.

Agbada, C. O., and York, P. (1994). "Dehydration of theophylline monohydrate powder: Effect of particle size and sample weight." *I. Pharm. J.*, 106, 33-40.

Allen, F. H. (2002). "The Cambridge structural database: A quarter of a million crystal structures and rising." *Acta Cryst.*, B58, 380-388.

Almarsson, Ö., and Zaworotka, J. M. (2004). "Crystal engineering of the composition of pharmaceutical phases. Do pharmaceutical co-crystals represent a new path to improved medicines?" *Chem. Commun.*, 1889-1896.

Alsaidan, S. M., Alsughayer, A. A., and Eshra, A. G. (1998). "Improved Dissolution Rate of Indometacin by Adsorbents." *Drug Dev. Ind.Pharm.*, 24, 389-394.

Armstrong, N. A., and Haines-Nutt, R. F. (1974). "Elastic recovery and surface area changes in a compacted powder system." *Powder Technology*, 9, 287-290.

Banerjee, R., Bhatt, P. M., Ravindra, N. V., and Desirju, G. R. (2005). "Saccharin salts of active pharmaceutical ingredients, their crystal structures, and increased water solubilities." *Crystal Growth Des.*, 5(6), 2299-2309.

Batchelor, E., Klinowski, J., and Jones, W. (2000). "Crystal engineering using co-crystallization of phenazine with dicarboxylic acids." *J. Mater. Chem.*, 10, 839-848.

Blagden, N., de Matas, M., Gavan, P. T., and York, P. (2007). "Crystal engineering of active pharmaceutical ingredients to improve solubility and dissolution rates." *Adv. Drug Deliv. Rev.*, 59, 617-630.

Boldyrev, V. V., and Takacova, K. (2000). "Mechanochemistry of solids: Past, present, and prospects." *J.Mater. Synth. Proc.*, 8, 121-132.

Bolhuis, G., and Chowan, Z. (1996). "Materials for direct compaction." *Pharmaceutical Powder Compaction Technology. New York: Marcel Dekker*, 419-501.

Bolhuis, G. K., Rechman, G., Lerk, C. F., Van Kamp, H. V., and Zuurman, K. (1985). "Evaluation of a hydrous alpha lactose, a new excipient in direct compression." *Drug Dev Ind Pharm.*, 8, 1657-1681.

Botha, S. A., and Lotter, A. P. (1989). "Compatibility study between ketoprofen and tablet excipients using differential scanning calorimetry." *Drug Development and Industrial Pharmacy*, 15, 415-426.

Bothe, H., and Cammenga, H. K. (1980). "Composition, properties, stability and thermal dehydration of crystalline caffeine hydrate." *Thermochim. Acta*, 40, 29-39.

Braga, D., Desirju, G. R., Miller, J. S., Orpen, A. G., and Price, S. L. (2002). "Innovation in crystal engineering." *Cryst Eng Comm*, 4, 500-509.

Braga, D., Grepioni, F., and Desirju, G. R. (1998). "Crystal engineering and organometalic architecture." *Chem. Rev.,*, 98, 1375-1405.

Brandstaetter, M., and Burger, A. (1997). *abcd. J. Therm. Anal.*, 50, 559.

Brittain, H. (1995). *Physical Characterisation of Pharmaceutical Solids, Marcel Dekker, Inc.*

Brockedon, W. (1843). *British Pat 9973*.

Bruno, I. J., Cole, J. C., Edgington, P. R., Kessler, M. K., Macrae, C. F., McCabe, P., Pearson, J., and Taylor, R. (2002). "New software for searching the Cambridge structural database and visualising crystal structures." *Acta Cryst.*, B58, 389-397.

Byrn, S. R. (1999). *Solid state chemistry of drugs 2nd ed., SSCI, West Lafayette, Indiana.*

Caira, M. R., Nassimbeni, L. R., and Wildervanck, A. F. (1995). "Selective formation of hydrogen-bonded co-crystals between sulfonamide and aromatic carboxylic acids in the solid-state." *J. Chem.Soc.- Perkin Trans.*, 2, 2213-2216.

Carrow, C. J., and Wheeler, K. A. (1998). "Structural studies of trimeric pyridinium carboxylate carboxylic acid co-crystals." *Mater.Res.Bull.*, 263-275.

Childs, S., Chyall, L., Dunlap, J., Smolenskaya, V., and Stahly, G. (2004). "Crystal engineering approach to forming co-crystals of amine hydrochlorides with organic

acids. Molecular complexesof fluoxetine hydrochloride with benzoic, succinic, and fumaric acids." *J. Am. Chem. Soc.*, 126, 13335-13342.

Cohen, J. L. (1975). "Theophylline. In: Florey, K.(ED), Anhydrous profiles of drug substances." *Acadein Press, New York*, 466-493.

Colacio-Rodriguez, E., Salas-Peregrin, J. M., Sanchez-Sanchez, M. P., and Mata-Arjuna, A. (1983). "Thermal studies on purine complex. ll. Thermal behaviour of some metal complexes of theophylline." *Thermochim. Acta*, 66, 245-253.

Cooper, A. R., and Eaton, L. E. (1962). "Compaction behaviour of several ceramic powders." *J. Amer. Ceram. Soc.*, 45, 97-101.

Davis, R. E., Lorimer, K. A., Wilkowski, M. A., and Rivers, J. H. (2004). "Studies of phase relationships in co-crystal systems." *ACA*, 39, 41-61.

De Boer, A. H., Vromans, H., Lerk, C. F., Bulhuis, G. K., Kussendrager, K. D., and Bosch, H. (1986). "The consolidation behaviour of sieve fraction of crystalline lactose monohydrate." *Pharm. Weekbl. Sci.*, 8, 145-150.

Debnath, S., and Suryanarayanan, R. (2004). "Influence of processing-induced phase transformations on the dissolution rate of theophylline tablets." *Pharm. Sci. Teh*, 5(1).

Desiraju, G. R. (1989). "Crystal engineering: The design of organic solids." *El sevier*.

Desiraju, G. R. (1995). "Supramolecular synthons in crystal engineering- a new organic synthesis." *Angew. Chem. Int. Ed. Engl.*,, 34, 2311-32-27.

Desiraju, G. R., and Steiner, T. (1999). "The weak hydrogen bond: Applications to structural chemistry and biology." *Clarendon Press New York*, 9.

Duberg, M., and Nystroem, C. (1986). "Studies on direct compression of tablets XVII. Porosity- Pressure curves for the characterization of volume reduction mechanisms in powder compression." *Powder Technol.*, 46, 67-75.

Duberg, M., and Nyström, C. (1982). "Studies on direct compression of tablets Vl. Evaluation of methods for the estimation of particle fragmentation during compaction." *Acta Pharm. Suec.*, 19, 421-436.

Duddu, S. P., Das, N. G., Kelly, T. P., and Sokoloski, T. D. (1995). "Microcalorimetric investigation of phase transitions: Is water desorption from theophylline. HOH a single-step process." *I. Pharm. J.*, 114, 247-256.

Dunitz, J. (2003). "Crystal and co crystal: A second opinion." *Cryst Eng Comm*, 5, 506.

Edwards, H. G. M., Lawson, E., de Matas, M., Shields, L., and York, P. (1997). "Metamorphosis of caffeine hydrate and anhydrous caffeine." *J. Chem. Soc., Perkin Trans.*, 2, 1985-1990.

Edwards, M. R., Jones, W., and Motherwell, W. D. S. (2002). "Influence of dicarboxylic acid structure on tape networks in co-crystals of 2-pyridone." *Cryst. Eng.*, 5, 25-36.

Etter, M. C. (1985). "Aggregate structure of carboxylic acids and amides." *Isr.J.Chem.*, 25, 312-319.

Etter, M. C. (1990). "Encoding and decoding hydrogen bond patterns of organic compounds." *Acc. Chem. Res.*, 23, 120-126.

Etter, M. C. (1991). "Hydrogen bonds as design in organic chemistry." *J.phys. Chem.*, 95, 4601.

Etter, M. C., Reutzel, S. M., and Choo, C. G. (1993). "Self-organization of adenine and thymine in the solid-state." *J. Am. Chem. Soc.*, 115, pp 4411-4412.

Fell, J. T., and Newton, J. M. (1970). "The prediction of tensile strength of tablets." *J.Pharm. Pharmacol.*, 22, 247-248.

Fell, J. T., and Newton, T. M. (1971). "Assessment of compression characteristics of powder." *J. Pharm. Sci.*, 60, 1429.

Ferrari, F., Bertoni, M., Bonferoni, M., Rossi, S., Gazzaniga, A., Conte, U., and Caramella, C. (1995). "Influence of porosity and formula solubility on disintegrant efficiency in tablets." *STP Pharma Sci.*, 5, 116-121.

Ferraro, J. R. (1996). "Spectroscopy: A history of Raman spectroscopy." 11, 18-25.

Finn, R. C., Zubieta, J., and Haushalter, R. C. (2003). "Crystal chemistry of organically templated vanadium phosphates and organophosphonates." *Prog. Inorg. Chem.,*, 51, 421-601.

Fleischman, S. G., Kuduva, S. S., McMahon, J. A., Moulton, B., Walsh, R. D. B., Rodriguez-Hornedo, N., and Zaworotko, M. J. (2003). "Crystal engineering of the composition of pharmaceutical phases: multiple -component crystalline solids involving carbamazepine." *Cryst. Growth Des.*, 3, 909-919.

Forster, A., Hempenstall, J., and Rades, T. (2001). "Characterization of glass solutions of poorly water-soluble drugs produced by melt extrusion with hydrophilic amorphous polymers." *Journal of Pharmacy and Pharmacology*, 53 (3), 303-315.

Fox, C. D., Richman, M. D., Reier, G. E., and Shangraw, R. F. (1963). *Drug & Cosmet. Ind. 92*, 2, 161-164, 258-261.

Fuhrer, C. (1962). *Dtsch.Apoth.Ztg.*, 102, 827.

Fuhrer, C. (1977). "Substance behaviour in direct compression." *Labo. Pharma. Probl. Tech.*, 25, 759-762.

Fujii, M., Okada, H., Shibata, Y., Teramachi, H., Kondoh, M., and Watanabe, Y. (2005). "Preparation, characterization, and tableting of a solid dispersion of indomethacin with crospovidone." *International Journal of Pharmaceutics*, 293, 145-153.

Garekani, H. A., Ford, J. L., Roubinstein, M. H., and Rajabi-Siahaboomi, A. R. (1999). "Formation and compression characteristics of prismatic polyhedral and thin plate-like crystals of paracetamol." *In. J. Pharm.*, 187, 77-89.

Ghosh, M., Basak, A. K., Mazumdar, S. K., and Sheldrick, B. (1991). "Structure and conformation of the 1-1 molecular-complex sulfaproxyline-caffeine." *Acta Cryst.*, 47, 577-580.

Gombas, A., Antal, I., Szabo-Revesz, P., Marton, S., and Eros, I. (2003). "Quantitative determination of crystallinity of ?-lactose monohydrate by Near Infrared Spectroscopy." *I. Pharm. J.*, 256, 25-32.

Graven, B. M., and Gartland, G. L. (1974). "2-1 Crystal complex of 5,5-diethylbarbituric acid (barbital) and caffeine." *Acta Cryst.*, B30, 1191-1195.

Haleblian, J. K. (1975). "Characterization of habits and crystalline modification of solids and their pharmaceutical application." *J.Pharm. Sci.*, 64, 1269-1288.

Hamed, A. (1995). "Instrumental methods of analysis." *IN GENARO, A. (Ed.) Remington: The science and practice of pharmacy. 19th ed. Easton, Pensylvania, Mack Publishing Company*.

Hancock, B. C., and Zografi, G. (1997). "Characterization and significance of the amorphous state in pharmaceutical systems." *J. Pharm.Sci.*, 86, 1-12.

Harnby, N., Edwards, M. F., and Nienow, A. W. (1989). *Mixing in the Process Industries/ Butterworth and Co Ltd., London.*

Harris, K. D. M., and Thomas, J. M. (1990). "Structural aspect of the chlorocyclohexene thiourea inclusion system." *Chem. Soc. Faradady Trans.*, 86, 1095-1101.

Heckel, R. W. (1961a). "Density-Pressure Relationships in Powder Compaction." *Trans. Metal. Soc. AIME*, 221, 671-675.

Heckel, R. W. (1961b). "An analysis of powder compaction phenomena." *Trans. Metal. Soc. AIM E.*, 221, 1001-1008.

Hermann, J., Remon, J. P., Visavarungroj, N., Scwartz, J. B., and Klinger, G. H. (1988). "Formation of theophylline monohydrate during the pelletisation of microcrystalline cellulose-anhydrous theophylline blends." *Int. J.Ppharm.*, 42, 15-18.

Herssy, J. A., and Rees, J. E. (1970). "Particle Size Analysis Conference. Bradford, England."

Herssy, J. A., Rees, J. E., and Cole, E. T. (1973). "Density changes in lactose tablets." *J. Pharm. Sci.*, 62, 2060.

Hickey, M. B., Peterson, M. L., Scoppettuolo, L. A., Morrisette, S. L., Vetter, A., Guzman, H. R., Remenar, J. F., Zhang, Z., Tawa, M. D., Haley, S., Zaworotka, J. M., and Almarsson, Ö. (2007). "Performance comparison of a co-crystal of carbamazepine with marketed product." *Euopean Journal of Pharmaceutics and Biopharmaceutics*, 67, 112-119.

Hiestand, E. N., Amidon, G. E., Smith, D. P., and Tiffany, B. D. (1981). "Powder and Bulk Solids Handling and Processing Conf. Rosement, Illinois." *Proc. Int.*

Hiestand, E. N., Wells, J. E., Peot, C. B., and Ochs, J. F. (1977). "Physical properties of tableting." *J.Pharm. Sci.*, 66, 510-519.

Higuchi, T., Shimamoto, T., Eriksen, S. P., and Yashiki, T. (1965). "Physics of tablet compression. XIV. Lateral die wall pressure during and after compression." *J.Pharm. Sci.*, 54, 111-118.

Huang, C. M., Leiserow, L., and Schmidt, G. M. J. (1973). "Molecular packing modes. 11. Crystal-structures of 2-1 complexes of benzamide with succinic acid and furamide with oxalic acid." *J.Chem.Soc.Perkin Trans.*, 2, 503-508.

Jayasankar, A., Good, D. J., and Rodriguez-Hornedo, N. (2007). *Mol. Pharmaceut.*, 4, 360-372.

Jayasankar, A., Somwanthanaroj, A., Shao, Z. J., and Rodriguez-Hornedo, N. (2006). "Crystal formation by solid-state grinding and during storage." *Phram.Res.*, 23, 2381-2392.

Joiris, E., Martino, P. D., Berneron, C., Guyot-Hermann, A. M., and Guyot, J. C. (1998). *Compression behaviour of orthorhombic paracetamol. Pharm. Res*, 15, 1122-1130.

Kachrimanis, K., Nikolakakis, L., and Malamataris, S. (2003). "Influence of interparticle bonding." *J. pharm. Sci.*, 92(7), 1489-1501.

Kahnkari, R. K., and Grant, D. J. W. (1995). "Pharmaceutical hydrates." *Thermochim. Acta*, 248, 61-79.

Karehill, P. G., Alderborn, G., Borjesson, E., Glazer, M., and Nyström, C. (1990). "Studies on direct compression of tablets- Investigation of bonding mechanisms of some directly compressed materials by addition and removal of magnesium stearate." *Powder Technol.*

Kawakita, K., and Ludde, K. H. (1971). "Some consideration on powder compression equation." *Powder Technol.*, 4, 61-68.

Kitaigorodskii, A. (1984). "Mixed crystals." *New York: Springer- Verlag*.

Klug, H. P., and Alexander, L. E. (1970). "X-ray diffraction procedures: For Polycrystalline and Amorphous Materials." 992.

Knoechel, E. L., Sperry, C. C., Ross, H. E., and Lintner, C. J. (1967). "Instrumented rotary tablet machines. I. Design, construction, and performance as pharmaceutical research and development tools." *J. Pharm. Sci.*, 56, 109.

Kofler, L., and Kofler, A. (1952). "Thermal micromethods for the study of organic compounds and their mixtures." *Wagner, Innsbruck*.

Kuroda, R., Higashiguchi, K., Hasebe, S., and Imai, Y. (2004). *Cryst Eng Comm*, 6, 463-468.

Kwei, G. Y., Novak, L. B., Hettrick, L. A., Reiss, E. R., Ostovic, D., Loper, A. E., Lui, C. Y., Higgins, R. J., Chen, I. W., and Lin, J. H. (1995). "Regiospecefic intestinal-absorption of the HIV protease inhibitor L-735,524 in Beagle dogs." *Pharm. Res.*, 12, 884-888.

Leger, J. M., Alberola, S., and Carby, A. (1977). "Crystal structure of 1/1 complex of sulfacetamide and caffeine." *Acta Cryst.*, B33, 1455-1459.

Lehto, V. P., and Laine, E. (1998). "A kinetic study of polymorphic transition of anhydrous caffeine with microcalorimeter." *Thermochim. Acta*, 317, 47-58.

Leigh, S., Carless, J. E., and Burt, B. W. (1967). "Compression characteristics of some pharmaceutical materials." *J.Pharm. Sci.*, 56, 888.

Lewis, C. J., and Shotton, E. (1965). *J.Pharm. Pharmacol.*, 17Suppl., 82S.

Ling, A. R., and Baker, J. L. (1893). "Halogen derivatives of quinone part lll. Derivatives of quinhydrone." *J. Chem. Soc.*, 63, 1314-1327.

Lloyed, G. R., Craig, D. Q. M., and Smith, A. (1999). "A calorimetric investigation into the interaction between paracetamol and polyethlene glycol 4000 in physical mixes and solid dispersions." *European Journal of Pharmaceutics and Biopharmaceutics*, 48, 59-65.

Long, W. M. (1960). *Powder metallurgy*, 6, 73.

Lu, M. (2002). "Improving Poorly Water-Soluble Drug Delivery Through Stabilized Amorphous Systems, Universty of Bradford, Bradford." *PhD Thesis*.

Lynch, D. E., Smith, G., Byriel, K. A., and Kennard, C. H. L. (1991). "Molecular co-crystals of carboxylic acids. 1. The crystal-structures of the adducts of indole-3-acetic-acid with pyridin-2-(1h)-one,3,5-dinitrobenzoic acid and 1,3,5-trinitrobenzene." *Australian J.Chem.*, 44(6), pp 808-819.

Mackenzie, R. (1979). "Nomenclature in thermal analysis part IV." *Thermochim. Acta*, 28, 1-6.

Mashadi, A. B., and Newton, J. M. (1987). "The characterisation of the mechanical properties of microcrystalline cellulose - A fracture mechanics approach." *J. Pharm. Pharmacol.*, 39, 961-965.

McKenna, A., and McCafferty, D. F. (1982). "Effect of particle size on the compaction mechanism and tensile strength of tablets." *J. Pharm. Pharmacol.*, 34, 347-351.

Mercer, A., and Trotter, J. (1978). "Crystal and molecular structure of 1,3,7-trimethyl-2,6-purinedione hydrochloride dihydrate (caffeine hydrochloride dihydrate)." *Acta Cryst.*, B34, 450-453.

Miyamae, A., Kema, H., Kawabata, T., Yasuda, T., M., O., and Matsuda, Y. (1994). "X-ray-powder diffraction study on the grinding effect of the polymorphs of a novel and orally effective uricosuric agent." *Drug Dev. Ind. Pharm.*, 20, 2881-2897.

Moribe, K., Tsuchiya, M., Tozuka, Y., Yamaguchi, K., Oguchi, T., and Yamamoto, K. (2006). "Equimolar complex formation of urea or thiourea with 2-alkoxy-benzamide: structural factors required for the equimolar complex formation." *J. Inc.Phenom*, 54, 9-16.

Morishima, K., Kawashima, Y., Takeuchi, H., Niwa, T., and Hino, T. (1994). "Tableting properties of bucillamine agglomerates prepared by spherical crystallization technique." *Int. J. Pharm.*, 105, pp, 11-18.

Morissette, S. L., Almarsson, O., Peterson, M. L., Remenar, L. F., Read, M. J., Lemmo, A. V., Ellis, S., Cima, M. J., and Gardner, C. R. (2004). "High-throughput crystallization: polymorphs, salts, co-crystals and solvates of pharmaceutical solids." *Adv. Drug Deliv. Rev.*, 56, 275-300.

Mura, P., Cirri, M., Faucci, M. T., Gines-Dordo, J. M., and Bettinetti, G. P. (2002). "Investigation of the effects of grinding and co-grinding on physicochemical properties of glisentide." *Journal of Pharmaceutical and Biomedical Analysis*, 30, 227-237.

Murali Mohan Babu, G. V., Prasad, C. D. S., and Ramana Murthy, K. V. (2002). "Evaluation of modified gum karaya as carrier for the dissolution enhancement of poorly water-soluble drug nimodipine." *International Journal of Pharmaceutics*, 234, 1-17.

Nangia, A. (2005). "Pseudopolymorph: Retain this widely accepted term." *Crystal Growth Des.*, 5:ASAP DOI: 10. 1021/ cg050343e.

Nelson, E., Naqvi, S. M., Busse, L. W., and Higuchi, T. (1954). "The physics of tablet compression: relationship of ejection and upper punch and lower punch forces during compressional process: application of measurements to comparison of tablet lubricants." *J. Am. Pharm.Ass. Soc.*, 43, 496-601.

Nichlas, G., and Frampton, C. S. (1998). "Physicochemical characterization of the orthorhombic polymorph of paracetamol crysallized from solution." *J. Pharm.Sci.*, 87, 684-693.

Oguchi, T., Kazama, K., Yonemochi, E., Churimaworapan, S., Choi, W. S., Limmatavapirat, S., and Yamamoto, K. (2000). "Specific complexation of

ursodeoxycholic acid with guest compounds induced by co-grinding." *Phys. Chem.*, 2, 2815-2820.

Oswald, I. D. H., Allan, D. R., MCGregor, P. A., Motherwell, W. D. S., Parsons, S., and Pulham, C. R. (2002). "The formation of paracetamol (acetaminophen) adducts with hydrogen-bond acceptors." *Acta Cryst.*, B58, 1057-1066.

Otsuka, M., Hasegawa, H., and Matsuda, Y. (1997). "Effect of polymorphic transformation during the extrusion-granulation process on the pharmaceutical properties of carbamazepine granules." *Chem. Pharm. Bull.*,, 45, 894-898.

Otsuka, M., and Kaneniwa, N. (1988). "The hydration kinetics of theophylline monohydrate powder and tablet." *Chem. Pharm. Bull.*, 36, 4914-4920.

Pedireddi, V. R., Chatterjee, S., Ranganthan, A., and Rao, C. N. R. (1998). "A study of supramolecular hydrogen bonded complexes formed by aliphatic dicarboxylic acids with azaaromatic donors." *Tetrahydron*, 54, 9457-9474.

Pedireddi, V. R., Jones, W., Charlton, A. P., and Docherty, R. (1996). "Creation of crystalline supramolecular arrays: a comparison of co-crystal formation from solution and by solid-state grinding." *Chem. Commun.*, pp-987-988.

Pedireddi, V. R., and PrakashaReddy, J. (2002). "Unique homo and hetero carboxylic acid dimer-mediated supramolecular assembly: rational analysis of crystal structure of 3,5-dinitrobenzoic acid and 4-(N-methylamino) benzoic acid,." *Tetrahedron Lett.*, 43, 4927-4930.

Penner, G. H., Polson, J. M., Stuart, C., Ferguson, G., and Kaitner:abcd, B. (1992). "Deuterium NMR and X-ray Crystallographic studies of guest and host motions in the thiourea/ 1,4-di-tert-butylbenzene inclusion compound." *J. Phys.Chem.*, 96, 5121-5129.

Phadnis, N. V., and Suryanayanan, R. (1997). "Polymorphism in anhydrous theophylline-implications on the dissolution rate of theophylline tablets." *J.Pharm. Sci.*, 86, 1256-1263.

Picker, K. M. (2001). "Time dependence of elastic recovery of characterization of tableting materials." *Pharm. Dev. Technol.*, 6, 61-70.

Pirttimaeki, J., and Laine, E. (1994). *Eur.J. Pharm. Sci.*, 1, 203-208.

Portalone, G., and Colapietro, M. (2004). "First example of co-crystals of polymorphic maleic hydrazide." *J. Chem. Crystallogr.*, 34, 609-612.

Price, R., and Young, M. P. (2005). "On the physical transformations of processed pharmaceutical solids." *Micron*, 36, 519-524.

Puttipipatkhachorn, S., Yonemochi, E., Oguchi, T., Yamamoto, K., and Nakai, Y. (1990). "Effect of grinding on dehydration of crystal water of theophylline." *Chem. Pharm. Bull.*, 38, 2233-2236.

Rastogi, R. P., Bassi, P. S., and Chadha, S. L. (1963). "Mechanism of the reaction between hydrocarbons and picric acid in the solid-state." *J. Phys. Chem.*, 67(12), 2569.

Rees, J. E., and Rue, P. J. (1978). "Time-dependent deformation of some direct compression excipients." *J.Pharm. Pharmacol*, 4, 131.

Remenar, J. F., Morisette, S. L., Peterson, M. L., Moulton, B., MacPhee, M. J., Guzman, H. R., and Almarsson, O. (2003). "Crystal engineering of novel co-crystals of a triazole drug with 1,4-dicarboxylic acids." *J. Am. Chem. Sci.,*, 125, 8456-8457.

Rhines, F. N. (1947). "Seminar on pressing of metal powders." *AIME Trans*, 171, 518-534.

Roberts, R., and Rowe, R. (1987). "The Young modulus of pharmaceutical materials." *Int. J. Pharm.*, 37, 15-18.

Roberts, R. J., Rowe, R. C., and York, P. (1991). "The relationship between Youngs modulus of elasticity of organic solids and their molecular structure." *Powder Technol.*, 65, 139-146.

Rodriguez-Hornedo, N., Lechuga, -. B., D., and Wu, H. J. (1992). "Phase transition and heterogeneous/epitaxial nucleation of hydrated and anhydrous theophylline crystals." *I. Pharm. J.*, 85, 149-162.

Rodriguez-Spong, B., Price, C. P., Jayasankar, A., Matzger, A. J., and Rodriguez-Hornedo, N. (2004). "General principles of pharmaceutical solids polymorphism: a supramolecular prespective." *Adv. Drug Deliv. Rev.*, 56, 241-274.

Rumpf, H. (1958). "Grundlagen und Methoden des Granulierens." *Chem. Ing.Tech.*, 30, 144-158.

Rumpf, H. (1962). "The strength of granules and agglomerates." *In: W. A. Knepper, Editor, International Symposium on Agglomeration, Interscience, New York*, 379-418.

Rusa, C. C., Luca, C., Tonelli, A. E., and Rusa, M. (2002). "Structural investigations of the poly(epsilon-caprolactam)-urea inclusion compound." *Polymer*, 43, 3969-3972.

Ryshkewitch, E. (1953). "Compression strength of porous sintered alumina and zircona." *J. Am. Cer. Soc.*, 36, 65-68.

Saito, M., Ugajin, T., Nozawa, Y., Sadzuka, Y., Miygishima, A., and Sonobe, T. (2002). "Preparation and dissolution characteristics of griseofulvin solid dispersions with saccharides." *International Journal of Pharmaceutics*, 249, 71-79.

Salole, E. G., and Al-Sarraj, F. A. (1985). "Spironolactone crystal forms." *Drug Dev Ind Pharm.*, 11(4), 855-864.

Seiler, P., and Dunitz, J. D. (1982). "Low-temperature crystallization of orthorhombic ferocene -structure-analysis at 98-K." *Acta Crystalograr., Sect. B-Struct.*, 38, 1741-1745.

Serajuddin, A. T. M., and Pudipeddi, M. (2002). *Handbook of Pharmaceutical Salts, P. H. Stahl and C. G. Wermuth, Zurich and Wiley-VCH:Weiheim.*, 138.

Shan, N., Bond, A. D., and Jones, W. (2002b). "Crystal engineering using 4,4-apos;-bipyridyl with di- and tricarboxylic acids." *Cryst. Eng.*, 5, 9-24.

Shan, N., Bond, A. D., and Jones, W. (2002c). "Supramolecular synthons in the co-crystal structures of 2-aminopyrimidine with diols and carboxylic acids." *Tetrahedron Lett.*, 43, 3101-3104.

Shan, N., Toda, F., and Jones, W. (2002). "Mechanochemistry and co-crystal formation: effect of solvent on reaction kinetics." *Chem. Commun.*, 20, pp 2372-2373.

Shefter, E., Fung, H. L., and Mok, O. (1973). "Dehydration of crystalline theophylline monohydrate and ampicillin trihydrate." *J.Pharm. Sci.*, 62, 791-794.

Shefter, E., and Higuchi, T. (1963). "Dissolution behaviour of crystalline solvated and nonsolvated forms of some pharmaceuticals." *J. Pharm. Sci.,*, 52, 781-791.

Shell, J. (1963). "X-ray and crystalographic application in pharmaceutical systems. Crystal habit quantitation." *J. Pharm. Sci.*, 52, 100-101.

Shin, S. C., Oh, I. J., Lee, Y. B., Choi, H. K., and Choi, J. S. (1998). "Enhanced dissolution of furosemide by coprecipitating or cogrinding with crospovidone." *International Journal of Pharmaceutics*, 175, 17-24.

Shotton, E., Deer, J. J., and Ganderton, D. (1963). "The instrumentation of a rotary tablet machine." *J.Pharm. Pharmacol.*, 15 Suppl.(106T), 106-14.

Shotton, E., and Obiorah, B. A. (1960). *J.Pharm. Pharmacol.*, 12 Suppl., 87T.

Skoog, D., Holler, F., and Nieman, T. (1998). "Principles of Instrumental Analysis." *Brooks/ cole thermson learning*.

Stahl, P. H., and Wermuth, C. G. (2002). *In. Handbook of Pharmaceutical Salts, Wiley-VCH*, 265-327.

Staniforth, J. N., Rees, J. E., Kayes, J. B., Priest, R. C., and Cotterill, N. J. (1981). "The design of a direct compression tablet excipient." *Drug Dev. Ind. Pharm.*, 7, 179-190.

Stanley-Wood, N. G. (1983). *Enlargement and compaction of particulate solids Butterworth & Co. Edn. London*.

Subramanian, S., and Zaworotka, J. M. (1995). "Manifestations of noncovalent bonding in the solid-state. 6.H-4(cyclam) (4+) cyclam= 1,4,8,11-tetraazacycltetra-decane) as a template for crystal engineering of network hydrogen bonded solids." *Can. J. Chem.*, 73, 414-424.

Sugimoto, M., Okagaki, T., Narisawa, S., Koida, Y., and Nakajima, K. (1998). "Improvement of dissolution characteristics and bioavailability of poorly water-soluble drugs by novel cogrinding method using water-soluble polymer." *International Journal of Pharmaceutics*, 160, 11-19.

Suihko, E., Ketolainen, J., Poso, A., Ahlgren, M., Gynther, J., and Paronen, P. (1997). "Dehydration of theophylline monohydrate: A two step process." *I. Pharm. J.*, 158, 47-55.

Suihko, E., Pekka, V., Ketolainen, J., Laine, E., and Paronen, P. (2001). "Dynamic solid-state tableting properties of four theophylline forms." *I.J. Pharm.*, 217, 225-236.

Suzuki, E., Shimomura, K., and Sekiguchi, K. (1989). "Thermochemical study of theophylline and its hydrate." *Chem. Pharm. Bull.*, 37, 493-497.

Takahashi, Y., Nakashima, T., Ishihara, K., Nakagawa, H., Sugimoto, I. (1985). "Polymorphism of Fostedil: Characterization and polymorphic change by mechanical treatments." *Drug Dev. Ind.Pharm.*, 11, 1543-1563.

Takemoto, K., and Sonoda, N. (1984). "Inclusion compounds of urea, thiourea and selenourea." *In. J. L. Atwood, J. E.D. Devis and D. D. MacNicol(eds.), Academic Press, London*, 2.

Tantishiyakul, V., Kaewnopparat, N., and Ingkatawornwong, S. (1996). "Properties of solid dispersion of piroxicalm in polyvinylpyrrolidone." *International Journal of Pharmaceutics*, 143, 59-66.

Ticehurst, M. D., Sorey, R. A., and Watt, C. (2002). "Application of slurry bridging experiments at cotrolled water activities to predict the solid-state conversion between anhydrous and anhydrated forms using theophylline as a model drug." *I. Pharm. J.*, 247, 1-10.

Trask, A., W.D.S., M., and Jones, W. (2004). "Solvent-drop grinding: Green polymorph control of crystallization." *Chem. Commun.*, 890-891.

Trask, A. V., and Jones, W. (2005). "Crystal engineering of organic co-crystals by the solid-state grinding approach." *In. Top. Curr. Chem.*, 41-70.

Trask, A. V., Motherwell, W. D. S., and Jones, W. (2005a). "Pharmaceutical co-crystallization: engineering a remedy for caffeine hydrate." *Cryst. Growth Des.*, 5, 1013-1021.

Trask, A. V., Shan, N., Motherwell, W. D. S., Jones, W., Feng, S., Tan, R. B. H., and Carpenter, K. J. (2005b). "Selective polymorph transformation via solvent -drop grinding." *Chem. Commun.*, 880-882.

Trask, A. W., WDS., M., and Jones, W. (2006). "Physical stability enhancement of theophylline via co-crystallization." *I. Pharm. J.*, 320, 114-123.

Tuladhar, M. D., Carless, J. E., and Summers, M. P. (1982). "The effects of polymorphism, particle size and compression pressure on the dissolution rate of phenylbutazone tablets." *J. Pharm. Pharmacol.*, 35, 269-274.

Urakami, K., Shono, Y., Higashi, A., Umemoto, K., and Goda, M. (2002). "A novel method for estimation of transition temperature for polymorphic pairs in pharmaceuticals using heat of solution and solubility data." *Chem. Pharm. Bull.,*, 50, 263-267.

Van Kamp, H. V., Bolhuis, G. K., Kussendrager, K., and Lerk, C. (1986a). "Studies on tableting properties of lactose 4. Dissolution and disintegration properties of different types of crystalline lactose." *Int. J. Pharm.*, 28, 229-238.

Videnova-Adrabinska, V. (1996). "The hydrogen bond as a design element in crystal engineering. Two- and three-dimensional building blocks of crystal architecture." *J. Mol. Struct.*, 374, 199-222.

Walsh, R. D. B., Bradner, M. W., Fleischman, S. G., Morales, L. A., Moulton, B., Rodriguez-Hornendo, N., and Zaworotko, M. J. (2003). "Crystal engineering of the composition of pharmaceutical phases." *Chem. Commun*, 186-187.

Watanbe, T., Hasegawa, S., Wakiyama, N., Kusai, A., and Senna, M. (2003). "Comparison between polyvinylpyrrolidone and silica nanoparticles as carriers for indomethacin in a solid state dispersion." *International Journal of Pharmaceutics*, 250, 283-286.

Watanbe, T., Ohano, I., Wakiyama, N., Kusai, A., and Senna, M. (2002). "Stabilization of amorphous indomethacin by co-grinding in a ternary mixture." *International Journal of Pharmaceutics*, 241, 103-111.

Watanbe, T., Wakiyama, N., Usi, F., Ikeda, M., Isobe, T., and Senna, M. (2001). "Stability of amorphous indomethacin compounded with silica." *International Journal of Pharmaceutics*, 226, 81-91.

Watano, S., Okomto, T., Tsuhari, M., Koizumi, I., and Osako, Y. (2002). "Development of a novel vertical high shear kneader and its performance in wet kneading of pharmaceutical powders." *Chem.Pharm. Bull.*, 50, 341-345.

Windheuser, J. J., Misra, J., Eriksen, S. P., and Higuchi, T. (1963). "Physics of tablet compression. Xlll. Development of die wall pressure during compression of various materials." *J. Pharm. Sci.*, 52, 767.

Wöhler, F. (1844). "Untersuchungen ueber das chinon. Annalen." *A Textbook of Spectroscopy, Anmol Publications PVT. LTD., New Delhi*, 51, 153.

Wong, M. W. Y., and Mitchell, A. G. (1992). "Physicochemical characterization of phase change produced during wet granulation of chlorpromazine hydrochloride and its effects on tableting." *Int. J. Pharm.*, 88, 261-273.

Yamako, T., Nakamachi, H., and Miyata, K. (1982). "Studies on the characteristics of carbochromen hydrochloride crystals. II. Polymorphism and cracking in the tablets." *Chem. Pharm. Bull.*,, 30, 3695-3700.

Yonemochi, E., Kitahara, S., Maeda, S., Yamamura, S., Oguchi, T., Yamamoto, K. (1999). "Physicochemical properties of amorphous clarithromycin obtained by grinding and spray drying." *Eur.J. Pharm. Sci*, 7, 331-338.

York, P. (1978). "Particle slippage and arrangement during compression of pharmaceutical powders." *J. Pharm. pharmacol.*, 30, 6-10.

Yoshinari, T., Forbes, R. T., and York, P. (2003). "The improved compaction properties of manitol after a moisture-induced polymorphic transition." *Int. J. Pharm.*, 258, 121-131.

Zaworotka, M. (2005). *Polymorphism in co-crystals and pharmaceutical co-crystals,XX Congress of the International Union of Crystallography, Florence*.

Zhang, J., Wu, L., and Fan, Y. (2003). "Heterosynthons in molecular complexes of azopyridine and 1,2-bis(4-pyridyl)ethylene with dicarboxylic acids." *J. Mol. Struct.*, 660, 119-129.